AUDITORY EFFERENT SYSTEM: NEW INSIGHTS FROM CORTEX TO COCHLEA

EDITED BY: Paul H. Delano and Ana B. Elgoyhen
PUBLISHED IN: Frontiers in Systems Neuroscience

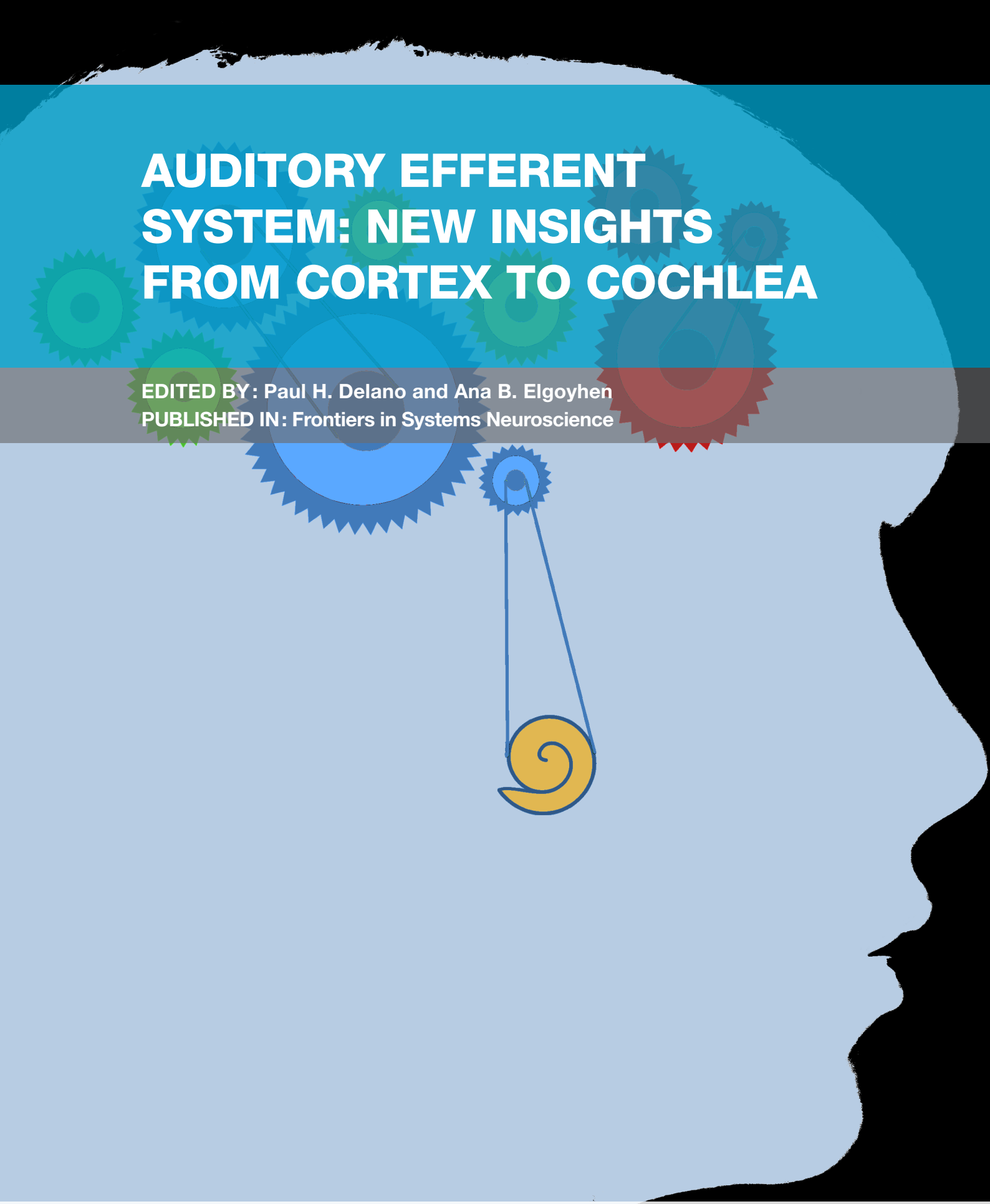

frontiers Research Topics

frontiers

ISSN 1664-8714
ISBN 978-2-88919-935-8
DOI 10.3389/978-2-88919-935-8

About Frontiers

Frontiers is more than just an open-access publisher of scholarly articles: it is a pioneering approach to the world of academia, radically improving the way scholarly research is managed. The grand vision of Frontiers is a world where all people have an equal opportunity to seek, share and generate knowledge. Frontiers provides immediate and permanent online open access to all its publications, but this alone is not enough to realize our grand goals.

Frontiers Journal Series

The Frontiers Journal Series is a multi-tier and interdisciplinary set of open-access, online journals, promising a paradigm shift from the current review, selection and dissemination processes in academic publishing. All Frontiers journals are driven by researchers for researchers; therefore, they constitute a service to the scholarly community. At the same time, the Frontiers Journal Series operates on a revolutionary invention, the tiered publishing system, initially addressing specific communities of scholars, and gradually climbing up to broader public understanding, thus serving the interests of the lay society, too.

Dedication to Quality

Each Frontiers article is a landmark of the highest quality, thanks to genuinely collaborative interactions between authors and review editors, who include some of the world's best academicians. Research must be certified by peers before entering a stream of knowledge that may eventually reach the public - and shape society; therefore, Frontiers only applies the most rigorous and unbiased reviews.

Frontiers revolutionizes research publishing by freely delivering the most outstanding research, evaluated with no bias from both the academic and social point of view.

By applying the most advanced information technologies, Frontiers is catapulting scholarly publishing into a new generation.

What are Frontiers Research Topics?

Frontiers Research Topics are very popular trademarks of the Frontiers Journals Series: they are collections of at least ten articles, all centered on a particular subject. With their unique mix of varied contributions from Original Research to Review Articles, Frontiers Research Topics unify the most influential researchers, the latest key findings and historical advances in a hot research area! Find out more on how to host your own Frontiers Research Topic or contribute to one as an author by contacting the Frontiers Editorial Office: **researchtopics@frontiersin.org**

AUDITORY EFFERENT SYSTEM: NEW INSIGHTS FROM CORTEX TO COCHLEA

Topic Editors:
Paul H. Delano, Universidad de Chile, Chile
Ana B. Elgoyhen, Consejo Nacional de Investigaciones Científicas y Técnicas (CONICET) & Universidad de Buenos Aires, Argentina

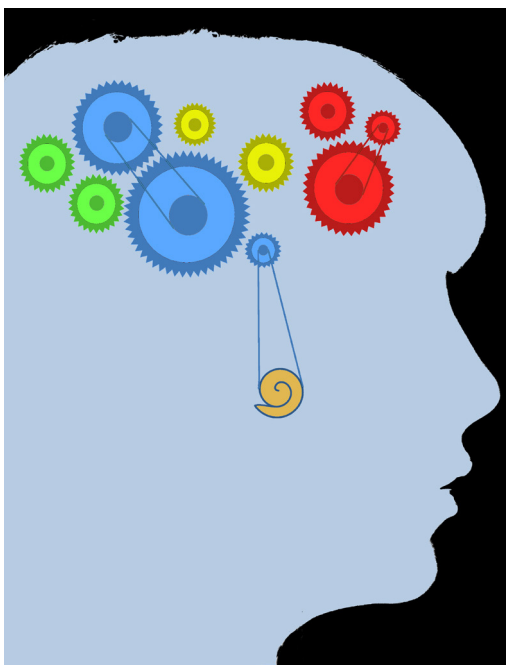

Schematic Diagram of the Descending Projections from the Auditory Cortex to the Cochlea. Figure by Jorratt, CC BY 4.0.

The main function of the sensory systems is the transducing of external stimuli into bioelectrical signals, which are conducted through afferent pathways from sensory epithelia to the brain. However, it is known that descending projections are ubiquitous in the different sensory modalities, and in the case of auditory efferents connect the cerebral cortex with sensory receptor cells.

Several functions have been attributed to the efferent system, including protection to acoustic trauma, unmasking of auditory stimuli in background noise, balance of interaural sensitivity and some cognitive functions like modulation of cochlear sensitivity during selective attention to auditory or visual stimuli. In addition there is evidence of a possible involvement of the efferent system in the etiology or treatment of some clinical pathologies like tinnitus.

In this e-book, entitled "Auditory Efferent System: New Insights from Cortex to Cochlea", we aimed to give an overview of the advances concerning the descending projections from the auditory cortex to subcortical nuclei and the olivocochlear system. In addition, different theoretical proposals of efferent functions are presented. We think that this e-book is an important contribution to the understanding of the efferent system in mammals, merging auditory-cortex literature with studies performed in the olivocochlear system.

Citation: Delano, P. H., Elgoyhen, A. B., eds. (2016). Auditory Efferent System: New Insights from Cortex to Cochlea. Lausanne: Frontiers Media. doi: 10.3389/978-2-88919-935-8

Table of Contents

frontiers in Systems Neuroscience

EDITORIAL
published: 07 June 2016
doi: 10.3389/fnsys.2016.00050

Editorial: Auditory Efferent System: New Insights from Cortex to Cochlea

Paul H. Delano[1,2]* *and Ana B. Elgoyhen*[3,4]*

[1] Programa de Fisiología y Biofísica, Instituto de Ciencias Biomédicas (ICBM), Facultad de Medicina, Universidad de Chile, Santiago, Chile, [2] Departamento de Otorrinolaringología, Hospital Clínico de la Universidad de Chile, Santiago, Chile, [3] Facultad de Medicina, Instituto de Investigaciones en Ingeniería Genética y Biología Molecular, Dr. Héctor N. Torres (INGEBI), Consejo Nacional de Investigaciones Científicas y Técnicas (CONICET) Buenos Aires, Argentina, [4] Tercera Cátedra de Farmacología, Universidad de Buenos Aires, Buenos Aires, Argentina

Keywords: auditory efferent, olivocochlear, top-down, corticofugal, outer hair cells

The Editorial on the Research Topic

Auditory Efferent System: New Insights from Cortex to Cochlea

The outer hair cells (OHCs) of the mammalian cochlea are unique. In average, there are about 15,000 mechanical receptor cells in each human cochlea, and OHCs constitute three quarters of them. They possess the cellular machinery to achieve two fundamental physiological mechanisms of the nervous system: mechanotransduction and electromotility. Through the process known as electromotility, OHCs convert membrane voltage changes into mechanical force. Electromotility depends on a unique motor protein called prestin and results in important auditory functions such as cochlear amplification and fine tuning of the cochlear basilar membrane. The OHCs receive efferent projections from the central nervous system through medial olivocochlear neurons (MOC), located in the brainstem. MOC neurons release acetylcholine which activates unique nicotinic receptors constituted by α9/α10 subunits. In addition to the olivocochlear system, there are massive descending projections from the auditory cortex to the thalamus, inferior colliculus, cochlear nucleus, and superior olivary complex. All these descending pathways could modulate cochlear responses through olivocochlear neurons. Taken together, the corticofugal projections and the olivocochlear system constitute a complex efferent neural network from cortex to the cochlear receptor that regulates synapses between MOC and OHC.

In this e-book, entitled "Auditory efferent system: new insights from cortex to cochlea," we aimed to give an overview of the advances concerning the descending projections from the auditory cortex to subcortical nuclei and the olivocochlear system. In addition, different theoretical proposals of efferent functions are presented.

Guinan gives an expert comprehensive review of the different methods used to assess the olivocochlear function in human and animal experiments. One key aspect discussed in this perspective article is the need to separate crossed and uncrossed MOC effects on otoacoustic emissions. Moreover, more rigorous statistical analyses, like bootstrap methods are proposed.

Aguilar et al. used contralateral acoustic stimulation with broad-band noise in humans and measured behavioral consequences on pure tone thresholds. They found that MOC activation was variable among subjects, as it increased the absolute detection thresholds in some individuals but not in others. Their results suggest that the intensity range of the mechanical suppression produced by MOC activation in humans is different for 500 and 4000 Hz tones.

Otoacoustic emissions have been widely used as a non-invasive tool to evaluate the olivocochlear reflex in animals as well as in humans. Zhao et al. used broad-band noise to assess MOC function with stimulus frequency otoacoustic emissions. Similar to distortion product otoacoustic emissions, they found a shift toward higher frequencies with contralateral acoustic stimulation. These results suggest that the effects of contralateral broad-band noise stimulation on otoacoustic emissions and hearing thresholds are driven by a common set of mechanisms.

OPEN ACCESS

Edited and reviewed by:
Maria V. Sanchez-Vives, Catalan Institution for Research and Advanced Studies (ICREA) and August Pi i Sunyer Biomedical Research Institute (IDIBAPS), Spain

***Correspondence:**
Paul H. Delano
pdelano@med.uchile.cl;
Ana B. Elgoyhen
abelgoyhen@gmail.com

Received: *13 February 2016*
Accepted: *25 May 2016*
Published: *07 June 2016*

Citation:
Delano PH and Elgoyhen AB (2016) Editorial: Auditory Efferent System: New Insights from Cortex to Cochlea. Front. Syst. Neurosci. 10:50. doi: 10.3389/fnsys.2016.00050

Aedo et al. show that suppression of the compound action potential of the auditory nerve with contralateral acoustic stimuli are larger in awake chinchillas compared to anesthetized animals. Moreover, the frequency selectivity of contralateral suppression for tones above 4 kHz is shifted around ¼ octave from the ipsilateral tone. These results show that the strongest olivocochlear effects are produced by contralateral tones at frequencies equal or close to those of ipsilateral tones.

Katz and Elgoyhen present an enlightening review on medial olivocochlear synapses of cochlear hair cells. They discuss how synaptic plasticity mechanisms regulate the efficacy of these synapses at the pre and postsynaptic levels.

Smith and Keil propose an interesting debate about the evolutionary role of the medial olivocochlear system. Loud noises in natural environments are infrequent and consequently it seems improbable that the olivocochlear system evolved to protect against high intensity sounds. They argue that in a biological context, probably the main function of the efferent system is to increase the signal-to-noise ratio during detection of target signals.

On the other hand, Fuente presents a systematic mini-review of the role of MOCs for protection from acoustic trauma in animal models and in human subjects. Animal experiments have clearly shown that olivocochlear fibers can protect from acoustic injuries, however human data is still contradictory and more research is needed.

Terreros and Delano review recent exciting findings showing that auditory cortex activity modulates the most initial auditory processing, including the cochlea, auditory nerve, and cochlear nucleus. In addition, a working model for the different loops of the corticofugal auditory pathways is proposed.

Mellott et al. used retrograde and anterograde tracers to demonstrate that corticofugal projections from the auditory cortex contact excitatory and inhibitory cells in the nucleus of the brachium of the inferior colliculus. Importantly, these findings evidence complex interactions in the efferent loops at the midbrain level.

Malmierca et al. review one key aspect of brain functioning such as the role of corticofugal projections in sensory adaptation. Notably, they evidence that stimulus sensory adaptation in the midbrain is modulated by the corticofugal pathways, and propose a model of predictive coding in the auditory system.

Kong et al. use electrical microstimulation of the auditory cortex to study corticofugal projections to the dorsal cochlear nucleus in mice. These authors describe that the corticofugal effects on the dorsal cochlear nucleus are frequency specific, similar to the corticofugal modulation of ventral cochlear nucleus.

Finally, Lamas et al. design an original approach to investigate the influences of auditory cortex on prestin expression in OHCs. They report changes in prestin oligomerization after surgical removal of the auditory cortex, suggesting that the corticofugal pathways could modulate OHC electromotility.

Some of the unknown fields that should be addressed by future research in the auditory efferent system include physiology of the cortico-olivocochlear neural dynamics, establishment of a reliable and non-invasive clinical measure of the olivocochlear reflex strength in humans and pharmacological development of selective drugs for human use.

AUTHOR CONTRIBUTIONS

All authors listed, have made substantial, direct and intellectual contribution to the work, and approved it for publication.

ACKNOWLEDGMENTS

We thank all the authors and reviewers that contribute to this Research topic. PD is funded by Proyecto Anillo ACT1403. ABE is funded by ANPCyT Argentina.

Conflict of Interest Statement: The authors declare that the research was conducted in the absence of any commercial or financial relationships that could be construed as a potential conflict of interest.

frontiers in
SYSTEMS NEUROSCIENCE

PERSPECTIVE ARTICLE
published: 12 August 2014
doi: 10.3389/fnsys.2014.00142

Olivocochlear efferent function: issues regarding methods and the interpretation of results

John J. Guinan Jr. [1,2] *

[1] Eaton Peabody Laboratory of Auditory Physiology, Department of Otolaryngology, Massachusetts Eye and Ear Infirmary, Boston, MA, USA
[2] Department of Otology and Laryngology, Harvard Medical School, Boston, Massachusetts, USA

Edited by:
Paul Hinckley Delano, Universidad de Chile, Chile

Reviewed by:
Paul Hinckley Delano, Universidad de Chile, Chile
Sumitrajit Dhar, Northwestern University, USA

***Correspondence:**
John J. Guinan Jr., Eaton Peabody Laboratory of Auditory Physiology, Department of Otolaryngology, Massachusetts Eye and Ear Infirmary, 243 Charles St., Boston, MA 02114, USA
e-mail: jjg@epl.meei.harvard.edu

As studies of the olivocochlear (OC) efferent system have matured, issues have been identified that need to be taken into account in the design of new studies and in the interpretation of existing work. The need for high signal-to-noise ratios (SNRs), multiple alternations of conditions, and avoiding middle-ear-muscle activation have been previously highlighted. Less well-known issues include: Contralateral medial OC (MOC) effects may not be good proxies for ipsilateral (ipsi) MOC effects; MOC-induced changes in otoacoustic emissions (OAEs) may not accurately show MOC-induced changes in auditory-nerve (AN) responses; measuring OAE differences from before to after psychophysical trials yields the transient OAE change but not tonic MOC activation; tonic MOC activation may be measurable by several techniques including by OAE differences in trials in which the subject's judgment was correct vs. trials that were incorrect; SNRs can be preserved by Bootstrap statistical tests; differences in task difficulty may outweigh differences in subject attention; lateral efferent effects are little understood and may be tied to MOC effects; to assess whether MOC strength predicts protection from acoustic trauma, prospective tests in humans are needed.

Keywords: olivocochlear efferents, medial olivocochlear, MOC, attention, task difficulty, auditory psychophysics

INTRODUCTION

The goal of this perspective is to provide little-appreciated observations that will help in interpreting the existing efferent literature and in guiding future work. To do this, some general review is necessary (for references see: Guinan, 1996, 2006, 2012a).

The olivocochlear (OC) efferents consist of medial (MOC) and lateral (LOC) groups that innervate outer hair cells (OHCs) and auditory-nerve (AN) dendrites under inner hair cells (IHCs), respectively. MOC neurons with crossed and uncrossed projections to the cochlea both receive inputs from the opposite cochlear nucleus and form MOC reflexes (MOCRs). The result is that uncrossed fibers mediate the contralateral (contra) MOCR, and crossed fibers mediate the ipsilateral (ipsi) MOCR (which is a double-crossed reflex) (Liberman and Brown, 1986).

DO IPSILATERAL AND CONTRALATERAL SOUNDS PRODUCE SIMILAR EFFECTS IN THE COCHLEA?

In most psychophysical studies of the detection of a signal in noise, the signal and noise are both in the same ear, the ipsi ear, so the noise elicits MOC activity through the ipsi MOCR. However, for technical reasons, most human physiologic studies monitor MOC effects using otoacoustic emissions (OAE) in the ipsi ear, but activate MOC efferents with contra noise. Using such a paradigm to correlate across-subject MOCR strengths with signal-in-noise discriminations is comparing contra MOCR strengths to ipsi MOCR effects.

Ipsi and contra MOCRs may be different in the brainstem and/or in the cochlea. Crossed and uncrossed MOC efferents originate in similar brainstem regions and appear to terminate on OHCs in similar ways. Anatomically, no difference in crossed and uncrossed MOC fibers has been described regarding where on OHCs they synapse or in the transmitters they use, but many anatomical experiments were not able to distinguish crossed from uncrossed MOC fibers. One ipsi/contra difference is that relative to ipsi MOCR fibers, contra MOCR fibers have an apical offset in their OHC terminations and a larger span of innervation (Brown, 2014). MOC fibers also terminate on type II auditory nerve fibers within the organ of Corti, and, in some species, on spiral-ganglion cells (Rask-Andersen et al., 2000; Thiers et al., 2008). Both of these are places where ipsi and contra reflex innervation may be different.

Physiological evidence shows ipsi-contra similarities and differences in MOC activation and MOC effects. Most experiments have been only done on one species, but anatomical results suggest there may be little difference in these results across most mammalian species. In cats, the MOC inhibition of AN responses is similar in magnitude for crossed and uncrossed MOC fibers on an inhibition-per-MOC-fiber basis (Gifford and Guinan, 1987). In humans, OAE changes are twice as large for ipsi noise as for contra noise when the MOC-elicitors are half-octave-bands—which is consistent with a 2 to 1 ratio of ipsi to contra MOCR fibers. However, ipsi and contra noises elicit similar-amplitude OAE inhibitions when the noises are broad band

(Lilaonitkul and Guinan, 2009). Thus the growth of MOCR activation with bandwidth is different for ipsi and contra MOCRs, which means that in the brainstem, the reflexes' neural summation across frequency is different. Within the cochlea, ipsi and contra MOCRs produce different relationships between the changes in OAE phase and OAE amplitude (Lilaonitkul and Guinan, 2012). Overall, while ipsi and contra MOCRs show many similarities, in summation across frequency, cochlear effects, and cochlear innervation anatomy, they are different.

Does measuring contra-MOCR strength adequately substitute for measuring ipsi-MOCR strength? Contra-MOCR strength varies greatly across humans (Backus and Guinan, 2007). It seems reasonable to expect ipsi and contra reflex strengths to vary similarly across subjects and to be correlated. However, since the reflexes are different in some respects, it cannot be assumed that their strengths are strongly correlated.

MOC-INDUCED CHANGES IN OAEs VS. IN AUDITORY NERVE (AN) RESPONSES

MOC activation in humans can be assessed by the MOC-induced changes in OAEs, but how well changes in OAEs represent changes in neural responses is not known. The important MOC-induced functional change is in the neural response. MOC-induced OAE and neural changes have been compared in a few studies that suggest that OAE changes are not good indicators of neural changes (Puria et al., 1996; Chabert et al., 2002; Zhao et al., 2012; Lichtenhan et al., 2014).

The changes with sound level of MOC effects on OAEs vs. on neural responses are informative. Many studies have shown that MOC-induced changes in basilar membrane (BM) responses, OAEs, and AN compound potentials (CAPs) are largest at threshold and decrease as sound level is increased. For AN fibers with high spontaneous rates (SRs), MOC-induced inhibition is greatest at low sound levels, but for low-SR fibers, MOC inhibition is highest at mid-to-high sound levels (Guinan and Stankovic, 1996). It might seem that MOC effects on low-SR fibers can be ignored because they are only a small fraction of AN fibers. However, low-SR fibers are the main ones whose firing rate grows at mid-to-high sound levels, and their responses most likely play an outsized role in behavioral discriminations at these levels. Additionally, the motion at the top of the organ of Corti is different from BM motion in tuning and growth with sound level (Zha et al., 2012). Motion at the top of the organ of Corti drives IHCs, not BM motion. Finally, the coupling between organ of Corti motion and the drive to IHC stereocilia is complex (Guinan, 2012b). Overall, one should beware of thinking that the MOC effects on AN responses (and thus, in psychophysical tests) follow MOC inhibition of BM motion and are always largest at low sound levels.

ISSUES IN COMPARING MOC EFFECTS AND PSYCHOPHYSICAL PERFORMANCE

As noted earlier, contra MOCR measurements may not accurately represent ipsi MOCR activation, so comparisons of psychophysical performance and MOC activation are best done using the ipsi MOCR. How is the ipsi MOCR to be measured? One possible test is the DPOAE-onset-adaptation test (Liberman et al., 1996). In humans (where, in contrast to animals, efferents cannot be cut as a control), this test does not distinguish MOC effects from intrinsic cochlear adaptation. The heavy dominance of ipsi adaptation over contra adaptation in humans (Kim et al., 2001) indicates that human ipsi DPOAE adaptation contains a large intrinsic component. Another technique that works in animals but not humans is measurement of DPOAE 2F1-F2 adaptation (F1 and F2 are the primary-tone frequencies) at frequencies near DPOAE response dips. In animals dips arise from OHC stereocilia nonlinearity (Lukashkin and Russell, 2002) and the MOCR directly changes OHC properties. In contrast, in humans most dips are due to interference between DPOAE distortion and reflection components (Talmadge et al., 1999) and the depth of these dips is due to how well they cancel which is only indirectly affected by the MOCR.

Another issue in measuring ipsi MOCR effects is that ipsi elicitor sounds suppress concurrent ipsi OAEs. This can be avoided by using MOCR elicitors with no energy near the OAE-probe frequency, but such a choice may not be compatible with the psychophysical test. For most psychophysical tests (e.g., signal-in-noise discriminations), ipsi OAE measurements cannot be done simultaneously with the stimuli being discriminated. An alternative is to measure MOC effects from OAEs before and immediately after each psychophysical trial. The difference in OAE amplitudes from before to after the trial provides a measure of the trial-locked *change* in MOC activation. However, the difference misses any tonic MOC activation, i.e., MOC activation that begins at the beginning of a block of trials and continues throughout the block during both the pre- and post-trial measurements.

If the subject's mental getting ready at the beginning of a task brings about tonic MOC activation (presumably from cortical activation of descending pathways), then when the same sounds are heard without a task (called "passive listening"), perhaps there is no tonic MOC activation. In passive listening, the difference between OAE measurements before and after the trial sounds is from transient MOC activation. If during pre-measurements in passive listening there is no tonic activation, then any OAE differences in the pre-trial measurements from active compared to passive listening would reveal tonic MOC activation during the active-listening trials. To avoid effects of drift and differences across measurement sessions, interleaving blocks of task and no-task trials within a measurement session is probably necessary. On the interleaved no-task blocks, the subject must "relax" and not attempt discriminations, i.e., not tonically activate their efferents. A long training period may be required for subjects to achieve good performance in tasks with alternation of MOC activation. Not all subjects may be able to do this, i.e., to achieve performance on blocks alternating MOC-on/MOC-off that equals their performance when doing long sequences of just MOC-on or just MOC-off.

One method to reveal tonic MOC activation would be to interleave a task that has a MOC perceptual benefit and a task in which MOC activation would be detrimental (e.g., detecting a tone in quiet at a frequency far from spontaneous OAEs (SOAEs)—see Dewey et al., 2014). Optimum performance would require MOC activation in the first case, and turning-off MOC activation in the

second case. Alternating these would allow tonic MOC activation to be detected by comparing the pre-trial OAE levels. Again, a long training period may be required to achieve good performances. Whenever there is long training, presumably there is learning involved and this may change the OAE results over time and make it difficult to obtain the stationary periods necessary for good averaging.

A powerful but difficult to apply method is the correct/incorrect comparison. In a series of trials using identical stimuli, some subject judgments are correct and some are incorrect. Since the stimuli are the same (with random permutations in presentation order), differences in subject judgments are presumably due to internal variations within the subject (e.g., in subject alertness, MOC activation, etc.). If correct trials, on average, have more MOC activation than incorrect trials, this would be strong evidence that the MOC activation actually produced the perceptual benefit, since all stimulus variables are the same (although correlation doesn't prove causation). With this method, transient activation during each trial is shown by the difference in before-trial to after-trial OAE amplitudes, and variation in tonic activation may be revealed by comparing the pre-trial OAE amplitudes from correct vs. incorrect trials. A variant of this method was used in chinchillas who skipped making a choice on many trials (which is not allowed in the normal human paradigm) with the result that a difference in MOC activation was found between trials when the animal made a choice vs. the skipped trials, but not between correct and incorrect trials (Delano et al., 2007).

STATISTICAL TESTS

Both the pre-to-post trial method and the correct/incorrect comparison method require many trials to achieve adequate signal-to-noise ratios (SNRs). The best SNR is achieved by computing differences using *all* of the available trials. If the data are broken into N subsets to have N tokens for a statistical test, then each token has poorer SNR than the grand average. One way to keep the highest SNR is to use a bootstrap method.

The bootstrap method is described initially with a correct/incorrect comparison. First, OAEs should have passed SNR criteria to remove those with excessive noise. Also, to minimize effects of drift, pre and post data from a trial should both be used or both excluded. Suppose there are Nc and Ni correct and incorrect noise-minimized trials: (1) Pre-trial and post-trial OAE averages are done using all of the Nc trials and separately using all of the Ni trials. The statistic of interest (the "real-stat") is then computed from these averages. (2) The null-hypothesis is that there is no difference between Nc and Ni trials, so all trials are pooled (i.e., their actual correct/incorrect value is ignored). From this pool, Nc trials are randomly chosen to form a pseudo-Nc set which are averaged. The remaining Ni trials become the pseudo-Ni set and are averaged. Both selections must be done without replacement so the noise from a trial is never added in twice (different random noises add orthogonally, but the same noise added to itself adds linearly and would produce a noise summation that is not equivalent to the noise summation in step 1). The statistic of interest (the "pseudo-stat") is then computed from these averages exactly as in step 1. (3) Step 2 is done 1000 times (10,000 is even better), each with a different randomization, yielding 1000 pseudo-stats which show the "null-hypothesis" distribution. (4) If there are fewer than 50 out of 1000 pseudo-stats that have more extreme values than the real-stat, then the real stat is statistically significant at the 0.05 level. Since usually Nc > Ni, the average of the correct trials will generally have a lower noise level than the average of the incorrect trials. However, no noise correction is needed in the statistical test because the real and pseudo averages use the same number of trials. However, the Nc > Ni difference in noise level can bias the average difference and needs to be considered in the interpretation of this difference. Control computations should be done to check that the Nc and Ni noise-levels-per-trial are not different and to inform the interpretation. If instead of correct/incorrect, the pre/post difference is tested, then the null hypothesis is that there is no pre/post difference. On each trial, pre and post values are pooled and are randomly assigned to be pseudo-pre and pseudo-post when calculating the pseudo distributions. The rest of the bootstrap is done as in the correct/incorrect comparison.

TASK DIFFICULTY AND THE COMPARISON OF TASK/NO-TASK CONDITIONS

A potentially important but little considered issue is task difficulty. It is well established that the pupillary reflex varies with task difficulty, including for auditory tasks (Kahneman and Beatty, 1966; Zekveld and Kramer, 2014). Like the pupillary reflex, the MOCR is a brainstem-level reflex that receives descending inputs. Furthermore, MOC activation has been shown to vary with task difficulty (Delano et al., 2007). To validate that a difference in MOC activation is due to selective attention and not to task difficulty, the task difficulty must be kept constant in the tasks compared. This might be done by setting the parameters so the compared tasks yield the same percentage of correct trials. Reports that claim to show differences in MOC activation due to selective attention (e.g., differences ascribed to auditory vs. visual attention) should be examined closely to determine if the supposed selective attention difference may actually be from differences in task difficulty.

It is well known that pushing a button can cause noise. Less well known is that subjects sometimes make small settling movements at the beginning of trials that add noise at the earphone. Large noises from gross motion can be removed easily by an artifact rejection system. However, small noises (which can be revealed by averaging two adjacent responses after reversing one) vary in amplitude over a wide range and are difficult to reject. Care must be taken to insure that differences between pre and post-task OAEs are not contaminated by differences in pre-post noise levels.

There are several areas of the MOC literature in which the existing reports appear to give contradictory results (e.g., attention increases MOC activation, or decreases MOC activation). Some of these may become clearer when the above considerations are taken into account. Less weight should be given to studies that have methodological deficiencies based on the issues presented above. However, even well-done studies can be expected to depend on the stimulus parameters explored and reported

differences may be due to difference in the parameters used. Too many studies look only at one condition, or a very few conditions, and then state conclusions as if these conclusions apply widely. More studies are needed that vary the sound parameters over a large enough range to capture how the MOC effect varies with the parameters.

LOC FUNCTION AND MOC-LOC INTERACTIONS

There is good evidence that LOC activity reduces acoustic trauma and auditory aging (Liberman et al., 2014). There is no direct evidence for activation of LOC neurons by sound, but it is presumed they respond to sound, in part because they are located in a brainstem auditory nucleus. Neurons in this brainstem region are excited by ipsi sound and inhibited by contra sound. If LOC neurons respond with the same laterality pattern, then those that inhibit AN fibers (some LOCs excite and some inhibit), may balance left-right cochlear outputs to optimize sound localization from interaural intensity differences (Guinan, 1996). Darrow et al. (2006) presented data favoring this hypothesis, but Larsen and Liberman (2010) presented data opposing this hypothesis. LSO fibers are unmyelinated, conduct slowly and change AN firing over the course of minutes (Groff and Liberman, 2003) so whatever they do is likely to be on a slow time scale.

There are several ways in which the MOC and LOC systems interact. MOC activity reduces cochlear amplifier gain which reduces AN firing rates, and thus MOC activity may reduce LOC activity. Likewise, LOC fibers change AN activity and thus influence MOC firing. MOC-LOC interaction also occurs within the tunnel of Corti where LOC fibers synapse on MOC fibers (Liberman, 1980), but it is unknown whether these synapses are excitatory or inhibitory. Overall, there is ample opportunity for MOC-LOC interactions so that their effects may be correlated across subjects and circumstances. Thus, effects attributed to one system, may be due in part to, or influenced by, the other system.

TESTS TO PREDICT SUSCEPTIBILITY TO ACOUSTIC TRAUMA AND AUDITORY AGING: ISSUES

Considering the strong evidence that the MOC and LOC systems help protect from both acoustic trauma and auditory aging, it would be highly desirable to have tests for MOC and LOC function. At present, there is no LOC test, but MOC function can be tested in humans by sound-evoked MOC effects on OAEs. Many prior studies of MOC function in humans used group averages, but for prediction in an individual the MOC test must be accurate in the individual. This requires achieving an adequate SNR in each subject, something which is especially difficult when small MOC effects are to be measured in the most-vulnerable subjects. SNRs of 25 dB or more are likely to be needed (e.g., Goodman et al., 2013, Figure 8). To minimize test time, an averaging stopping rule should be used that is based on achieving the SNR to detect a pre-determined low-amplitude MOC effect (Guinan, 2006, 2012a). One little-discussed issue is: "How many frequencies need to be tested?" Related questions are: "How much does MOC activation vary across frequency in different subjects?" What does finding MOC activation at an easy-to-test frequency (e.g., one with large OAEs) indicate about the MOC activation at hard-to-test frequencies? More work on these questions is needed.

One possibility is that MOC activation at non-traumatic levels is aimed at gaining perceptual benefits, but for protection at very high sound levels other brainstem mechanisms are activated, similar to those that activate the middle-ear-muscle system. The relative strengths of such low-level and high-level MOC systems may vary across individuals. Animal work indicates that MOC tests at low sound levels can be predictive of MOC anti-trauma strength (Maison and Liberman, 2000) but this does not rule out low-to-high-level differences. Prospective tests in humans are needed to show how well MOC tests predict susceptibility to acoustic trauma, e.g., MOC tests applied at the start of a person's work in a loud-sound environment (e.g., Lapsley Miller et al., 2006).

CONCLUSION

There are many potential problems in studying efferents. Some have clear solutions. Others do not. In all cases it is important to be aware of the potential problems so that experiments can be designed well and interpreted properly.

ACKNOWLEDGMENTS

I thank Dr. Jeffery Lichtenhan for comments on the manuscript. Supported by NIH RO1-DC005977.

REFERENCES

Backus, B. C., and Guinan, J. J. Jr. (2007). Measurement of the distribution of medial olivocochlear acoustic reflex strengths across normal-hearing individuals via otoacoustic emissions. *J. Assoc. Res. Otolaryngol.* 8, 484–496. doi: 10.1007/s10162-007-0100-0

Brown, M. C. (2014). Single-unit labeling of medial olivocochlear neurons: the cochlear frequency map for efferent axons. *J. Neurophysiol.* 111, 2177–2186. doi: 10.1152/jn.00045.2014

Chabert, R., Magnan, J., Lallemant, J. G., Uziel, A., and Puel, J. L. (2002). Contralateral sound stimulation suppresses the compound action potential from the auditory nerve in humans. *Otol. Neurotol.* 23, 784–788. doi: 10.1097/00129492-200209000-00029

Darrow, K. N., Maison, S. F., and Liberman, M. C. (2006). Cochlear efferent feedback balances interaural sensitivity. *Nat. Neurosci.* 9, 1474–1476. doi: 10.1038/nn1807

Delano, P. H., Elgueda, D., Hamame, C. M., and Robles, L. (2007). Selective attention to visual stimuli reduces cochlear sensitivity in chinchillas. *J. Neurosci.* 27, 4146–4153. doi: 10.1523/jneurosci.3702-06.2007

Dewey, J. B., Lee, J., and Dhar, S. (2014). Effects of contralateral acoustic stimulation on spontaneous otoacoustic emissions and hearing threshold fine structure. *J. Assoc. Res. Otolaryngol.* in press.

Gifford, M. L., and Guinan, J. J. Jr. (1987). Effects of electrical stimulation of medial olivocochlear neurons on ipsi and contra cochlear responses. *Hear. Res.* 29, 179–194. doi: 10.1016/0378-5955(87)90166-3

Goodman, S. S., Mertes, I. B., Lewis, J. D., and Weissbeck, D. K. (2013). Medial olivocochlear-induced transient-evoked otoacoustic emission amplitude shifts in individual subjects. *J. Assoc. Res. Otolaryngol.* 14, 829–842. doi: 10.1007/s10162-013-0409-9

Groff, J. A., and Liberman, M. C. (2003). Modulation of cochlear afferent response by the lateral olivocochlear system: activation via electrical stimulation of the inferior colliculus. *J. Neurophysiol.* 90, 3178–3200. doi: 10.1152/jn.00537.2003

Guinan, J. J. Jr. (1996). "The physiology of olivocochlear efferents," in *The Cochlea*, eds P. J. Dallos, A. N. Popper and R. R. Fay (New York: Springer-Verlag), 435–502.

Guinan, J. J. Jr. (2006). Olivocochlear efferents: anatomy, physiology, function and the measurement of efferent effects in humans. *Ear Hear.* 27, 589–607. doi: 10.1097/01.aud.0000240507.83072.e7

Guinan, J. J. Jr. (2012a). "Efferent system," in *Translational Perspectives in Hearing Science. Normal Aspects of Hearing.*, eds K. L. Tremblay and R. Burkard (San Diego: Plural Pub. Inc.), 283–323.

Guinan, J. J. Jr. (2012b). How are inner hair cells stimulated? Evidence for multiple mechanical drives. *Hear. Res.* 292, 35–50. doi: 10.1016/j.heares.2012.08.005

Guinan, J. J. Jr., and Stankovic, K. M. (1996). Medial efferent inhibition produces the largest equivalent attenuations at moderate to high sound levels in cat auditory-nerve fibers. *J. Acoust. Soc. Am.* 100, 1680–1690. doi: 10.1121/1.416066

Kahneman, D., and Beatty, J. (1966). Pupil diameter and load on memory. *Science* 154, 1583–1585. doi: 10.1126/science.154.3756.1583

Kim, D. O., Dorn, P. A., Neely, S. T., and Gorga, M. P. (2001). Adaptation of distortion product otoacoustic emission in humans. *J. Assoc. Res. Otolaryngol.* 2, 31–40.

Lapsley Miller, J. A., Marshall, L., Heller, L. M., and Hughes, L. M. (2006). Low-level otoacoustic emissions may predict susceptibility to noise-induced hearing loss. *J. Acoust. Soc. Am.* 120, 280–296. doi: 10.1121/1.2204437

Larsen, E., and Liberman, M. C. (2010). Contralateral cochlear effects of ipsilateral damage: no evidence for interaural coupling. *Hear. Res.* 260, 70–80. doi: 10.1016/j.heares.2009.11.011

Liberman, M. C. (1980). Efferent synapses in the inner hair cell area of the cat cochlea: an electron microscopic study of serial sections. *Hear. Res.* 3, 189–204. doi: 10.1016/0378-5955(80)90046-5

Liberman, M. C., and Brown, M. C. (1986). Physiology and anatomy of single olivocochlear neurons in the cat. *Hear. Res.* 24, 17–36. doi: 10.1016/0378-5955(86)90003-1

Liberman, M. C., Liberman, L. D., and Maison, S. F. (2014). Efferent feedback slows cochlear aging. *J. Neurosci.* 34, 4599–4607. doi: 10.1523/JNEUROSCI.4923-13.2014

Liberman, M. C., Puria, S., and Guinan, J. J. Jr. (1996). The ipsilaterally evoked olivocochlear reflex causes rapid adaptation of the $2f_1$-f_2 distortion product otoacoustic emission. *J. Acoust. Soc. Am.* 99, 3572–3584. doi: 10.1121/1.414956

Lichtenhan, J., Wilson, U., and Guinan, J. J. Jr. (2014). Quantifying efferent-induced inhibition of cochlear amplifier gain from changes in human compound action potentials. *Asso. Res. Otolaryngol. Abstr.* 37, 122–122.

Lilaonitkul, W., and Guinan, J. J. Jr. (2009). Human medial olivocochlear reflex: effects as functions of contralateral, ipsilateral and bilateral elicitor bandwidths. *J. Assoc. Res. Otolaryngol.* 10, 459–470. doi: 10.1007/s10162-009-0163-1

Lilaonitkul, W., and Guinan, J. J. Jr. (2012). Frequency tuning of medial-olivocochlear-efferent acoustic reflexes in humans as functions of probe frequency. *J. Neurophysiol.* 107, 1598–1611. doi: 10.1152/jn.00549.2011

Lukashkin, A. N., and Russell, I. J. (2002). Modifications of a single saturating nonlinearity account for post-onset changes in 2f1–f2 distortion product otoacoustic emission. *J. Acoust. Soc. Am.* 112, 1561–1568. doi: 10.1121/1.1502903

Maison, S. F., and Liberman, M. C. (2000). Predicting vulnerability to acoustic injury with a noninvasive assay of olivocochlear reflex strength. *J. Neurosci.* 20, 4701–4707.

Puria, S., Guinan, J. J. Jr., and Liberman, M. C. (1996). Olivocochlear reflex assays: effects of contralateral sound on compound action potentials vs. ear-canal distortion products. *J. Acoust. Soc. Am.* 99, 500–507. doi: 10.1121/1.414508

Rask-Andersen, H., Tylstedt, S., Kinnefors, A., and Illing, R. (2000). Synapses on human spiral ganglion cells: a transmission electron microscopy and immunohistochemical study. *Hear. Res.* 141, 1–11. doi: 10.1016/s0378-5955(99)00179-3

Talmadge, C. L., Long, G. R., Tubis, A., and Dhar, S. (1999). Experimental confirmation of the two-source interference model for the fine structure of distortion product otoacoustic emissions. *J. Acoust. Soc. Am.* 105, 275–292. doi: 10.1121/1.424584

Thiers, F. A., Nadol, J. B. Jr., and Liberman, M. C. (2008). Reciprocal synapses between outer hair cells and their afferent terminals: evidence for a local neural network in the mammalian cochlea. *J. Assoc. Res. Otolaryngol.* 9, 477–489. doi: 10.1007/s10162-008-0135-x

Zekveld, A. A., and Kramer, S. E. (2014). Cognitive processing load across a wide range of listening conditions: insights from pupillometry. *Psychophysiology* 51, 277–284. doi: 10.1111/psyp.12151

Zha, D., Chen, F., Ramamoorthy, S., Fridberger, A., Choudhury, N., Jacques, S. L., et al. (2012). In vivo outer hair cell length changes expose the active process in the cochlea. *PLoS One* 7:e32757. doi: 10.1371/journal.pone.0032757

Zhao, W., Berezina, M. A., and Guinan, J. J. Jr. (2012). A comparison of medial olivocochlear efferent effects on auditory nerve compound action potentials and Stimulus Frequency Otoacoustic Emissions (SFOAEs) in guinea pigs. *Asso. Res. Otolaryngol. Abstr.* 35, 78.

Conflict of Interest Statement: The author declares that the research was conducted in the absence of any commercial or financial relationships that could be construed as a potential conflict of interest.

Received: 12 June 2014; paper pending published: 27 June 2014; accepted: 23 July 2014; published online: 12 August 2014.

*Citation: Guinan JJ Jr. (2014) Olivocochlear efferent function: issues regarding methods and the interpretation of results. Front. Syst. Neurosci. **8**:142. doi: 10.3389/fnsys.2014.00142*

This article was submitted to the journal Frontiers in Systems Neuroscience.

frontiers in
SYSTEMS NEUROSCIENCE

ORIGINAL RESEARCH ARTICLE
published: 15 January 2015
doi: 10.3389/fnsys.2014.00251

Contralateral efferent suppression of human hearing sensitivity

Enzo Aguilar[1,2†], Peter T. Johannesen[1,2] and Enrique A. Lopez-Poveda[1,2,3]*

[1] *Auditory Computation and Psychoacoustics, Instituto de Neurociencias de Castilla y León, Universidad de Salamanca, Salamanca, Spain*
[2] *Grupo de Audiología, Instituto de Investigación Biomédica de Salamanca, Universidad de Salamanca, Salamanca, Spain*
[3] *Departamento de Cirugía, Facultad de Medicina, Universidad de Salamanca, Salamanca, Spain*

Edited by:
Paul Hinckley Delano, Universidad de Chile, Chile

Reviewed by:
John J. Guinan, Massachusetts Eye and Ear Infirmary; and Harvard Medical School, USA
Luis Robles, Universidad de Chile, Chile

***Correspondence:**
Enrique A. Lopez-Poveda, Auditory Computation and Psychoacoustics, Instituto de Neurociencias de Castilla y León, Universidad de Salamanca, Calle Pintor Fernando Gallego 1, 37007 Salamanca, Spain
e-mail: ealopezpoveda@usal.es

†Present address:
Enzo Aguilar, Escuela de Fonoaudiología, Facultad de Ciencias de la Salud, Universidad de Talca, Chile

The present study aimed at characterizing the suppressing effect of contralateral medial olivocochlear (MOC) efferents on human auditory sensitivity and mechanical cochlear responses at sound levels near behavioral thresholds. Absolute thresholds for pure tones of 500 and 4000 Hz with durations between 10–500 ms were measured in the presence and in the absence of a contralateral broadband noise. The intensity of the noise was fixed at 60 dB SPL to evoke the contralateral MOC reflex without evoking the middle-ear muscle reflex. In agreement with previously reported findings, thresholds measured without the contralateral noise decreased with increasing tone duration, and the rate of decrease was faster at 500 than at 4000 Hz. Contralateral stimulation increased thresholds by 1.07 and 1.72 dB at 500 and 4000 Hz, respectively. The mean increase (1.4 dB) just missed statistical significance (p = 0.08). Importantly, the across-frequency mean threshold increase was significantly greater for long than for short probes. This effect was more obvious at 4000 Hz than at 500 Hz. Assuming that thresholds depend on the MOC-dependent cochlear mechanical response followed by an MOC-independent, post-mechanical detection mechanism, the present results at 4000 Hz suggest that MOC efferent activation suppresses cochlear mechanical responses more at lower than at higher intensities across the range of intensities near threshold, while the results at 500 Hz suggest comparable mechanical suppression across the threshold intensity range. The results are discussed in the context of central masking and of auditory models of efferent suppression of cochlear mechanical responses.

Keywords: temporal integration, absolute threshold, auditory efferents, audiometry, central masking, auditory models, auditory suppression

INTRODUCTION

Physiological studies in non-human mammals have shown that activation of olivocochlear efferents suppresses cochlear mechanical responses. The amount of suppression is greater at low than at moderate or high sound input levels (Murugasu and Russell, 1996; Dolan et al., 1997; Russell and Murugasu, 1997; Cooper and Guinan, 2006; Guinan and Cooper, 2008). Olivocochlear efferents may be activated in a reflexive manner by contralateral stimulation (Guinan, 2006, 2010). On the other hand, otoacoustic emissions (OAEs) are a byproduct of cochlear mechanical responses (Kemp, 1978, 2002). For these reasons, researchers have often looked at the suppression of OAEs by contralateral stimulation as a way to physiologically characterize the suppressing effects of the contralateral medial olivocochlear reflex (MOCR) in humans (Guinan et al., 2003; Atcherson et al., 2008; Sun, 2008; Lilaonitkul and Guinan, 2009a,b; Francis and Guinan, 2010). Comparatively, few studies have looked at the suppressing effects of the contralateral MOCR on human auditory sensitivity. This is the aim of the present study.

Typically, auditory sensitivity is assessed by measuring the detection threshold of pure tones. It has been long known that pure-tone detection thresholds increase with contralateral stimulation (Wegel and Lane, 1924). Contralateral pure tones increase thresholds between 3 and 15 dB, depending on the frequency and the temporal position of the test tone relative to that of the contralateral tone. Typically, threshold increases are larger for test tones at the frequency and at the onset of the contralateral tone than in other conditions (Zwislocki et al., 1967, 1968; Mills et al., 1996). This phenomenon was originally referred to as "central masking" because the contralateral stimulus was regarded as a "masker" and the threshold increase was interpreted to occur by interaction of that "masker" with the test tone somewhere in the central auditory nervous system (Zwislocki et al., 1967).

Smith et al. (2000) related central masking with MOC suppression. They used macaques and measured absolute thresholds for pure tones of 1 s of duration in the presence and in the absence of a continuous, band-limited (two-octave wide) contralateral noise centered at the test tone frequency. They reported mean threshold shifts of 2, 4 and 6 dB at 1, 2, and 4 kHz, respectively, for a contralateral noise at 60 dB of sensation level (SL). Most importantly, they showed that the shift decreased in magnitude,

or even disappeared, after sectioning of MOC efferents. Hence, they argued that central masking is probably due to the suppressing effects of the MOCR and concluded that the term "central masking" is probably incorrect.

Kawase et al. (2003) measured the suppressor effect of the contralateral MOCR on audiometric thresholds for pure tones at frequencies of 500–8000 Hz. They used a continuous broadband noise as the contralateral MOCR elicitor and their test tones had 50 ms of duration. They showed that their contralateral noise increased audiometric thresholds more at low than at high frequencies (see their Figure 2), and that the magnitude of the increase was proportional to the intensity of the contralateral stimulus. Their results are broadly consistent with more recent studies reporting greater OAE suppression at low than at high frequencies (Lilaonitkul and Guinan, 2009a).

Human auditory sensitivity not only depends on the frequency of the test tone; it also depends on its duration. Absolute thresholds decrease with increasing tone duration and the rate of decrease varies depending on tone frequency (Watson and Gengel, 1969). Several explanatory mechanisms have been proposed for this phenomenon, including the idea that threshold is based on the integration of sound intensity (Watson and Gengel, 1969) or sound pressure (Heil and Neubauer, 2003) over time, on taking "multiple-looks" at neural responses elicited by the test tones in search for excess neural activity (Viemeister and Wakefield, 1991), or on the greater probability of firing of auditory nerve fibers for longer than for shorter stimuli (Meddis, 2006).

Whatever the actual mechanism, threshold probably depends on the magnitude of the cochlear mechanical response elicited by the stimulus and a post-mechanical detection mechanism. In the absence of efferent suppression, human mechanical cochlear responses are probably linear at intensities near absolute threshold (Plack and Skeels, 2007). Assuming that the post-cochlear detection mechanism is independent of MOC activation, comparisons of the threshold-vs.-duration functions measured with and without contralateral stimulation can give us some insight about the magnitude of MOC suppression of basilar membrane (BM) responses at different sound levels near threshold. For example, if the amount of suppression were comparable across levels near threshold, as is illustrated by Model 1 in **Figure 1**, MOC activation would shift the threshold-vs.-duration function vertically without a change in the function slope. By contrast, if the magnitude of MOC suppression were greater at lower than at higher sound levels (throughout the threshold range), as is illustrated by Model 2 in **Figure 1**, or if BM responses were compressive at threshold for short tones and linearized by MOC suppression, as illustrated by Model 3 in **Figure 2**, then MOC activation would shift the threshold-vs.-duration function with a concomitant

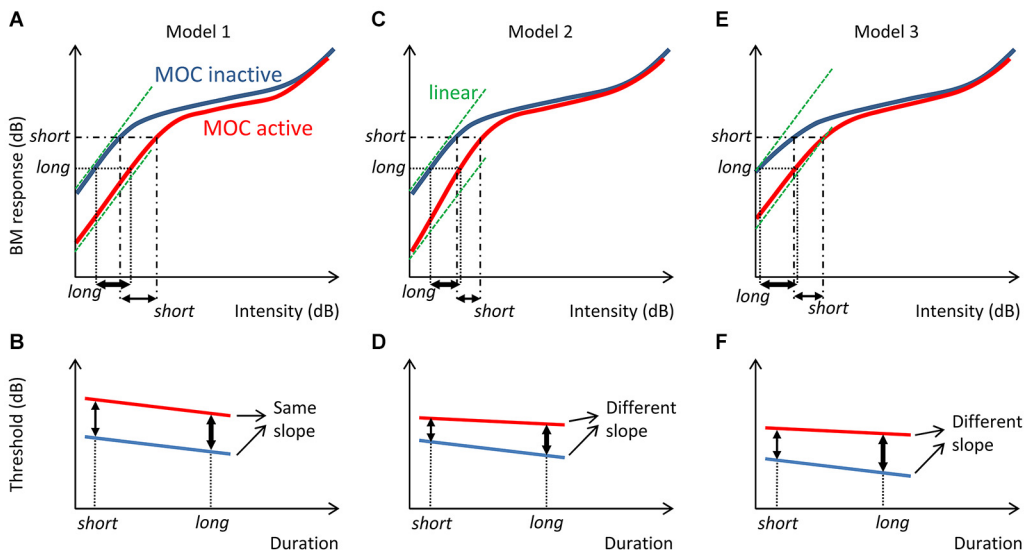

FIGURE 1 | Three possible models of contralateral MOC suppression of basilar membrane (BM) responses and their effects on threshold-vs.-duration functions. The left panels (Model 1) illustrate the case where BM responses are linear (slope = 1 dB/dB) at behavioral threshold both with and without MOC activation and MOC activation suppresses BM responses by a constant amount at all levels near threshold, a model adapted from (Ferry and Meddis, 2007). Assuming that a short tone requires a greater BM response than a longer tone to evoke just detectable responses **(A)**, MOC activation would vertically shift the threshold-vs.-duration function without changing the function slope **(B)**. The middle panels (Model 2) illustrate an alternative model where BM responses are linear at threshold and MOC activation suppresses BM responses more at low than at moderate input threshold levels **(C)**. In other words, in this case MOC activation would turn a linear BM input/output function near threshold into expansive (slope > 1 dB/dB). In this case, MOC activation would vertically shift the threshold-vs.-duration function with a concomitant change in slope **(D)**. The right panels illustrate a third model (Model 3) where BM responses are slightly compressive (slope < 1 dB/dB) at threshold and MOC activation suppresses BM responses more at low than at moderate input levels in the threshold range, thus causing the compressive BM input/output curve to become linear near threshold **(E)**. In this case, MOC activation would also vertically shift the threshold-vs.-duration function with a concomitant change in slope **(F)**. For reference, the green dashed lines illustrate hypothetical linear input/output relationships.

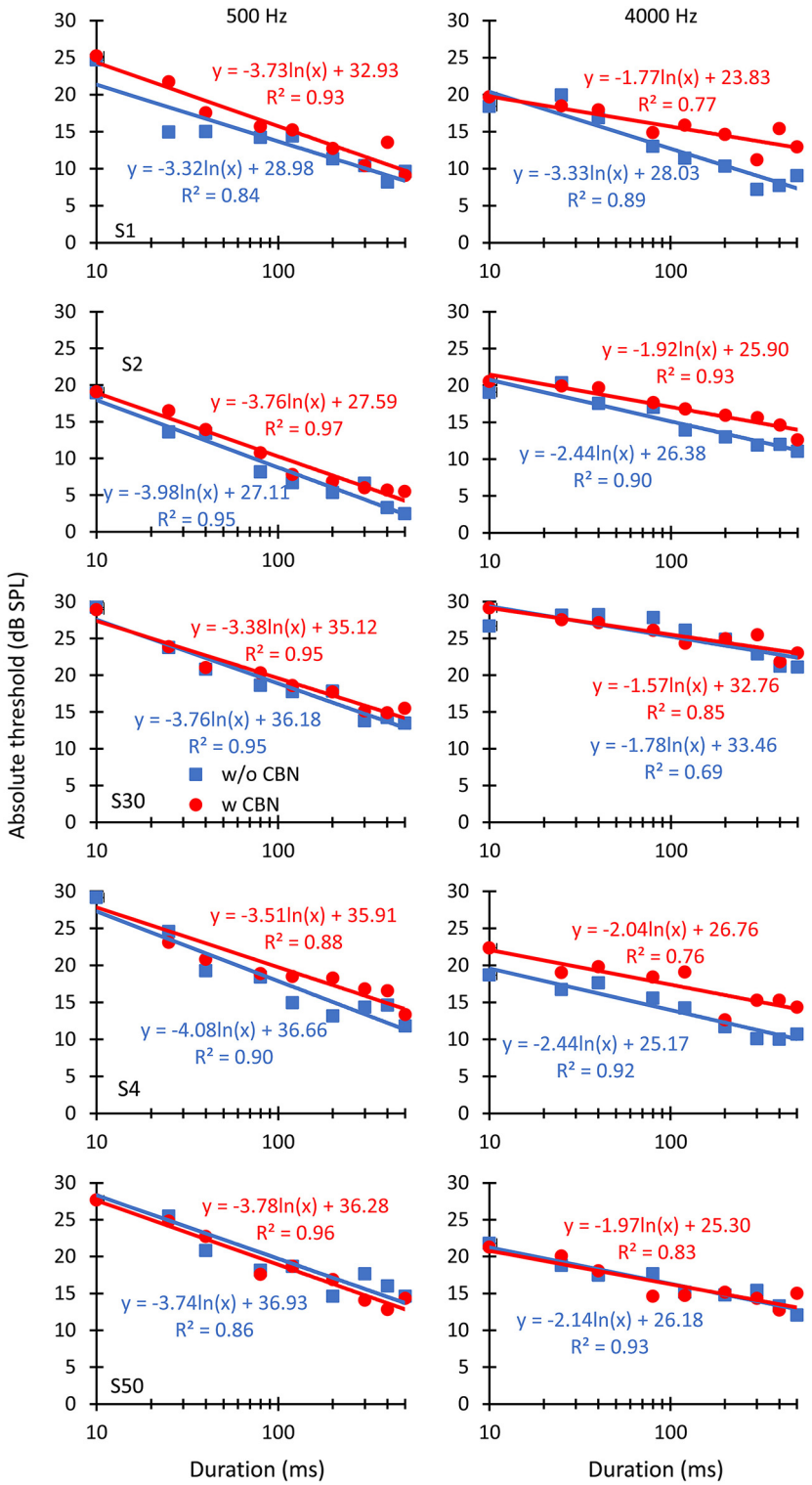

FIGURE 2 | The effect of contralateral stimulation on individual absolute detection thresholds for pure tones of different durations. The left and right columns illustrate results for pure tone frequencies of 500 and 4000 Hz, respectively. Each row illustrates results for an individual listener, as indicated in the left panels. Symbols depict mean thresholds in the absence ("w/o CBN", squares) and in the presence ("w CBN", circles) of a CBN, as indicated by the inset in the left panel of the middle row. Lines illustrate least-squares fits to the data using the logarithmic functions given next to the data. R^2 is the proportion of variance in the data predicted by the fits.

change in slope. The aim of the present study was to test these hypotheses by comparing threshold-vs.-duration functions measured in the presence and in the absence of a 60-dB SPL contralateral broadband noise (CBN) used as the MOCR elicitor.

METHODS

STIMULI

The task consisted of measuring absolute detection thresholds of pure tones of various different durations in the presence and in the absence of a CBN used as the MOCR elicitor. Pure tones had frequencies of 500 and 4000 Hz, and durations of 10, 25, 40, 80, 120, 200, 300, 400, and 500 ms. All of them were gated with onset and offset raised-cosine ramps of 5-ms of duration. The level of the CBN was set fixed at 60 dB SPL. It has been shown elsewhere that this type of noise is capable of activating the MOCR without activating the middle-ear muscle reflex (Lilaonitkul and Guinan, 2009a,b; Aguilar et al., 2013). The CBN had a duration of 1010 ms and it was gated with 5-ms raised-cosine onset and offset ramps. It started 500 ms before the tone onset and ended 10 ms after the offset of the longest tone. The MOCR is almost fully activated about 330 ms after the elicitor onset (Backus and Guinan, 2006). Therefore, we assumed that MOCR was activated at the onset of the test tone and remained active over the whole tone duration.

PROCEDURE

Absolute detection thresholds were measured using a two-interval, two-alternative, forced-choice adaptive procedure. Two intervals were presented to the participants accompanied by flash lights in a computer monitor. One of the intervals was silent in the test ear while the other contained the test tone; the CBN was presented to the contralateral ear in the two intervals. The inter-stimulus time interval (defined as the silent period between the offset and the onset of the CBN in the two intervals) was 500 ms. The test tone was presented in either the first or the second interval at random and participants were instructed to identify the interval containing the tone by pressing a key on the computer keyboard. Feedback was given to the participants. The level of the test tone decreased after two successive correct responses and increased after an incorrect response (two-down, one-up adaptive rule). Absolute threshold was thus defined as the tone level giving 71% correct responses in the psychometric function (Levitt, 1971). The level of test tone changed by 6 dB until the third reversal in level occurred, and it changed by 2 dB thereafter. The procedure continued until 12 level reversals were measured and absolute threshold was obtained as the mean of the tone levels at the last 10 reversals. The threshold estimate was discarded when the corresponding standard deviation exceeded 6 dB. At least three valid thresholds estimates were obtained for each condition and their average was taken as the absolute threshold. When the standard deviation of the three threshold estimates exceeded 6 dB, additional estimates were obtained and included in the mean.

Stimuli were generated with custom-made Matlab software and played via an RME Fireface 400 soundcard at a sampling rate of 44.1 kHz, and with 24-bit resolution. Stimuli were presented to the participants using Etymotic ER-2 insert earphones. These earphones are designed to give a flat frequency response at the eardrum and have a nominal inter-aural attenuation of 70+ dB that minimizes cross-hearing. Listeners sat in a double-wall sound attenuating booth during all measurements.

Stimuli were calibrated by coupling the earphones to a sound level meter (B&K 2238) through a Zwislocki coupler (Knowles DB-100). Calibration was performed at 1 kHz and the measured sensitivity was applied to all other frequencies.

Experimental procedures were approved by the Human Experimentation Ethics Committee of the University of Salamanca (Spain). Informed consent was obtained from all participants.

SUBJECTS

Three women (S1, S4, and S50) and two men (S2—the first author, and S30) with no history of hearing impairment participated in the study. All of them had normal tympanometry and clinical audiometric thresholds within 20 dB hearing level (HL; ANSI, 1996). Their ages were 31 (S1), 31 (S2), 27 (S4), 33 (S30), and 25 (S50) years. Subjects were volunteers and were not paid for their service.

RESULTS

ABSOLUTE THRESHOLDS

Individual and mean threshold-vs.-duration functions are shown in **Figures 2**, **3**, respectively. A first question is whether the CBN increases absolute thresholds, as would be expected (e.g., **Figure 1**), and whether the magnitude of the increase is different at the two probe frequencies or for different probe durations. Visual inspection of **Figures 2**, **3** suggests that the CBN raised thresholds at the two test frequencies for some listeners (S1, S2 or S4) but not for others (S30 and S50). When it occurred, the threshold increase was typically greater for long than for short durations, particularly at 4000 Hz. A three-way repeated-measures analysis of the variance (ANOVA) was used to test for the effects of duration, probe frequency, the presence of contralateral stimulation, and their possible interactions on mean absolute thresholds. Results revealed a statistically significant interaction between duration and frequency ($F_{(8,32)} = 29.55$, $p < 0.001$). All other possible interactions between pairs of factors or between the three factors were not statistically significant. The analysis also revealed a significant effect of duration ($F_{(8,32)} = 160.87$, $p < 0.001$) and an almost-significant effect of contralateral stimulation ($F_{(1,4)} = 5.64$, $p = 0.080$) but not a significant effect of frequency.

In summary, thresholds were: (1) lower for longer than for shorter probes (**Figure 3**); and (2) higher in the presence than in the absence of the CBN (**Figure 4A**), although the effect of the CBN just missed statistical significance. On average, the CBN increased thresholds slightly more at 4000 than at 500 Hz (1.72 vs. 1.07 dB, respectively), but the effect of frequency on the mean increase was not statistically significant.

SLOPE OF THE THRESHOLD-VS.-DURATION FUNCTION

Figures 2, **3** show that in the absence of contralateral stimulation, absolute thresholds always decreased with increasing tone duration and the rate of decrease (i.e., the slope of the function)

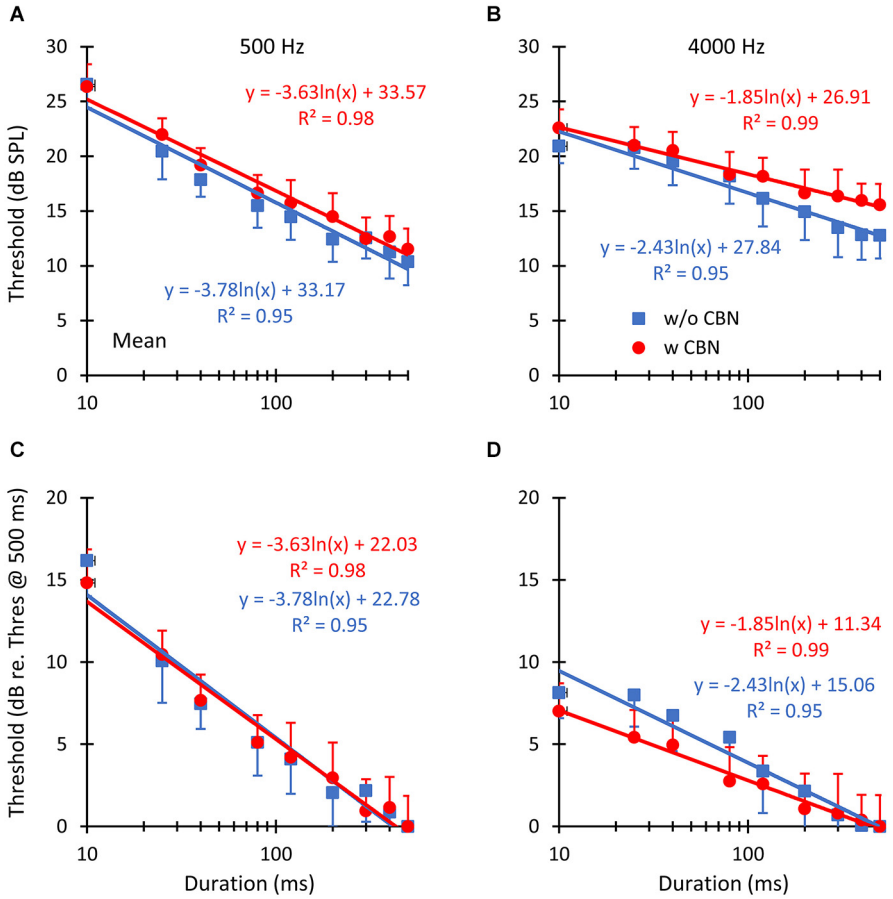

FIGURE 3 | The *mean* effect of contralateral stimulation on absolute detection thresholds for pure tones of different durations. The left and right columns illustrate results for pure tone frequencies of 500 and 4000 Hz, respectively. Symbols depict mean thresholds in the absence ("w/o CBN", squares) and in the presence ("w CBN", circles) of a CBN, as indicated by the inset in panel B. Error bars illustrate one standard error of the mean. Lines illustrate least-squares fits to the data using the logarithmic functions given next to the data. The two rows show identical data in units of dB SPL **(A,B)** or dB re threshold for the 500-ms tone **(C,D)**.

generally appeared steeper at 500 than at 4000 Hz. These results are consistent with those reported by early studies (Watson and Gengel, 1969). The question here is whether the contralateral stimulation alters the slope of the threshold-vs.-duration function and if so, whether the change is different at the two test frequencies. To better address this question, logarithmic functions were fitted *ad hoc* to the individual data. The fits are shown in **Figures 2**, **3** as straight lines together with their corresponding equations and goodness-of-fit statistic, R^2 (the proportion of predicted variance). The high values of R^2 support the chosen model.

Figure 4B illustrates the effect of the CBN on the mean slope at the two test frequencies. **Table 1** gives corresponding numeric values. A two-way repeated-measures ANOVA was carried out to test for the effects of frequency, the presence or absence of contralateral stimulation, and their possible interaction on the *slope* of the threshold-vs.-duration function. The test revealed that when the data for the two CBN conditions were combined, mean slopes were significantly steeper at 500 than at 4000 Hz: mean slopes were −3.70 vs. −2.14 dB/ln(ms) at 500 and 4000 Hz respectively ($F_{(1,4)}$ = 99.37, p = 0.001). The test also revealed that when the data for the two frequencies were combined, mean slopes were significantly shallower with than without contralateral stimulation: mean slopes were −2.74 vs. −3.10 dB/ln(ms) with and without CBN, respectively ($F_{(1,4)}$ = 16.73, p = 0.015). **Figure 4B** shows that the CBN reduced the mean slope more at 4000 than at 500 Hz (see also **Figures 3C,D**). Although the ANOVA revealed that this effect (i.e., the interaction of frequency with CBN effects on the slope) was not statistically significant ($F_{(1,4)}$ = 1.16, p = 0.342), a *post hoc* analysis suggested that the mean slope decrease (**Table 1**) was almost significant at 4000 Hz (two-tailed paired t-test, N = 5, p = 0.088) and not significant at 500 Hz (two-tailed, paired t test, N = 5, p = 0.446).

In summary, the rate of decrease of absolute threshold with increasing duration (i.e., the slope of the threshold-vs.-duration function) was (1) faster at 500 than at 4000 Hz; and (2) decreased in the presence of a CBN. The CBN reduced the rate of decrease more at 4000 Hz than at 500 Hz (**Table 1**). At 4000 Hz, the reduction in slope just missed statistical significance.

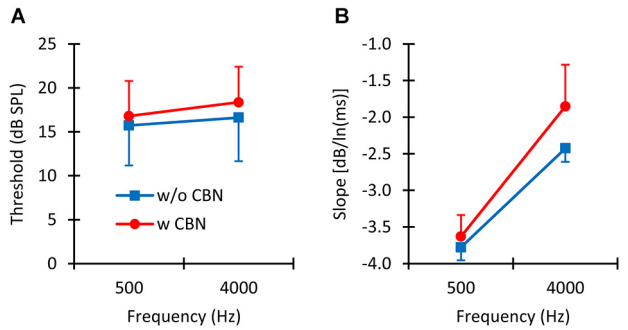

FIGURE 4 | The mean effect of contralateral stimulation. **(A)** Mean absolute detection thresholds with (w CBN) and without (w/o CBN) contralateral stimulation at the two test frequencies. **(B)** Mean slope of the threshold-vs.-duration functions with and without contralateral stimulation at the two test frequencies. Error bars illustrate one standard deviation.

Table 1 | Slope (in units of dB/ln(ms)) of the threshold-vs.-duration functions.

	w/o CBN	w CBN	Mean
500 Hz	−3.77 ± 0.29	−3.63 ± 0.18	−3.70
4000 Hz	−2.43 ± 0.57	−1.85 ± 0.19	−2.14
Mean	−3.10	−2.74	

Central cells give mean of the individual slopes across the five listeners plus and minus one standard deviation.

DISCUSSION

The aim of the present study was to investigate the effect of MOC activation on the detection threshold of pure tones of different durations. We used a CBN with a level of 60 dB SPL as the MOCR elicitor because it has been shown in previous reports that this noise appears sufficient to evoke an MOCR without activating a middle-ear muscle reflex (see Figure 1 in Aguilar et al., 2013; see also Lilaonitkul and Guinan, 2009a). Therefore, it is reasonable to assume that the reported effects of the CBN are caused by the activation of contralateral MOC efferents.

We have shown that in the absence of contralateral acoustic stimulation, (1) pure-tone absolute thresholds decrease with increasing tone duration; and (2) that the rate of decrease is steeper at 500 Hz than at 4000 Hz (compare the slope of the blue lines in **Figures 3C,D**; see also **Table 1**). This aspect of the results is not new and is broadly consistent with what was shown by Watson and Gengel (1969).

We have also shown that the CBN employed here increases absolute thresholds on average by 1.07 and 1.72 dB at 500 and 4000 Hz, respectively (**Figure 4A**), presumably by activation of the MOCR. (We note, however, that the increase just missed statistical significance ($p = 0.08$) because the effect of the CBN was largely variable across listeners (**Figure 2**)). It is hard to compare this result with conclusions from previous studies because the magnitude of MOC suppression depends on the intensity and time course of the MOC elicitor in relation to the probe (Zwislocki et al., 1967; Kawase et al., 2003). Even studies that used an MOCR elicitor comparable to the one employed here show mixed effects, not always consistent with the present data. For example, Lilaonitkul and Guinan (2009a) showed that a contralateral MOCR elicitor suppressed human stimulus frequency OAEs more at 500 than at 4000 Hz (their Figure 3). Smith et al. (2000) reported that for macaques, the contralateral MOCR elicitor increased threshold shifts more at 4000 than at 500 Hz (their Figure 2). Kawase et al. (2003) showed that the MOCR elicitor shifted absolute thresholds by approximately equal amounts at the two frequencies, but the magnitude of the shift was around 6 dB, hence greater than the magnitude observed in the present data (1.4 dB). Aguilar et al. (2013) analyzed the effect of the CBN on psychoacoustical tuning curves and concluded that suppression was greater at 500 than at 4 kHz. The reason for the discrepancies across studies is uncertain. It might be related to differences in experimental species, procedures, and/or MOCR elicitor-probe timing configurations. Indeed, previous studies on the effect of the MOCR on OAEs or psychoacoustical tuning curves were concerned with effects at supra-threshold conditions while the present study focuses on effects at absolute threshold.

The main novelty of the present results is that *on average* the magnitude of threshold increase caused by the CBN was greater for long than for short probe durations; in other words, that the CBN made the threshold-vs.-duration functions shallower (**Figure 4B**). This effect was more obvious at 4000 Hz than at 500 Hz (**Figures 3C,D** and **Table 1**), even though in statistical terms the effect was not significantly different at the two frequencies. Assuming that threshold shifts are caused by a reduction of mechanical cochlear responses only (i.e., that MOC activation does not affect post-mechanical detection mechanism) and based on the rationale illustrated in **Figure 1**, the present results suggests that at 4000 Hz MOC activation reduces cochlear mechanical responses more at lower than at higher input levels in the threshold range, while at 500 Hz the reduction of cochlear mechanical responses is comparable at all levels in the threshold range. In other words, the present results at 500 Hz appear consistent with Model 1 in **Figure 1**, while the results at 4000 Hz appear consistent with either Model 2 or Model 3.

Model 1, however, has been successfully used elsewhere to mimic the effects of MOC activation on the vibration of basal BM regions and on the spike rate of auditory nerve fibers with high characteristic frequencies (Ferry and Meddis, 2007). It has also been successfully used to model the effects of the contralateral MOCR on psychoacoustical tuning curves at 500 and 4000 Hz (Aguilar et al., 2013; Lopez-Poveda et al., 2013). That the present data at 4000 Hz are *not* consistent with such model is thus puzzling and the reason uncertain. One possibility is that in testing Model 1, previous studies put more emphasis in getting accurate model predictions at levels above around 30 dB SPL than at the lower levels measured here. Indeed, Figure 2 in Ferry and Meddis (2007) reveals that Model 1 is comparatively less accurate at mimicking the efferent effects on BM input/output curves at low than at moderate input levels.

On the other hand, Model 2 assumes that linear BM responses at threshold become *expansive* with MOC efferent activation,

something not supported by experimental BM input/output curves from basal cochlear regions. Instead, direct recordings of BM motion from basal cochlear regions suggest that BM input/output curves are slightly compressive near behavioral thresholds and become more linear with MOC efferent activation (e.g., Figure 2 in Cooper and Guinan (2006); Figure 2 in Murugasu and Russell (1996)). In other words, physiological recordings in non-human mammals suggest that the present human data at 4000 Hz would be consistent with Model 3.

That the effect of MOC activation on the slope of the threshold-vs.-duration function was not significantly different at the two test frequencies was possibly due to the large variability of the data across subjects (**Figures 2**, **4B**). We note, however, that the effect of the CBN on the slope was almost statistically significant at 4000 Hz ($p = 0.088$) but far from significant at 500 Hz. The available mechanical measurements indicate considerable differences between cochlear mechanics in the apex vs. in the base (Robles and Ruggero, 2001; Cooper, 2004). Therefore, although admittedly uncertain, it is conceivable that the more obvious MOC effects at 4000 than at 500 Hz do reflect actual differences in cochlear mechanics between basal and apical cochlear regions.

One might think that the comparatively larger threshold increase for longer tones could be due to inhibition from the ipsilateral MOCR that would be evoked by the longer test tones and less so by the shorter tones. This, however, is unlikely because all the tones involved in the present study had levels at behavioral threshold, and tones at threshold elicit little or no MOC activity.

The threshold shifts reported here are interpreted to be primarily caused by suppression of cochlear mechanical responses by MOC efferent activation. Electrically stimulated ears lack contralateral MOC efferent modulation of cochlear mechanical responses and yet contralateral masking has been reported to occur on electrically stimulated ears of cochlear implant users with residual hearing in the non-implanted ear (James et al., 2001) as well as in bilateral cochlear implant users (Lin et al., 2013). Therefore, it is conceivable that central masking does occur in spite of the evidence given by Smith et al. (2000) and that it may have contributed to the present results to some uncertain extent.

CONCLUSIONS

1. Activation of the contralateral MOCR by broadband noise at 60 dB SPL increased the absolute detection thresholds of pure tones for some listeners but not for others. The average increase was 1.07 and 1.72 dB at 500 and 4000 Hz, respectively, and just missed statistical significance because of the wide across-subject variability.
2. On average, the threshold increase due to MOCR activation was significantly greater for longer (500 ms) than for shorter (10 ms) probes. This effect was more obvious at 4000 than at 500 Hz.
3. Assuming that detection thresholds depend on the MOC-dependent cochlear mechanical response followed by an MOC-independent, post-mechanical detection mechanism, the present results at 4000 Hz suggest that MOC efferent activation suppresses cochlear mechanical responses more at lower than at higher intensities across the range of intensities near threshold, while the results at 500 Hz suggest that MOC efferent activation suppresses cochlear mechanical responses similarly across the range of intensities near threshold. In other words, the present results would be consistent with Model 1 in **Figure 1** at 500 Hz and with Model 3 at 4000 Hz.

ACKNOWLEDGMENTS

We thank Almudena Eustaquio-Martin for technical support, and Joshua S. Stohl for pointing at the studies of central masking in cochlear-implant users referred to in the Discussion. We also thank the two reviewers for their suggestions. Work supported by the Spanish MICINN (ref. BFU2009-07909) to Enrique A. Lopez-Poveda, and by the Chilean CONICYT to Enzo Aguilar. Publication of this study was supported by the Spanish MINECO (ref. BFU2012-39544-C02) to Enrique A. Lopez-Poveda.

REFERENCES

Aguilar, E., Eustaquio-Martin, A., and Lopez-Poveda, E. A. (2013). Contralateral efferent reflex effects on threshold and suprathreshold psychoacoustical tuning curves at low and high frequencies. *J. Assoc. Res. Otolaryngol.* 14, 341–357. doi: 10.1007/s10162-013-0373-4

ANSI. (1996). *S3.6 Specification for Audiometers.* New York: American National Standards Institute.

Atcherson, S. R., Martin, M. J., and Lintvedt, R. (2008). Contralateral noise has possible asymmetric frequency-sensitive effect on the 2F1–F2 otoacoustic emission in humans. *Neurosci. Lett.* 438, 107–110. doi: 10.1016/j.neulet.2008.04.050

Backus, B. C., and Guinan, J. J. (2006). Time-course of the human medial olivocochlear reflex. *J. Acoust. Soc. Am.* 119, 2889–2904. doi: 10.1121/1.2169918

Cooper, N. P. (2004). "Compression in the peripheral auditoy system," in *Compression: From Cochlea to Cochlear Implants*, eds S. P. Bacon, R. R. Fay and A. N. Popper (New York: Springer-Verlag), 18–61.

Cooper, N. P., and Guinan, J. J. (2006). Efferent-mediated control of basilar membrane motion. *J. Physiol.* 576, 49–54. doi: 10.1113/jphysiol.2006.114991

Dolan, D. F., Guo, M. H., and Nuttall, A. L. (1997). Frequency-dependent enhancement of basilar membrane velocity during olivocochlear bundle stimulation. *J. Acoust. Soc. Am.* 102, 3587–3596. doi: 10.1121/1.421008

Ferry, R. T., and Meddis, R. (2007). A computer model of medial efferent suppression in the mammalian auditory system. *J. Acoust. Soc. Am.* 122, 3519–3526. doi: 10.1121/1.2799914

Francis, N. A., and Guinan, J. J. (2010). Acoustic stimulation of human medial olivocochlear efferents reduces stimulus-frequency and click-evoked otoacoustic emission delays: implications for cochlear filter bandwidths. *Hear. Res.* 267, 36–45. doi: 10.1016/j.heares.2010.04.009

Guinan, J. J. (2006). Olivocochlear efferents: anatomy, physiology, function and the measurement of efferent effects in humans. *Ear. Hear.* 27, 589–607. doi: 10.1097/01.aud.0000240507.83072.e7

Guinan, J. J. (2010). Cochlear efferent innervation and function. *Curr. Opin. Otolaryngol. Head Neck Surg.* 18, 447–453. doi: 10.1097/MOO.0B013e32833e05d6

Guinan, J. J., Backus, B. C., Lilaonitkul, W., and Aharonson, V. (2003). Medial olivocochlear efferent reflex in humans: Otoacoustic Emission (OAE) measurement issues and the advantages of stimulus frequency OAEs. *J. Assoc. Res. Otolaryngol.* 4, 521–540. doi: 10.1007/s10162-002-3037-3

Guinan, J. J., and Cooper, N. P. (2008). Medial olivocochlear efferent inhibition of basilar-membrane responses to clicks: evidence for two modes of cochlear mechanical excitation. *J. Acoust. Soc. Am.* 124, 1080–1092. doi: 10.1121/1.2949435

Heil, P., and Neubauer, H. (2003). A unifying basis of auditory thresholds based on temporal summation. *Proc. Natl. Acad. Sci. U S A* 100, 6151–6156. doi: 10.1073/pnas.1030017100

James, C., Blamey, P., Shallop, J. K., Incerti, P. V., and Nicholas, A. M. (2001). Contralateral masking in cochlear implant users with residual hearing in the non-implanted ear. *Audiol. Neurootol.* 6, 87–97. doi: 10.1159/000046814

Kawase, T., Ogura, M., Sato, T., Kobayashi, T., and Suzuki, Y. (2003). Effects of contralateral noise on the measurement of auditory threshold. *Tohoku J. Exp. Med.* 200, 129–135. doi: 10.1620/tjem.200.129

Kemp, D. T. (1978). Stimulated acoustic emissions from within the human auditory system. *J. Acoust. Soc. Am.* 64, 1386–1391. doi: 10.1121/1.382104

Kemp, D. T. (2002). Otoacoustic emissions, their origin in cochlear function, and use. *Br. Med. Bull.* 63, 223–241. doi: 10.1093/bmb/63.1.223

Levitt, H. (1971). Transformed up-down methods in psychoacoustics. *J. Acoust. Soc. Am.* 49, 467–477. doi: 10.1121/1.1912375

Lilaonitkul, W., and Guinan, J. J. (2009a). Human medial olivocochlear reflex: effects as functions of contralateral, ipsilateral and bilateral elicitor bandwidths. *J. Assoc. Res. Otolaryngol.* 10, 459–470. doi: 10.1007/s10162-009-0163-1

Lilaonitkul, W., and Guinan, J. J. (2009b). Reflex control of the human inner ear: a half-octave offset in medial efferent feedback that is consistent with an efferent role in the control of masking. *J. Neurophysiol.* 101, 1394–1406. doi: 10.1152/jn.90925.2008

Lin, P., Lu, T., and Zeng, F. G. (2013). Central masking with bilateral cochlear implants. *J. Acoust. Soc. Am.* 133, 962–969. doi: 10.1121/1.4773262

Lopez-Poveda, E. A., Aguilar, E., Johannesen, P. T., and Eustaquio-Martín, A. (2013). "Contralateral efferent regulation of human cochlear tuning: behavioral observations and computer model simulations," in *Basic Aspects of Hearing: A Compilation of Papers from the 16th International Symposium on Hearing*, eds B. C. J. Moore, H. Gockel, R. P. Carlyon, I. M. Winter and R. D. Patterson (New York: Springer), 47–54.

Meddis, R. (2006). Auditory-nerve first-spike latency and auditory absolute threshold: a computer model. *J. Acoust. Soc. Am.* 119, 406–417. doi: 10.1121/1.2139628

Mills, J. H., Dubno, J. R., and He, N. (1996). Masking by ipsilateral and contralateral maskers. *J. Acoust. Soc. Am.* 100, 3336–3344. doi: 10.1121/1.416974

Murugasu, E., and Russell, I. J. (1996). The effect of efferent stimulation on basilar membrane displacement in the basal turn of the guinea pig cochlea. *J. Neurosci.* 16, 325–332.

Plack, C. J., and Skeels, V. (2007). Temporal integration and compression near absolute threshold in normal and impaired ears. *J. Acoust. Soc. Am.* 122, 2236–2244. doi: 10.1121/1.2769829

Robles, L., and Ruggero, M. A. (2001). Mechanics of the mammalian cochlea. *Physiol. Rev.* 81, 1305–1352.

Russell, I. J., and Murugasu, E. (1997). Medial efferent inhibition suppresses basilar membrane responses to near characteristic frequency tones of moderate to high intensities. *J. Acoust. Soc. Am.* 102, 1734–1738. doi: 10.1121/1.420083

Smith, D. W., Turner, D. A., and Henson, M. M. (2000). Psychophysical correlates of contralateral efferent suppression. I. The role of the medial olivocochlear system in "central masking" in nonhuman primates. *J. Acoust. Soc. Am.* 107, 933–941. doi: 10.1121/1.428274

Sun, X. M. (2008). Contralateral suppression of distortion product otoacoustic emissions and the middle-ear muscle reflex in human ears. *Hear. Res.* 237, 66–75. doi: 10.1016/j.heares.2007.12.004

Viemeister, N. F., and Wakefield, G. H. (1991). Temporal integration and multiple looks. *J. Acoust. Soc. Am.* 90, 858–865. doi: 10.1121/1.401953

Watson, C. S., and Gengel, R. W. (1969). Signal duration and signal frequency in relation to auditoy sensitivitiy. *J. Acoust. Soc. Am.* 46, 989–997. doi: 10.1121/1.1911819

Wegel, R. L., and Lane, C. E. (1924). The auditory masking of one pure tone by another and its probable relation to the dynamics of the inner ear. *Phys. Rev.* 23, 266–285. doi: 10.1103/physrev.23.266

Zwislocki, J. J., Buining, E., and Glantz, J. (1968). Frequency distribution of central masking. *J. Acoust. Soc. Am.* 43, 1267–1271. doi: 10.1121/1.1910978

Zwislocki, J. J., Damianopoulos, E. N., Buining, E., and Glantz, J. (1967). Central masking: some steady-state and transient effects. *Percept. Psychophys.* 2, 59–64. doi: 10.3758/bf03212462

Conflict of Interest Statement: The authors declare that the research was conducted in the absence of any commercial or financial relationships that could be construed as a potential conflict of interest.

Received: 17 November 2014; accepted: 21 December 2014; published online: 15 January 2015.

Citation: Aguilar E, Johannesen PT and Lopez-Poveda EA (2015) Contralateral efferent suppression of human hearing sensitivity. Front. Syst. Neurosci. ***8****:251. doi: 10.3389/fnsys.2014.00251*

This article was submitted to the journal Frontiers in Systems Neuroscience.

frontiers in Systems Neuroscience

ORIGINAL RESEARCH
published: 10 December 2015
doi: 10.3389/fnsys.2015.00168

Efferent Modulation of Stimulus Frequency Otoacoustic Emission Fine Structure

*Wei Zhao[1], James B. Dewey[2], Sriram Boothalingam[2] and Sumitrajit Dhar[2,3]**

[1] L.E.K. Consulting, Boston, MA, USA, [2] Roxelyn and Richard Pepper Department of Communication Sciences and Disorders, Northwestern University, Evanston, IL, USA, [3] Knowles Hearing Center, Northwestern University, Evanston, IL, USA

Otoacoustic emissions, sounds generated in the inner ear, have become a convenient non-invasive tool to examine the efferent modulation of cochlear mechanics. Activation of the medial olivocochlear (MOC) efferents has been shown to alter the magnitude of these emissions. When the effects of efferent activation on the detailed spectral structures of these emissions have been examined, a shift of the spectral patterns toward higher frequencies has been reported for distortion product and spontaneous otoacoustic emissions. Stimulus frequency otoacoustic emissions (SFOAEs) have been proposed as the preferred emission type in the study of efferent modulation due to the simplicity of their production leading to the possibility of clearer interpretation of results. The effects of efferent activation on the complex spectral patterns of SFOAEs have not been examined to the best of our knowledge. We have examined the effects of activating the MOC efferents using broadband noise in normal-hearing humans. The detailed spectral structure of SFOAEs, known as fine structure, was recorded with and without contralateral acoustic stimulation. Results indicate that SFOAEs are reduced in magnitude and their fine structure pushed to higher frequencies by contralateral acoustic stimulation. These changes are similar to those observed in distortion product or spontaneous otoacoustic emissions and behavioral hearing thresholds. Taken together with observations made about magnitude and phase changes in otoacoustic emissions and hearing thresholds upon contralateral acoustic stimulation, all changes in otoacoustic emission and hearing threshold fine structure appear to be driven by a common set of mechanisms. Specifically, frequency shifts in fine structure patterns appear to be linked to changes in SFOAE phase due to contralateral acoustic stimulation.

Keywords: otoacoustic emissions, stimulus frequency otoacoustic emissions, fine structure, auditory efferents, medial olivocochlear bundle

OPEN ACCESS

Edited by:
Paul Hinckley Delano, Universidad de Chile, Chile

Reviewed by:
Maria Eugenia Gomez-Casati, INGEBI-CONICET Buenos Aires, Argentina
Jeffery Lichtenhan, Washington University in St. Louis, USA

****Correspondence:***
Sumitrajit Dhar
s-dhar@northwestern.edu

Received: *31 August 2015*
Accepted: *19 November 2015*
Published: *10 December 2015*

Citation:
Zhao W, Dewey JB, Boothalingam S and Dhar S (2015) Efferent Modulation of Stimulus Frequency Otoacoustic Emission Fine Structure. Front. Syst. Neurosci. 9:168. doi: 10.3389/fnsys.2015.00168

INTRODUCTION

Stimulus frequency otoacoustic emissions (SFOAEs) are low-level signals evoked by tonal probes, generated in the cochlea and recorded in the ear canal (Kemp and Chum, 1980). At moderate to high probe levels, SFOAEs arise from both linear coherent reflection and non-linear distortion mechanisms, characterized by long and short group delays, respectively (Shera and Guinan, 1999;

Talmadge et al., 2000; Goodman et al., 2003). At low probe levels, linear coherent reflection is thought to dominate SFOAE generation (Zweig and Shera, 1995) with non-linear mechanisms theorized to be contributing at moderate and high probe levels (Talmadge et al., 2000). A quasi-periodic pattern, demonstrated in SFOAE level spectra, expected in phase and delay as well, is referred to as fine structure (Talmadge et al., 2000) or microstructure (Goodman et al., 2003). Multiple internal reflections in the cochlea, variation in effective reflectance along the cochlear partition, and the interaction between linear coherent reflection and non-linear distortion mechanisms have been implicated in generating and influencing SFOAE fine structure (Zweig and Shera, 1995; Talmadge et al., 2000). In guinea pigs, variation in effective reflectance along the cochlear partition accounts for the origin of SFOAE fine structure with moderate probe levels, whereas interference between SFOAE components of long and short phase-gradient delays account for SFOAE fine structure at higher probe levels (Goodman et al., 2003). Multiple internal reflections generate the fine structure in both the amplitude and phase of the basilar membrane transfer function in sensitive chinchilla cochlea (Shera and Cooper, 2013). In humans, knowledge of the origin of SFOAE fine structure as well as its probe level-dependency has potential clinical implications and can lead to the selection of optimal test conditions for the assessment of the cochlea as well as the auditory efferents.

Activation of the medial olivocochlear (MOC) efferents reduces the gain of the cochlear amplifier thereby decreasing the input to the auditory nerve (Galambos, 1956; Fex, 1962; Murugasu and Russell, 1996; Cooper and Guinan, 2003). MOC efferents have traditionally been associated with many possible functional roles, such as protection against acoustic trauma, facilitation of speech perception in noise, and auditory attention (for review, see Guinan, 2006). More recently, MOC efferents have been demonstrated to delay age-related changes in the cochlea (Liberman et al., 2014), play a role in perceptual learning (de Boer and Thornton, 2008), and be associated with localization in the presence of background noise (Andeol et al., 2011; Irving et al., 2011). SFOAEs have been employed for assessing the strength of MOC efferents (Backus and Guinan, 2007). However, the efferent influence on SFOAE fine structure has not been explored. Activation of the MOC pathway by contralateral noise not only alters the levels of OAEs, but also shifts distortion product otoacoustic emission (DPOAE) fine structure (e.g., Deeter et al., 2009), spontaneous otoacoustic emissions (SOAEs; e.g., Zhao and Dhar, 2010; Zhao and Dhar, 2011), and even hearing threshold fine structure (e.g., Dewey et al., 2014) toward higher frequencies. Since the fine structures of OAEs and hearing thresholds as well as the spacing between SOAEs are thought to originate from a set of common mechanisms involving mechanical resonance and multiple internal reflections in the cochlea, the MOC efferents should be expected to alter SFOAE fine structure in similar ways.

In this study, we recorded SFOAEs in humans at low to moderate probe levels (20 and 40 dB SPL) with and without activating the MOC efferents by a 60 dB SPL contralateral broadband noise. The origin of, and MOC influence on, SFOAE fine structure were explored.

MATERIALS AND METHODS

Subjects

Eleven subjects (9 female and 2 male) between 21 and 31 years of age with normal hearing thresholds in both ears (20 dB HL or better at octave frequencies between 250 and 8000 Hz) participated in the experiment. These eleven subjects were chosen from a pool of over 50 specifically because their middle ear acoustic reflex thresholds, measured using broadband noise in the contralateral ear using a clinical impedance audiometer, were higher than 90 dB SPL. SFOAEs were recorded in one ear per subject. All procedures were approved by the Northwestern University Institutional Review Board. A written, informed consent was obtained from each subject. Measurements were conducted in a sound-treated audiological test booth.

Signal Generation and Recording

Stimuli were generated by a Macintosh computer connected to a MOTU 828 MKII I/O device (sampling rate 44100 Hz, 24 bit), amplified, and presented via transducers (MB Quart 13.01 HX) coupled to an Etymotic Research ER-10B probe assembly using custom software. Signals from subjects' ear canals were passed from the ER-10B microphone to a preamplifier (20 dB gain), then digitized by the MOTU and stored on disk for analysis.

Measurement Procedure

Stimulus frequency otoacoustic emissions were obtained via the compression method (Kemp and Chum, 1980) using tones swept in frequency. A probe tone (20 and 40 dB SPL) and a compressor tone (60 dB SPL) were swept from 800 to 1800 Hz at a rate of 20 s/octave. MOC activity was elicited by a 60 dB SPL contralateral broadband noise (100–10000 Hz). A total of five conditions were interleaved: probe alone at 20 or 40 dB SPL, compressor alone at 60 dB SPL, probe at 20 or 40 dB SPL paired with contralateral noise. Six runs per condition were recorded and averaged. The total ear canal pressure at the probe frequency was estimated using a custom least-squares fit algorithm (Long and Talmadge, 1997).

Analysis

Stimulus frequency otoacoustic emissions were extracted by scaling the ear canal complex pressure in the compressor condition and subtracting it from that recorded in each of the other conditions. SFOAE without and with contralateral noise are denoted as baseline SFOAE and SFOAEmoc, respectively (**Figure 1**). The magnitude and phase of the vector pressure change between the two are denoted as ΔP and α. Throughout the paper, baseline SFOAE, SFOAEmoc and ΔP are color coded using blue, red and green traces, respectively.

Absence of middle-ear muscle (MEM) contraction was confirmed by a phase-gradient delay of ΔP around 10 ms near 1500 Hz (see **Figures 2A,B**) indicating that ΔP was dominated

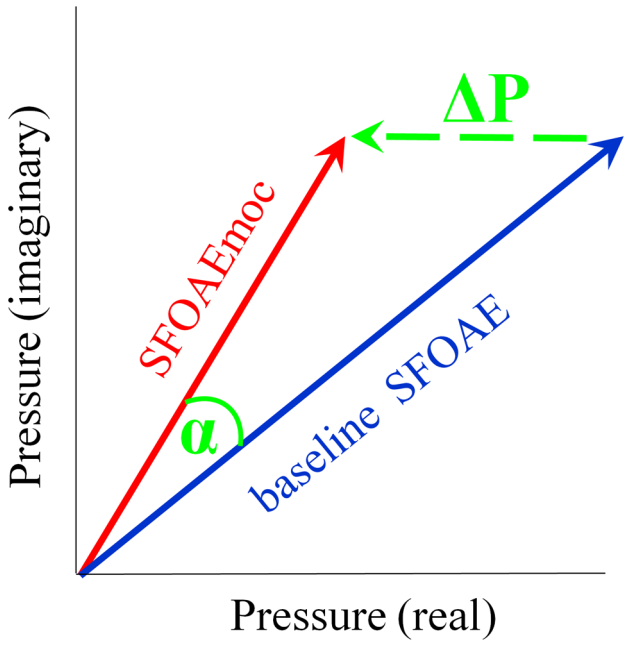

FIGURE 1 | Schematic of medial olivocochlear (MOC) modulation of stimulus frequency otoacoustic emissions (SFOAE). SFOAE without and with contralateral noise are denoted as baseline SFOAE (blue) and SFOAEmoc (red), respectively. MOC effects were assessed via both the vector pressure change ΔP (green) and phase change α.

by MOC-mediated changes in SFOAE pressure, and not MEM-induced changes in the stimulus pressure reflected at the eardrum (Guinan et al., 2003). This elegant method of differentiating between MOC- and MEM-mediated changes takes advantage of the expected phase-frequency relationship of SFOAEs versus middle ear reflectance. The phase gradient delay of the change vector is expected to be around 10 ms only when the change in ear canal pressure is actually due to a change in the SFOAE. In contrast, the phase gradient delay is expected to approximately 0 ms when the change in ear canal pressure is due to a change in middle ear reflectance caused by an MEM reflex.

The extracted complex ear canal SFOAE estimate was converted from the spectral to the temporal domain by performing an inverse Fast Fourier Transform (IFFT, 300-Hz Hann window, 20-Hz steps; Kalluri and Shera, 2001). The magnitude of the IFFT output was normalized to its own maximal value in order to assess the weight of SFOAE components with varying delays, which appear as a vertical bands of energy separated in time (see **Figure 3**). The output of the IFFT analysis was found to be sensitive to parameters such as the width of the analysis window and the degree of overlap between adjacent windows. These parameters significantly affected the number of vertical bands of energy observed and the gap in delay between them. We developed confidence in the results of the IFFT by subjecting synthetic data with known reflections and delays to the analysis. To be further conservative in our approach, we limited the included data to those within 20 dB of the peak in all cases. Even after adopting this cautious approach we recommend that the reader attach limited value to the specific number of vertical bands of energy and the delays between them in **Figures 3, 4,** and **6**.

Equivalence of SFOAE Extraction Methods

To assess our method of using probes swept in frequency, we compared SFOAEs extracted by using discrete-frequency vs. swept-frequency tones, and by the compression versus suppression methods in two subjects. For discrete tones, the following triplet was applied, each portion of the triplet lasting 2 s: a 20/40 dB SPL probe tone, followed by a 20/40 dB SPL probe tone plus a 60 dB SPL suppressor 47 Hz below the probe frequency, followed by a 60 dB SPL compressor tone. This triplet was applied for probe frequencies between 800 and 1800 Hz in 20-Hz steps and repeated six times for each probe frequency. SFOAE recording and extraction via the compression method using swept-frequency tones was identical to the process described above. Discrete- tones and swept-frequency tones were interleaved to minimize probe drift across time. SFOAEs extracted by the suppression method using discrete-frequency tones, by the compression method using discrete tones, and by the compression method using swept-frequency tones were indistinguishable (**Supplementary Figure S1**) as has been demonstrated before (Kalluri and Shera, 2007b, 2013). It should be noted that the equivalence between otoacoustic emissions recorded using swept- and discrete-frequency tones is heavily dependent on various signal characteristics and analysis variables. The rate of frequency sweep is one such important variable and our claim of the equivalence of results between swept- and discrete-frequency tones is made specifically and only for slow frequency sweeps (20 s/octave) used here. In contrast, AlMakadma et al. (2015) have recently demonstrated differences in DPOAEs recorded using fast (1 s/octave) sweeps in stimulus frequency depending on the direction of the frequency change.

RESULTS

Baseline SFOAE Fine Structure: Manifestations in the Spectral and Temporal Domains

Examples of baseline SFOAEs evoked by two probe levels (20 and 40 dB SPL) between 800 and 1800 Hz from two subjects are presented as a function of probe frequency in **Figure 2** for subjects WTPF13 and WTPF76. Thin and thick lines represent SFOAEs evoked by 20 and 40 dB SPL probes, respectively. For both probe levels, the SFOAE phase slope was approximately parallel with the reference line of a 10 ms delay (**Figures 2A,B**), indicating the dominance of a generation mechanism consistent with the properties of coherent reflection (Shera and Guinan, 1999). SFOAE phase slopes from all eleven individual subjects included in this study are shown in **Supplementary Figure S2**. Each of these exhibit a phase slope of approximately 10 ms with occasional discontinuities at unpredictable frequencies. On

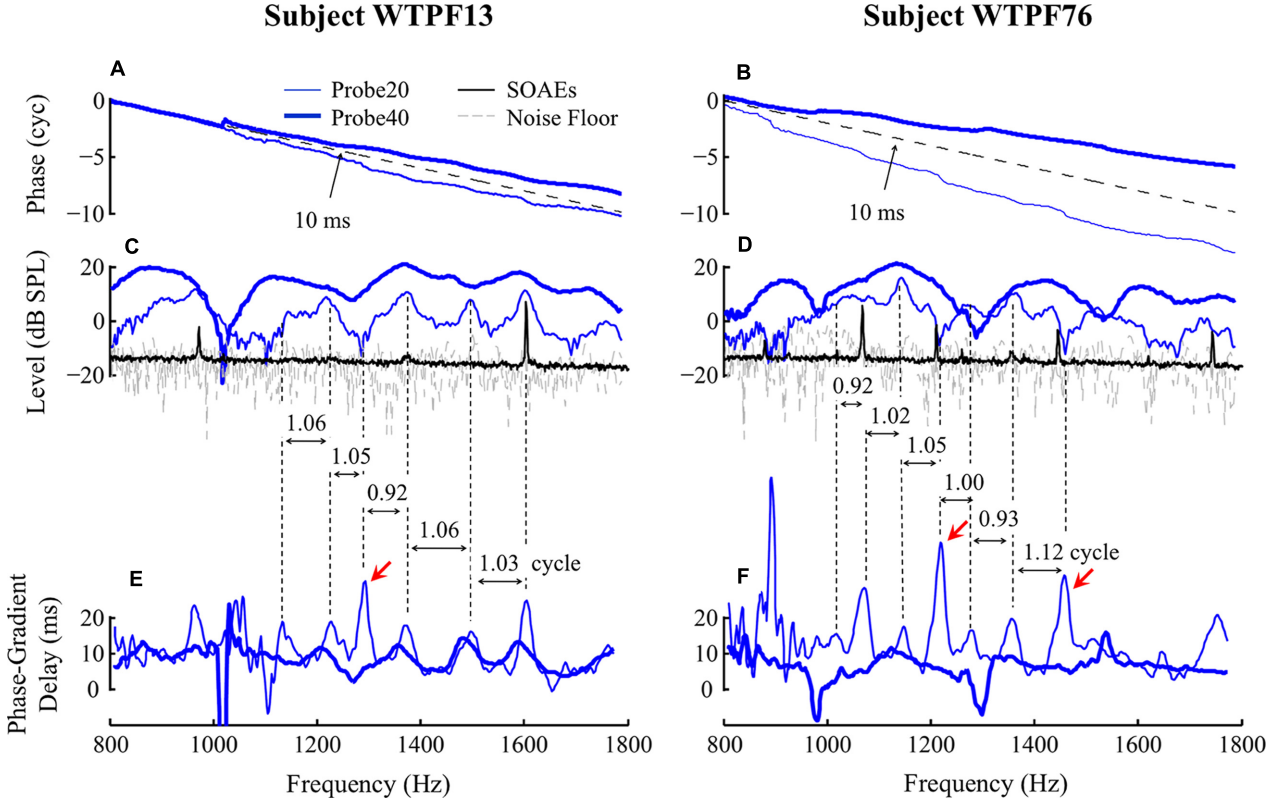

FIGURE 2 | Baseline SFOAE as a function of probe frequency for subjects WTPF13 and WTPF76 (columns). Data obtained using 20 and 40 dB SPL probes are represented using thin and thick traces, respectively. SFOAE phase slopes are parallel with the phase slope of 10-ms delay (dashed reference line in **A,B**). Fine structure patterns of SFOAE level **(C,D)** and phase-gradient delay **(E,F)** are presented along with SOAE in panels **(C)** and **(D)** using the black traces. Vertical dashed lines are used to mark the alignment between fine structure patterns of level and delay. Red arrows indicate (the less common) alignment between SFOAE level valleys and phase-gradient delay peaks.

informal inspection, SFOAE phase slopes for the 20 dB SPL probe seem steeper than those with the 40 dB SPL probe.

Stimulus frequency otoacoustic emissions levels presented in **Figures 2C,D** appear to display a quasi-periodic fine structure. Not only does the 40 dB SPL probe yield higher level SFOAEs, the two probes also yield SFOAE fine structure with different morphologies, in location of peaks, spacing between them, as well as peak-to-valley depth. For subject WTPF13, SFOAEs evoked by the 20 dB SPL probe demonstrate good alignment between local peaks in SFOAE level and SOAEs (black trace in **Figure 2C**). Phase accumulation between adjacent SFOAE level peaks is around one cycle (**Figure 2C**). Similar phase accumulation between adjacent SFOAE level peaks can also be observed for subject WTPF76 (**Figure 2D**). However, the alignment between SOAEs and SFOAE level peaks is less evident for this subject (**Figure 2D**). The relationship between the location of SFOAE level peaks, SOAEs, and the phase accumulation between them is not as clear for SFOAEs evoked by the 40 dB SPL probe.

Stimulus frequency otoacoustic emissions phase-gradient delay, computed as the negative of the phase slope, is presented as a function of probe frequency in **Figures 2E,F** for probe levels of 20 and 40 dB SPL using thin and thick traces, respectively. The SFOAE delay versus frequency function also demonstrates periodicity that resembles the SFOAE level-frequency fine structure. SFOAEs evoked using the 20 dB SPL probe are associated with more prominent fine structure in both level and delay than those with the 40 dB SPL probe. For the 20 dB SPL probe, local peaks of the SFOAE delay-frequency function were most commonly aligned with local peaks of the SFOAE level-frequency function. However, delay peaks were occasionally also found to be aligned with level valleys (marked by red arrows in **Figures 2E,F**). Phase accumulation between adjacent peaks of the SFOAE delay-frequency function was approximately one cycle as demonstrated by the vertical dashed lines.

The temporal-domain representation of SFOAE pressure yielded by inverse Fourier analysis is represented in **Figure 3** for eight subjects, for 20 and 40 dB SPL probes. $F\{\text{Pressure}\}$ is presented in dB and color-coded. Each vertical color band corresponds to an SFOAE component with a distinct delay. Each raw heat plot resulting from the Fourier transform is normalized to its own maximal value for better assessment of the relative strength of SFOAE components of different delays. Only data within 20 dB of the peak were included. This resulted in the rejection of some artifacts of the Fourier analysis, which manifested as ripples in the temporal domain.

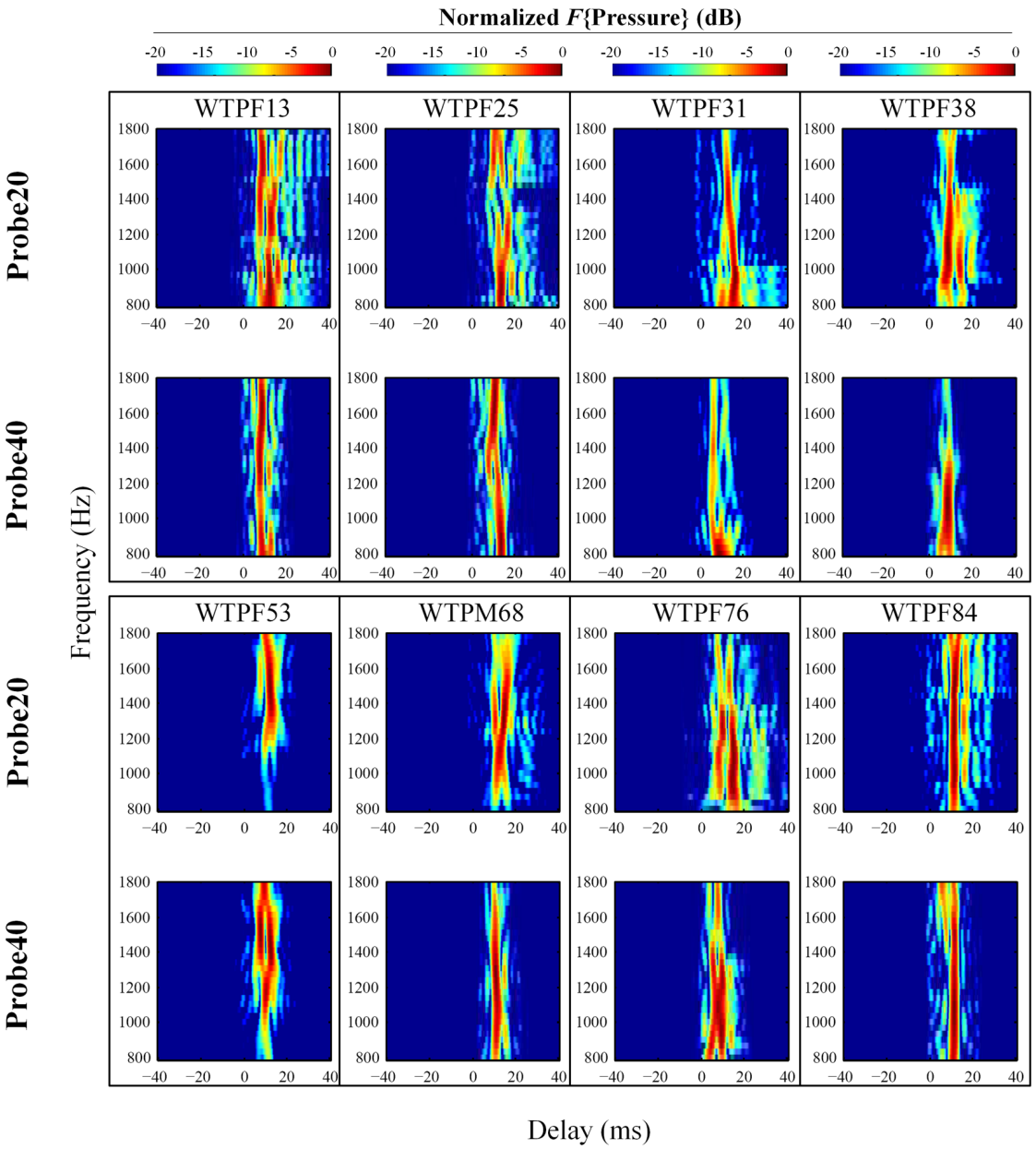

FIGURE 3 | Normalized results of inverse Fast Fourier Transform (IFFT) analysis on baseline SFOAE in eight subjects for 20 and 40 dB SPL probes. In order to evaluate the weighting of components with different phase-gradient delays, each heat plot was normalized to its own maximal value. Only signals within 20 dB of the peak were retained. SFOAE components with different phase-gradient delays appear as vertical color bands on the SFOAE frequency versus phase-gradient delay heat plots.

Stimulus frequency otoacoustic emissions recorded using a 20 dB SPL probe receive greater contribution from SFOAE components with longer delays (sometimes up to 40 ms), whereas components of SFOAEs recorded using a 40 dB SPL probe cluster around 10 ms (**Figure 3**). Multiple, evenly spaced, bands can be observed for SFOAEs recorded using the 20 dB SPL probe. In some subjects, components with delays around 5 ms are demonstrated only in SFOAEs evoked by the 40 dB SPL probe (**Figure 4**).

Efferent Influence on SFOAE Fine Structure

Efferent influence on SFOAE responses for both 20 and 40 dB SPL probes from subject WTPF13 is presented in **Figure 5**. Baseline SFOAE, SFOAEmoc, and ΔP are presented in blue, red, and green traces, respectively. MOC activity was elicited by a 60 dB SPL contralateral broadband noise. Absence of MEM contraction was confirmed by a phase-gradient delay of ΔP near 10 ms (**Figures 5C–F**). MOC activation suppresses SFOAE

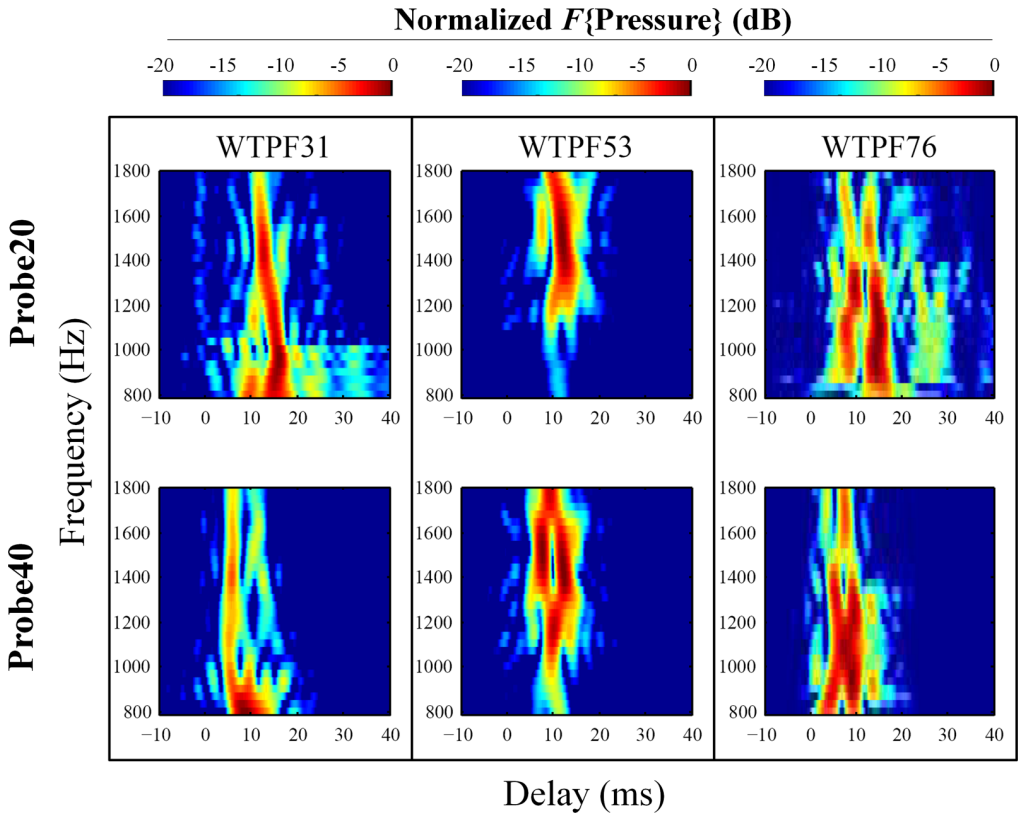

FIGURE 4 | Expanded heat plots of data from subjects WTPF31, WTPF53, and WTPF76 from Figure 3. SFOAE components with delays less than 10 ms are almost exclusive to the 40 dB SPL probe (bottom row).

levels and shifts SFOAE fine structure laterally toward higher frequencies (**Figures 5A,B**). The phase slope of baseline SFOAE, SFOAEmoc and ΔP are parallel with the dashed reference lines representing a delay of 10-ms (**Figures 5C,D**). The phase-gradient delay versus frequency function is also shifted toward higher frequencies by MOC activation (**Figures 5E,F**). Finally, the SFOAE phase change α also exhibits periodicity as a function of probe frequency (**Figures 5G,H**), much like the periodicity in the SFOAE level-frequency function (**Figures 5A,B**) and the delay-frequency function (**Figures 5E,F**). The phase change (α) is almost always a phase advance, reaching up to 90 degrees (**Figures 5G,H**).

Examples of the results of IFFT analysis on baseline SFOAE, ΔP and SFOAEmoc are presented in **Figure 6** (subject WTPF13). Comparing the first and last columns of **Figure 6** reveals the greatest differences between SFOAEmoc (right column) and baseline SFOAE (left column) for components with long delays. This trend is more prominent for the 20 dB SPL probe level. As a result, ΔP (middle column) is dominated by long-latency components (>10 ms) perhaps indicating a greater dependence of later reflections on cochlear gain and consequently greater inhibition upon MOC activation.

Group results averaged across eleven subjects are displayed in **Figure 7**. Individual differences in the delays of discrete bands have a smearing effect on the average data, such that the dominant component near 10 ms in the average is wider than those from individual subjects (e.g., **Figure 6**), and no discrete bands are discernable above 20 ms. The contribution from components with delays greater than 10 ms is reduced for SFOAEs evoked by the 40 dB SPL probe as compared to those recorded using the 20 dB SPL probe. Interestingly ΔP exhibits a prominent band of energy near 0 ms in ΔP for the 40 dB SPL probe only (**Figure 7E**).

DISCUSSION

The goals of this study were to examine the modulation of SFOAE fine structure by the MOC efferent system. The general effect of MOC stimulation on SFOAEs has been studied extensively (e.g., Lilaonitkul and Guinan, 2009). SFOAEs and TEOAEs, both considered reflection emissions, have been preferred over DPOAEs in acknowledgment of the inherent complexity of DPOAE generation (multiple sites and multiple mechanisms; Guinan et al., 2003). SFOAEs are also available for study in a greater number of normal-hearing humans as compared to SOAEs. However, despite previous investigations into SFOAE fine structure, the components contributing to this fine structure, as well as their alteration by the MOC efferents have not been fully explored. Our results indicate

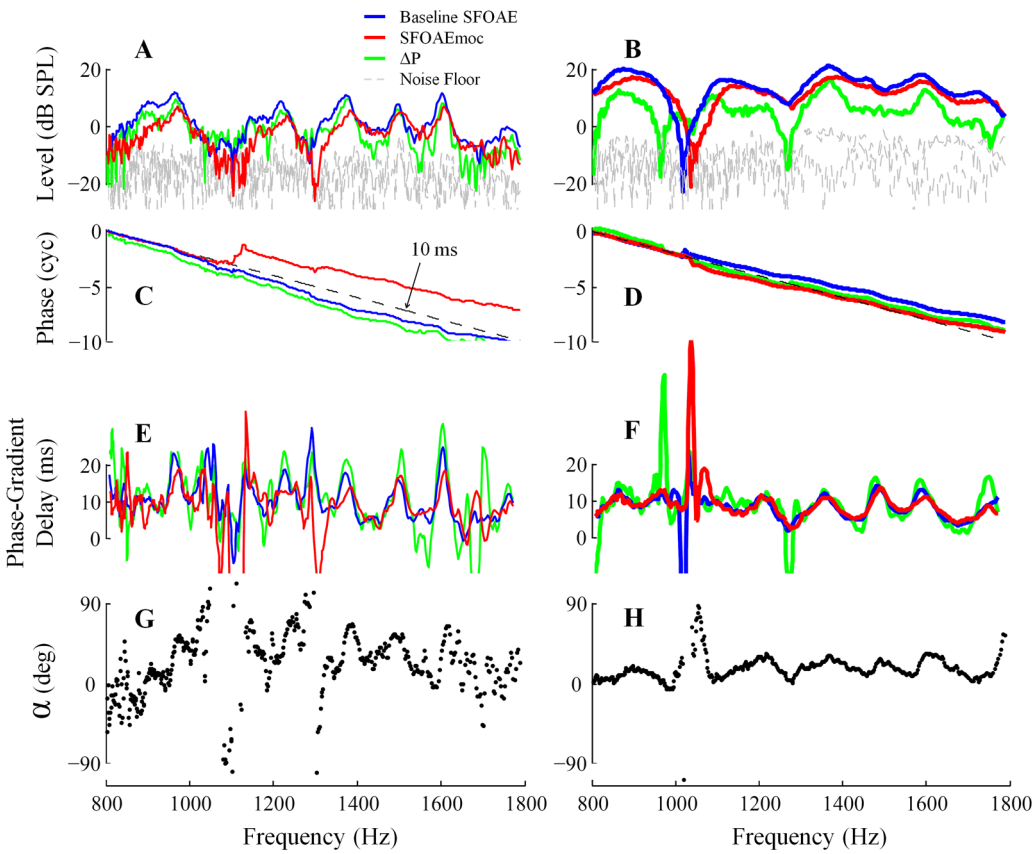

FIGURE 5 | Medial olivocochlearmodulation of SFOAE as a function of probe frequency for subject WTPF13. Level, phase, delay, and phase change (α) are presented in separate rows with data from 20 and 40 dB SPL probes in the two columns. Representations of the baseline SFOAE, SFOAEmoc, and ΔP are made using different colors.

that lower probe levels evoke contributions from SFOAE components with greater phase-gradient delays and these long-latency components are affected by efferent stimulation, more so than the shorter latency components. We also observed a shift of SFOAE fine structure toward higher frequencies, much like the observation in DPOAE fine structure (Abdala et al., 2009; Deeter et al., 2009), SOAEs (e.g., Zhao and Dhar, 2010), and behavioral threshold fine structure (Dewey et al., 2014).

SFOAE Components

Processing the complex SFOAE pressure through an IFFT algorithm revealed roughly three groups of components segregated by differing delays (**Figures 3** and **4**). For both probe levels of 20 and 40 dB SPL, a prominent band of SFOAE energy was observed around 10 ms, consistent with previous observations (Kalluri and Shera, 2007a). Bands of SFOAE pressure at delays greater than 10 ms, often spaced regularly in time, were observed frequently for the 20 dB SPL probe condition (**Figure 3**). These can be interpreted as the outcome of multiple intracochlear reflections. Such reflections are predicted in various models of OAEs (Shera and Zweig, 1991; Dhar et al., 2002) and have been observed for DPOAEs and SFOAEs previously (Dhar et al., 2002; Goodman et al., 2003). Consistent with theoretical expectations, the band of SFOAE pressure around 10 ms was greater in magnitude as compared with the bands with greater delays. The dominance of a band of energy with a delay of approximately 10 ms in a frequency band around 1.5 kHz supports the notion of SFOAEs being generated near the peak of the traveling wave of the probe tone. This limited spatial distribution of SFOAE generators is consistent with model predictions (e.g., Shera and Guinan, 1999) as well as experimental results (Lichtenhan, 2012).

More prominent SFOAE components with delays shorter than 10 ms were observed for the 40 dB SPL probe condition. Often this early band of SFOAE energy was observed with a delay in the vicinity of 5 ms. This component with a shorter delay is consistent with the existence of sources of SFOAE basal to the peak of the traveling wave created by the probe (Mertes and Goodman, 2013; Charaziak and Siegel, 2015), the possibility of a fast mode of transport (as compared to a traditional mechanical traveling wave) of the SFOAE signal

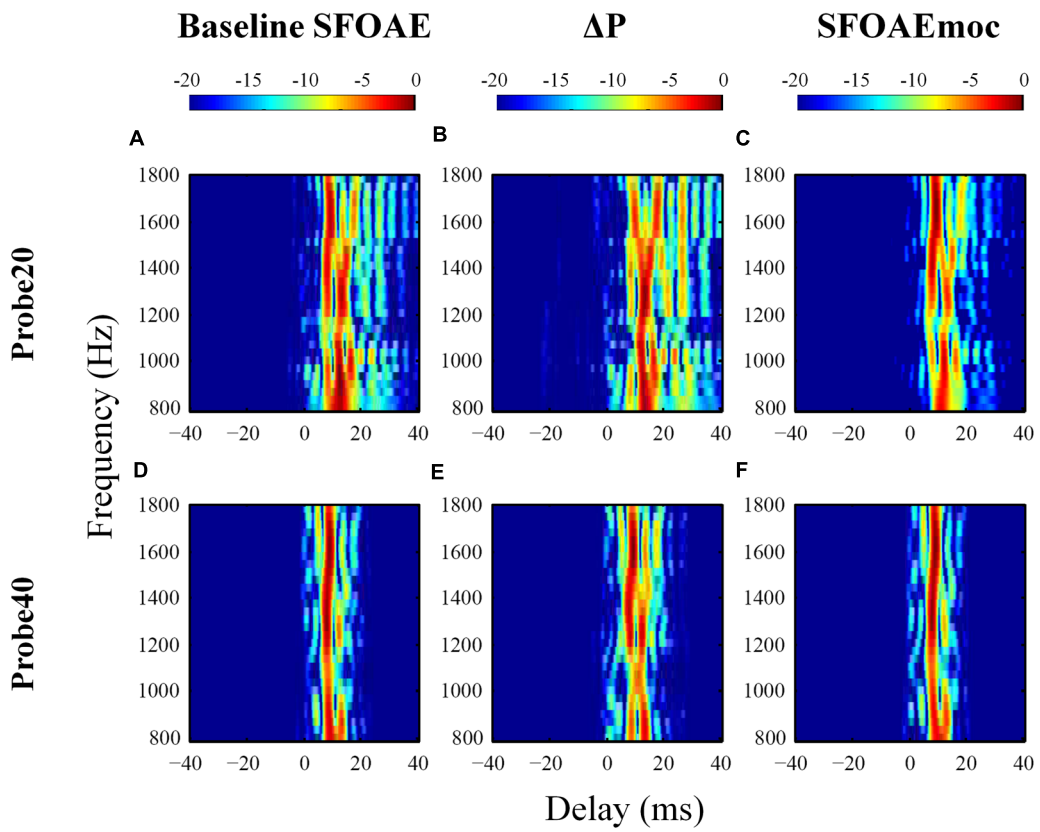

FIGURE 6 | Normalized results from IFFT analysis on baseline SFOAE (left column), ΔP (middle column) and SFOAEmoc (right column) from subject WTPF13. Compared with baseline SFOAE, ΔP appears to receive greater contribution from components of delays above 10 ms.

back to the ear canal (Siegel et al., 2005), as well as a non-linear generation mechanism (Talmadge et al., 2000). That the early latency component was most observable for the 40 dB SPL probe might suggest a greater contribution from a non-linear SFOAE generation mechanism, increased involvement of basal sources, or a combination of both at moderate probe levels.

SFOAE Fine Structure

Fine structure was observed in both SFOAE level and group delay for both probe levels. The morphology of fine structure was different between the two probe conditions with narrower and perhaps better defined peaks and valleys observed more frequently for the 20 dB SPL probe condition (**Figure 2**). For this low probe level, the peaks in SFOAE group delay were separated by approximately one cycle of phase accumulation. These peaks in group delay were found to be aligned almost exclusively with peaks in SFOAE level and SOAEs. This observation would be consistent with the expectations from a model of global resonance leading to both SFOAE fine structure (at low probe levels) and SOAEs (Kemp, 1980; Shera, 2003). However, we occasionally observed peaks in SFOAE group delay for the 20 dB SPL probe condition to be aligned with valleys in SFOAE level (marked by red arrows in **Figure 2**). The origin of this association is unclear at this time.

For the 40 dB SPL probe condition, SFOAE fine structure appears to be more broadly spaced. The lack of multiple intracochlear reflections for this probe level along with a shorter delay for the main component suggests that the source of fine structure may be different for this probe condition as compared to that for a 20 dB SPL probe. In this case, SFOAE fine structure could arise from variation in the effective reflectance along the cochlear partition (Goodman et al., 2003) or due to interference between a linear reflection component and a non-linear distortion component (Talmadge et al., 2000; Goodman et al., 2003). Regardless, differences in SFOAE fine structure morphology with probe level may indicate level-dependent variations in the dominant SFOAE generation mechanisms and the relative contributions of multiple internal reflections.

Efferent Modulation of SFOAE

Contralateral noise-induced MOC activity reduces SFOAE level (**Figures 5A,B**) and advances SFOAE phase (**Figures 5G,H**). The reduction in SFOAE level is consistent with a decrease in cochlear

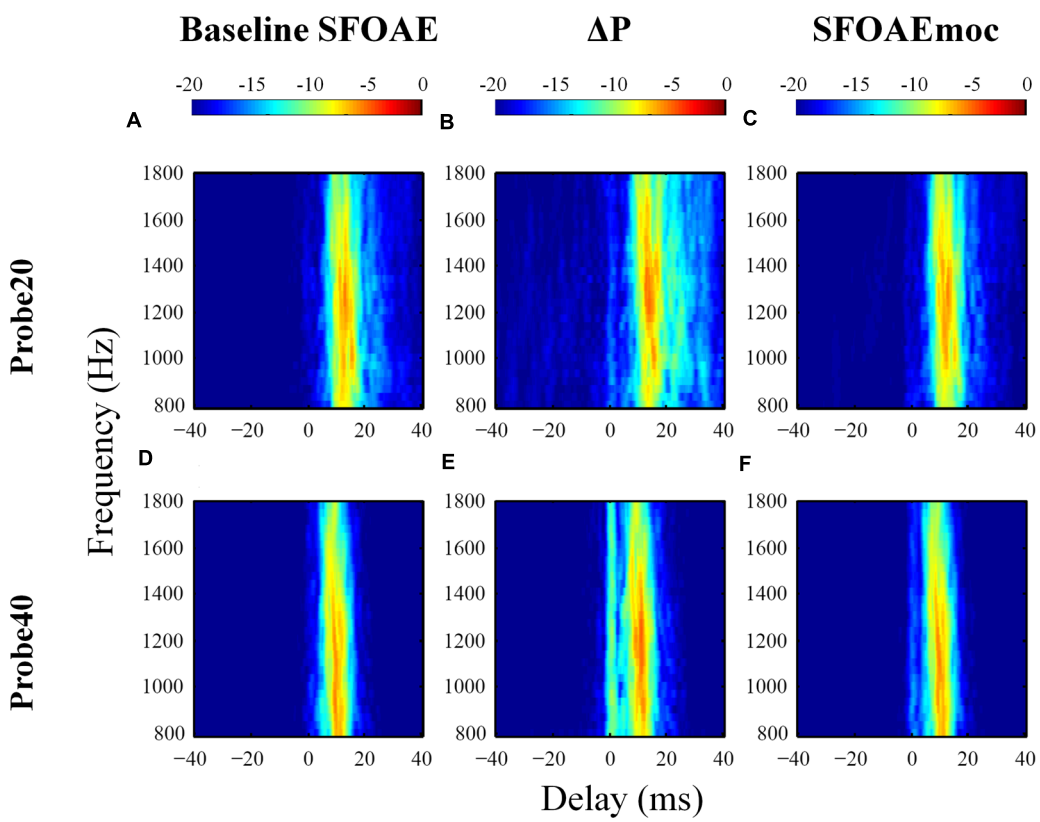

FIGURE 7 | Normalized IFFT results averaged across eleven subjects in a format similar to Figure 6. Distinctive long-latency bands in individuals (**Figure 6**) are smeared after averaging across subjects. ΔP receives greater contribution from long-latency components than baseline SFOAE. A 0-ms band is observed in ΔP only for the 40 dB SPL probe.

amplifier gain due to MOC activation. Long-latency components (>10 ms) that arguably correspond to multiple intracochlear reflections appear to be attenuated more than earlier components relative to the baseline by MOC activation (**Figures 6** and **7**). MOC activity reduces the SFOAE generating reflectance and the influence of this reduction is visible more in each successive reflection due to their roughly exponential dependence on the reflectance.

Medial olivocochlear-induced advance in SFOAE phase, denoted by α here, has previously been reported with coarse frequency resolution (Figure 5 in Francis and Guinan, 2010), and is consistent with the advance in basilar membrane vibration phase upon MOC activation (Murugasu and Russell, 1996). The quasi-periodic pattern observed when α is plotted as a function of frequency mimics that of the phase-gradient delay versus frequency function of the baseline SFOAE (**Figure 5**).

Medial olivocochlear activity shifts SFOAE fine structure toward higher frequencies (**Figures 5A,B**). Similar shifts have been observed in DPOAE fine structure (Abdala et al., 2009; Deeter et al., 2009) and SOAE frequency (Mott et al., 1989; Harrison and Burns, 1993; Zhao and Dhar, 2010). The models that account for DPOAE and SOAE shifts are based on a change in stiffness of the basilar membrane leading to a phase advance (Mott et al., 1989). Our results suggest a similar shift in SFOAE phase resulting in a shift in SFOAE fine structure toward higher frequencies. It can further be concluded that the shift in SFOAE phase is at the root of the shift toward higher frequencies of all evoked OAE fine structure, SOAEs, and even behavioral hearing threshold fine structure.

Plotting the two-dimensional SFOAE pressure vector as a function of probe frequency yields a spiral in a three-dimensional space (**Figure 8A**). The blue and red spirals are baseline SFOAE and SFOAEmoc, respectively. MOC modulation of SFOAE fine structure can be dissected in two perpendicular directions: shrinkage along the radial axis and shift along the axial axis. These changes are better visualized by projecting the two spirals to the real pressure-frequency plane and the imaginary pressure-frequency plane (**Figures 8B,C**). It is appealing to relate the shrinkage along the radial axis to the reduction in the cochlear amplifier gain, and the shift along the axial axis to the stiffness change of the basilar membrane that alters the cochlear characteristic frequency map.

A vertical band near 0 ms was found in the IFFT analysis of ΔP in some of the subjects (as in **Figure 6**) and in

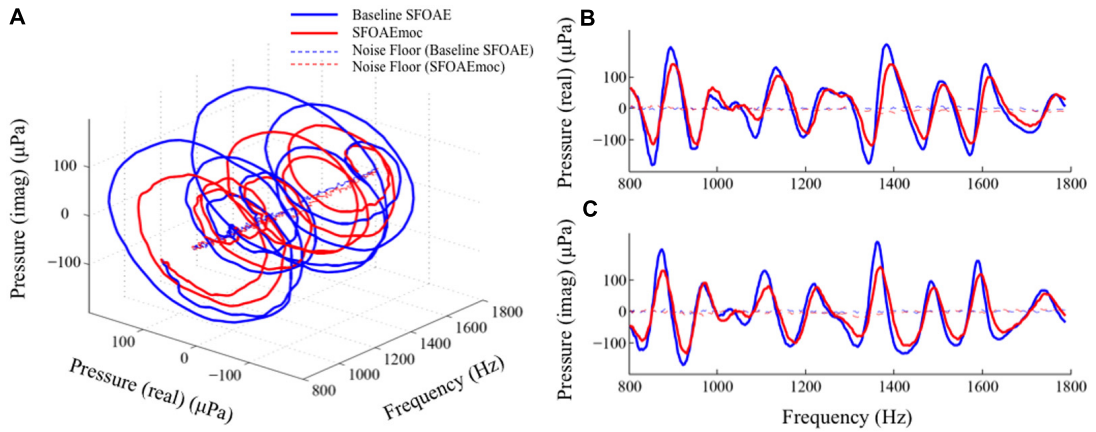

FIGURE 8 | Alternative views of MOC-induced SFOAE fine structure shift. The complex SFOAE pressure is transformed into a spiral in three-dimensional space **(A)**. MOC modulation on this spiral can be dissected in two perpendicular directions: a radial shrinkage and an axial advance. Projecting this spiral to the pressure (real) – frequency plane **(B)** and the pressure (imaginary) – frequency plane **(C)** provides better views of MOC effects along the two perpendicular directions.

the averaged data (**Figure 7**). It would be convenient to associate this 0 ms component with activation of the MEM reflex. However, the phase gradient of ΔP did not indicate domination by the MEM reflex. Thus, even if the MEM reflex was activated in some subjects with the 40 dB SPL probe, it did not dominate the overall changes in SFOAE pressure. Alternately, it is also possible that MOC activation generated a non-linear distortion component, not documented before.

Clinical Considerations

Disruption of, or changes in, the efferent modulation of otoacoustic emissions is of clinical interest. For example, efferent modulation of otoacoustic emissions is different in adults and children with learning disabilities (e.g., Garinis et al., 2008). The strength of efferent modulation is associated with the ability to locate a signal in space in the presence of background noise (Andeol et al., 2011; Irving et al., 2011; Liberman et al., 2014). Clinicians are expressing increasing interest in measuring efferent modulation of otoacoustic emissions for these reasons.

In typical clinical applications, TEOAEs or DPOAEs are measured with and without broadband noise in the contralateral ear and the difference in magnitude caused by the background noise is taken as a measure of the strength of efferent modulation of otoacoustic emissions. Shifts in DPOAE fine structure due to efferent stimulation causes significant complications in the interpretation of clinical data. Because the entire fine structure pattern is not evident in clinical measures at isolated frequencies, a shift in fine structure can manifest as an enhancement of DPOAE level due to efferent stimulation. If SFOAEs were used for clinical measures of efferent function, the same complications due to fine structure shift would be expected to complicate interpretation. In the absence of full characterization of fine structure, multiple measures at strategic frequencies near the frequency of interest could help avoid confusion, as at least one measure would then be expected to fall near the peak of fine structure yielding a stable estimate of efferent strength (see Deeter et al., 2009 for details). While we have focused on frequency shifts in fine structure as the source of the occasional enhancement in otoacoustic emission levels observed in the literature, another possible cause leading to the same effect in at least quadratic DPOAE levels (e.g., f_2–f_1) could be a change in the operating point of outer hair cells (Abel et al., 2009).

Closing Summary

To the best of our knowledge, these results are the first demonstration of an MOC-induced shift of SFOAE fine structure. This observation not only accounts for occasionally observed SFOAE enhancement by contralateral noise, but also bears clinical relevance as to the selection of SFOAE probe frequency (peak vs. valley) for examining the strength of MOC efferents. Finally, we argue that the shifts in all OAE and behavioral fine structures are driven by a common source – efferent-induced changes in SFOAE phase.

FUNDING

This research was funded by grant number DC008420 from the National Institute on Deafness and Other Communication Disorders, and by Northwestern University.

ACKNOWLEDGMENTS

The authors would like to thank Jonathan Siegel, Christopher Shera, Rachael Baiduc, Gayla Poling, Abby Rogers, and Sumaya Sidique for helpful discussions, and Carrick Talmadge and Ping Luo for the use of their data processing tools. Parts of this work were presented at the 2011 annual convention of the Association for Research in Otolaryngology.

SUPPLEMENTARY MATERIAL

The Supplementary Material for this article can be found online at: http://journal.frontiersin.org/article/10.3389/fnsys.2015.00168

FIGURE S1 | Comparison of stimulus frequency otoacoustic emissions (SFOAEs) obtained through the suppression and the compression methods using discrete or swept-frequency tones (Subjects WTPM18 and WTPF76). SFOAE level yielded by the suppression method using discrete tones, the compression method using discrete tones, and the compression method using swept-frequency tones are represented by red, blue, and green colors, respectively.

FIGURE S2 | Stimulus frequency otoacoustic emissions phase slopes are distinctive across subjects ($N = 11$). For both probe levels, phase slopes are approximately parallel with the 10-ms phase slope (dashed line).

REFERENCES

Abdala, C., Mishra, S. K., and Williams, T. L. (2009). Considering distortion product otoacoustic emission fine structure in measurements of the medial olivocochlear reflex. *J. Acoust. Soc. Am.* 125, 1584–1594. doi: 10.1121/1.3068442

Abel, C., Wittekindt, A., and Kossl, M. (2009). Contralateral acoustic stimulation modulates low-frequency biasing of DPOAE: efferent influence on cochlear amplifier operating state? *J. Neurophysiol.* 101, 2362–2371. doi: 10.1152/jn.00026.2009

AlMakadma, H. A., Henin, S., Prieve, B. A., Dyab, W. M., and Long, G. R. (2015). Frequency-change in DPOAE evoked by 1 s/octave sweeping primaries in newborns and adults. *Hear. Res.* 328, 157–165. doi: 10.1016/j.heares.2015.08.012

Andeol, G., Guillaume, A., Micheyl, C., Savel, S., Pellieux, L., and Moulin, A. (2011). Auditory efferents facilitate sound localization in noise in humans. *J. Neurosci.* 31, 6759–6763. doi: 10.1523/JNEUROSCI.0248-11.2011

Backus, B. C., and Guinan, J. J. Jr. (2007). Measurement of the distribution of medial olivocochlear acoustic reflex strengths across normal-hearing individuals via otoacoustic emissions. *J. Assoc. Res. Otolaryngol.* 8, 484–496. doi: 10.1007/s10162-007-0100-0

Charaziak, K. K., and Siegel, J. H. (2015). Tuning of SFOAEs evoked by low-frequency tones is not compatible with localized emission generation. *J. Assoc. Res. Otolaryngol.* 16, 317–329. doi: 10.1007/s10162-015-0513-0

Cooper, N. P., and Guinan, J. J. Jr. (2003). Separate mechanical processes underlie fast and slow effects of medial olivocochlear efferent activity. *J. Physiol.* 548(Pt 1), 307–312. doi: 10.1113/jphysiol.2003.039081

de Boer, J., and Thornton, A. R. (2008). Neural correlates of perceptual learning in the auditory brainstem: efferent activity predicts and reflects improvement at a speech-in-noise discrimination task. *J. Neurosci.* 28, 4929–4937. doi: 10.1523/JNEUROSCI.0902-08.2008

Deeter, R., Abel, R., Calandruccio, L., and Dhar, S. (2009). Contralateral acoustic stimulation alters the magnitude and phase of distortion product otoacoustic emissions. *J. Acoust. Soc. Am.* 126, 2413–2424. doi: 10.1121/1.3224716

Dewey, J. B., Lee, J., and Dhar, S. (2014). Effects of contralateral acoustic stimulation on spontaneous otoacoustic emissions and hearing threshold fine structure. *J. Assoc. Res. Otolaryngol.* 15, 897–914. doi: 10.1007/s10162-014-0485-5

Dhar, S., Talmadge, C. L., Long, G. R., and Tubis, A. (2002). Multiple internal reflections in the cochlea and their effect on DPOAE fine structure. *J. Acoust. Soc. Am.* 112, 2882–2897. doi: 10.1121/1.1516757

Fex, J. (1962). Auditory activity in centrifugal and centripetal cochlear fibres in cat. A study of a feedback system. *Acta Physiol. Scand. Suppl.* 189, 1–68.

Francis, N. A., and Guinan, J. J. Jr. (2010). Acoustic stimulation of human medial olivocochlear efferents reduces stimulus-frequency and click-evoked otoacoustic emission delays: implications for cochlear filter bandwidths. *Hear. Res.* 267, 36–45. doi: 10.1016/j.heares.2010.04.009

Galambos, R. (1956). Suppression of auditory nerve activity by stimulation of efferent fibers to cochlea. *J. Neurophysiol.* 19, 424–437.

Garinis, A. C., Glattke, T., and Cone-Wesson, B. K. (2008). TEOAE suppression in adults with learning disabilities. *Int. J. Audiol.* 47, 607–614. doi: 10.1080/14992020802129402

Goodman, S. S., Withnell, R. H., and Shera, C. A. (2003). The origin of SFOAE microstructure in the guinea pig. *Hear. Res.* 183, 7–17. doi: 10.1016/S0378-5955(03)00193-X

Guinan, J. J. Jr (2006). Olivocochlear efferents: anatomy, physiology, function, and the measurement of efferent effects in humans. *Ear Hear.* 27, 589–607. doi: 10.1097/01.aud.0000240507.83072.e7

Guinan, J. J. Jr., Backus, B. C., Lilaonitkul, W., and Aharonson, V. (2003). Medial olivocochlear efferent reflex in humans: otoacoustic emission (OAE) measurement issues and the advantages of stimulus frequency OAEs. *J. Assoc. Res. Otolaryngol.* 4, 521–540. doi: 10.1007/s10162-002-3037-3

Harrison, W. A., and Burns, E. M. (1993). Effects of contralateral acoustic stimulation on spontaneous otoacoustic emissions. *J. Acoust. Soc. Am.* 94, 2649–2658. doi: 10.1121/1.407349

Irving, S., Moore, D. R., Liberman, M. C., and Sumner, C. J. (2011). Olivocochlear efferent control in sound localization and experience-dependent learning. *J. Neurosci.* 31, 2493–2501. doi: 10.1523/JNEUROSCI.2679-10.2011

Kalluri, R., and Shera, C. A. (2001). Distortion-product source unmixing: a test of the two-mechanism model for DPOAE generation. *J. Acoust. Soc. Am.* 109, 622–637. doi: 10.1121/1.1334597

Kalluri, R., and Shera, C. A. (2007a). Comparing stimulus-frequency otoacoustic emissions measured by compression, suppression, and spectral smoothing. *J. Acoust. Soc. Am.* 122, 3562–3575. doi: 10.1121/1.2793604

Kalluri, R., and Shera, C. A. (2007b). Near equivalence of human click-evoked and stimulus-frequency otoacoustic emissions. *J. Acoust. Soc. Am.* 121, 2097–2110. doi: 10.1121/1.2435981

Kalluri, R., and Shera, C. A. (2013). Measuring stimulus-frequency otoacoustic emissions using swept tones. *J. Acoust. Soc. Am.* 134, 356–368. doi: 10.1121/1.4807505

Kemp, D. T. (1980). Towards a model for the origin of cochlear echoes. *Hear. Res.* 2, 533–548. doi: 10.1016/0378-5955(80)90091-X

Kemp, D. T., and Chum, R. (1980). Properties of the generator of stimulated acoustic emissions. *Hear. Res.* 2, 213–232. doi: 10.1016/0378-5955(80)90059-3

Liberman, M. C., Liberman, L. D., and Maison, S. F. (2014). Efferent feedback slows cochlear aging. *J. Neurosci.* 34, 4599–4607. doi: 10.1523/JNEUROSCI.4923-13.2014

Lichtenhan, J. T. (2012). Effects of low-frequency biasing on otoacoustic and neural measures suggest that stimulus-frequency otoacoustic emissions originate near the peak region of the traveling wave. *J. Assoc. Res. Otolaryngol.* 13, 17–28. doi: 10.1007/s10162-011-0296-x

Lilaonitkul, W., and Guinan, J. J. Jr. (2009). Human medial olivocochlear reflex: effects as functions of contralateral, ipsilateral, and bilateral elicitor bandwidths. *J. Assoc. Res. Otolaryngol.* 10, 459–470. doi: 10.1007/s10162-009-0163-1

Long, G. R., and Talmadge, C. L. (1997). Spontaneous otoacoustic emission frequency is modulated by heartbeat. *J. Acoust. Soc. Am.* 102(Pt 1), 2831–2848. doi: 10.1121/1.420339

Mertes, I. B., and Goodman, S. S. (2013). Short-latency transient-evoked otoacoustic emissions as predictors of hearing status and thresholds. *J. Acoust. Soc. Am.* 134, 2127–2135. doi: 10.1121/1.4817831

Mott, J. B., Norton, S. J., Neely, S. T., and Warr, W. B. (1989). Changes in spontaneous otoacoustic emissions produced by acoustic stimulation of the contralateral ear. *Hear. Res.* 38, 229–242. doi: 10.1016/0378-5955(89)90068-3

Murugasu, E., and Russell, I. J. (1996). The effect of efferent stimulation on basilar membrane displacement in the basal turn of the guinea pig cochlea. *J. Neurosci.* 16, 325–332.

Shera, C. A. (2003). Mammalian spontaneous otoacoustic emissions are amplitude-stabilized cochlear standing waves. *J. Acoust. Soc. Am.* 114, 244–262. doi: 10.1121/1.1575750

Shera, C. A., and Cooper, N. P. (2013). Basilar-membrane interference patterns from multiple internal reflection of cochlear traveling waves. *J. Acoust. Soc. Am.* 133, 2224–2239. doi: 10.1121/1.4792129

Shera, C. A., and Guinan, J. J. Jr. (1999). Evoked otoacoustic emissions arise by two fundamentally different mechanisms: a taxonomy for mammalian OAEs. *J. Acoust. Soc. Am.* 105(2 Pt 1), 782–798. doi: 10.1121/1.426948

Shera, C. A., and Zweig, G. (1991). Reflection of retrograde waves within the cochlea and at the stapes. *J. Acoust. Soc. Am.* 89, 1290–1305. doi: 10.1121/1.400654

Siegel, J. H., Cerka, A. J., Recio-Spinoso, A., Temchin, A. N., van Dijk, P., and Ruggero, M. A. (2005). Delays of stimulus-frequency otoacoustic emissions and cochlear vibrations contradict the theory of coherent reflection filtering. *J. Acoust. Soc. Am.* 118, 2434–2443. doi: 10.1121/1.2005867

Talmadge, C. L., Tubis, A., Long, G. R., and Tong, C. (2000). Modeling the combined effects of basilar membrane nonlinearity and roughness on stimulus frequency otoacoustic emission fine structure. *J. Acoust. Soc. Am.* 108, 2911–2932. doi: 10.1121/1.1321012

Zhao, W., and Dhar, S. (2010). The effect of contralateral acoustic stimulation on spontaneous otoacoustic emissions. *J. Assoc. Res. Otolaryngol.* 11, 53–67. doi: 10.1007/s10162-009-0189-4

Zhao, W., and Dhar, S. (2011). Fast and slow effects of medial olivocochlear efferent activity in humans. *PLoS ONE* 6:e18725. doi: 10.1371/journal.pone.0018725

Zweig, G., and Shera, C. A. (1995). The origin of periodicity in the spectrum of evoked otoacoustic emissions. *J. Acoust. Soc. Am.* 98, 2018–2047. doi: 10.1121/1.413320

Conflict of Interest Statement: The authors declare that the research was conducted in the absence of any commercial or financial relationships that could be construed as a potential conflict of interest.

frontiers in
SYSTEMS NEUROSCIENCE

ORIGINAL RESEARCH ARTICLE
published: 02 March 2015
doi: 10.3389/fnsys.2015.00021

Stronger efferent suppression of cochlear neural potentials by contralateral acoustic stimulation in awake than in anesthetized chinchilla

Cristian Aedo[1,2], Eduardo Tapia[1,2], Elizabeth Pavez[1,2], Diego Elgueda[2†], Paul H. Delano[2,3] and Luis Robles[2]*

[1] Departamento de Tecnología Médica, Facultad de Medicina, Universidad de Chile, Santiago, Chile
[2] Programa de Fisiología y Biofísica, ICBM, Facultad de Medicina, Universidad de Chile, Santiago, RM, Chile
[3] Departamento de Otorrinolaringología, Hospital Clínico, Universidad de Chile, Santiago, Chile

Edited by:
Ana Elgoyhen, Instituto de Investigaciones en Ingeniería Genética y Biología Molecular, Argentina

Reviewed by:
John J. Guinan, Massachusetts Eye and Ear Infirmary and Harvard Medical School, USA
Maria Eugenia Gomez-Casati, Instituto de Investigaciones en Ingeniería Genética y Biología Molecular, Argentina

***Correspondence:**
Luis Robles, Programa de Fisiología y Biofísica, ICBM, Facultad de Medicina, Universidad de Chile, Independencia 1027, Santiago, RM, 8380453, Chile
e-mail: lrobles@med.uchile.cl

†Present address:
Diego Elgueda, Institute for Systems Research and Neuroscience and Cognitive Science Program, University of Maryland, College Park, Maryland, USA

There are two types of sensory cells in the mammalian cochlea, inner hair cells, which make synaptic contact with auditory-nerve afferent fibers, and outer hair cells that are innervated by crossed and uncrossed medial olivocochlear (MOC) efferent fibers. Contralateral acoustic stimulation activates the uncrossed efferent MOC fibers reducing cochlear neural responses, thus modifying the input to the central auditory system. The chinchilla, among all studied mammals, displays the lowest percentage of uncrossed MOC fibers raising questions about the strength and frequency distribution of the contralateral-sound effect in this species. On the other hand, MOC effects on cochlear sensitivity have been mainly studied in anesthetized animals and since the MOC-neuron activity depends on the level of anesthesia, it is important to assess the influence of anesthesia in the strength of efferent effects. Seven adult chinchillas (*Chinchilla laniger*) were chronically implanted with round-window electrodes in both cochleae. We compared the effect of contralateral sound in awake and anesthetized condition. Compound action potentials (CAP) and cochlear microphonics (CM) were measured in the ipsilateral cochlea in response to tones in absence and presence of contralateral sound. Control measurements performed after middle-ear muscles section in one animal discarded any possible middle-ear reflex activation. Contralateral sound produced CAP amplitude reductions in all chinchillas, with suppression effects greater by about 1–3 dB in awake than in anesthetized animals. In contrast, CM amplitude increases of up to 1.9 dB were found in only three awake chinchillas. In both conditions the strongest efferent effects were produced by contralateral tones at frequencies equal or close to those of ipsilateral tones. Contralateral CAP suppressions for 1–6 kHz ipsilateral tones corresponded to a span of uncrossed MOC fiber innervation reaching at least the central third of the chinchilla cochlea.

Keywords: olivocochlear, auditory efferent, contralateral MOC reflex, CAP suppression, frequency tuning, anesthesia

INTRODUCTION

The cochlea of mammals has two types of sensory cells: outer (OHC) and inner (IHC) hair cells. The IHCs make synaptic contact with the afferent fibers of the auditory nerve while the OHCs are fundamentally innervated by auditory efferent axons. The auditory efferent system originates in the auditory cortex and projects mainly through two pathways. One is directed to the medial geniculate body of the thalamus, wherein it makes synapses with the afferent fibers and returns to the cortex (Winer and Prieto, 2001). The other pathway descends to the inferior colliculus and superior olivary complex finally projecting through medial olivocochlear (MOC) fibers to both cochleae (Vetter et al., 1993). The MOC fibers are myelinated axons that originate in the ventral nucleus of the trapezoid body and that segregate into crossed and uncrossed fibers that make synaptic contact with OHCs in the contra- and ipsilateral cochleae, respectively. The lateral olivocochlear (LOC) system is constituted by unmyelinated neurons that project mainly to the ipsilateral cochlea making synaptic contacts beneath IHCs (Warr and Guinan, 1979). Based on the available experimental evidence several possible roles have been assigned to the auditory efferent system, such as: reduction of the masking effect produced by noise or tones (Kawase et al., 1993), a protective role in preventing loss of sensitivity caused by exposure to high-intensity sounds (Rajan, 1995), modulation of responses to auditory stimuli within the sleep-wake cycle (Velluti, 1997), modulation of cochlear sensitivity according to attentional processes (Delano et al., 2007) and a balancing effect on interaural sensitivity (Darrow et al., 2006). (For review see Guinan, 2006; Robles and Delano, 2008).

It has been shown that stimulation of the MOC efferent system by means of electrical pulses delivered at the floor

of the fourth ventricle produces a decrease in the amplitude of auditory-nerve compound action potentials (CAP) and a concomitant increase in cochlear microphonic (CM) potentials (Galambos, 1956; Fex, 1959; Desmedt and Monaco, 1961; Gifford and Guinan, 1987; Elgueda et al., 2011). Auditory efferent fibers can also be activated by acoustic stimulation of the contralateral ear producing a decrease in single auditory-nerve fiber and CAP responses to ipsilateral tones (Buño, 1978; Liberman, 1989; Warren and Liberman, 1989a). This efferent suppression produced by contralateral sounds, known as the "contra MOC reflex" (de Venecia et al., 2005) is mediated by MOC uncrossed fibers. In all species studied so far uncrossed MOC fibers comprise a smaller percentage of the total than the crossed MOC fibers (Robles and Delano, 2008). However, there are significant differences in the distribution of MOC fibers among species. The finding that the chinchilla displays the lowest percentage of uncrossed fibers among all studied mammals has raised questions about the strength and frequency distribution of the contra MOC reflex in this species (Iurato et al., 1978; Azeredo et al., 1999). In fact, as reported in Azeredo et al. (1999), the relative paucity of MOC uncrossed fibers and their strong apical bias may have been contributing factors in the early unsuccessful attempts to demonstrate CAP suppression with contralateral noise in the chinchilla.

The aims of this work are: to determine the strength of the contra MOC reflex at different locations along the cochlea in the chinchilla, to ascertain whether the suppression due to contralateral tones is tuned to the ipsilateral-tone frequency and to compare the CAP and CM efferent effects in the awake and anesthetized chinchilla.

MATERIALS AND METHODS

ANIMALS

Seven adult Chinchillas (*Chinchilla laniger*) weighing between 400 and 700 grams were used. All procedures involving animals were made in accordance with NIH Guidelines for the Care and Use of Laboratory Animals, publication No. 86–23, revised 1996, and were approved by the Institutional Bioethics Committee (Comité de Bioética de Investigación en Animales, Facultad de Medicina, Universidad de Chile, permit number CBA #0262). All surgeries were performed under ketamine and xylazine anesthesia, and every effort was made to minimize animal suffering.

SURGERY

Chinchillas were premedicated with atropine (0.04 mg/kg I.M.), xylazine (3–8 mg/kg I.M.) and then anesthetized with ketamine (20–40 mg/kg, I.M.). After the surgery, they were treated with analgesics (Ketofen®, 3 mg/kg I.M.) and antibiotics (Baytril®, 5 mg/kg I.M.) every 12 h for 5 days. A craniotomy was performed in the lateral tympanic bulla and a cochlear electrode (Nichrome® 200 μm diameter) was placed on the round window niche membrane and connected to an external connector that was chronically implanted on the animal's skull. The middle-ear ossicles remained intact to preserve the physiologic conduction of sound to the cochlea. During surgery rectal temperature was maintained constant at 35–37°C by means of a heating pad. All surgical procedures were performed under a microscope (Zeiss®, OpMi-1) with magnification of up to 40x.

STIMULATION PROTOCOL AND DATA ACQUISITION

The effects produced by contralateral stimulation on cochlear potentials were measured in all chinchillas, first in awake and later in anesthetized condition. For the measurements in the awake condition the animals were kept in a custom-made motion restrainer that limited their movements with minimum discomfort in sessions of less than 45 min duration. The restrainer device consisted in a cloth hammock in which the animal was suspended and a padded ring that was adjusted around its neck to restrict the head movements. A week before the surgical electrode implantation, the animals were trained during 3–5 days in sessions not exceeding 45 min to stay quiet on the restrainer device.

All experiments were performed in a double-walled sound-attenuating room, isolated from external noises and vibrations. The same stimulation protocol was used in anesthetized and awake animals. Acoustic stimuli were digitally generated with a National Instruments® (PCI-6071E) multifunction data acquisition device, attenuated by programmable attenuators (PA-5, Tucker Davis Technologies®, TDT System 3) and delivered through insertion phones (EC1 electrostatic speakers, TDT). Cochlear potentials were recorded in response to tones at different sound pressure levels (40–80 dB SPL for ipsilateral stimuli and 50–75 dB for contralateral stimuli) and frequencies ranging from 1–6 kHz. Acoustical stimuli were presented with alternated polarity in order to allow us to separate CAPs from CMs. Responses to stimuli of each polarity were independently averaged and later added together to cancel CMs and isolate CAP responses. Each stimulus sequence consisted of 3 consecutive series of 32 stimuli presented at a 1 Hz rate: control, efferent and recovery. In the control series the ipsilateral tones (15 ms duration) were presented alone. In the efferent series the ipsilateral tones (15 ms duration) were preceded by a contralateral tone or noise (500 ms duration) followed by a silent period (15 ms duration). In the recovery series the ipsilateral tones (15 ms duration) were again presented alone (**Figure 1**). The noise stimulus was digitally generated and filtered (0.5–32 kHz) uniform white noise (LabWindows®, white noise subroutine). Cochlear potentials were amplified (10,000X), filtered (0.1–10 kHz) and digitized (40,000 points/s) by a National Instruments® (PCI-6024E) card. CAP amplitudes were measured between the maximum and minimum of N1 and P1 waves (first and second peaks) of the average of 32 responses. Subtraction of the averaged responses to stimuli of the two polarities allowed the computation of the CM amplitudes by performing a Fast Fourier Transform (FFT) in a 12.8 ms window that excluded the CAP response. Efferent effects on CAP and CM responses were expressed in dB referred to the control amplitudes. In the case of efferent effects on CMs that were fairly small we used a threshold of 0.5 dB for CM amplitude changes. This threshold was established by measuring, in two animals, the variability of repeated measures of CM amplitude for the same parameters of ipsilateral stimulation, without efferent activation. The variability obtained ranged from 1 to 3 % or 0.1 to 0.25 dB, therefore to make sure the changes

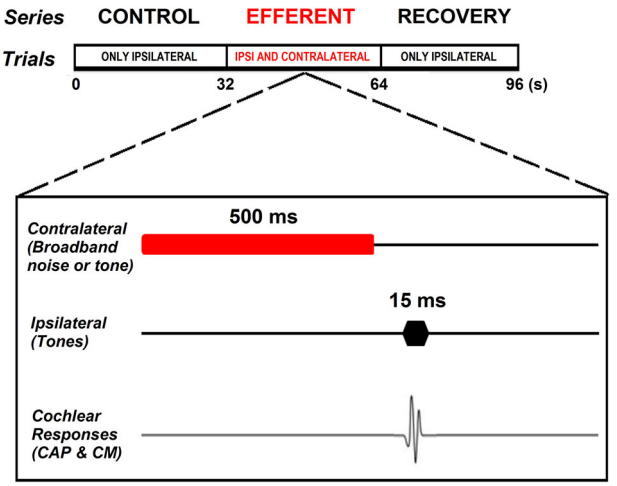

FIGURE 1 | Experimental paradigm. Each stimulation sequence consisted of three consecutive series of 32 stimuli presented at 1 Hz rate: control, efferent and recovery. Control series consisting of ipsilateral tones (15 ms duration) presented alone. Efferent series in which the ipsilateral tone (15 ms duration) was preceded by a contralateral tone or noise (500 ms duration) followed by a silent period (15 ms duration). Recovery series in which the ipsilateral tones (15 ms duration) were again presented alone.

were not due to the variability of the responses we set a threshold equal twice the maximum variability. In two chinchillas at the end of the experiment we injected tetrodotoxin (TTX, 3 μM), a powerful neurotoxin that blocks voltage-dependent Na^+ ion channels, through the round window of the contralateral cochlea to block neural responses and repeated some of the measurements of contralateral-ear suppression. Data analysis was performed using custom-made C programs (LabWindows®). The significance of the differences between the experimental and control series was checked using *t*-tests or ANOVA for normal distributed data or the Mann-Whitney test (SigmaPlot® v12.5) for non-normal data (as evaluated by the Shapiro-Wilk test).

RESULTS

The effect of contralateral broad-band noise on the magnitudes of the CAP and CMs generated in response to ipsilateral tones (1–6 kHz) was measured in seven chinchillas in awake and anesthetized condition. CAP-amplitude reductions produced by contralateral noise ranged from 1 to 7 dB in anesthetized and from 1 to 10 dB in awake animals. In contrast, no measurable contralateral-sound effects were obtained on CMs in anesthetized chinchillas. In awake state efferent effects on CM were found in only three chinchillas that displayed CM amplitude increases ranging from 0.5 to 1.9 dB. **Figure 2** depicts the effects of contralateral broad-band noise on CAP and CM responses obtained in the awake chinchilla that displayed the largest CM increases, concomitant to CAP reductions. Since contralateral-sound effects on CM potentials were obtained in only three awake animals the following description and analysis of results will be limited to the effects on CAP responses.

Figure 3 shows reductions produced by contralateral noise (40–50 dB SPL) in the amplitude of CAP responses to ipsilateral tones at four frequencies in one anesthetized chinchilla. In the figure green and red symbols indicate CAP amplitudes in absence and presence of contralateral stimulation, respectively. As exemplified in this figure, in all cases the presence of the contralateral sound produced an abrupt decrease in CAP amplitude that could be seen in the first CAP response after the onset of the contralateral stimulation series and an equally abrupt return to the control value at the offset of stimulation.

Figure 4 shows input-output curves of CAP amplitudes in response to ipsilateral tones at frequencies of 3 and 4 kHz and intensities from 20 to 80 dB SPL obtained in absence and presence of contralateral broad-band noise (50 dB SPL; red curves) in one awake (blue) and anesthetized (green) chinchilla. All of the curves show a monotonic CAP amplitude increase with increasing stimulation intensity that in some cases reaches saturation at levels above 80 dB SPL (not shown). The figure compares CAP suppressions obtained at the two ipsilateral tone frequencies that displayed the strongest efferent effects. At both frequencies, in awake condition, all amplitude differences reached statistical significance for ipsilateral tones <60 dB SPL, while in anesthetized condition, most amplitude differences were significant for ipsilateral tones <50 dB SPL.

Contralateral stimulation with pure tones also produced CAP reductions in anesthetized as well as in awake animals; however, the magnitude of the effect was highly dependent on the frequency of the contralateral tone. **Figure 5** displays examples of the reductions of CAP responses to ipsilateral tones at four frequencies (2–6 kHz) produced by contralateral tones of different frequencies in awake and anesthetized animals. The efferent suppression produced by contralateral tones was always tuned to a frequency equal or close to the ipsilateral stimulus tone and, as in the case with contralateral noise, it was stronger in awake than in anesthetized animals. To give an idea of the differences in frequency tuning of efferent suppression observed in the different animals we present in **Figure 6** the superposition of the curves of CAP reduction obtained, at four ipsilateral frequencies, for all contralateral frequencies tested in all animals in awake and anesthetized condition (intensity levels: 50–60 dB SPL ipsilateral and 60–70 dB SPL contralateral tones). Significant effects were obtained with frequency and with awake or anesthesia conditions as assessed by a two-way ANOVA (ipsilateral frequency vs. awake/anesthesia as factors): awake vs. anesthesia: $F_{(1)} = 5.681$, $p = 0.018$; ipsilateral frequency: $F_{(3)} = 14.199$, $p < 0.001$. However, there was no interaction between these factors: $F_{(3)} = 0.182$, $p = 0.908$. The magnitudes and extent of the CAP reductions were also dependent on the intensity of the contralateral tone. **Figure 7** compares the magnitudes of CAP suppressions obtained in one animal, for a 4 kHz ipsilateral tone in anesthetized and awake condition, with contralateral tones at frequencies ranging from 1800 to 6200 Hz and intensities at 58 and 68 dB SPL. In both conditions, awake and anesthetized, the efferent suppression effects were stronger and extended on a wider range of frequencies for the more intense contralateral tones.

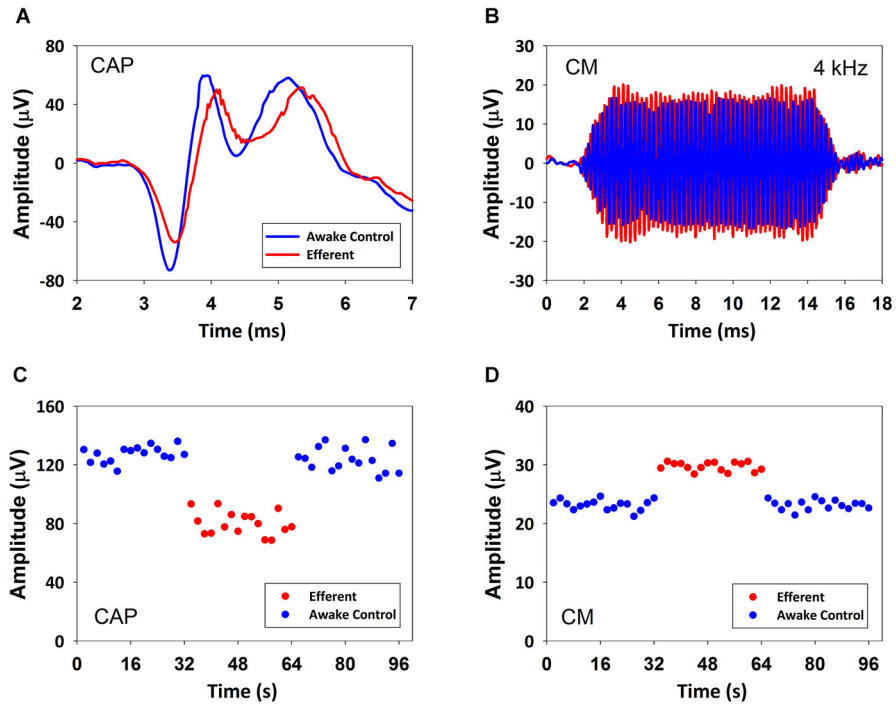

FIGURE 2 | CAP suppression and CM increase produced by contralateral acoustical stimulation in an awake chinchilla. **(A)** Average CAP traces of 32 responses to ipsilateral tones in absence (blue) and presence (red) of contralateral acoustical stimulation. **(B)** Average CM traces of 32 responses to ipsilateral tones in absence (blue) and presence (red) of contralateral acoustical stimulation. **(C)** CAP response amplitudes in repeated trials in absence (blue) and presence (red) of contralateral acoustical stimulation. Each symbol represents the average CAP amplitude (N1 to P1 in μV) of two consecutive trials. Significant CAP reductions were obtained with contralateral acoustical stimulation (two tailed *t*-test, $T_{(30)} = 19.618$, $p = 1.157*10^{-18}$). **(D)** CM response amplitudes in repeated trials in absence (blue) and presence (red) of contralateral acoustical stimulation. Each symbol represents the average CM amplitude of two consecutive trials. Amplitudes (rms in μV) were obtained by fast Fourier transform (FFT). Significant CM enhancements were obtained with contralateral acoustical stimulation (two tailed *t*-test, $T_{(30)} = -22.329$, $p = 3.031*10^{-20}$). In all panels ipsilateral tones were 4 kHz at 60 dB SPL and contralateral broad-band noise was at 55 dB SPL.

We have compared the CAP suppressions obtained in awake and anesthetized animals for 1–6 kHz ipsilateral frequencies and similar stimulation intensity levels: 50–60 dB SPL ipsilateral tones and 60–70 dB SPL contralateral tones. **Figure 8** depicts the maximum CAP reductions produced by contralateral stimulation, in each animal, at each ipsilateral frequency in awake and anesthetized condition (blue and green symbols, respectively). The figure also displays the average of the maximum CAP reductions produced by contralateral tones for all animals at each ipsilateral frequency in awake and anesthetized condition (blue and green dashed lines, respectively). As shown in the figure, the average CAP suppressions produced by contralateral tones in all chinchillas were significantly larger, at almost all frequencies, in the awake than in the anesthetized condition (Mann-Whitney test, 1 kHz: $U_{(7)} = 6.0$, $T = 71.0$, $p = 0.017$; 2 kHz: $U_{(7)} = 0.0$, $T = 77$, $p < 0.001$; 3 kHz: $U_{(7)} = 7.5$, $T = 69.5$, $p = 0.026$; 4 kHz: $U_{(5)} = 2.0$, $T = 38$, $p = 0.032$; 6 kHz: $U_{(3)} = 3.0$, $T = 12$, $p = 0.7$).

As mentioned above, the efferent CAP suppression produced by contralateral tones was always tuned in frequency; that is, there was a most effective contralateral frequency, close or equal to the ipsilateral-tone frequency, that produced maximal suppression (**Figures 5–7**). **Figure 9** shows the relationship between the most effective contralateral frequencies and ipsilateral frequencies for all data obtained in awake and anesthetized animals (blue and green symbols, respectively). In both conditions, the most effective contralateral suppressor frequencies for ipsilateral frequencies <4 kHz were nearly equal to the ipsilateral frecuencies, while for ipsilateral frequencies ≥4 kHz they were consistently lower than ipsilateral frequencies, as shown by the average values of the most effective contralateral frequencies (dashed lines). This different relation between most effective contralateral and ipsilateral frequencies is also illustrated in **Figure 10**, which depicts CAP suppressions as a function of the difference (in octaves) between most effective suppressor and ipsilateral frequencies for the data obtained in all animals, but segregated into two groups according to the values of ipsilateral frequency. In awake, as well as, in anesthetized animals CAP suppressions display distributions that, for ipsilateral frequencies <4 kHz are centered at most effective suppressor frequencies equal to ipsilateral frequencies, while for ipsilateral frequencies ≥4 kHz exhibit an offset of −0.26 octaves between most effective suppressor and ipsilateral frequencies. The figure shows that CAP-suppression curves for ipsilateral frequencies ≥4 kHz display higher tuning than those of ipsilateral frequencies <4 kHz, but that there are no changes in the pattern of tuning with and without anesthesia.

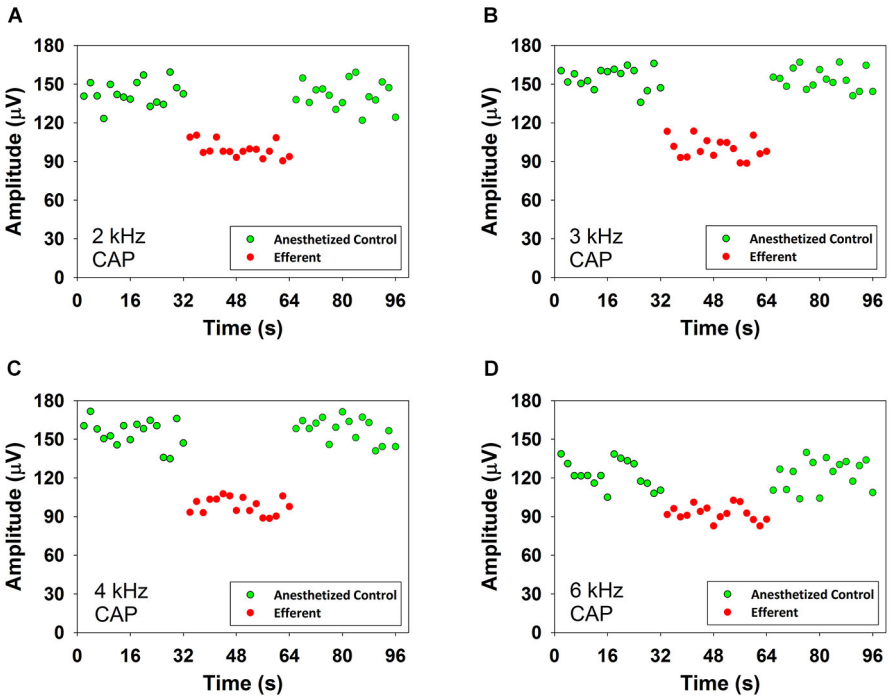

FIGURE 3 | CAP suppression produced by contralateral acoustical stimulation in an anesthetized chinchilla. Reductions of CAP amplitudes in response to ipsilateral tones obtained in the presence of contralateral broad-band noise (55 dB SPL). Each symbol represents the average CAP amplitude of two consecutive trials. The red circles correspond to responses to ipsilateral tones preceded by contralateral efferent stimulation. The green circles correspond to responses to ipsilateral tones alone, before and after contralateral efferent stimulation. Panel **(A)**: 2 kHz at 47 dB SPL, panel **(B)**: 3 kHz at 50 dB SPL, panel **(C)**: 4 kHz at 44 dB SPL and panel **(D)**: 6 kHz at 40 dB SPL. Significant CAP reductions were obtained with contralateral acoustical stimulation at 2 kHz (two tailed *t*-test, $T_{(30)} = 15.324$, $p = 9.919*10^{-16}$), 3 kHz (two tailed *t*-test, $T_{(30)} = 18.924$, $p = 3.150*10^{-18}$), 4 kHz (two tailed *t*-test, $T_{(30)} = 9.920$, $p = 5.509*10^{-11}$) and 6 kHz (two tailed *t*-test, $T_{(30)} = 18.391$, $p = 6.957*10^{-18}$).

In order to discard any possibility that the reduction in CAP amplitude could be produced by activation of the middle-ear reflex, in one anesthetized animal the experimental protocol for frequency tuning of CAP suppression was repeated after section of the tensor tympani muscle and detachment of the stapedius muscle from its insertion. As shown in **Figure 11**, at four ipsilateral frequencies, no significant differences were found in contralateral CAP suppression for the magnitudes obtained before and after the middle-ear muscle section.

In addition, we performed two kinds of controls to show that CAP suppression was mediated by MOC neurons activated from the contralateral ear and was not due to ipsilateral forward masking or ipsilateral activation of MOC fibers produced by crosstalk of contralateral stimuli to the ipsilateral ear. First, in two animals we injected tetrodotoxin (TTX), a powerful neurotoxin blocker of voltage-dependent Na^+ ion channels, into the contralateral cochlea. After minutes of the TTX injection, in both animals, the toxin abolished the contralateral-ear neural responses and also their suppressive effect on ipsilateral CAPs (**Figure 12**). The disappearance of the CAP suppression after the TTX contralateral injection showed that the effect was mediated by the neural response of the contralateral ear. Second, in one chinchilla we determined that the interaural attenuation was higher than 40 dB at all frequencies of contralateral stimulation. Then, after measuring the CAP suppression produced by a contralateral tone, we evaluated the CAP suppression produced by an ipsilateral tone at an intensity 40 dB lower than that of the contralateral tone. CAP suppression was found for the contralateral tone stimulation, but not for the 40 dB-lower ipsilateral tone, thus showing that the CAP suppression measured in the experiments was exclusively produced by MOC neurons activated from the contralateral ear.

DISCUSSION

The effect of contralateral sound stimulation on cochlear responses has been studied recording auditory-nerve fiber and CAP responses and distortion product otoacoustic emissions (DPOAEs) in cat, guinea pig and mice (Buño, 1978; Liberman, 1989; Warren and Liberman, 1989a,b; Puel and Rebillard, 1990; Popelár et al., 2001; Boyev et al., 2002; Chambers et al., 2012). In the cat it has been shown that contralateral tones and broad-band noise produce a decrease in the responses of single auditory-nerve fibers to ipsilateral tones that is greatest for auditory fibers with CF near 2 kHz and that could reach up to about 70% (Warren and Liberman, 1989a). Severing of the olivocochlear bundle at the internal auditory meatus completely eliminated the suppressive effects of contralateral sound, while severing only the crossed olivocochlear fibers did not eliminate them, thus indicating that these contralateral-sound suppressive effects were mediated by

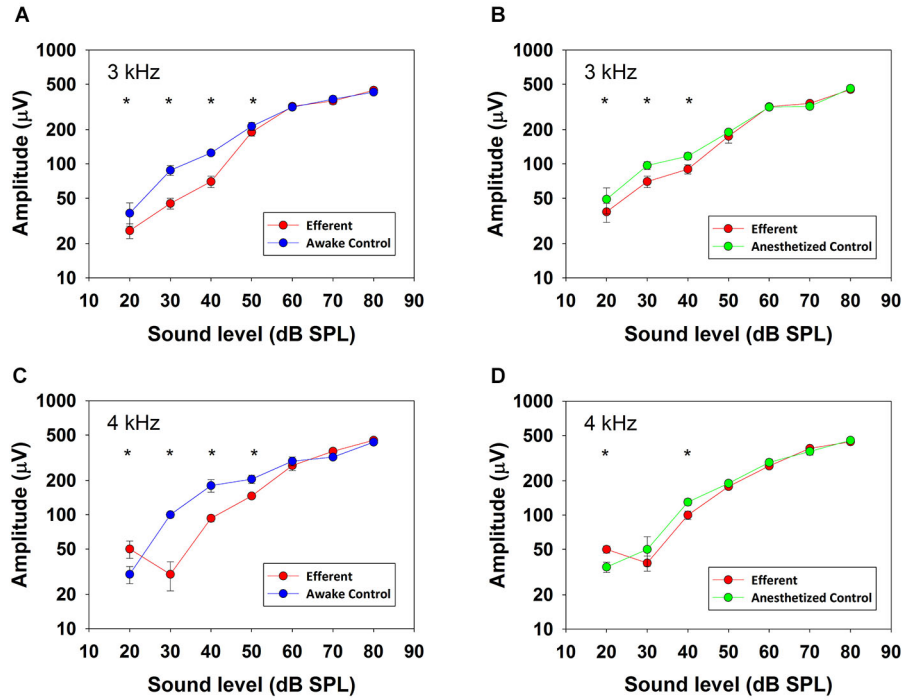

FIGURE 4 | CAP input–output curves. CAP amplitudes obtained in one chinchilla without (blue and green) and with (red) contralateral acoustical stimulation (broad-band noise at 50 dB SPL) in awake (blue) and anesthetized (green) condition. Vertical lines indicate standard deviations. Efferent-activation produced by contralateral stimulation is more effective at low ipsilateral stimulus intensities and efferent reductions are higher in awake than in anesthetized animals. Asterisks indicate statistically significant differences. Panel **(A)**: 3 kHz, 20 dB: (Mann-Whitney, $U_{(32)} = 30.0$, $T = 1522$, $p < 0.001$); 3 kHz, 30 dB: (Mann-Whitney, $U_{(32)} = 0.0$, $T = 528.0$, $p < 0.001$); 3 kHz, 40 dB: (Mann-Whitney, $U_{(32)} = 0.0$, $T = 1522.0$, $p < 0.001$); 3 kHz, 50 dB: (Mann-Whitney, $U_{(32)} = 126.0$, $T = 1426.0$, $p < 0.001$). Panel **(B)**: 3 kHz, 20 dB: (Mann-Whitney, $U_{(32)} = 170.0$, $T = 1382.0$, $p < 0.001$); 3 kHz, 30 dB: (Mann-Whitney, $U_{(32)} = 5.0$, $T = 1547.0$, $p < 0.001$); 3 kHz, 40 dB: (Mann-Whitney, $U_{(32)} = 0.0$, $T = 528.0$, $p < 0.001$). Panel **(C)**: 4 kHz, 20 dB: (Mann-Whitney, $U_{(32)} = 266.0$, $T = 1286.0$, $p < 0.001$); 4 kHz, 30 dB: (Mann-Whitney, $U_{(32)} = 0.0$, $T = 528.0$, $p < 0.001$); 4 kHz, 40 dB: (Mann-Whitney, $U_{(32)} = 0.0$, $T = 528.0$, $p < 0.001$); 4 kHz, 50 dB: (Mann-Whitney, $U_{(32)} = 179.0$, $T = 707.0$, $p < 0.001$). Panel **(D)**: 4 kHz, 20 dB: (Mann-Whitney, $U_{(32)} = 266.0$, $T = 1286.0$, $p < 0.001$); 4 kHz, 40 dB: (Mann-Whitney, $U_{(32)} = 2.0$, $T = 1550.0$, $p < 0.001$).

uncrossed olivocochlear fibers (Warren and Liberman, 1989a). Suppressive effects of contralateral noise and tones on CAP responses have also been reported in anesthetized cats and guinea pigs (Liberman, 1989; Puria et al., 1996; Larsen and Liberman, 2009). These suppressive effects, as in the case of auditory-nerve responses, were mediated by uncrossed olivocochlear fibers. Furthermore, Liberman (1989) recording CAP and single olivocochlear-fiber responses in the same animals obtained good correlation between the strength of CAP suppression and the sound-evoked discharge rates of single olivocochlear neurons. All of this evidence indicates that the effects of contralateral sound stimulation are dependent on the uncrossed MOC efferent fibers.

As mentioned in the Introduction, among all species studied, the chinchilla is the one that presents the lowest percentage of uncrossed MOC fibers (about 20%; Azeredo et al., 1999). Since these are the efferent fibers comprising the neural pathway that mediates contralateral sound suppression, their scarcity in the chinchilla raised doubts about the strength and frequency distribution of the contralateral-sound suppression that could be found in this species. In fact, early works in chinchilla reported unsuccessful attempts to suppress CAP responses and DPOAEs with contralateral noise stimulation (Azeredo et al., 1999). In contrast with the outcome of those early attempts, more recent studies in chinchilla have succeed in finding contralateral-sound suppressive effects on ipsilateral DPOAEs (James et al., 2005; Harrison et al., 2008; Wolter et al., 2014) and in the present work we are reporting consistent contralateral-sound suppression of CAP responses in the seven chinchillas studied.

EFFERENT MODULATION OF COCHLEAR RESPONSES IN CHINCHILLA

Two types of efferent effects on cochlear responses with different temporal courses have been described: fast effects that have time constants of tens of milliseconds and slow effects that have time constants three orders of magnitude larger (Sridhar et al., 1995; Cooper and Guinan, 2003). Although our experimental paradigm allowed the assessment of both fast and slow MOC effects, we only found fast amplitude changes in cochlear potentials. In all animals CAP amplitudes abruptly decreased at the onset of the contralateral stimulation series and abruptly returned to control values at the offset, without evidence of slower changes of amplitude during the 32 s stimulation period. Similar abrupt amplitude increases,

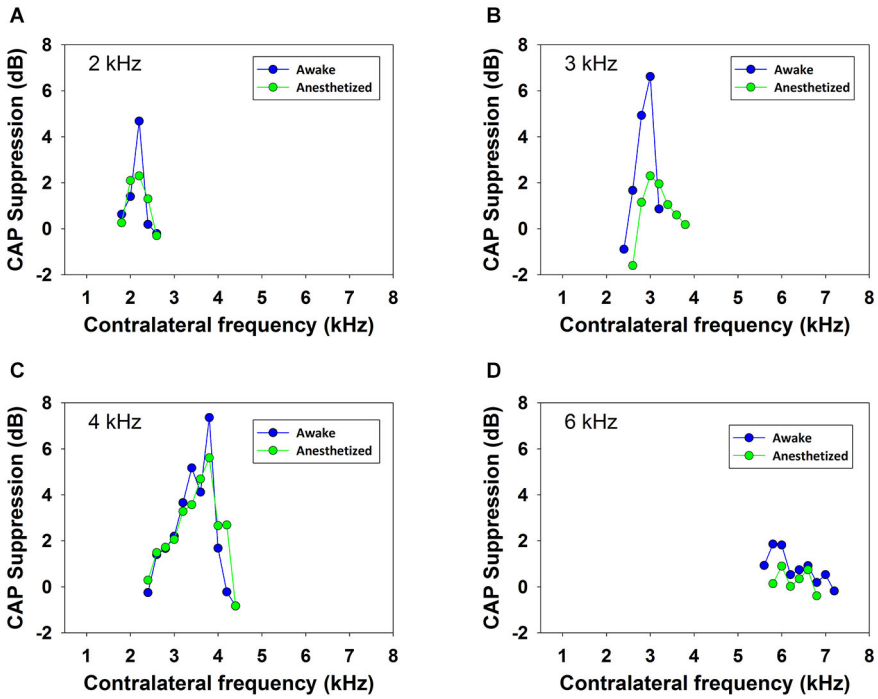

FIGURE 5 | Frequency tuning of ipsilateral CAP reduction produced by contralateral tone stimulation. Efferent reduction of CAP amplitudes produced by the presence of contralateral acoustical stimulation in four animals, in awake (blue) and anesthetized (green) condition, for ipsilateral tones at frequencies of 2, 3, 4 and 6 kHz. Intensities of the ipsilateral and contralateral tones were, panel **(A)**: 55 and 69 dB SPL, panel **(B)**: 58 and 64 dB SPL, panel **(C)**: 56 and 62 dB SPL and panel **(D)**: 53 and 58 dB SPL.

instead of decreases, were observed in the CM responses of the three awake chinchillas that exhibited CM efferent effects (see **Figures 2**, **3**). However, it is possible that our contralateral stimulation period could have been too short to produce slow effects, as other studies using other contralateral stimulation paradigms in chinchilla have reported slow efferent effects after 1 min of contralateral stimulation (Bowen et al., 2014).

We have found in chinchilla large CAP-amplitude suppressions produced by contralateral broad-band noise as well as by contralateral tones. But, a comparison of the magnitudes of contralateral CAP suppression obtained in our study in chinchilla with values reported in other species is difficult because of the dependance of suppression on the different paradigms and parameters of stimulation used by different authors. However, in spite of the lower percentage of uncrossed MOC fibers in chinchilla, our highest values of suppression of about 10 dB (computed as equivalent or effective attenuation; Desmedt, 1962; Liberman, 1989) are similar to those reported in cat (Liberman, 1989).

We were able to demonstrate contralateral CAP suppression for ipsilateral tones with frequencies in the range of 1–6 kHz. This would indicate a span of efferent innervation reaching at least the central third of the cochlea, according to the chinchilla cochlea frequency-position map (Müller et al., 2010). The only anatomical study on efferent fiber distribution available in chinchilla shows that uncrossed MOC fibers have a strong bias toward the more apical cochlear regions: no uncrossed MOC fibers were found in the most basal cochlear region, only 12% of MOC fibers in the basal turn, about 30% in the second turn and 57% in the apical turn (Iurato et al., 1978). This anatomical distribution of uncrossed MOC fibers is compatible with our finding of contralateral suppression for ipsilateral tones with frequencies of 1–6 kHz. The largest suppressions produced by contralateral tones in this study were for ipsilateral frequencies at 3 and 4 kHz. In the cat the largest CAP suppressions were found for an ipsilateral frequency of 1.5 kHz (Liberman, 1989). In both cases maximal suppressions occurred for frequencies corresponding to locations in the mid turn of the cochlea (Greenwood, 1990; Müller et al., 2010).

As mentioned in Results, we consistently found that contralateral sounds produced substantial CAP-amplitude reductions and no measurable effects on CMs in anesthetized chinchillas and small CM enhancements in only three of the seven awake chinchillas. This absence or weakness of efferent effects on CMs in the present results is consistent with results obtained in a previous study in which we electrically stimulated MOC fibers in chinchilla and obtained significant CAP reductions of up to 11 dB (for 2 kHz tones) accompanied by much smaller CM increases of $<$2.5 dB (Elgueda et al., 2011). The lesser efferent effects on CMs than on CAPs have also being reported for sustained contralateral noise that elicits sizable CAP suppressions and

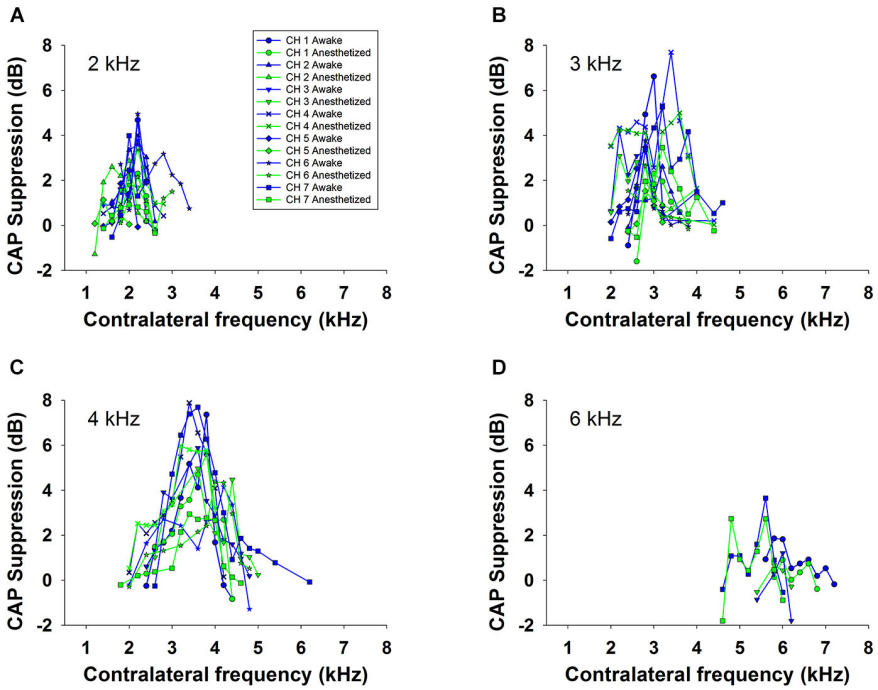

FIGURE 6 | Frequency tuning of ipsilateral CAP reduction produced by contralateral tone stimulation in all animals. Superposition of the curves of CAP suppression produced by contralateral acoustical stimulation in all animals, in awake (blue) and anesthetized (green) condition, for ipsilateral tones at, panel **(A)**: 2 kHz, panel **(B)**: 3 kHz, panel **(C)**: 4 kHz and panel **(D)**: 6 kHz. Intensities of the tones were: 50 to 60 dB SPL for the ipsilateral and 60 to 70 dB SPL for the contralateral tones.

only small CM enhancements (Larsen and Liberman, 2009). In contrast, auditory cortex deactivation in chinchilla, in most cases, produced decreases in both CM and CAP responses (León et al., 2012). In that case, as mentioned by the authors, the effects may have involved not only the activity of medial, but also lateral OC efferent fibers.

COMPARISON OF SUPPRESSION IN ANESTHETIZED AND AWAKE ANIMALS

Contralateral-sound suppression of cochlear responses has been mostly studied in anesthetized animals and it is known that the activity of medial OC neurons is dependent on the level of anesthesia (Liberman and Brown, 1986). Accordingly, to assess the physiological importance of this suppression effect it is important to measure it in awake animals. A study that compared contralateral-sound suppression of DPOAEs in anesthetized and awake guinea pigs found that suppression was much weaker in urethane-anesthetized than in awake animals, and that it was even weaker in pentobarbitone-anesthetized animals (Guitton et al., 2004). In this study we have compared the contralateral suppression of CAP responses in anesthetized and awake chinchillas finding that the mean values of suppression were higher by 1–3 dB in the awake than in the anesthetized condition (see **Figure 8**). These results add to previous evidence (Boyev et al., 2002; Guitton et al., 2004; Chambers et al., 2012) showing that when comparing the strength of efferent suppression measured in awake human subjects with that in experimental animals one must keep in mind that the latter is mostly measured in anesthetized animals and, consequently, is consistently underestimated.

FREQUENCY TUNING OF CONTRALATERAL SUPPRESSION

In all chinchillas, in anesthetized and awake condition, we found that the contralateral-tone CAP suppression was frequency tuned; that is, suppression had a peak for contralateral tones at frequencies equal or near those of the ipsilateral tones and decreased at a fast-rate for higher and lower frequencies (**Figures 5–7**). This tuning of contralateral suppression indicates a correspondence between the tonotopic distribution of afferent and efferent cochlear neural fibers. Afferent fibers from a contralateral cochlear location with a certain characteristic frequency activate MOC efferent neurons that innervate ipsilateral cochlear locations having similar characteristic frequencies. The close correspondence that we have found between the most effective contralateral frequencies and ipsilateral frequencies (**Figure 9**) is similar to that reported for auditory-nerve responses in cat (Warren and Liberman, 1989b). However, in the cat the most effective contralateral frequencies displayed a slight deviation from ipsilateral frequencies for ipsilateral tones at frequencies less than 3 kHz while in our case the deviation was for ipsilateral frequencies $\geq$4 kHz. These results are also in agreement with anatomical data of single olivocochlear neurons in cat and guinea pig showing that the cochlear region innervated by an efferent neuron corresponds

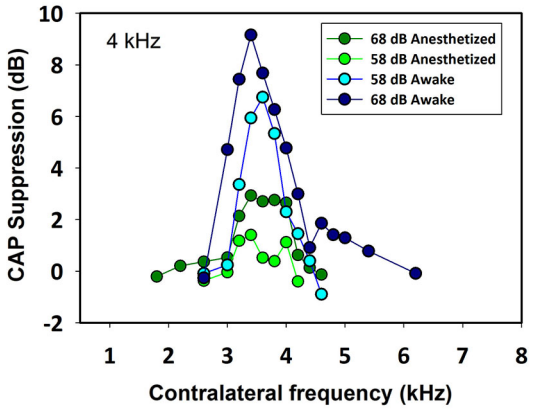

FIGURE 7 | Frequency tuning curves of ipsilateral CAP reduction produced by contralateral tones at two intensities in an awake and anesthetized chinchilla. The magnitude and extent of the CAP reduction depend on the contralateral stimulus frequency and intensity. In this case, for a 4 kHz ipsilateral tone (48 dB SPL) the greatest CAP reductions were obtained for contralateral frequencies between 3400 and 4000 Hz. As in all other animals, the efferent effect was better tuned and stronger in awake than in anesthetized condition. Awake vs. anesthetized, 68 dB SPL (Mann-Whitney, $U_{(32)} = 0.0$, $T = 392$, $p < 0.001$), 58 dB SPL (Mann-Whitney, $U_{(32)} = 0.0$, $T = 392$, $p < 0.001$); 68 dB SPL vs. 58 dB SPL, awake (Mann-Whitney, $U_{(32)} = 45.0$, $T = 181$, $p = 0.002$), anesthetized (Mann-Whitney, $U_{(32)} = 0.0$, $T = 136$, $p < 0.001$).

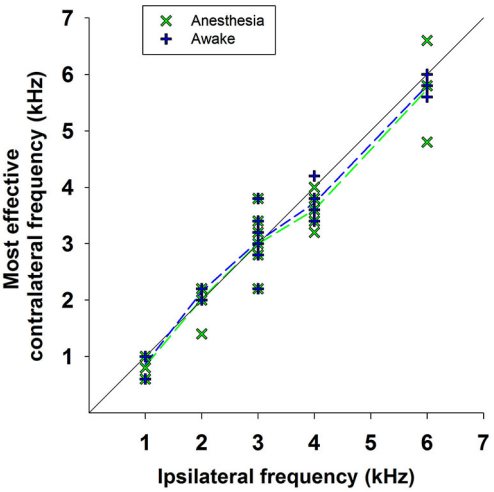

FIGURE 9 | Most effective contralateral suppressor frequencies vs. ipsilateral frequencies. Relationship between the frequencies of the most effective contralateral suppressors and the ipsilateral tones for all data obtained in awake (blue symbols) and anesthetized (green symbols) animals. The dashed lines indicate the average values of the most effective contralateral suppressors frequencies for all measurements at each ipsilateral frequency in awake (blue dashed line) and anesthetized (green dashed line) animals.

(or is close) to the place innervated by afferent neurons with the same characteristic frequency (Robertson and Gummer, 1985; Liberman and Brown, 1986). The widths of the frequency tuning curves for CAP suppression that we obtained in chinchilla would correspond to efferent innervation spans of about 4 to 8% of total cochlear length; these values are in between those obtained by fiber labeling in cat (2.2–11.2%) by Liberman and Brown (1986) and in guinea pig (<1–2% and 1.4–7.8%) by Robertson (1984) and Robertson and Gummer (1985), and Brown (1987), respectively.

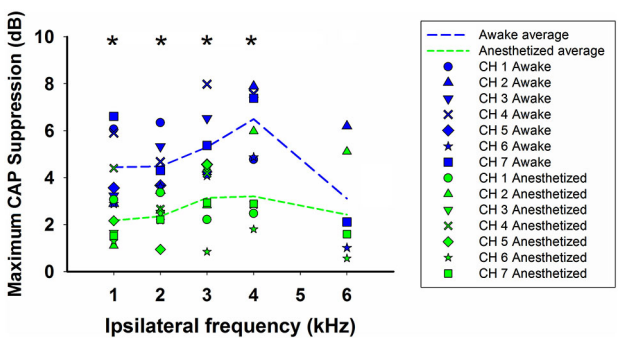

FIGURE 8 | Summary of efferent CAP suppression in awake and anesthetized animals. Symbols depict maximum CAP supressions produced by contralateral stimulation, in each animal, at each ipsilateral frequency in awake (blue) and anesthetized (green) condition. The dashed lines display the average of the maximum CAP reductions produced by contralateral tones for all animals at each ipsilateral frequency in awake (blue) and anesthetized condition (green). Intensities of ipsilateral and contralateral tones were 50–60 and 60–70 dB SPL, respectively. Asterisks indicate statistical significance.

Our finding of narrow frequency tuning curves for contralateral CAP suppression, although in good agreement with suppression tuning curves previously obtained for auditory-nerve and CAP responses in anesthetized cats (Liberman, 1989; Warren and Liberman, 1989b), are in contradiction with two completely different frequency-selectivity characteristics of suppression recently reported using OAEs in humans. Stimulus frequency OAE measurements in humans indicate that the strength of contralateral suppression depends on the integration of the effect from almost the entire length of the contralateral cochlea (Lilaonitkul and Guinan, 2009). On the other hand, spontaneous OAE measurements indicate that contralateral suppression is tuned to a fixed narrow frequency band, between 500 and 1,000 Hz, independent of the spontaneous OAE frequency (Zhao and Dhar, 2012). As mentioned above, the narrow tuning of MOC effects that we have observed agrees well with previous evidence on cochlear efferent innervation, while the results obtained using different types of OAEs to assess MOC-effect tuning in humans are contradictory and difficult to interpret.

CONTROLS TO DISCARD ANY MIDDLE-EAR INVOLVEMENT IN SUPPRESSIVE EFFECTS

As mentioned above, there is solid experimental evidence indicating that the suppressive effects of contralateral sounds on cochlear responses are mediated by efferent uncrossed MOC fibers (Warren and Liberman, 1989a). However, there is always a possibility, especially when using high levels of stimulation, that the suppressive effects on CAP responses could be partially

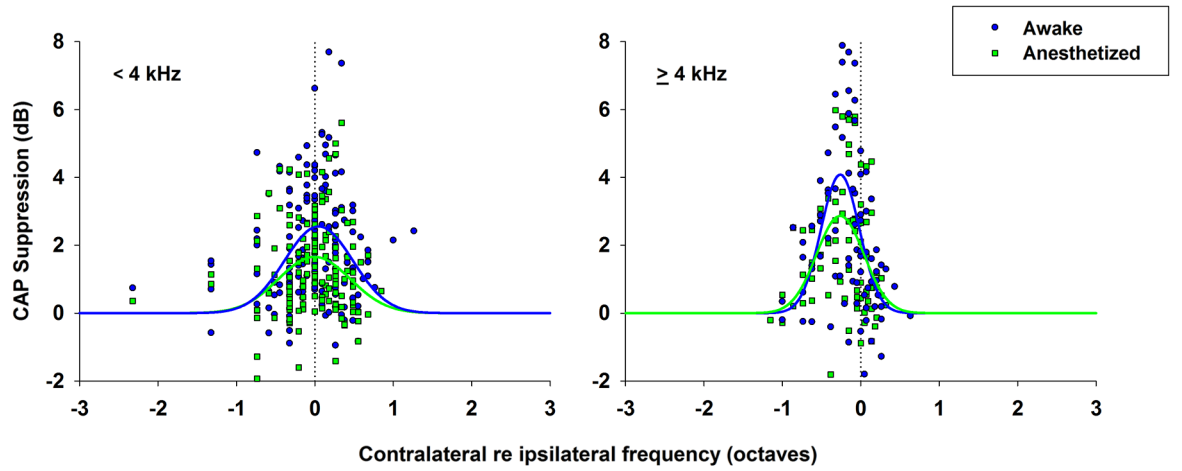

FIGURE 10 | CAP suppression as a function of contralateral suppressor frequency re ipsilateral frequency. CAP suppressions as a function of the difference between contralateral frequencies and ipsilateral frequencies (in octaves) for all data in awake (blue circles) and anesthetized (green squares) animals. Normal distributions fitted to data, awake (blue line), anesthetized (green line). (Left) CAP suppression for ipsilateral frequencies <4 kHz. Awake, $f(x) = 2.56\, e^{-0.5\left(\frac{x-0.0483}{0.435}\right)^2}$; anesthetized, $f(x) = 1.66\, e^{-0.5\left(\frac{x+0.0067}{0.435}\right)^2}$. (Right) CAP suppression for ipsilateral frequencies ≥ 4 kHz. Awake, $f(x) = 4.084\, e^{-0.5\left(\frac{x+0.262}{0.245}\right)^2}$; anesthetized, $f(x) = 2.868\, e^{-0.5\left(\frac{x+0.263}{0.301}\right)^2}$.

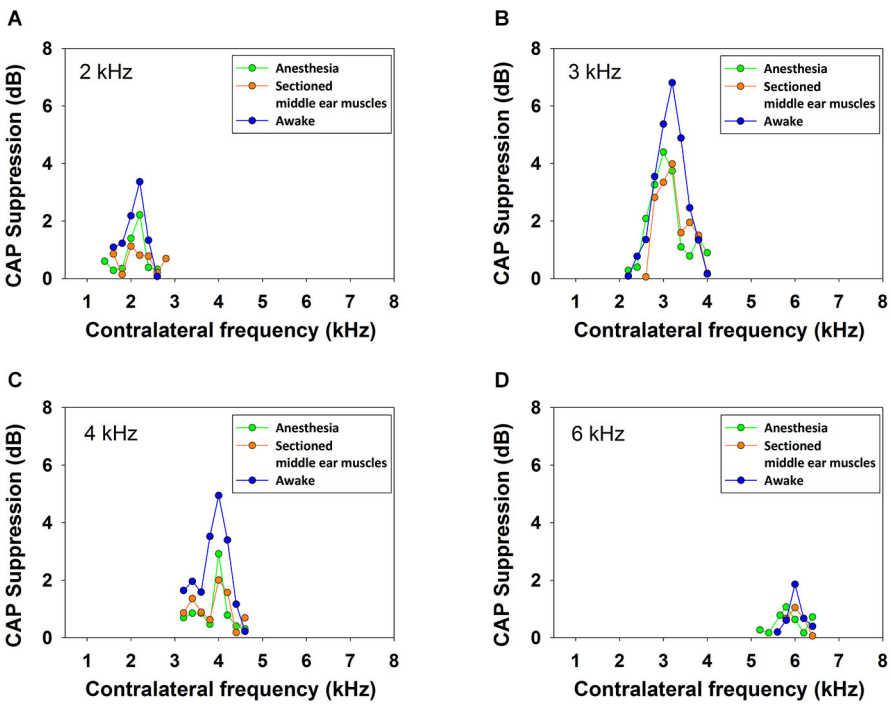

FIGURE 11 | Frequency tuning curves in awake and anesthetized chinchilla with intact and sectioned middle-ear muscles. Efferent reduction of CAP amplitudes produced by contralateral acoustical stimulation (70 dB SPL) in one animal, awake (blue), anesthetized (green) and anesthetized with detached middle-ear muscles (orange), for ipsilateral tones (50 dB SPL) at, panel **(A)**: 2 kHz, panel **(B)**: 3 kHz, panel **(C)**: 4 kHz and panel **(D)**: 6 kHz. There were no significant differences between the results obtained in the anesthetized animal before and after middle-ear muscles detachment.

produced by activation of the middle-ear reflex that also reduces cochlear sensitivity. Several facts assure us that the CAP-amplitude reductions observed in these experiments were due to activation of the MOC system and not the middle-ear reflex. First, all contralateral suppressions (other than those in CAP input-output curves) were measured at or below 70 dB SPL intensity

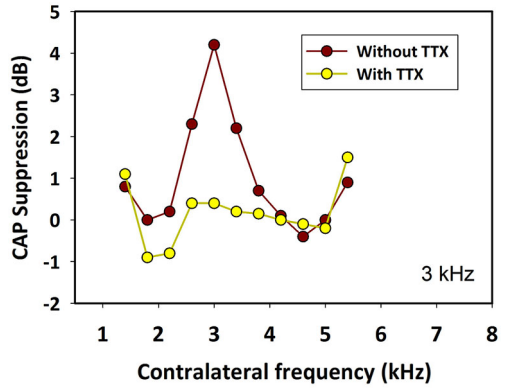

FIGURE 12 | Effect of tetrodotoxin (TTX) in the contralateral cochlea. Ipsilateral CAP-reduction tuning curves before (brown) and after (yellow) injection of tetrodotoxin into the contralateral cochlea. The toxin abolished contralateral neural responses and their suppressive effect on ipsilateral CAPs. Ipsilateral tones at 3 kHz and 50 dB SPL. Contralateral tones at 70 dB SPL.

levels, and the strongest suppression effects were always found at much lower levels. Second, no differences in contralateral CAP reduction were found in one control animal in which the CAP-suppression frequency tuning was measured before and after middle-ear muscle section (**Figure 11**). Third, in the three awake chinchillas in which we did find efferent effects on CMs, contralateral sounds produced CAP reductions concomitant with CM enhancements. The presence of these opposite effects of contralateral stimulation on CAP and CM potentials is strong evidence that they were not produced by middle-ear reflex activation (Guinan, 1996; Robles and Delano, 2008). Fourth, the fact that CAP suppressions produced by contralateral tones were always sharply tuned to frequencies equal or close to that of the ipsilateral tone discards any possibility that they could be a consequence of middle-ear reflex activation.

In conclusion, we have shown that: (1) In spite of the lower percentage of uncrossed MOC fibers present in chinchilla, contralateral sounds produce consistent CAP amplitude reductions for 1–6 kHz ipsilateral frequencies. (2) The contralateral tones producing the CAP suppression are frequency tuned to a frequency equal or close to that of the ipsilateral tone. (3) The contralateral produced CAP suppressions correspond to a span of uncrossed MOC fiber innervation reaching at least the central third of the chinchilla cochlea. (4) The contralateral CAP suppression is consistently higher in awake than in anesthetized condition.

ACKNOWLEDGMENTS

Supported by Fondecyt 1120256 and Fundación Guillermo Puelma.

REFERENCES

Azeredo, W. J., Kliment, M. L., Morley, B. J., Relkin, E., Slepecky, N. B., Sterns, A., et al. (1999). Olivocochlear neurons in the chinchilla: a retrograde fluorescent labelling study. *Hear. Res.* 134, 57–70. doi: 10.1016/s0378-5955(99)00069-6

Bowen, M., Aedo, C., León, A., Dragicevic, C. D., Terreros, G., Robles, L., et al. (2014). "Awake state and auditory cortex microstimulation enhance contralateral-noise suppression of cochlear responses in chinchillas," in 37th Annual MidWinter Meeting of the Association for Research in Otolaryngology. Abstract Book, 37:52.

Boyev, K. P., Liberman, M. C., and Brown, M. C. (2002). Effects of anesthesia on efferent-mediated adaptation of the DPOAE. *J. Assoc. Res. Otolaryngol.* 3, 362–373. doi: 10.1007/s101620020044

Brown, M. C. (1987). Morphology of labeled efferent fibers in the guinea pig cochlea. *J. Comp. Neurol.* 260, 605–618. doi: 10.1002/cne.902600412

Buño, W. Jr. (1978). Auditory nerve fiber activity influenced by contralateral ear sound stimulation. *Exp. Neurol.* 59, 62–74. doi: 10.1016/0014-4886(78)90201-7

Chambers, A. R., Hancock, K. E., Maison, S. F., Liberman, M. C., and Polley, D. B. (2012). Sound-evoked olivocochlear activation in unanesthetized mice. *J. Assoc. Res. Otolaryngol.* 13, 209–217. doi: 10.1007/s10162-011-0306-z

Cooper, N. P., and Guinan, J. J. (2003). Separate mechanical processes underlie fast and slow effects of medial olivocochlear efferent activity. *J. Physiol.* 548, 307–312. doi: 10.1111/j.1469-7793.2003.00307.x

Darrow, K. N., Maison, S. F., and Liberman, M. C. (2006). Cochlear efferent feedback balances interaural sensitivity. *Nat. Neurosci.* 9, 1474–1476. doi: 10.1038/nn1807

Delano, P. H., Elgueda, D., Hamame, C. M., and Robles, L. (2007). Selective attention to visual stimuli reduces cochlear sensitivity in chinchillas. *J. Neurosci.* 27, 4146–4153. doi: 10.1523/jneurosci.3702-06.2007

Desmedt, J. E. (1962). Auditory-evoked potentials from cochlea to cortex as influenced by activation of the efferent olivocochlear bundle. *J. Acoust. Soc. Am.* 34, 1478–1496. doi: 10.1121/1.1918374

Desmedt, J. E., and Monaco, P. (1961). Mode of action of the efferent olivocochlear bundle on the inner ear. *Nature* 192, 1263–1265. doi: 10.1038/1921263a0

de Venecia, R. K., Liberman, M. C., Guinan, J. J., and Brown, M. C. (2005). Medial olivocochlear reflex interneurons are located in the posteroventral cochlear nucleus: a kainic acid lesion study in guinea pigs. *J. Comp. Neurol.* 487, 345–360. doi: 10.1002/cne.20550

Elgueda, D., Delano, P. H., and Robles, L. (2011). Effects of electrical stimulation of olivocochlear fibers in cochlear potentials in the chinchilla. *J. Assoc. Res. Otolaryngol.* 12, 317–327. doi: 10.1007/s10162-011-0260-9

Fex, J. (1959). Augmentation of cochlear microphonic by stimulation of efferent fibres to the cochlea; preliminary report. *Acta Otolaryngol.* 50, 540–541. doi: 10.3109/00016485909129230

Galambos, R. (1956). Suppression of auditory activity by stimulation of efferent fibers to the cochlea. *J. Neurophysiol.* 19, 424–437.

Gifford, M. L., and Guinan, J. J. Jr. (1987). Effects of electrical stimulation of medial olivocochlear neurons on ipsilateral and contralateral cochlear responses. *Hear. Res.* 29, 179–194. doi: 10.1016/0378-5955(87)90166-3

Greenwood, D. D. (1990). A cochlear frequency-position function for several species—29 years later. *J. Acoust. Soc. Am.* 87, 2592–2605. doi: 10.1121/1.399052

Guinan, J. J. Jr. (1996). "The physiology of olivocochlear efferents," in *The Cochlea*, eds P. J. Dallos, A. N. Popper and R. R. Fay (New York: Springer-Verlag), 435–502.

Guinan, J. J. Jr. (2006). Olivocochlear efferents: anatomy, physiology, function and the measurement of efferent effects in humans. *Ear Hear.* 27, 589–607. doi: 10.1097/01.aud.0000240507.83072.e7

Guitton, M. J., Avan, P., Puel, J. L., and Bonfils, P. (2004). Medial olivocochlear efferent activity in awake guinea pigs. *Neuroreport* 15, 1379–1382. doi: 10.1097/01.wnr.0000131672.15566.64

Harrison, R. V., Sharma, A., Brown, T., Jiwani, S., and James, A. L. (2008). Amplitude modulation of DPOAEs by acoustic stimulation of the contralateral ear. *Acta Otolaryngol.* 128, 404–407. doi: 10.1080/00016480701784965

Iurato, S., Smith, C. A., Eldredge, D. H., Henderson, D., Carr, C., Ueno, Y., et al. (1978). Distribution of the crossed olivocochlear bundle in the chinchilla's cochlea. *J. Comp. Neurol.* 182, 57–76. doi: 10.1002/cne.901820105

James, A. L., Harrison, R. V., Pienkoesky, M., Dajani, H. R., and Mount, R. J. (2005). Dynamics of the real time DPOAE contralateral suppression in chinchillas and humans. *Int. J. Audiol.* 44, 118–129. doi: 10.1080/14992020400029996

Kawase, T., Delgutte, B., and Liberman, M. C. (1993). Antimasking effects of the olivocochlear reflex: II. Enhancement of auditory-nerve response to masked tones. *J. Neurophysiol.* 70, 2533–2549.

Larsen, E., and Liberman, M. C. (2009). Slow build-up of cochlear suppression during sustained contralateral noise: central modulation of olivocochlear efferents? *Hear. Res.* 256, 1–10. doi: 10.1016/j.heares.2009.02.002

León, A., Elgueda, D., Silva, M. A., Hamamé, C. M., and Delano, P. H. (2012). Auditory cortex basal activity modulates cochlear responses in chinchillas. *PLoS One* 7:e36203. doi: 10.1371/journal.pone.0036203

Liberman, M. C. (1989). Rapid assessment of sound-evoked olivocochlear feedback: suppression of compound action potential by contralateral sound. *Hear. Res.* 38, 47–56. doi: 10.1016/0378-5955(89)90127-5

Liberman, M. C., and Brown, M. C. (1986). Physiology and anatomy of single olivocochlear neurons in the cat. *Hear. Res.* 24, 17–36. doi: 10.1016/0378-5955(86)90003-1

Lilaonitkul, W., and Guinan, J. J. Jr. (2009). Human medial olivocochlear reflex: effects as functions of contralateral, ipsilateral and bilateral elicitor bandwidths. *J. Assoc. Res. Otolaryngol.* 10, 459–470. doi: 10.1007/s10162-009-0163-1

Müller, M., Hoidis, S., and Smolders, J. W. (2010). A physiological frequency-position map of the chinchilla cochlea. *Hear. Res.* 268, 184–193. doi: 10.1016/j.heares.2010.05.021

Popelár, J., Erre, J. P., Syka, J., and Aran, J. M. (2001). Effects of contralateral acoustical stimulation on three measures of cochlear function in the guinea pig. *Hear. Res.* 152, 128–138. doi: 10.1016/s0378-5955(00)00244-6

Puel, J. L., and Rebillard, G. (1990). Effect of contralateral sound stimulation on the distortion product 2F1–F2: evidence that the medial efferent system is involved. *J. Acoust. Soc. Am.* 87, 1630–1635. doi: 10.1121/1.399410

Puria, S., Guinan, J. J. Jr., and Liberman, M. C. (1996). Olivocochlear reflex assays: effects of contralateral sound on compound action potentials versus ear-canal distortion products. *J. Acoust. Soc. Am.* 99, 500–507. doi: 10.1121/1.414508

Rajan, R. (1995). Frequency and loss dependence of the protective effects of the olivocochlear pathways in cats. *J. Neurophysiol.* 74, 598–615.

Robertson, D. (1984). Horseradish peroxidase injection of physiologically characterized afferent and efferent neurons in the guinea pig spiral ganglion. *Hear. Res.* 15, 113–121. doi: 10.1016/0378-5955(84)90042-x

Robertson, D., and Gummer, M. (1985). Physiological and morphological characterization of efferent neurons in the guinea pig cochlea. *Hear. Res.* 20, 63–77. doi: 10.1016/0378-5955(85)90059-0

Robles, L., and Delano, P. H. (2008). "Efferent system," in *Handbook of The Senses, Audition*, eds P. Dallos and D. Oertel (San Diego: Academic Press), 413–445.

Sridhar, T. S., Liberman, M. C., Brown, M. C., and Sewell, W. F. (1995). A novel cholinergic "slow effect" of efferent stimulation on cochlear potentials in the guinea pig. *J. Neurosci.* 15, 3667–3678.

Velluti, R. A. (1997). Interactions between sleep and sensory physiology. *J. Sleep Res.* 6, 61–77. doi: 10.1046/j.1365-2869.1997.00031.x

Vetter, D. E., Saldaña, E., and Mugnaini, E. (1993). Input from the inferior colliculus to medial olivocochlear neurons in the rat: a double label study with PHA-L and cholera toxin. *Hear. Res.* 70, 173–186. doi: 10.1016/0378-5955(93)90156-u

Warr, W. B., and Guinan, J. J. Jr. (1979). Efferent innervation of the organ of Corti: two separate systems. *Brain Res.* 173, 152–155. doi: 10.1016/0006-8993(79)91104-1

Warren, E. H., and Liberman, M. C. (1989a). Effects of contralateral sound on auditory-nerve responses. I. Contributions of cochlear efferents. *Hear. Res.* 37, 89–104. doi: 10.1016/0378-5955(89)90032-4

Warren, E. H., and Liberman, M. C. (1989b). Effects of contralateral sound on auditory-nerve responses. II. Dependence on stimulus variables. *Hear. Res.* 37, 105–121. doi: 10.1016/0378-5955(89)90033-6

Winer, J. A., and Prieto, J. J. (2001). Layer V in cat primary auditory cortex (AI): cellular architecture and identification of projection neurons. *J. Comp. Neurol.* 434, 379–412. doi: 10.1002/cne.1183

Wolter, N. E., Harrison, R. V., and James, A. L. (2014). Separating the contributions of olivocochlear and middle ear muscle reflexes in modulation of distortion product otoacoustic emission levels. *Audiol. Neurotol.* 19, 41–48. doi: 10.1159/000356174

Zhao, W., and Dhar, S. (2012). Frequency tuning of the contralateral medial olivocochlear reflex in humans. *J. Neurophysiol.* 108, 25–30. doi: 10.1152/jn.00051.2012

Conflict of Interest Statement: The authors declare that the research was conducted in the absence of any commercial or financial relationships that could be construed as a potential conflict of interest.

Received: 08 November 2014; accepted: 08 February 2015; published online: 02 March 2015.

*Citation: Aedo C, Tapia E, Pavez E, Elgueda D, Delano PH and Robles L (2015) Stronger efferent suppression of cochlear neural potentials by contralateral acoustic stimulation in awake than in anesthetized chinchilla. Front. Syst. Neurosci. **9**:21. doi: 10.3389/fnsys.2015.00021*

This article was submitted to the journal Frontiers in Systems Neuroscience.

frontiers in
SYSTEMS NEUROSCIENCE

REVIEW ARTICLE
published: 02 December 2014
doi: 10.3389/fnsys.2014.00224

Short-term plasticity and modulation of synaptic transmission at mammalian inhibitory cholinergic olivocochlear synapses

***Eleonora Katz*[1,2]* and *Ana Belén Elgoyhen*[1,3]**

[1] *Instituto de Investigaciones en Ingeniería Genética y Biología Molecular "Dr. Héctor N. Torres" (INGEBI), Consejo Nacional de Investigaciones Científicas y Técnicas (CONICET), Buenos Aires, Argentina*
[2] *Departamento de Fisiología, Biología Molecular y Celular "Prof. Héctor Maldonado", Facultad de Ciencias Exactas y Naturales, Universidad de Buenos Aires, Buenos Aires, Argentina*
[3] *Tercera Cátedra de Farmacología, Facultad de Medicina, Universidad de Buenos Aires, Buenos Aires, Argentina*

Edited by:
Paul Hinckley Delano, Universidad de Chile, Chile

Reviewed by:
Elisabeth Glowatzki, Johns Hopkins University, USA
Sonja Pyott, University of North Carolina Wilmington, USA

***Correspondence:**
Eleonora Katz, Instituto de Investigaciones en Ingeniería Genética y Biología Molecular "Dr. Héctor N. Torres" (INGEBI), Consejo Nacional de Investigaciones Científicas y Técnicas (CONICET), Vuelta de Obligado 2490, Buenos Aires, 1428 CABA, Argentina
e-mail: eleokatz@gmail.com

The organ of Corti, the mammalian sensory epithelium of the inner ear, has two types of mechanoreceptor cells, inner hair cells (IHCs) and outer hair cells (OHCs). In this sensory epithelium, vibrations produced by sound waves are transformed into electrical signals. When depolarized by incoming sounds, IHCs release glutamate and activate auditory nerve fibers innervating them and OHCs, by virtue of their electromotile property, increase the amplification and fine tuning of sound signals. The medial olivocochlear (MOC) system, an efferent feedback system, inhibits OHC activity and thereby reduces the sensitivity and sharp tuning of cochlear afferent fibers. During neonatal development, IHCs fire Ca^{2+} action potentials which evoke glutamate release promoting activity in the immature auditory system in the absence of sensory stimuli. During this period, MOC fibers also innervate IHCs and are thought to modulate their firing rate. Both the MOC-OHC and the MOC-IHC synapses are cholinergic, fast and inhibitory and mediated by the $\alpha9\alpha10$ nicotinic cholinergic receptor (nAChR) coupled to the activation of calcium-activated potassium channels that hyperpolarize the hair cells. In this review we discuss the biophysical, functional and molecular data which demonstrate that at the synapses between MOC efferent fibers and cochlear hair cells, modulation of transmitter release as well as short term synaptic plasticity mechanisms, operating both at the presynaptic terminal and at the postsynaptic hair-cell, determine the efficacy of these synapses and shape the hair cell response pattern.

Keywords: medial olivocochlear system, efferent innervation, cochlear hair cells, synaptic transmission, calcium channels, calcium-activated potassium channels, $GABA_B$ receptors, short-term synaptic plasticity

INTRODUCTION

The organ of Corti, the mammalian sensory epithelium of the inner ear, has two types of mechanoreceptor cells, inner hair cells (IHCs) and outer hair cells (OHCs). In this sensory epithelium, vibrations produced by sound waves are transformed into electrical signals that depolarize the hair cell membranes (Hudspeth, 1997). Inner hair cells the phonoreceptors proper, release glutamate upon depolarization by incoming sounds and activate the auditory nerve fibers innervating them (Fuchs et al., 2003). Outer hair cells respond to variations in membrane voltage with changes in their length due to their electromotile property (Brownell et al., 1985). This enhances sound-evoked motion within the cochlear partition thereby amplifying the input to the IHCs. A descending efferent feedback pathway from the central nervous systems (CNS) reduces the sensitivity and sharp tuning of cochlear afferent fibers (Ashmore, 2008).

This efferent innervation is supplied by descending olivocochlear (OC) neurons (Rasmussen, 1955) and can be divided into two separate systems, namely the lateral and medial OC (MOC) systems (Warr, 1975, 1992; Guinan et al., 1983). In adult mammals, lateral OC (LOC) neurons whose somata are in the lateral superior olive (LSO) in the brainstem, project mainly to the ipsilateral cochlea and innervate the dendrites of spiral ganglion neurons (SGN) below the IHCs. Medial olivocochlear neurons, whose somata are in the medial periolivary region, project mostly (50–80% depending on species and cochlear region) to the contra lateral cochlea and make synaptic contacts with the OHC (Smith and Rasmussen, 1963; Liberman, 1980; Ginzberg and Morest, 1984; Liberman and Brown, 1986; Maison et al., 2003). The LOC and MOC systems are cholinergic but other neurotransmitters and neuromodulators like γ-aminobutiric acid (GABA), calcitonine gene-related peptide (CGRP) have also been found to be present in both types of OC fibers. In addition dopamine, and opiod peptides might also be expressed in LOC synaptic terminals (for an in depth description of the pharmacology and neurochemistry of the OC systems see Sewell, 2011). In rodents, the

first efferent fibers can be traced toward sensory epithelia around embryonic day (E) 13 (Fritzsch and Nichols, 1993; Fritzsch, 1996). Medial olivocochlear efferent neurons mature early and project transiently to the IHC region of the cochlea before reaching their final targets, the OHCs (Simmons et al., 1996; Simmons, 2002). By postnatal day (P) 0, efferent axons make transient axo-somatic synapses with the IHCs and start to appear below the OHC area by P2, the first synapses are seen by P4 (Simmons et al., 1996; Bruce et al., 2000; Simmons, 2002; Rontal and Echteler, 2003). At around the onset of hearing, P12 in altricial rodents, axo-somatic synapses on IHCs have almost completely disappeared and only the axo-dendritc synapses between LOC fibers onto Type I SGN can be observed below the IHC area (Simmons et al., 1996). At this stage, OC innervation acquires the adult profile described above, where only OHCs present MOC axo-somatic synapses (Simmons, 2002).

THE MEDIAL OLIVOCOCHLEAR SYSTEM INHIBITS OHC ACTIVITY

Medial olivocochlear neurons are activated by several feedback loops both from the periphery and cortical processing centers and regulate various aspects of auditory processing. Namely, the dynamic range of hearing (Guinan, 2011), the detection of relevant auditory signals (Maison et al., 2001), selective attention (Delano et al., 2007), and protection from noise-induced trauma (Rajan, 2000; Maison et al., 2002, 2013b; Taranda et al., 2009). When MOC fibers are activated by electrical stimuli, both sound-evoked movements in the cochlea and auditory nerve responses are reduced. This indicates that the MOC system reduces the gain of the cochlea by directly inhibiting OHC electromotile activity (Guinan, 2011). It has been demonstrated that the strength of cochlear inhibition is proportional to the firing frequency of MOC fibers (Galambos, 1956; Wiederhold and Kiang, 1970). Moreover, *in vitro* experiments using electrical stimulation suggest that the higher the rate of MOC activity, the higher the strength of synaptic inhibition at the MOC-OHC synapse (Ballestero et al., 2011).

THE MOC SYSTEM INHIBITS IHC SPONTANEOUS ACTIVITY BEFORE THE ONSET OF HEARING

Altricial rodents are deaf at birth and start to hear at around P12. Before hearing, IHCs fire action potentials which result from the activation of an inward Ca^{2+} current and the slowly activating delayed rectifier potassium channel IK_{neo} (Kros et al., 1998; Marcotti et al., 2003b; Johnson et al., 2011). There is no consensus however regarding the origin of these calcium action potentials in immature IHCs, as it has also been suggested that they are evoked by ATP released from supporting cells present in the organ of Kolliker (Tritsch et al., 2007). Notwithstanding, these Ca^{2+} action potentials, whether spontaneous or evoked by ATP, release the neurotransmitter glutamate at the first auditory synapse in the absence of sensory stimuli (Beutner and Moser, 2001; Glowatzki and Fuchs, 2002) and promote activity in the immature auditory system (Johnson et al., 2011; Sendin et al., 2014) which might be involved in directing the first stages of central synapse formation (Kandler, 2004). As mentioned above, mature IHCs are mainly innervated by the dendrites of SGN afferent fibers. However, during early postnatal development, IHCs receive transient axo-somatic contacts from MOC efferent fibers, even before they reach their final targets, the OHCs (Simmons et al., 1996; Simmons, 2002). This innervation, like that on mature OHCs, is cholinergic and inhibitory (Glowatzki and Fuchs, 2000; Elgoyhen et al., 2001; Katz et al., 2004). From P1 to P12, when exogenous ACh is applied or when the efferent fibers are electrically stimulated (Glowatzki and Fuchs, 2000; Goutman et al., 2005), IHCs are hyperpolarized and consequently, Ca^{2+} action potential frequency is reduced or even abolished. Interestingly, just after birth, at P0, the MOC-IHC synapse was found to be excitatory and to increase action potential frequency in the IHCs (Roux et al., 2011). Therefore, it is likely that this transient innervation interferes with the generation of Ca^{2+} action potentials (Marcotti et al., 2003a, 2004; Johnson et al., 2011; Sendin et al., 2014) thereby modulating the release of glutamate which occurs in the absence of sensory stimulation before the onset of hearing (Beutner and Moser, 2001; Glowatzki and Fuchs, 2002).

THE MOC-HAIR CELL SYNAPSE

MOLECULAR AND FUNCTIONAL PROPERTIES OF THE POSTSYNAPTIC RESPONSE

Hair cells are inhibited by the MOC system in a few milliseconds, however, this MOC-hair cell synapses differ from other inhibitory fast synapses which are mediated by a chloride conductance through GABA and/or glycine receptors (Alger, 1991; Betz et al., 1999). Medial olivocochlear-hair cell synapses are mediated by the activation of nicotinic cholinergic receptors (nAChR) that mediate fast excitatory synaptic responses (Dani and Bertrand, 2007; Martyn et al., 2009). The cellular mechanisms of this cholinergic inhibition and the molecular constituents involved are common among vertebrates (Art et al., 1984; Fuchs, 1992; Erostegui et al., 1994a,b; Evans, 1996; Fuchs, 1996; Nenov et al., 1996; Glowatzki and Fuchs, 2000; Oliver et al., 2000; Katz et al., 2011). At the MOC-hair cell synapse inhibition is brought about by ACh acting on a cholinergic nicotinic receptor highly permeable to Ca^{2+}, the α9α10 nAChR functionally coupled to the opening of Ca^{2+}-activated K^+ channels that hyperpolarize the OHC (Erostegui et al., 1994a; Evans, 1996; Nenov et al., 1996; Oliver et al., 2000; Wersinger et al., 2010; Ballestero et al., 2011; Wersinger and Fuchs, 2011). Pharmacological and immunohistochemical studies (Murthy et al., 2009a,b; Elgoyhen and Katz, 2012) together with molecular studies involving genetically modified mouse models (Vetter et al., 1999, 2007; Kong et al., 2008; Murthy et al., 2009a,b; Taranda et al., 2009) support this hypothesis.

Inhibition in cochlear hair cells is brought about by a nicotinic receptor, the α9α10 nAChR, coupled to the activation of calcium-activated potassium channels, namely, SK2 type channels (Glowatzki and Fuchs, 2000; Oliver et al., 2000; Gómez-Casati et al., 2005; Elgoyhen and Katz, 2012; see **Figures 1**, **2**) or BK channels (Wersinger et al., 2010; Wersinger and Fuchs, 2011). It has been described that when SK2 channels are blocked by apamin, a specific antagonist of these potassium channels, the cholinergic response at the cellular level changes from inhibitory to excitatory (Glowatzki and Fuchs, 2000; Katz et al., 2004; Marcotti et al., 2004; Gómez-Casati et al., 2005). Surprisingly, SK2 knockout mice lack these cholinergic excitatory efferent effects. The nAChRs are profoundly affected by deletion of the

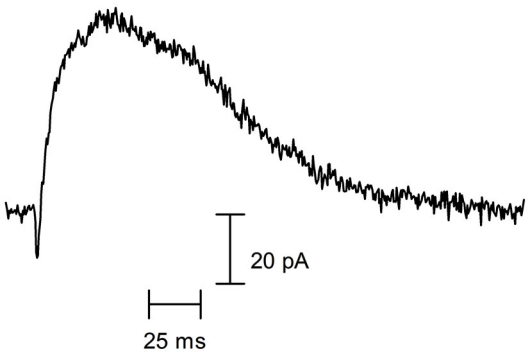

FIGURE 1 | Cholinergic synaptic currents of rodent cochlear hair cells. Representative spontaneous synaptic current recorded in a P10 OHC from a mouse apical cochlear coil, voltage-clamped at −60 mV (recording performed by Jimena Ballestero). As can be observed, a rapid inward current (mediated by the α9α10 nAChR) is curtailed by a larger and longer-lasting outward current (mediated by the SK2 K^+ channel).

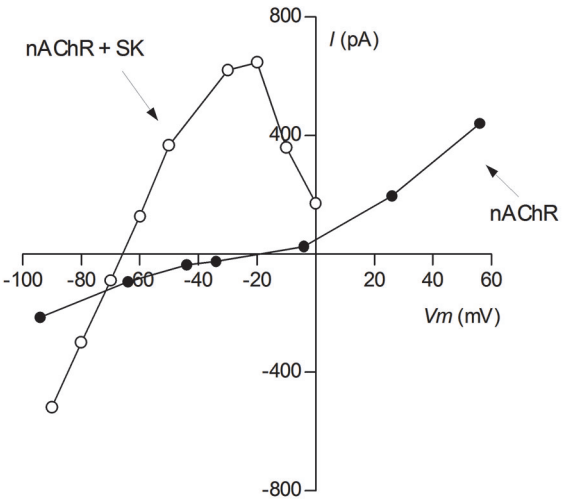

FIGURE 2 | Voltage sensitivity of cholinergic currents. Ionic currents were evoked by bath application of 100 μM ACh to voltage-clamped P9-11 rat IHCs. Reprentative I-V curves of isolated cholinergic currents (nAChR; intracellular solution CsCl-BAPTA + 1 nM apamin) and of those coupled to the SK2 channel (nAChR + SK2; intracellular solution KCl-EGTA) (This I-V curve was reproduced with permission from Figure 1A in Gómez-Casati et al., 2005).

SK2 gene whereas this deletion does not affect voltage-gated conductances in the hair cells. SK2-knockout OHCs and neonatal IHCs are completely insensitive to exogenous ACh and lack efferent synaptic currents, implying absent or dysfunctional nAChRs (Kong et al., 2008). It has been therefore suggested that the SK2 channel might have a central role at these synapses and that the nAChR/SK2 channel complex is assembled before being inserted in the hair cell membrane (Kong et al., 2008). However, during normal development, the transient efferent innervation to the IHCs is excitatory at the first postnatal day, meaning that the α9α10 nAChR is functional prior to the functional expression of the SK2 channel and its coupling to the cholinergic response (Roux et al., 2011). From P2 until P12–14, a stage at which this synapse disappears, cholinergic responses are inhibitory and always coupled to the activation of the SK2 channel (Katz et al., 2004; Goutman et al., 2005; Roux et al., 2011). Therefore, the absence of cholinergic responses in SK null mice could be due to the fact that OC fiber degeneration is also observed in these mice (Kong et al., 2008; Murthy et al., 2009a). Thus, apart from the lack of the SK2 protein to stabilize the synaptic complex, the lack of innervation, as shown at the neuromuscular junction (Sanes and Lichtman, 1999) and the absence of cross talk between the pre- and the postsynapse could also lead to alteration/disruption of the molecular components necessary for a cholinergic response.

It was recently shown that large conductance, calcium and voltage-gated (BK) potassium channels expressed by the OHCs at the area of efferent contacts, are the basis for ACh-mediated hyperpolarization in higher frequency regions of the rat cochlea (Wersinger et al., 2010). This differs from rat cochlear low frequency regions or the chicken hearing organ, where hair cell hyperpolarization is served by SK potassium channels (Fuchs and Murrow, 1992; Glowatzki and Fuchs, 2000; Wersinger and Fuchs, 2011). The calcium affinity of BK channels is two orders of magnitude lower than that of SK channels, requiring higher calcium influx for activation (Fakler and Adelman, 2008). Therefore, the amount of calcium entering through the α9α10 nAChR must play a key role in cholinergic inhibition in different regions of the cochlear axis and also in different species. In agreement with this notion, it has been shown recently that the Ca^{2+} permeability of α9α10 nAChRs is not uniform across species (Lipovsek et al., 2012, 2014). The Ca^{2+} permeability in chicken α9α10 nAChRs is unexpectedly low and similar to that of heteromeric neuronal nAChRs whereas in rat α9α10 nAChRs is high and similar to that of homomeric α7- and α8-containing receptors (Sgard et al., 2002; Weisstaub et al., 2002; Gómez-Casati et al., 2005; Lipovsek et al., 2012, 2014). Therefore, the increased Ca^{2+} permeability in the mammalian lineage (Lipovsek et al., 2014) might have evolved to help activate low-Ca^{2+}-affinity, high-conductance BK channels in mammalian basal OHCs, whereas Ca^{2+} influx provided by the non mammalian nAChR suffices to activate the high-Ca^{2+}-affinity, low-conductance SK channels (Fakler and Adelman, 2008; Wersinger et al., 2010; Wersinger and Fuchs, 2011; Lipovsek et al., 2012, 2014). To test this hypothesis further, it would be interesting to evaluate whether there are variations in the nAChR Ca^{2+} permeability between apical (coupled to SK) and basal OHCs (coupled to BK). The role of BK channels has been recently evaluated *in vivo* by comparing MOC efferent-mediated inhibition in BK knockout mice with that of their wild-type littermates. It was found that, both BK and SK channel significantly contribute to the MOC-efferent inhibition along most of the cochlear axis, except in the apical 20% of the cochlea, where it is difficult to evaluate the effects *in vivo* (Maison et al., 2013a).

Cholinergic inhibition of hair cells, therefore, relies on a rise in postsynaptic calcium to activate calcium-dependent potassium channels, irrespective of whether the α9α10 nAChR is coupled

either to the SK2 or to the BK channel or both. In addition, it has been postulated that inhibition involves the near-membrane postsynaptic cistern (Smith and Sjostrand, 1961; Saito, 1983; Fuchs, 2014; Fuchs et al., 2014). Since the synaptic cistern is co-extensive with the efferent terminals, lying only 14 nm apart from the postsynaptic membrane (Fuchs et al., 2014), it defines a restricted diffusion space that might play an important role in calcium kinetics. This synaptic cistern has been proposed to serve as a calcium store, similar to the sarcoplasmic reticulum that supports contraction in muscle. The participation of a calcium store is supported by the effects of ryanodine and other store-active agents (Sridhar et al., 1997; Evans et al., 2000; Lioudyno et al., 2004). Experiments *in vitro* performed in OHCs, show that caffeine, a store depleting compound, potentiates whereas ryanodine (a modulator of calcium induced-calcium release) and ciclopiazonic acid (an antagonist of the sarcoplasmic/endoplasmic reticulum calcium ATPase, SERCA) reduce the amplitude of synaptic ACh currents and also the amplitude of currents evoked by exogenously applied ACh (Evans et al., 2000; Lioudyno et al., 2004). Evaluation of the MOC-efferent effects in experiments performed *in vivo* show that cochlear perfusion with ryanodine, ciclopiazonic acid and thapsigargin (another SERCA antagonist), enhances the magnitude of the efferent effects (Sridhar et al., 1997). Even though the *in vitro* and *in vivo* results show differences in the effects of both ryanodine and store-active compounds in the magnitude and sign of their effects, they nevertheless suggest that cholinergic inhibition might be due to both influx of calcium from the extracellular space and calcium release from the synaptic cistern (Fuchs, 2014). However, the short time course of efferent synaptic currents (Oliver et al., 2000) and the voltage-dependence of ACh-evoked currents (Martin and Fuchs, 1992) suggest that the cholinergic response is due only to calcium influx. Very recently, it was proposed (Fuchs, 2014) that the cisterns could act both as a store that releases calcium or as a sink, a fixed buffer that absorbs calcium allowing the rapid decay of cholinergic currents (Glowatzki and Fuchs, 2000; Oliver et al., 2000; Katz et al., 2004; Gómez-Casati et al., 2005; Ballestero et al., 2011). Thus, depending on the degree of activity, and therefore on the amount of calcium accumulated in the cisterns, cholinergic inhibition would take place by calcium influx from the extracellular space or by a combination of calcium influx and calcium release from internal stores (Fuchs, 2014).

MOLECULAR AND FUNCTIONAL PROPERTIES OF TRANSMITTER RELEASE AT MOC-HAIR CELL SYNAPSES

Calcium channels coupled to ACh release at MOC synaptic terminals

Neurotransmitter release at fast synapses takes place when the action potential invades and depolarizes the synaptic terminal which promotes the activation of Ca^{2+} channels and the consequent increase in cytosolic Ca^{2+} (Katz and Miledi, 1969). The release of neurotransmitter is triggered by Ca^{2+} influx through presynaptic voltage-gated Ca^{2+} channels (VGCC; Katz and Miledi, 1969). In mammals, fast synaptic transmission at both central and peripheral synapses is mediated by multiple types of VGCCs, including N-type, P/Q type and R-type (Katz et al., 1997; Plant et al., 1998; Reid et al., 2003; Catterall and Few, 2008; Catterall, 2011). Voltage-gated Ca^{2+} channels are formed by at least four different subunits (α1, α2-δ, β, sometimes also γ). The existence of multiple pore-forming α1 subunits accounts for the biophysical and pharmacological diversity of VGCCs. So far, 10 different α1 genes have been found and they have been divided into three families: $Ca_v1.1$ (α1S), $Ca_v1.2$ (α1C), $Ca_v1.3$ (α1D) and $Ca_v1.4$ (α1F) all giving rise to L-type Ca^{2+} currents; $Ca_v2.1$ (α1A), $Ca_v2.2$ (α1B) and $Ca_v2.3$ (α1E) giving rise to P/Q, N and R-type Ca^{2+} currents, respectively; and $Ca_v3.1$ (α1G), $Ca_v3.2$ (α1H) and $Ca_v3.3$ (α1I) all giving rise to T-type currents (Catterall, 1998, 2011; Catterall and Few, 2008). In the mouse cochlea, the occurrence of the α1 subunits $Ca_v1.2$ (L-type), $Ca_v1.3$ (L-type) and $Ca_v2.3$ (R-type) has been shown by PCR analysis (Green et al., 1996). In addition, the α1A (P/Q-type) and α1G (T-type) were also found, by analyzing the ion channel transcriptome, to be expressed in the mammalian inner ear (Gabashvili et al., 2007).

Transmitter release from the IHC ribbon synapse has been shown to be mediated by L-type currents (Platzer et al., 2000; Brandt et al., 2003) and that the $Ca_v1.3$ subunit is the predominant α1 subunit in neonatal IHCs and OHCs (Platzer et al., 2000; Michna et al., 2003; Layton et al., 2005). Using immunocytochemical techniques, Waka et al. (2003), reported that from P2 to P14 the predominant VGCC type expressed by medial efferent fibers is the $Ca_v2.3$, or R-type VGCC, whereas as of P14 onwards the predominant subunit is $Ca_v1.2$, suggesting that L-type channels might be involved in the release of ACh from MOC efferent fibers in adult mice.

By using an electrophysiological and pharmacological approach in the acutely isolated cochlear mouse preparation at P9–11, it has been shown that ACh release at the efferent-IHC synapse is supported by both N ($Ca_v2.2$) and P/Q-type ($Ca_v2.1$) VGCCs (Zorrilla de San Martín et al., 2010). At different synapses as well as at different developmental stages, differences in the relative contribution of P/Q- and N-type VGCC to synaptic transmission have been reported (Iwasaki et al., 2000; Ishikawa et al., 2005). Moreover, is has been shown that transmitter release is more strongly dependent on the Ca^{2+} concentration for P/Q- than for N-type VGCCs. In cerebellar synapses, Ca^{2+} cooperativity is around 4 and 2.5 for P/Q- and N-type VGCCs, respectively (Mintz et al., 1995). At the MOC-IHC synapse, cooperativity is around 2.5 (Zorrilla de San Martín et al., 2010), suggesting that at the transient MOC-IHC synapse, at least two Ca^{2+} ions are necessary to trigger the release of one ACh vesicle (Dodge and Rahamimoff, 1967). Notwithstanding, in the above mentioned work, Ca^{2+} cooperativity was assayed without discriminating between the two types of VGCC that support release. Therefore, it would be interesting to study whether the N- or the P/Q-type VGCC is more efficiently coupled to the release machinery at the MOC-IHC synapse.

Inhibition of ACh release by L-type VGCC functionally coupled to BK channels

BK channel activation requires membrane depolarization and high intracellular Ca^{2+} (Fakler and Adelman, 2008). These two conditions are usually achieved during the release of neurotransmitter. Therefore, BK channels have been shown to accelerate the repolarizing phase of the action potential and thereby terminate

the release process (Vergara et al., 1998; Fakler and Adelman, 2008). It has been reported that activation of BK channels requires Ca^{2+} influx through closely coupled L-type VGCCs (Storm, 1987; Lingle et al., 1996; Prakriya et al., 1996). BK channels have low Ca^{2+} affinity (Fakler and Adelman, 2008), therefore, the formation of macromolecular complexes between BK channels and VGCC is necessary for reliably activating BK channels by Ca^{2+} influx without affecting other Ca^{2+}-dependent intracellular processes (Fakler and Adelman, 2008).

Before the onset of hearing, BK channels were shown by immunofluorescence to be present at the MOC synaptic terminals making axo-somatic contacts with the IHCs (Zorrilla de San Martín et al., 2010). Moreover, by electrophysiological recordings and the use of specific BK channel and L-type VGCC agonists and antagonists, it has been demonstrated that BK channels are functionally coupled to the activation of L-type VGCC (Zorrilla de San Martín et al., 2010). Those experiments show that when an action potential invades MOC synaptic terminals, P/Q-, N-, and L-type VGCCs are activated. Influx of Ca^{2+} via P/Q- and N-type VGCCs, closely associated to the release machinery, support release. Whereas, influx of Ca^{2+} via L-type VGCCs functionally associated to BK channels, and possibly farther away from the release machinery (Urbano et al., 2001; Flink and Atchison, 2003), together with membrane depolarization, would activate BK channels. BK channel activation would accelerate the repolarization of the MOC synaptic terminal membrane and ACh release would be reduced (Storm, 1987; Marcantoni et al., 2007) (this model is schematized in **Figure 3**).

It remains to be determined if, as reported for the transient MOC-IHC synapse (Zorrilla de San Martín et al., 2010), BK channels are also functionally expressed at the MOC synaptic terminals innervating the OHCs. So far, results from *in vivo* experiments with $slo^{-/-}$ mice, which lack the BK alpha subunit, suggest that in adult mice, BK channels are not expressed by the efferent presynaptic terminals contacting the OHCs (Maison et al., 2013a). The authors argue that if BK channels were functionally expressed by the efferent terminals contacting OHCs, the knockout phenotype should show increased efferent effects, due to increased ACh release at the MOC-OHC synapse as shown at the MOC-IHC synapse (Zorrilla de San Martín et al., 2010). However, $Slo^{-/-}$ mice were found to be characterized by reduced efferent effects (Maison et al., 2013a) which is more consistent with the postsynaptic role of BK channels at the MOC-OHC synapse (Wersinger et al., 2010). It can be misleading, however, to directly compare results from *in vitro* synaptic physiology with results obtained from *in vivo* experiments as those used to evaluate the MOC efferent effects. Notwithstanding, one can also argue that the lack of BK channels during development might have altered synaptic strength at the MOC-OHC synapse by changing the balance between regulatory mechanisms, namely GABA acting through presynaptic $GABA_B$ receptors (Wedemeyer et al., 2013), the coupling of L-type VGCC to BK channels (Zorrilla de San Martín et al., 2010) as well as NO released from the postsynaptic cell upon efferent stimulation (Kong et al., 2013). Moreover, the size of the efferent terminals in the $slo^{-/-}$ mice is reduced throughout the cochlear spiral (Maison et al., 2013a), this suggests that the lack of BK channel functional expression alters the normal MOC-hair cell synapse development and could also explain in part the reduced magnitude of efferent suppression in these mice. BK channels have been shown, at the light-microscopic level, to be expressed at the interface between presynaptic MOC terminals and the postsynaptic OHC membrane (Hafidi et al., 2005; Engel et al., 2006; Wersinger et al., 2010; Maison et al., 2013a), suggesting a postsynaptic localization for these calcium-activated K^+ channels. However, an electron microscopic study carried out in adult mice shows by immunogold labeling that at the MOC-OHC synapse, BK channels are localized at both pre and postsynaptic membranes (Sakai et al., 2011). Therefore, in order to determine whether BK channels are functionally expressed by the MOC synaptic terminals contacting OHCs, it is necessary to evaluate the strength of synaptic transmission by electrophysiological experiments in wild-type mice in the presence of specific blockers of these channels both during development and adulthood.

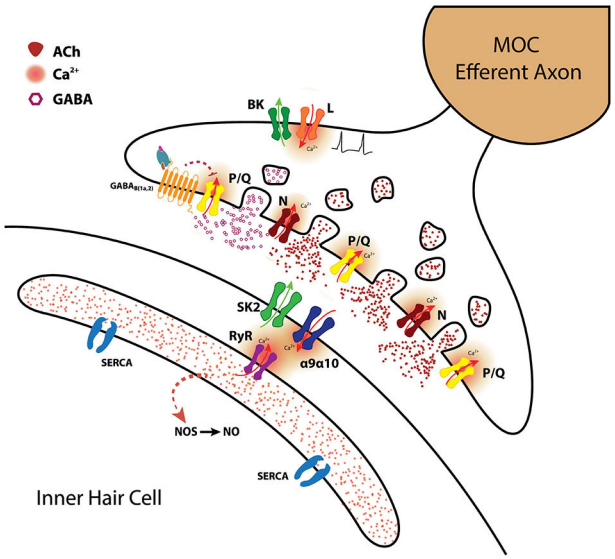

FIGURE 3 | The MOC-hair cell synapse. Schematic representation of the molecules and mechanisms involved in synaptic transmission at MOC-hair cell synapses from the apical region of the organ of Corti. ACh release is supported by both P/Q and N-type VGCC. BK channels activated by Ca^{2+} entering through L-type VGCC accelerate action potential repolarization and thus diminish the amount of ACh being released (Zorrilla de San Martín et al., 2010). γ-aminobutiric acid probably co-released with ACh, activates presynaptic $GABA_{B(1a,2)}R$ which inhibit ACh release by altering the activity of P/Q-type VGCC (Wedemeyer et al., 2013). The inhibitory postsynaptic response is mediated by α9α10 nAChR coupled to the activation of SK2 K^+ channels (Glowatzki and Fuchs, 2000; Elgoyhen et al., 2001; Katz et al., 2004; Gómez-Casati et al., 2005). Ca^{2+}-induced Ca^{2+} release from the postsynaptic cisterns closely apposed to the IHC synaptic region probably also contributes to SK2 activation (Fuchs, 2014). Nitric oxide synthetized by the IHC in response to 1 Hz stimulation of the MOC fibers enhances transmitter release by the MOC synaptic terminals acting as a retrograde messenger (Kong et al., 2013). (SERCA: sarcoendoplasmic reticulum calcium ATPase; RyR: Ryanodine receptor; NOS: nitric oxide synthase; NO: nitric oxide) This drawing was kindly performed by Marcelo Moglie.

Inhibition of ACh release by the GABAergic system

Medial olivocochlear synapses are mainly cholinergic, however, a profuse GABAergic innervation has been described close to

the IHC and OHC regions (Fex and Altschuler, 1986; Vetter et al., 1991; Eybalin, 1993; Maison et al., 2003). In addition, it has been shown that GABA co-localizes with ACh in almost all efferent terminals of the OC system in adult mice (Maison et al., 2003). Experiments carried out *in vivo* with mice lacking different $GABA_A$ receptor subunits presented cochlear dysfunction and suggest that the GABAergic component of the OC system contributes to the long-term maintenance of hair cells and superior cervical ganglion (SCG) neurons in the inner ear (Maison et al., 2006). Furthermore, the phenotypic analysis of $GABA_{B1}$ knockout mice indicated that GABAergic signaling might be required for normal OHC amplifier function (Maison et al., 2009). Moreover, OHC stiffness and motility have been shown to be sensitive to exogenously applied GABA (Gitter and Zenner, 1992; Batta et al., 2004). Guinea pig OHCs have been shown to hyperpolarize upon GABA application to the extracellular medium (Gitter and Zenner, 1992) which suggests that those cells might express $GABA_A$ postsynaptic receptors. However, postsynaptic GABA-activated currents were not found either in mouse IHCs (P9–11) or OHCs (P12–16) indicating that postsynaptic $GABA_A$ receptors if present, are not functional in the organ of Corti of developing mice (Wedemeyer et al., 2013). Two other evidences support the notion that fast synaptic transmission at the MOC-hair synapse is cholinergic and mediated only by the postsynaptic α9α10 nAChR: (1) no postsynaptic currents are observed in the OHCs and the IHCs in response to either K^+ elevation or electrical stimulation of the MOC efferent axons if the α9α10 nAChR is pharmacologically blocked (Glowatzki and Fuchs, 2000; Oliver et al., 2000; Ballestero et al., 2011); and (2) no postsynaptic currents are observed in α9 knockout mice (Vetter et al., 2007).

Interestingly, using pharmacological and electrophysiological approaches, together with mutant mouse lines lacking specific $GABA_BR$ subtypes, a physiological role for GABA in MOC efferent synaptic transmission has been recently demonstrated (Wedemeyer et al., 2013). Activation of presynaptic $GABA_BRs$ by baclofen, a selective $GABA_BRs$ agonist, inhibits the release of ACh from OC-IHC terminals in P9–11 mouse cochlear explants. Moreover, incubation with a selective $GABA_BR$ antagonist, CGP35348, significantly increases the quantum content of evoked release, demonstrating the presence of pre-synaptic $GABA_B$ receptors. Furthermore, inhibition of transmitter release by GABA at the MOC-IHC synapse is most likely mediated through inhibition of P/Q- but not N-type VGCCs (Wedemeyer et al., 2013). In addition, CGP35348 also enhances evoked release at the MOC-OHC synapse in P9–16 mice, suggesting that presence of functional $GABA_B$ receptors at this synapse as well. The dimerization of two subunits, $GABA_{B1}$ and $GABA_{B2}$, is required to make up functional $GABA_BRs$ (Jones et al., 1998; Kaupmann et al., 1998; White et al., 1998; Kuner et al., 1999). The molecular variability of $GABA_BR$ is due to the existence of two different GB1 isoforms, 1a and 1b (Bettler et al., 2004). By making use of $GABA_B$ subunit specific KO mice, it was also shown that GABA acting on presynaptic $GABA_{B(1a,2)}R$ inhibited the release of ACh at the MOC-IHC synapse (Wedemeyer et al., 2013). Immunostaining experiments in transgenic $GABA_{B1}$-GFP mice, further demonstrated the expression of $GABA_BRs$ in OC terminals innervating both IHCs and OHCs during development (P9–16). Those results are consistent with evidence indicating that the GB1a isoform is mainly expressed by the presynaptic terminals whereas the GB1b is usually found at the postsynapse (Perez-Garci et al., 2006; Vigot et al., 2006). Therefore, GABA released at both the MOC-IHC and MOC-OHC cholinergic inhibitory synapses activates presynaptic $GABA_BRs$ that inhibit the release of ACh thus reducing inhibition. This agrees with the widely described role of GABA in presynaptic modulation of synaptic transmission at mammalian glutamatergic and GABAergic synapses (Gaiarsa et al., 1995a,b; Brenowitz et al., 1998; Chalifoux and Carter, 2011a,b).

Immunohistochemistry experiments have revealed that both $GABA_B$ receptors and GAD, the GABA synthetic enzyme, are present in the synaptic terminals contacting both IHCs and OHCs close to hearing onset (Wedemeyer et al., 2013). This is consistent with previous data showing that the GABAergic input to the mammalian cochlea arises solely from the OC system (Fex and Altschuler, 1986; Thompson et al., 1986; Vetter et al., 1991; Eybalin, 1993; Maison et al., 2003). However, in adult mice, $GABA_BRs$ have not been found in OC efferent terminals making synaptic contacts in the IHC or the OHC regions (Maison et al., 2009), a result that might indicate that presynaptic modulation of ACh release by $GABA_B$ receptors is limited to the developing MOC system. Adult IHCs are not innervated by the MOC system (Liberman, 1980; Simmons, 2002), so the lack of $GABA_BRs$ at the IHC area is not surprising. However, OHCs are innervated by MOC fibers since the second postnatal week throughout life (Liberman, 1980; Simmons, 2002). Expression of functional $GABA_BRs$ in MOC fibers innervating the OHCs (Wedemeyer et al., 2013) might be transient, and this needs to be further explored. Alternatively, $GABA_B$ receptors might be present in adult OHC efferent terminals but the expression level might be below that detected by immunostaining methods.

GABA and ACh were reported to be co-localized in the same MOC terminals (Maison et al., 2003). Therefore, it is likely that both neurotransmitters are co-released from the same terminal when the efferent fibers are activated. Co-release of these two neurotransmitters was described in retinal starburst amacrine cells, but in this case both GABA and ACh act at postsynaptic receptors (Duarte et al., 1999; Lee et al., 2010). At the OC-hair cell synapse, however, ACh release is modulated by putatively co-released GABA by activating $GABA_B$ autoreceptors. Presynaptic inhibition of ACh release via $GABA_BRs$ might be involved in shaping the short term plasticity properties of the MOC-hair cell synapses (see Section Short-term Plasticity at Olivocochlear Synapses).

Retrograde enhancement of ACh release by nitric oxide

It has been shown recently that nitric oxide (NO), probably released by the IHCs in response to low frequency stimulation (1 Hz) of the efferent MOC fibers, increases the efficacy of transmitter release at the MOC synaptic terminals acting as a retrograde signal (Kong et al., 2013). Both IHCs and OHCs can produce NO in response to ATP-evoked calcium influx (Shen et al., 2006), and NO synthase immunoreactivity has been described throughout the cochlear epithelium, including hair

cells, and afferent and efferent nerve endings (Heinrich et al., 1997; Riemann and Reuss, 1999). It still remains to be elucidated however, the mechanism by which NO enhances release. Nitric oxide stimulates guanylate cyclase to produce cyclic GMP, leading to cGMP-dependent phosphorylation of vesicular release proteins and thus might alter the synaptic protein interactions that regulate neurotransmitter release and synaptic plasticity (Meffert et al., 1996). In addition, NO might alter channel gating by direct nitrosylation of the channel protein (Bredt and Snyder, 1994). Therefore, it would be interesting to evaluate whether NO enhances the activity of either P/Q and/or N-type VGCCs or if it interferes with the negative feedback loop involving functionally coupled L-type VGCCs and BK channels described at the MOC-IHC transient synapse (Zorrilla de San Martín et al., 2010).

SHORT-TERM SYNAPTIC PLASTICITY

Synapses are endowed with an extraordinary capacity to change according to their previous history. Several forms of activity-dependent synaptic plasticity shape synaptic output (Zucker and Regehr, 2002). Short-term plasticity (STP) lasts from tens of milliseconds to several minutes and can modify synaptic strength, which can be reduced for hundreds of milliseconds to seconds (depression), or it can be enhanced for hundreds of milliseconds to seconds (facilitation), to tens of seconds to minutes (augmentation and post-tetanic potentiation, PTP). The interaction between multiple forms of plasticity will lead to the observed net plasticity at any given synapse. In many cases, facilitation, depression, PTP and longer lasting depression co-exist, but the relative salience of each mechanism is controlled by the initial release probability and the presynaptic activity pattern (Zucker and Regehr, 2002; Fioravante and Regehr, 2011). Synapses with a high probability of release tend to depress, whereas those with a low probability of release usually facilitate when challenged by two closely spaced stimuli (Fioravante and Regehr, 2011). The origin of STP is thought to be mainly of presynaptic origin, although under certain conditions postsynaptic mechanisms have been shown to be involved (Dittman et al., 2000; Schneggenburger et al., 2002; Wang and Manis, 2008). Regulation of VGCCs has not been generally considered as a major mechanism in STP, however it has been recently shown that regulation of VGCC can mediate STP (Catterall and Few, 2008; Catterall et al., 2013). There is accumulated evidence indicating that facilitation is caused by an elevated intracellular Ca^{2+} concentration that remains from the previous stimulus. Residual Ca^{2+} is thought to increase the release probability by binding to a Ca^{2+} sensor different from the one that mediates evoked exocytosis (Schneggenburger et al., 2002). Short-term synaptic depression upon high frequency stimulation is thought to arise due to depletion of a readily releasable pool of vesicles (RRP; Atluri and Regehr, 1996; Neher, 1998; Schneggenburger et al., 2002).

SHORT-TERM PLASTICITY AT OLIVOCOCHLEAR SYNAPSES

The main function of the vertebrate efferent system is well conserved among species. Namely, it inhibits the activity of hair cells and thereby regulates the dynamic range of hearing (see Guinan, 2011). A low probability of release at rest and facilitation of responses during high-frequency discharges has been reported in the turtle papilla (Art et al., 1984), at the transient MOC efferent synapse to mammalian IHCs before the hearing onset (Goutman et al., 2005) and more recently also at the MOC-OHC synapse (Ballestero et al., 2011). These well conserved synaptic mechanisms suggest they are relevant for regulating auditory function.

In rat P9–11 MOC-IHC synapses, transmitter release increases upon high frequency stimulation (40 Hz) of the MOC fibers due to presynaptic facilitation and postsynaptic summation (Goutman et al., 2005). Surprisingly, the same stimulation pattern, and using the same cochlear preparation produced depression in MOC-IHC synapses from P9–11 mice (Zorrilla de San Martin et al., 2012). The quantum content of ACh release at both synapses was found to be similar and low (around 1), so other factors (i.e., size or rate of replenishment of the readily releasable pool of vesicles (RRP), the Ca^{2+} channels supporting and/or modulating release) might account for this species differences.

By performing whole-cell recordings in voltage-clamped mouse OHCs while electrically stimulating the MOC efferent fibers innervating them (**Figure 4**), Ballestero et al. (2011) showed how synaptic transmission is tuned at the MOC-OHC synapse. At a stimulation frequency of Hz transmitter release at the MOC-OHC occurs with low probability (quantum content ∼0.4). When the stimulation frequency is raised, the efficacy of release increases due to presynaptic facilitation. In addition, the relatively slow decay of evoked inhibitory postsynaptic currents (eIPSCs) (combined nAChR and SK2 IPSCs; see **Figure 1**) causes temporal summation at frequencies >10 Hz. Facilitation and summation give rise to a frequency-dependent increase in the amplitude of inhibitory currents in OHCs (**Figure 5**; Ballestero et al., 2011).

The properties of the MOC-OHC synapse described by Ballestero et al. (2011) are consistent with *in vivo* studies performed to evaluate the MOC efferent effects on hearing. Electrical stimulation of MOC neurons only inhibits auditory function efficiently when high frequency trains are applied (Galambos, 1956; Wiederhold and Kiang, 1970; Mountain, 1980; Gifford and Guinan, 1987). Moreover, the strength of the efferent effect increases linearly upon increasing the stimulation rate, not only in mammals (Galambos, 1956; Wiederhold and Kiang, 1970; Brown and Nuttal, 1984; Gifford and Guinan, 1987) but also in other vertebrates (Flock and Russell, 1976; Art et al., 1984; Figure 12A). In addition, MOC firing rate increases with sound intensity (Robertson and Gummer, 1985; Brown, 1989; Brown et al., 1998) leading to a greater gain reduction upon exposure to intense sounds. This is in agreement with the hypothesis that the MOC system protects the auditory system from acoustic trauma (Rajan, 2000; Taranda et al., 2009).

Efferent synaptic terminals from various species were shown by electron microscopy studies to have a large number of synaptic vesicles (Lenoir et al., 1980; Nadol, 1988; Simmons et al., 1996; Bruce et al., 2000). Therefore, the low probability of release at the MOC-OHC synapse at low frequency stimulation (Ballestero et al., 2011) cannot be accounted for by vesicle availability (Schikorski and Stevens, 1997; Xu-Friedman and Regehr, 2004). Moreover, the fact that synaptic output at the MOC-OHC synapse

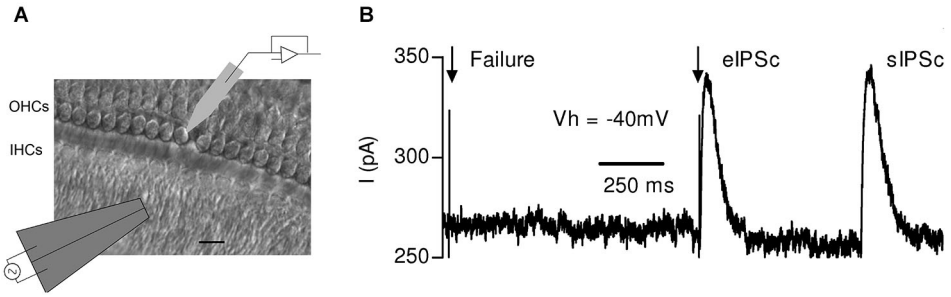

FIGURE 4 | Synaptic responses evoked by electrical stimulation of the MOC efferent fibers in mouse OHCs. (A) Schematic representation of the experimental setup: OHCs from the first row were recorded with a patch pipette while electrical shocks were delivered to the MOC fibers through an extracellular bipolar theta glass pipette positioned ~10–20 μm below the IHCs. Scale bar 10 μm.**(B)** Representative trace obtained in an OHC in response to two single electrical shocks (arrows). The figure shows one evoked and one spontaneous inhibitory postsynaptic current (eIPSC) and (sIPSC), respectively, and also a failure of response upon nerve stimulation. (Reproduced with permission from Figure 1 in Ballestero et al., 2011).

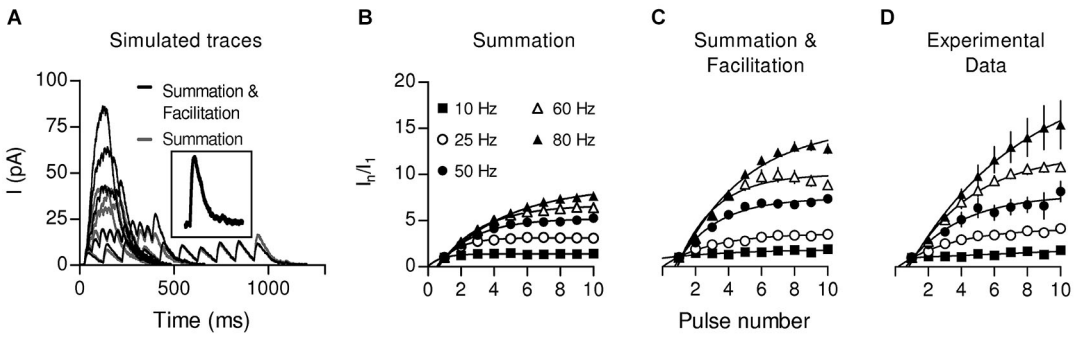

FIGURE 5 | Summation and Facilitation contribute to the increment of the postsynaptic response during high frequency stimulation. To estimate the effect of summation during high frequency stimulation, simulated responses were constructed from a single-shock response (**A**, inset) considering only temporal summation (gray traces) or considering facilitation by also taking into account the change in the probability of release (black traces) for every shock. Plots of normalized current vs. pulse number were constructed from the simulation considering only summation **(B)** or summation and facilitation **(C)**. **(D)** Plot of normalized current vs. pulse number derived from the experimental data. (Reproduced with permission from Figure 7 in Ballestero et al., 2011).

can be sustained during prolonged periods even at high stimulation frequencies (Ballestero et al., 2011), gives further support to the hypothesis that vesicle availability is not the limiting factor.

Some synapses have a low initial release probability and present strong facilitation. They respond with high efficacy only to high frequency stimulation (Lisman, 1997) and function as "high-pass filters" (Fortune and Rose, 2001). This mechanism, which implies that spontaneous or infrequent MOC discharges are ignored, would determine a threshold for efficient cochlear suppression. In mammals, this could be of great relevance as it was shown that MOC fibers fire regularly but with variable frequencies (Robertson and Gummer, 1985; Liberman and Brown, 1986; Brown, 1989). Moreover, summation and facilitation at the MOC-OHC synapse can grade efferent inhibition according to MOC discharge rate, thus fine tuning cochlear amplification. The firing rate of MOC fibers increases linearly with sound intensity (Robertson and Gummer, 1985; Liberman and Brown, 1986; Brown, 1989). Besides, upon activation by sound MOC fiber discharge rate is modulated by stimulus properties such as intensity, origin, and type (Brown et al., 1998). In this scenario, the short term plasticity properties of the MOC-OHC synapse seem to be highly relevant for encoding graded levels of efferent feedback. This has been illustrated in **Figure 6**, where it is shown that the reduction in auditory brain response amplitude upon increasing the frequency of MOC stimulation (Galambos, 1956; Art and Fettiplace, 1984; Gifford and Guinan, 1987) is in agreement with the increment in the amplitude of OHC synaptic responses when the frequency of stimulation of the MOC efferent fibers is increased (Ballestero et al., 2011).

DEVELOPMENTAL MOLECULAR AND FUNCTIONAL CHANGES AT THE MOC-IHC SYNAPSE

As described above, IHCs are transiently innervated by fibers of the MOC system which make functional axo-somatic contacts with these cells since birth until the onset of hearing (P12 in mice and rats) (Glowatzki and Fuchs, 2000; Simmons, 2002; Katz et al., 2004; Roux et al., 2011). During development, synaptic modifications take place concurrently in both postsynaptic cells and presynaptic terminals. The transient MOC-IHC synapse is no

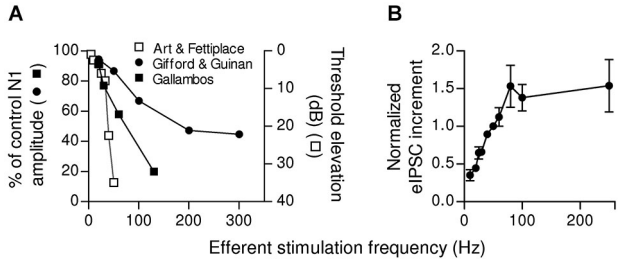

FIGURE 6 | Dependence of afferent function and OHCs inhibitory responses on the frequency of efferent stimulation. (A) Relationship between the frequency of MOC activation and inhibition of afferent activity in the cat (adapted from Galambos, 1956; Gifford and Guinan, 1987) and in the turtle (adapted from Art and Fettiplace, 1984). In the left y-axis efferent effect was quantified as the ratio between the amplitude of the N1 component of the compound action potential (CAP) produced by moderate sound stimulation (10–25 dB above threshold) with or without efferent stimulation (($N1_{w/shock}/N1_{ctrl}$)x100, (Galambos, 1956; Gifford and Guinan, 1987). The right y-axis shows the increase in sound intensity (Threshold shift in dB) necessary to evoke an afferent discharge as a function of the efferent stimulation frequency (Art and Fettiplace, 1984). **(B)** Increment in eIPSC amplitudes (mean ± SEM) after 10 shocks of efferent stimulation at different frequencies. Due to data variability, the values from different cells were normalized to the increment in the amplitude of the response at a stimulation frequency of 50 Hz. Note that in both afferent activity **(A)** and OHCs eIPSCs **(B)**, there is a range of frequencies where there is a linear relationship between the frequency of MOC activation and the increment in inhibition. (Reproduced with permission from Figure 12 in Ballestero et al., 2011).

exception and it undergoes dramatic changes both in the cholinergic sensitivity, the expression of key postsynaptic molecules (Katz et al., 2004; Marcotti et al., 2004; Roux et al., 2011), as well as in the pattern of innervation (Simmons, 2002; Katz et al., 2004; Roux et al., 2011). Thus, the expression of the nAChR α10 subunit and the SK2 channel are down regulated and disappear after the onset of hearing (Katz et al., 2004). This is accompanied by a retraction of the axo-somatic contacts to these cells (Simmons, 2002). Even though, the mRNA for the α9 subunit is present in IHCs throughout life (Elgoyhen et al., 1994, 2001), no cholinergic responses can be found in these cells after the onset of hearing (Katz et al., 2004; Roux et al., 2011). Cholinergic responses at P0 are excitatory as they are not coupled to the SK2 channel (Roux et al., 2011) and they dramatically increase from P1 towards P7–9, they start to decline at around P12 to completely disappear after P14, consistent with the down regulation of the expression of the α10 subunit and the SK2 channel (Katz et al., 2004; Roux et al., 2011).

Ca^{2+} channels coupled to transmitter release are developmentally regulated both at central synapses (Momiyama, 2003; Fedchyshyn and Wang, 2005) and at the neuromuscular junction (Rosato Siri and Uchitel, 1999). In agreement with this notion, it has been recently shown that there are significant changes in the types VGCC that support and/or modulate the release process at the MOC-IHC synapse during the short period at which it is functional. Namely, at P9–11, P/Q and N-type VGCC support release whereas Ca^{2+} through L-type VGCC activate BK channels (Zorrilla de San Martín et al., 2010). At P5–7, N-type channels are not functionally expressed by the transient MOC synaptic terminals and transmitter release is supported by P/Q and R-type VGCC (Zorrilla de San Martin et al., 2012; Kearney et al., 2014). Moreover, at P5–7, L-type VGCC, both support release and activate BK channels (Kearney et al., 2014), indicating that at an earlier stage of development, the presynaptic terminal might be less compartmentalized than at P9–11 (Zorrilla de San Martin et al., 2012). Moreover, it has been recently shown that at this earlier stage of development (P5–7), the mouse MOC-IHC synapse presents a lower initial probability of release than that at P9–11 and that it facilitates upon high frequency stimulation (10-pulse trains at 40 and 100 Hz lead to ∼2-fold increase in synaptic efficacy), whereas the same stimulation protocol applied at P9–11 synapses leads to progressive depression (Zorrilla de San Martin et al., 2012). Thus, the changes in expression of key molecules involved in synaptic transmission that take place both in the pre and the postsynapse at the transient MOC-IHC synapse (Katz et al., 2004; Roux et al., 2011; Zorrilla de San Martin et al., 2012; Kearney et al., 2014) during the short period at which it is functional, might underlie the changes in the STP properties of this synapse (Zorrilla de San Martin et al., 2012). In addition, developmental changes in STP properties of the transient MOC-IHC synapse might lead to fine tuning of the pattern of action potential frequency of IHCs (Goutman et al., 2005; Johnson et al., 2011; Sendin et al., 2014), affecting signaling at the first synapse of the auditory system during the course of its establishment.

Interestingly, it has been very recently demonstrated that the normal strengthening and silencing of inhibitory synaptic connections between the medial nucleus of the trapezoid body (MNTB) and the LSO before hearing onset is impaired in mice lacking a functional efferent innervation, the α9 KO mice (Clause et al., 2014). It is important to mention that MNTB neurons discharge following the spike patterns of SGN (Tritsch and Bergles, 2010; Tritsch et al., 2010) which are activated by glutamate release at the IHC-afferent fiber synapse. This release of glutamate occurs in the absence of sensory stimuli, before hearing onset, and is driven by Ca^{2+} action potentials in IHCs (Beutner and Moser, 2001; Glowatzki and Fuchs, 2002). Moreover, α9 nAChR subunit KO mice have severe deficits in the axonal pruning that occurs in normal mice during the first week after the onset of hearing (Clause et al., 2014). In addition, it has been also recently shown that the Ca^{2+} sensitivity of glutamate release at afferent IHC-ribbon synapses do not mature correctly in the α9 nAChR subunit KO mice (Johnson et al., 2013). The above mentioned results show that the timing and pattern of activity that occurs in the absence of sensory stimuli before hearing onset, is important for the correct development of a tonotopic map. In addition, these results give strong support to the hypothesis that efferent MOC modulation of the IHC action potential pattern (Glowatzki and Fuchs, 2000; Marcotti et al., 2004; Goutman et al., 2005; Johnson et al., 2011; Sendin et al., 2014) is a key factor in the correct establishment of the auditory pathway. Thus it can be hypothesized that the transient efferent innervation to IHCs could be involved in the functional maturation of IHCs, as well as in the correct development of the peripheral and central compartments of the auditory system.

CONCLUSIONS

Synaptic strength is a key variable for transmitting information, therefore synapses, both in the developing and mature nervous system, must be highly regulated in order to adapt to the changing demands of the environment. The MOC-hair cell synapse is endowed with at least three regulatory mechanisms: presynaptic inhibition of ACh release via the activation of BK channels that reduce action potential duration (Zorrilla de San Martín et al., 2010); inhibition of ACh release via $GABA_BRs$ reducing Ca^{2+} entry through P/Q-type VGCC (Wedemeyer et al., 2013) and enhancement of ACh release by a retrograde messenger, most likely, NO (Kong et al., 2013). These regulatory mechanisms acting in concert (see **Figure 3**) might determine the STP properties of MOC-hair cell synapses and thereby exert a tight control on the release probability. As reported for other synapses (Brenowitz et al., 1998; Brenowitz and Trussell, 2001), this regulation could be crucial for preventing depression and allow MOC fibers to continue releasing transmitter even at high activity rates. Moreover, as MOC firing rate increases with sound intensity (Brown et al., 1985; Robertson and Gummer, 1985) and this increment in firing rate enhances the efficacy of the MOC-OHC synapse (Ballestero et al., 2011), synaptic plasticity might be relevant for protecting the auditory system from noise-induced damage (Rajan, 2000; Maison et al., 2002, 2013a; Wang et al., 2002). Finally, since the efficacy of the MOC efferent innervation to diminish or silence spontaneous Ca^{2+} action potentials in IHCs improves as the MOC firing frequency increases (Goutman et al., 2005), STP might also be crucial for regulating the activity pattern of the first afferent synapse during the establishment of the auditory pathway.

REFERENCES

Alger, B. E. (1991). Gating of GABAergic inhibition in hippocampal pyramidal cells. *Ann. N Y Acad. Sci.* 627, 249–263. doi: 10.1111/j.1749-6632.1991.tb25929.x

Art, J. J., and Fettiplace, R. (1984). Efferent desensitization of auditory nerve fibre responses in the cochlea of the turtle *Pseudemys scripta elegans*. *J. Physiol.* 356, 507–523.

Art, J. J., Fettiplace, R., and Fuchs, P. (1984). Synaptic hyperpolarization and inhibition of turtle cochlear hair cells. *J. Physiol.* 365, 525–550.

Ashmore, J. (2008). Cochlear outer hair cell motility. *Physiol. Rev.* 88, 173–210. doi: 10.1152/physrev.00044.2006

Atluri, P. P., and Regehr, W. G. (1996). Determinants of the time course of facilitation at the granule cell to Purkinje cell synapse. *J. Neurosci.* 16, 5661–5671.

Ballestero, J., Zorrilla de San Martin, J., Goutman, J., Elgoyhen, A. B., Fuchs, P. A., and Katz, E. (2011). Short-term synaptic plasticity regulates the level of olivocochlear inhibition to auditory hair cells. *J. Neurosci.* 31, 14763–14774. doi: 10.1523/jneurosci.6788-10.2011

Batta, T. J., Panyi, G., Szucs, A., and Sziklai, I. (2004). Regulation of the lateral wall stiffness by acetylcholine and GABA in the outer hair cells of the guinea pig. *Eur. J. Neurosci.* 20, 3364–3370. doi: 10.1111/j.1460-9568.2004.03797.x

Bettler, B., Kaupmann, K., Mosbacher, J., and Gassmann, M. (2004). Molecular structure and physiological functions of GABA(B) receptors. *Physiol. Rev.* 84, 835–867. doi: 10.1152/physrev.00036.2003

Betz, H., Kuhse, J., Schmieden, V., Laube, B., Kirsch, J., and Harvey, R. J. (1999). Structure and functions of inhibitory and excitatory glycine receptors. *Ann. N Y Acad. Sci.* 868, 667–676. doi: 10.1111/j.1749-6632.1999.tb11343.x

Beutner, D., and Moser, T. (2001). The presynaptic function of mouse cochlear inner hair cells during development of hearing. *J. Neurosci.* 21, 4593–4599.

Brandt, A., Striessnig, J., and Moser, T. (2003). CaV1.3 channels are essential for development and presynaptic activity of cochlear inner hair cells. *J. Neurosci.* 23, 10832–10840.

Bredt, D. S., and Snyder, S. H. (1994). Nitric oxide: a physiologic messenger molecule. *Annu. Rev. Biochem.* 63, 175–195. doi: 10.1146/annurev.biochem.63.1.175

Brenowitz, S., David, J., and Trussell, L. (1998). Enhancement of synaptic efficacy by presynaptic GABA(B) receptors. *Neuron* 20, 135–141. doi: 10.1016/s0896-6273(00)80441-9

Brenowitz, S., and Trussell, L. O. (2001). Maturation of synaptic transmission at end-bulb synapses of the cochlear nucleus. *J. Neurosci.* 21, 9487–9498.

Brown, M. C. (1989). Morphology and response properties of single olivocochlear fibers in the guinea pig. *Hear. Res.* 40, 93–109. doi: 10.1016/0378-5955(89)90103-2

Brown, M. C., Kujawa, S. G., and Liberman, M. C. (1998). Single olivocochlear neurons in the guinea pig. II. Response plasticity due to noise conditioning. *J. Neurophysiol.* 79, 3088–3097.

Brown, J. J., Meikle, M. B., and Lee, C. A. (1985). Reduction of acoustically induced auditory impairment by inhalation of carbogen gas. II. Temporary pure-tone induced depression of cochlear action potentials. *Acta Otolaryngol.* 100, 218–228. doi: 10.3109/00016488509104784

Brown, M. C., and Nuttal, A. L. (1984). Efferent control of cochlear inner hair cell responses in guinea-pig. *J. Physiol.* 354, 625–646.

Brownell, W., Bader, C., Bertrand, D., and de Ribaupierre, Y. (1985). Evoked mechanical responses of isolated cochlear hair cells. *Science* 227, 194–196. doi: 10.1126/science.3966153

Bruce, L. L., Christensen, M. A., and Warr, W. B. (2000). Postnatal development of efferent synapses in the rat cochlea. *J. Comp. Neurol.* 423, 532–548. doi: 10.1002/1096-9861(20000731)423:3<532::aid-cne14>3.0.co;2-t

Catterall, W. A. (1998). Structure and function of neuronal Ca2+ channels and their role in neurotransmitter release. *Cell Calcium* 24, 307–323. doi: 10.1016/s0143-4160(98)90055-0

Catterall, W. A. (2011). Voltage-gated calcium channels. *Cold Spring Harb. Perspect. Biol.* 3:a003947. doi: 10.1101/cshperspect.a003947

Catterall, W. A., and Few, A. P. (2008). Calcium channel regulation and presynaptic plasticity. *Neuron* 59, 882–901. doi: 10.1016/j.neuron.2008.09.005

Catterall, W. A., Leal, K., and Nanou, E. (2013). Calcium channels and short-term synaptic plasticity. *J. Biol. Chem.* 288, 10742–10749. doi: 10.1074/jbc.r112.411645

Chalifoux, J. R., and Carter, A. G. (2011a). GABAB receptor modulation of synaptic function. *Curr. Opin. Neurobiol.* 21, 339–344. doi: 10.1016/j.conb.2011.02.004

Chalifoux, J. R., and Carter, A. G. (2011b). GABAB receptor modulation of voltage-sensitive calcium channels in spines and dendrites. *J. Neurosci.* 31, 4221–4232. doi: 10.1523/jneurosci.4561-10.2011

Clause, A., Kim, G., Sonntag, M., Weisz, C. J., Vetter, D. E., Rubsamen, R., et al. (2014). The precise temporal pattern of prehearing spontaneous activity is necessary for tonotopic map refinement. *Neuron* 82, 822–835. doi: 10.1016/j.neuron.2014.04.001

Dani, J. A., and Bertrand, D. (2007). Nicotinic acetylcholine receptors and nicotinic cholinergic mechanisms of the central nervous system. *Annu. Rev. Pharmacol. Toxicol.* 47, 699–729. doi: 10.1146/annurev.pharmtox.47.120505.105214

Delano, P. H., Elgueda, D., Hamame, C. M., and Robles, L. (2007). Selective attention to visual stimuli reduces cochlear sensitivity in chinchillas. *J. Neurosci.* 27, 4146–4153. doi: 10.1523/jneurosci.3702-06.2007

Dittman, J. S., Kreitzer, A. C., and Regehr, W. G. (2000). Interplay between facilitation, depression and residual calcium at three presynaptic terminals. *J. Neurosci.* 20, 1374–1385.

Dodge, F. A. Jr., and Rahamimoff, R. (1967). Co-operative action a calcium ions in transmitter release at the neuromuscular junction. *J. Physiol.* 193, 419–432.

Duarte, C. B., Santos, P. F., and Carvalho, A. P. (1999). Corelease of two functionally opposite neurotransmitters by retinal amacrine cells: experimental evidence and functional significance. *J. Neurosci. Res.* 58, 475–479. doi: 10.1002/(sici)1097-4547(19991115)58:4<475::aid-jnr1>3.0.co;2-o

Elgoyhen, A. B., Johnson, D. S., Boulter, J., Vetter, D. E., and Heinemann, S. (1994). α9: an acetylcholine receptor with novel pharmacological properties expressed in rat cochlear hair cells. *Cell* 79, 705–715. doi: 10.1016/0092-8674(94)90555-x

Elgoyhen, A. B., and Katz, E. (2012). The efferent medial olivocochlear-hair cell synapse. *J. Physiol. Paris* 106, 47–56. doi: 10.1016/j.jphysparis.2011.06.001

Elgoyhen, A. B., Vetter, D. E., Katz, E., Rothlin, C. V., Heinemann, S. F., and Boulter, J. (2001). α10: a determinant of nicotinic cholinergic receptor function in mammalian vestibular and cochlear mechanosensory hair cells. *Proc. Natl. Acad. Sci. U S A* 98, 3501–3506. doi: 10.1073/pnas.051622798

Engel, J., Braig, C., Rüttiger, L., Kuhn, S., Zimmermann, U., Blin, N., et al. (2006). Two classes of outer hair cells along the tonotopic axis of the cochlea. *Neuroscience* 143, 837–849. doi: 10.1016/j.neuroscience.2006.08.060

Erostegui, C., Nenov, A. P., Norris, C. H., and Bobbin, R. P. (1994a). Acetylcholine activates a K+ conductance permeable to Cs+ in guinea pig outer hair cells. *Hear. Res.* 81, 119–129. doi: 10.1016/0378-5955(94)90159-7

Erostegui, C., Norris, C. H., Nenov, A. P., and Bobbin, R. P. (1994b). Ionic mechanisms underlying the action of acetylcholine on outer hair cells. *Assoc. Res. Otolaryngol.* 506, 127.

Evans, M. (1996). Acetylcholine activates two currents in guinea-pig outer hair cells. *J. Physiol.* 491, 563–578.

Evans, M. G., Lagostena, L., Darbon, P., and Mammano, F. (2000). Cholinergic control of membrane conductance and intracellular free Ca2+ in outer hair cells of the guinea pig cochlea. *Cell Calcium* 28, 195–203. doi: 10.1054/ceca.2000.0145

Eybalin, M. (1993). Neurotransmitters and neuromodulators of the mammalian cochlea. *Physiol. Rev.* 73, 309–373.

Fakler, B., and Adelman, J. P. (2008). Control of K(Ca) channels by calcium nano/microdomains. *Neuron* 59, 873–881. doi: 10.1016/j.neuron.2008.09.001

Fedchyshyn, M. J., and Wang, L. Y. (2005). Developmental transformation of the release modality at the calyx of Held synapse. *J. Neurosci.* 25, 4131–4140. doi: 10.1523/jneurosci.0350-05.2005

Fex, J., and Altschuler, R. A. (1986). Neurotransmitter-related inmunihistochemistry of the organ of Corti. *Hear. Res.* 22, 249–263. doi: 10.1016/0378-5955(86)90102-4

Fioravante, D., and Regehr, W. G. (2011). Short-term forms of presynaptic plasticity. *Curr. Opin. Neurobiol.* 21, 269–274. doi: 10.1016/j.conb.2011.02.003

Flink, M. T., and Atchison, W. D. (2003). Iberiotoxin-induced block of Ca2+-activated K+ channels induces dihydropyridine sensitivity of ACh release from mammalian motor nerve terminals. *J. Pharmacol. Exp. Ther.* 305, 646–652. doi: 10.1124/jpet.102.046102

Flock, A., and Russell, I. (1976). Inhibition by efferent nerve fibres: action on hair cells and afferent synaptic transmission in the lateral line canal organ of the burbot Lota lota. *J. Physiol.* 257, 45–62.

Fortune, E. S., and Rose, G. J. (2001). Short-term synaptic plasticity as a temporal filter. *Trends Neurosci.* 24, 381–385. doi: 10.1016/s0166-2236(00)01835-x

Fritzsch, B. (1996). Development of the labyrinthine efferent system. *Ann. N Y Acad. Sci.* 781, 21–33. doi: 10.1111/j.1749-6632.1996.tb15690.x

Fritzsch, B., and Nichols, D. H. (1993). Dil reveals a prenatal arrival of efferents at the differentiating otocyst of mice. *Hear. Res.* 65, 51–60. doi: 10.1016/0378-5955(93)90200-k

Fuchs, P. A. (1992). Ionic currents in cochlear hair cells. *Prog. Neurobiol.* 39, 493–505. doi: 10.1016/0301-0082(92)90003-w

Fuchs, P. A. (1996). Synaptic transmission at vertebrate hair cells. *Curr. Opin. Neurobiol.* 6, 514–519. doi: 10.1016/s0959-4388(96)80058-4

Fuchs, P. A. (2014). A 'calcium capacitor' shapes cholinergic inhibition of cochlear hair cells. *J. Physiol.* 592, 3393–3401. doi: 10.1113/jphysiol.2013.267914

Fuchs, P. A., Glowatzki, E., and Moser, T. (2003). The afferent synapse of cochlear hair cells. *Curr. Opin. Neurobiol.* 13, 452–458. doi: 10.1016/s0959-4388(03)00098-9

Fuchs, P. A., Lehar, M., and Hiel, H. (2014). Ultrastructure of cisternal synapses on outer hair cells of the mouse cochlea. *J. Comp. Neurol.* 522, 717–729. doi: 10.1002/cne.23478

Fuchs, P. A., and Murrow, B. W. (1992). Cholinergic inhibition of short (outer) hair cells of the chick's cochlea. *J. Neurosci.* 12, 800–809.

Gabashvili, I. S., Sokolowski, B. H., Morton, C. C., and Giersch, A. B. (2007). Ion channel gene expression in the inner ear. *J. Assoc. Res. Otolaryngol.* 8, 305–328. doi: 10.1007/s10162-007-0082-y

Gaiarsa, J. L., Mclean, H., Congar, P., Leinekugel, X., Khazipov, R., Tseeb, V., et al. (1995a). Postnatal maturation of gamma-aminobutyric acidA and B-mediated inhibition in the CA3 hippocampal region of the rat. *J. Neurobiol.* 26, 339–349. doi: 10.1002/neu.480260306

Gaiarsa, J. L., Tseeb, V., and Ben-Ari, Y. (1995b). Postnatal development of pre- and postsynaptic GABAB-mediated inhibitions in the CA3 hippocampal region of the rat. *J. Neurophysiol.* 73, 246–255.

Galambos, R. (1956). Suppression of auditory nerve activity by stimulation of afferent fibers to the cochlea. *J. Neurophysiol.* 19, 424–437.

Gifford, M. L., and Guinan, J. J. Jr. (1987). Effects of electrical stimulation of medial olivocochlear neurons on ipsilateral and contralateral cochlear responses. *Hear. Res.* 29, 179–194. doi: 10.1016/0378-5955(87)90166-3

Ginzberg, R. D., and Morest, D. K. (1984). Fine structure of cochlear innervation in the cat. *Hear. Res.* 14, 109–127. doi: 10.1016/0378-5955(84)90011-x

Gitter, A. H., and Zenner, H. P. (1992). gamma-Aminobutyric acid receptor activation of outer hair cells in the guinea pig cochlea. *Eur. Arch. Otorhinolaryngol.* 249, 62–65. doi: 10.1007/bf00175674

Glowatzki, E., and Fuchs, P. (2000). Cholinergic synaptic inhibition of inner hair cells in the neonatal mammalian cochlea. *Science* 288, 2366–2368. doi: 10.1126/science.288.5475.2366

Glowatzki, E., and Fuchs, P. (2002). Transmitter release at the hair cell ribbon synapse. *Nat. Neurosci.* 5, 147–154. doi: 10.1038/nn796

Gómez-Casati, M. E., Fuchs, P. A., Elgoyhen, A. B., and Katz, E. (2005). Biophysical and pharmacological characterization of nicotinic cholinergic receptors in rat cochlear inner hair cells. *J. Physiol.* 566, 103–118. doi: 10.1113/jphysiol.2005.087155

Goutman, J. D., Fuchs, P. A., and Glowatzki, E. (2005). Facilitating efferent inhibition of inner hair cells in the cochlea of the neonatal rat. *J. Physiol.* 566, 49–59. doi: 10.1113/jphysiol.2005.087460

Green, G. E., Khan, K. M., Beisel, D. W., Drescher, M. J., Hatfield, J. S., and Drescher, D. G. (1996). Calcium channel subunits in the mouse cochlea. *J. Neurochem.* 67, 37–45. doi: 10.1046/j.1471-4159.1996.67010037.x

Guinan, J. J. (2011). "Physiology of the medial and lateral olivocochlear systems," in *Auditory and Vestibular Efferents*, eds D. K. Ryugo, R. R. Fay and A. N. Popper (New York: Springer), 39–81.

Guinan, J. J., Warr, W. B., and Norris, B. E. (1983). Differential olivocochlear projections from lateral vs. medial zones of the superior olivary complex. *J. Comp. Neurol.* 221, 358–370. doi: 10.1002/cne.902210310

Hafidi, A., Beurg, M., and Dulon, D. (2005). Localization and developmental expression of BK channels in mammalian cochlear hair cells. *Neuroscience* 130, 475–484. doi: 10.1016/j.neuroscience.2004.09.038

Heinrich, U. R., Maurer, J., Gosepath, K., and Mann, W. (1997). Electron microscopic localization of nitric oxide I synthase in the organ of Corti of the guinea pig. *Eur. Arch. Otorhinolaryngol.* 254, 396–400. doi: 10.1007/bf01642558

Hudspeth, A. (1997). How hearing happens. *Neuron* 19, 947–950. doi: 10.1016/s0896-6273(00)80385-2

Ishikawa, T., Kaneko, M., Shin, H. S., and Takahashi, T. (2005). Presynaptic N-type and P/Q-type Ca2+ channels mediating synaptic transmission at the calyx of Held of mice. *J. Physiol.* 568, 199–209. doi: 10.1113/jphysiol.2005.089912

Iwasaki, S., Momiyama, A., Uchitel, O. D., and Takahashi, T. (2000). Developmental changes in calcium channel types mediating central synaptic transmission. *J. Neurosci.* 20, 59–65.

Johnson, S. L., Eckrich, T., Kuhn, S., Zampini, V., Franz, C., Ranatunga, K. M., et al. (2011). Position-dependent patterning of spontaneous action potentials in immature cochlear inner hair cells. *Nat. Neurosci.* 14, 711–717. doi: 10.1038/nn.2803

Johnson, S. L., Wedemeyer, C., Vetter, D. E., Adachi, R., Holley, M. C., Elgoyhen, A. B., et al. (2013). Cholinergic efferent synaptic transmission regulates the maturation of auditory hair cell ribbon synapses. *Open Biol.* 3: 130163. doi: 10.1098/rsob.130163

Jones, K. A., Borowsky, B., Tamm, J. A., Craig, D. A., Durkin, M. M., Dai, M., et al. (1998). GABA(B) receptors function as a heteromeric assembly of the subunits GABA(B)R1 and GABA(B)R2. *Nature* 396, 674–679.

Kandler, K. (2004). Activity-dependent organization of inhibitory circuits: lessons from the auditory system. *Curr. Opin. Neurobiol.* 14, 96–104. doi: 10.1016/j.conb.2004.01.017

Katz, E., Elgoyhen, A. B., and Fuchs, P. (2011). "Cholinergic inhibition of hair cells," in *Auditroy and Vestibular Efferents*, eds D. K. Ryugo, R. R. Fay and A. N. Popper (New York: Springer), 103–133.

Katz, E., Elgoyhen, A. B., Gómez-Casati, M. E., Knipper, M., Vetter, D. E., Fuchs, P. A., et al. (2004). Developmental regulation of nicotinic synapses on cochlear inner hair cells. *J. Neurosci.* 24, 7814–7820. doi: 10.1523/jneurosci.2102-04.2004

Katz, B., and Miledi, R. (1969). Spontaneous and evoked activity of motor nerve endings in calcium ringer. *J. Physiol.* 203, 689–706.

Katz, E., Protti, D. A., Ferro, P. A., Rosato Siri, M. D., and Uchitel, O. D. (1997). Effects of Ca2+ channel blocker neurotoxins on transmitter release and presynaptic currents at the mouse neuromuscular junction. *Br. J. Pharmacol.* 121, 1531–1540. doi: 10.1038/sj.bjp.0701290

Kaupmann, K., Malitschek, B., Schuler, V., Heid, J., Froestl, W., Beck, P., et al. (1998). GABA(B)-receptor subtypes assemble into functional heteromeric complexes. *Nature* 396, 683–687.

Kearney, G. I., Zorrilla de San Martin, J., Wedemeyer, C., Elgoyhen, A. B., and Katz, E. (2014). Developmental changes in the voltage-gated Ca2+ channels (VGCC) that mediate acetylcholine (ACh) release at the transient efferent-inner hair cell synapse. *Asso. Res. Otolaryyngol. Abstr.* 495–495.

Kong, J. H., Adelman, J. P., and Fuchs, P. A. (2008). Expression of the SK2 calcium-activated potassium channel is required for cholinergic function in mouse cochlear hair cells. *J. Physiol.* 586, 5471–5485. doi: 10.1113/jphysiol.2008.160077

Kong, J. H., Zachary, S., Rohmann, K. N., and Fuchs, P. A. (2013). Retrograde facilitation of efferent synapses on cochlear hair cells. *J. Assoc. Res. Otolaryngol.* 14, 17–27. doi: 10.1007/s10162-012-0361-0

Kros, C. J., Ruppersberg, J. P., and Rusch, A. (1998). Expression of a potassium current in inner hair cells during development of hearing in mice. *Nature* 394, 281–284.

Kuner, R., Köhr, G., Grünewald, S., Eisenhardt, G., Bach, A., and Kornau, H. C. (1999). Role of heteromer formation in GABAB receptor function. *Science* 283, 74–77. doi: 10.1126/science.283.5398.74

Layton, M. G., Robertson, D., Everett, A. W., Mulders, W. H., and Yates, G. K. (2005). Cellular localization of voltage-gated calcium channels and synaptic vesicle-associated proteins in the guinea pig cochlea. *J. Mol. Neurosci.* 27, 225–244. doi: 10.1385/jmn:27:2:225

Lee, S., Kim, K., and Zhou, Z. J. (2010). Role of ACh-GABA cotransmission in detecting image motion and motion direction. *Neuron* 68, 1159–1172. doi: 10.1016/j.neuron.2010.11.031

Lenoir, M., Schnerson, A., and Pujol, R. (1980). Cochlear receptor development in the rat with emphasis on synaptogenesis. *Anat. Embryol. (Berl)* 160, 253–262. doi: 10.1007/bf00305106

Liberman, M. C. (1980). Efferent synapses in the inner hair cell area of the cat cochlea: an electron microscopic study of serial sections. *Hear. Res.* 3, 189–204. doi: 10.1016/0378-5955(80)90046-5

Liberman, M. C., and Brown, M. C. (1986). Physiology and anatomy of single olivocochlear neurons in the cat. *Hear. Res.* 24, 17–36. doi: 10.1016/0378-5955(86)90003-1

Lingle, C. J., Solaro, C. R., Prakriya, M., and Ding, J. P. (1996). Calcium-activated potassium channels in adrenal chromaffin cells. *Ion Channels* 4, 261–301. doi: 10.1007/978-1-4899-1775-1_7

Lioudyno, M., Hiel, H., Kong, J. H., Katz, E., Waldman, E., Parameshwaran-Iyer, S., et al. (2004). A "synaptoplasmic cistern" mediates rapid inhibition of cochlear hair cells. *J. Neurosci.* 24, 11160–11164. doi: 10.1523/jneurosci.3674-04.2004

Lipovsek, M., Fierro, A., Pérez, E. G., Boffi, J. C., Millar, N. S., Fuchs, P., et al. (2014). Tracking the molecular evolution of calcium permeability in a nicotinic acetylcholine receptor. *Mol. Biol. Evol.* doi: 10.1093/molbev/msu258. [Epub ahead of print].

Lipovsek, M., Im, G. J., Franchini, L. F., Pisciottano, F., Katz, E., Fuchs, P. A., et al. (2012). Phylogenetic differences in calcium permeability of the auditory hair cell cholinergic nicotinic receptor. *Proc. Natl. Acad. Sci. U S A* 109, 4308–4313. doi: 10.1073/pnas.1115488109

Lisman, J. E. (1997). Bursts as a unit of neural information: making unreliable synapses reliable. *Trends Neurosci.* 20, 38–43. doi: 10.1016/s0166-2236(96)10070-9

Maison, S. F., Adams, J. C., and Liberman, M. C. (2003). Olivocochlear innervation in the mouse: immunocytochemical maps, crossed versus uncrossed contributions and transmitter colocalization. *J. Comp. Neurol.* 455, 406–416. doi: 10.1002/cne.10490

Maison, S. F., Casanova, E., Holstein, G. R., Bettler, B., and Liberman, M. C. (2009). Loss of GABAB receptors in cochlear neurons: threshold elevation suggests modulation of outer hair cell function by type II afferent fibers. *J. Assoc. Res. Otolaryngol.* 10, 50–63. doi: 10.1007/s10162-008-0138-7

Maison, S. F., Luebke, A. E., Liberman, M. C., and Zuo, J. (2002). Efferent protection from acoustic injury is mediated via alpha9 nicotinic acetylcholine receptors on outer hair cells. *J. Neurosci.* 22, 10838–10846.

Maison, S., Micheyl, C., and Collet, L. (2001). Influence of focused auditory attention on cochlear activity in humans. *Psychophysiology* 38, 35–40. doi: 10.1111/1469-8986.3810035

Maison, S. F., Pyott, S. J., Meredith, A. L., and Liberman, M. C. (2013a). Olivocochlear suppression of outer hair cells in vivo: evidence for combined action of BK and SK2 channels throughout the cochlea. *J. Neurophysiol.* 109, 1525–1534. doi: 10.1152/jn.00924.2012

Maison, S. F., Rosahl, T. W., Homanics, G. E., and Liberman, M. C. (2006). Functional role of GABAergic innervation of the cochlea: phenotypic analysis of mice lacking GABA(A) receptor subunits α 1, α 2, α 5, α 6, β 2, β 3, or δ. *J. Neurosci.* 26, 10315–10326. doi: 10.1523/jneurosci.2395-06.2006

Maison, S. F., Usubuchi, H., and Liberman, M. C. (2013b). Efferent feedback minimizes cochlear neuropathy from moderate noise exposure. *J. Neurosci.* 33, 5542–5552. doi: 10.1523/jneurosci.5027-12.2013

Marcantoni, A., Baldelli, P., Hernandez-Guijo, J. M., Comunanza, V., Carabelli, V., and Carbone, E. (2007). L-type calcium channels in adrenal chromaffin cells: role in pace-making and secretion. *Cell Calcium* 42, 397–408. doi: 10.1016/j.ceca.2007.04.015

Marcotti, W., Johnson, S. L., Holley, M. C., and Kros, C. J. (2003a). Developmental changes in the expression of potassium currents of embryonic, neonatal and mature mouse inner hair cells. *J. Physiol.* 548, 383–400. doi: 10.1111/j.1469-7793.2003.00383.x

Marcotti, W., Johnson, S. L., and Kros, C. J. (2004). A transiently expressed SK current sustains and modulates action potential activity in immature mouse inner hair cells. *J. Physiol.* 560, 691–708. doi: 10.1113/jphysiol.2004.072868

Marcotti, W., Johnson, S. L., Rusch, A., and Kros, C. J. (2003b). Sodium and calcium currents shape action potentials in immature mouse inner hair cells. *J. Physiol.* 552, 743–761. doi: 10.1113/jphysiol.2003.043612

Martin, A. R., and Fuchs, P. A. (1992). The dependence of calcium-activated potassium currents on membrane potential. *Proc. Biol. Sci.* 250, 71–76. doi: 10.1098/rspb.1992.0132

Martyn, J. A., Fagerlund, M. J., and Eriksson, L. I. (2009). Basic principles of neuromuscular transmission. *Anaesthesia* 64(Suppl. 1), 1–9. doi: 10.1111/j.1365-2044.2008.05865.x

Meffert, M. K., Calakos, N. C., Scheller, R. H., and Schulman, H. (1996). Nitric oxide modulates synaptic vesicle docking fusion reactions. *Neuron* 16, 1229–1236. doi: 10.1016/s0896-6273(00)80149-x

Michna, M., Knirsch, M., Hoda, J. C., Muenkner, S., Langer, P., Platzer, J., et al. (2003). Cav1.3 (α1D) Ca2+ currents in neonatal outer hair cells of mice. *J. Physiol.* 553, 747–758. doi: 10.1113/jphysiol.2003.053256

Mintz, I. M., Sabatini, B. L., and Regehr, W. G. (1995). Calcium control of transmitter release at a cerebellar synapse. *Neuron* 15, 675–688. doi: 10.1016/0896-6273(95)90155-8

Momiyama, T. (2003). Parallel decrease in omega-conotoxin-sensitive transmission and dopamine-induced inhibition at the striatal synapse of developing rats. *J. Physiol.* 546, 483–490. doi: 10.1113/jphysiol.2002.031773

Mountain, D. C. (1980). Changes in endolymphatic potential and crossed olivocochlear bundle stimulation alter cochlear mechanics. *Science* 210, 71–72. doi: 10.1126/science.7414321

Murthy, V., Maison, S. F., Taranda, J., Haque, N., Bond, C. T., Elgoyhen, A. B., et al. (2009a). SK2 channels are required for function and long-term survival of efferent synapses on mammalian outer hair cells. *Mol. Cell. Neurosci.* 40, 39–49. doi: 10.1016/j.mcn.2008.08.011

Murthy, V., Taranda, J., Elgoyhen, A. B., and Vetter, D. E. (2009b). Activity of nAChRs containing alpha9 subunits modulates synapse stabilization via bidirectional signaling programs. *Dev. Neurobiol.* 69, 931–949. doi: 10.1002/dneu.20753

Nadol, J. B. Jr. (1988). Comparative anatomy of the cochlea and auditory nerve in mammals. *Hear. Res.* 34, 253–266. doi: 10.1016/0378-5955(88)90006-8

Neher, E. (1998). Vesicle pools and Ca2+ microdomains: new tools for understanding their roles in neurotransmitter release. *Neuron* 20, 389–399. doi: 10.1016/s0896-6273(00)80983-6

Nenov, A. P., Norris, C., and Bobbin, R. P. (1996). Acetylcholine responses in guinea pig outer hair cells. II. Activation of a small conductance Ca2+-activated K+ channel. *Hear. Res.* 101, 149–172. doi: 10.1016/s0378-5955(96)00143-8

Oliver, D., Klöcker, N., Schuck, J., Baukrowitz, T., Ruppersberg, J. P., and Fakler, B. (2000). Gating of Ca2+-activated K+ channels controls fast inhibitory

synaptic transmission at auditory outer hair cells. *Neuron* 26, 595–601. doi: 10.1016/s0896-6273(00)81197-6

Perez-Garci, E., Gassmann, M., Bettler, B., and Larkum, M. E. (2006). The GABAB1b isoform mediates long-lasting inhibition of dendritic Ca2+ spikes in layer 5 somatosensory pyramidal neurons. *Neuron* 50, 603–616. doi: 10.1016/j.neuron.2006.04.019

Plant, T. D., Schirra, C., Katz, E., Uchitel, O. D., and Konnerth, A. (1998). Single-cell RT-PCR and functional characterization of Ca2+ channels in motoneurons of the rat facial nucleus. *J. Neurosci.* 18, 9573–9584.

Platzer, J., Engel, J., Schrott-Fischer, A., Stephan, K., Bova, S., Chen, H., et al. (2000). Congenital deafness and sinoatrial node dysfunction in mice lacking class D L-type Ca2+ channels. *Cell* 102, 89–97. doi: 10.1016/s0092-8674(00)00013-1

Prakriya, M., Solaro, C. R., and Lingle, C. J. (1996). [Ca2+]i elevations detected by BK channels during Ca2+ influx and muscarine-mediated release of Ca2+ from intracellular stores in rat chromaffin cells. *J. Neurosci.* 16, 4344–4359.

Rajan, R. (2000). Centrifugal pathways protect hearing sensitivity at the cochlea in noisy environments that exacerbate the damage induced by loud sound. *J. Neurosci.* 20, 6684–6693.

Rasmussen, G. L. (1955). Descending, or "feedback-back" connections of the auditory system of the cat. *Am. J. Physiol.* 183, 653.

Reid, C. A., Bekkers, J. M., and Clements, J. D. (2003). Presynaptic Ca2+ channels: a functional patchwork. *Trends Neurosci.* 26, 683–687. doi: 10.1016/j.tins.2003.10.003

Riemann, R., and Reuss, S. (1999). Nitric oxide synthase in identified olivocochlear projection neurons in rat and guinea pig. *Hear. Res.* 135, 181–189. doi: 10.1016/s0378-5955(99)00113-6

Robertson, D., and Gummer, M. (1985). Physiological and morphological characterization of efferent neurones in the guinea pig cochlea. *Hear. Res.* 20, 63–77. doi: 10.1016/0378-5955(85)90059-0

Rontal, D. A., and Echteler, S. M. (2003). Developmental segregation in the efferent projections to auditory hair cells in the gerbil. *J. Comp. Neurol.* 467, 509–520. doi: 10.1002/cne.10931

Rosato Siri, M. D., and Uchitel, O. D. (1999). Calcium channels coupled to neurotransmitter release at neonatal rat neuromuscular junctions. *J. Physiol.* 514, 533–540. doi: 10.1111/j.1469-7793.1999.533ae.x

Roux, I., Wersinger, E., Mcintosh, J. M., Fuchs, P. A., and Glowatzki, E. (2011). Onset of cholinergic efferent synaptic function in sensory hair cells of the rat cochlea. *J. Neurosci.* 31, 15092–15101. doi: 10.1523/jneurosci.2743-11.2011

Saito, K. (1983). Fine structure of the sensory epithelium of guinea-pig organ of Corti: subsurface cisternae and lamellar bodies in the outer hair cells. *Cell Tissue Res.* 229, 467–481. doi: 10.1007/bf00207692

Sakai, Y., Harvey, M., and Sokolowski, B. (2011). Identification and quantification of full-length BK channel variants in the developing mouse cochlea. *J. Neurosci. Res.* 89, 1747–1760. doi: 10.1002/jnr.22713

Sanes, J. R., and Lichtman, J. W. (1999). Development of the vertebrate neuromuscular junction. *Annu. Rev. Neurosci.* 22, 389–442. doi: 10.1146/annurev.neuro.22.1.389

Schikorski, T., and Stevens, C. F. (1997). Quantitative ultrastructural analysis of hippocampal excitatory synapses. *J. Neurosci.* 17, 5858–5867.

Schneggenburger, R., Sakaba, T., and Neher, E. (2002). Vesicle pools and short-term synaptic depression: lessons from a large synapse. *Trends Neurosci.* 25, 206–212. doi: 10.1016/s0166-2236(02)02139-2

Sendin, G., Bourien, J., Rassendren, F., Puel, J. L., and Nouvian, R. (2014). Spatiotemporal pattern of action potential firing in developing inner hair cells of the mouse cochlea. *Proc. Natl. Acad. Sci. U S A* 111, 1999–2004. doi: 10.1073/pnas.1319615111

Sewell, W. F. (2011). "Pharmacology and Neurochemistry of Olivocochlear Efferents," in *Auditory and Vestibular Efferents*, eds D. K. Ryugo, R. R. Fay and A. N. Popper (New York: Springer), 83–101.

Sgard, F., Charpentier, E., Bertrand, S., Walker, N., Caput, D., Graham, D., et al. (2002). A novel human nicotinic receptor subunit, α10, that confers functionality to the α9-subunit. *Mol. Pharmacol.* 61, 150–159. doi: 10.1124/mol.61.1.150

Shen, J., Harada, N., Nakazawa, H., Kaneko, T., Izumikawa, M., and Yamashita, T. (2006). Role of nitric oxide on ATP-induced Ca2+ signaling in outer hair cells of the guinea pig cochlea. *Brain Res.* 1081, 101–112. doi: 10.1016/j.brainres.2005.12.129

Simmons, D. D. (2002). Development of the inner ear efferent system across vertebrate species. *J. Neurobiol.* 53, 228–250. doi: 10.1002/neu.10130

Simmons, D. D., Mansdorf, N. B., and Kim, J. H. (1996). Olivocochlear innervation of inner and outer hair cells during postnatal maturation: evidence for a waiting period. *J. Comp. Neurol.* 370, 551–562. doi: 10.1002/(sici)1096-9861(19960708)370:4<551::aid-cne10>3.0.co;2-m

Smith, C. A., and Rasmussen, G. L. (1963). Recent observations on the olivo-cochlear bundle. *Ann. Otol. Rhinol. Laryngol.* 72, 489–506. doi: 10.1177/000348946307200218

Smith, C. A., and Sjostrand, F. S. (1961). Structure of the nerve endings on the external hair cells of the guinea pig cochlea as studied by serial sections. *J. Ultrastruct. Res.* 5, 523–556. doi: 10.1016/s0022-5320(61)80025-7

Sridhar, T. S., Brown, M. C., and Sewell, W. F. (1997). Unique postsynaptic signaling at the hair cell efferent synapse permits calcium to evoke changes on two time scales. *J. Neurosci.* 17, 428–437.

Storm, J. F. (1987). Action potential repolarization and a fast after-hyperpolarization in rat hippocampal pyramidal cells. *J. Physiol.* 385, 733–759.

Taranda, J., Maison, S. F., Ballestero, J. A., Katz, E., Savino, J., Vetter, D. E., et al. (2009). A point mutation in the hair cell nicotinic cholinergic receptor prolongs cochlear inhibition and enhances noise protection. *PLoS Biol.* 7:e18. doi: 10.1371/journal.pbio.1000018

Thompson, G. C., Cortez, A. M., and Igarashi, M. (1986). GABA-like immunoreactivity in the squirrel monkey organ of Corti. *Brain Res.* 372, 72–79. doi: 10.1016/0006-8993(86)91459-9

Tritsch, N. X., and Bergles, D. E. (2010). Developmental regulation of spontaneous activity in the Mammalian cochlea. *J. Neurosci.* 30, 1539–1550. doi: 10.1523/jneurosci.3875-09.2010

Tritsch, N. X., Rodríguez-Contreras, A., Crins, T. T., Wang, H. C., Borst, J. G., and Bergles, D. E. (2010). Calcium action potentials in hair cells pattern auditory neuron activity before hearing onset. *Nat. Neurosci.* 13, 1050–1052. doi: 10.1038/nn.260

Tritsch, N. X., Yi, E., Gale, J. E., Glowatzki, E., and Bergles, D. E. (2007). The origin of spontaneous activity in the developing auditory system. *Nature* 450, 50–55. doi: 10.1038/nature06233

Urbano, F. J., Depetris, R. S., and Uchitel, O. D. (2001). Coupling of L-type calcium channels to neurotransmitter release at mouse motor nerve terminals. *Pflugers Arch.* 441, 824–831. doi: 10.1007/s004240000489

Vergara, C., Latorre, R., Marrion, N. V., and Adelman, J. P. (1998). Calcium-activated potassium channels. *Curr. Opin. Neurobiol.* 8, 321–329.

Vetter, D. E., Adams, J. C., and Mugnani, E. (1991). Chemically distinct rat olivocochlear neurons. *Synapse* 7, 21–43. doi: 10.1002/syn.890070104

Vetter, D. E., Katz, E., Maison, S. F., Taranda, J., Turcan, S., Ballestero, J., et al. (2007). The α10 nicotinic acetylcholine receptor subunit is required for normal synaptic function and integrity of the olivocochlear system. *Proc. Natl. Acad. Sci. U S A* 104, 20594–20599. doi: 10.1073/pnas.0708545105

Vetter, D., Lieberman, M., Mann, J., Barhanin, J., Boulter, J., Brown, M., et al. (1999). Role of α9 nicotinic ACh receptor subunits in the development and function of cochlear efferent innervation. *Neuron* 23, 93–103. doi: 10.1016/s0896-6273(00)80756-4

Vigot, R., Barbieri, S., Bräuner-Osborne, H., Turecek, R., Shigemoto, R., Zhang, Y. P., et al. (2006). Differential compartmentalization and distinct functions of GABAB receptor variants. *Neuron* 50, 589–601. doi: 10.1016/j.neuron.2006.04.014

Waka, N., Knipper, M., and Engel, J. (2003). Localization of the calcium channel subunits Cav1.2 (α1C) and Cav2.3 (α1E) in the mouse organ of Corti. *Histol. Histopathol.* 18, 1115–1123.

Wang, Y., Hirose, K., and Liberman, M. C. (2002). Dynamics of noise-induced cellular injury and repair in the mouse cochlea. *J. Assoc. Res. Otolaryngol.* 3, 248–268. doi: 10.1007/s101620020028

Wang, Y., and Manis, P. B. (2008). Short-term synaptic depression and recovery at the mature mammalian endbulb of Held synapse in mice. *J. Neurophysiol.* 100, 1255–1264. doi: 10.1152/jn.90715.2008

Warr, W. B. (1975). Olivocochlear and vestibular efferent neurons of the feline brain stem: their location, morphology and number determined by retrograde axonal transport and acetylcholinesterase histochemistry. *J. Comp. Neurol.* 161, 159–181. doi: 10.1002/cne.901610203

Warr, W. (1992). "Organization of olivocochlear efferent sytems in mammals," in *The Mammalian Auditory Pathway: Neuroanatomy*, eds W. Douglas, A. Popper and R. Fay (New York: Springler-Verlag), 410–448.

Wedemeyer, C., Zorrilla de San Martín, J., Ballestero, J., Gómez-Casati, M. E., Torbidoni, A. V., Fuchs, P. A., et al. (2013). Activation of presynaptic

GABA(B(1a,2)) receptors inhibits synaptic transmission at mammalian inhibitory cholinergic olivocochlear-hair cell synapses. *J. Neurosci.* 33, 15477–15487. doi: 10.1523/jneurosci.2554-13.2013

Weisstaub, N., Vetter, D. E., Elgoyhen, A. B., and Katz, E. (2002). The α9α10 nicotinic acetylcholine receptor is permeable to and is modulated by divalent cations. *Hear. Res.* 167, 122–135. doi: 10.1016/s0378-5955(02)00380-5

Wersinger, E., and Fuchs, P. A. (2011). Modulation of hair cell efferents. *Hear. Res.* 279, 1–12. doi: 10.1016/j.heares.2010.12.018

Wersinger, E., Mclean, W. J., Fuchs, P. A., and Pyott, S. J. (2010). BK channels mediate cholinergic inhibition of high frequency cochlear hair cells. *PLoS One* 5:e13836. doi: 10.1371/journal.pone.0013836

White, J. H., Wise, A., Main, M. J., Green, A., Fraser, N. J., Disney, G. H., et al. (1998). Heterodimerization is required for the formation of a functional GABA(B) receptor. *Nature* 396, 679–682.

Wiederhold, M. L., and Kiang, N. Y. S. (1970). Effects of electrical stimulation of the crossed olivocochlear bundle on cat single auditory nerve fibres. *J. Acoust. Soc. Am.* 48, 950–965.

Xu-Friedman, M. A., and Regehr, W. G. (2004). Structural contributions to short-term synaptic plasticity. *Physiol. Rev.* 84, 69–85. doi: 10.1152/physrev.00016.2003

Zorrilla de San Martin, J., Alvarez Heduan, F., Elgoyhen, A. B., and Katz, E. (2012). Functional development of the medial olivocochlear efferent innervation before the onset of hearing. *Asso. Res. Otolaryngology. Abstr.* 265–266.

Zorrilla de San Martín, J., Pyott, S., Ballestero, J., and Katz, E. (2010). Ca(2+) and Ca(2+)-activated K(+) channels that support and modulate transmitter release at the olivocochlear efferent-inner hair cell synapse. *J. Neurosci.* 30, 12157–12167. doi: 10.1523/jneurosci.2541-10.2010

Zucker, R. S., and Regehr, W. G. (2002). Short-term synaptic plasticity. *Annu. Rev. Physiol.* 64, 355–405. doi: 10.1146/annurev.physiol.64.092501.114547

Conflict of Interest Statement: The authors declare that the research was conducted in the absence of any commercial or financial relationships that could be construed as a potential conflict of interest.

Received: 23 September 2014; accepted: 06 November 2014; published online: 02 December 2014.

*Citation: Katz E and Elgoyhen AB (2014) Short-term plasticity and modulation of synaptic transmission at mammalian inhibitory cholinergic olivocochlear synapses. Front. Syst. Neurosci. **8**:224. doi: 10.3389/fnsys.2014.00224*

This article was submitted to the journal Frontiers in Systems Neuroscience.

frontiers in
SYSTEMS NEUROSCIENCE

HYPOTHESIS AND THEORY ARTICLE
published: 25 February 2015
doi: 10.3389/fnsys.2015.00012

The biological role of the medial olivocochlear efferents in hearing: separating evolved function from exaptation

David W. Smith [1,2] **** and Andreas Keil*** [1,3]

[1] *Program in Behavioral and Cognitive Neuroscience, Department of Psychology, University of Florida, Gainesville, FL, USA*
[2] *Center for Smell and Taste, University of Florida, Gainesville, FL, USA*
[3] *Center for the Study of Emotion and Attention, University of Florida, Gainesville, FL, USA*

Edited by:
Paul Hinckley Delano, Universidad de Chile, Chile

Reviewed by:
Miguel A. Merchán, University of Salamanca, Spain
Xavier G. A. Perrot, Université Claude Bernard - Lyon 1, France

****Correspondence:***
David W. Smith, Program in Behavioral and Cognitive Neuroscience, Department of Psychology and Center for Smell and Taste, University of Florida, 114 Psychology, Box 112250, Gainesville, FL, USA
e-mail: dwsmith@ufl.edu

Cochlear outer hair cells (OHCs) are remarkable, mechanically-active receptors that determine the exquisite sensitivity and frequency selectivity characteristic of the mammalian auditory system. While there are three to four times as many OHCs compared with inner hair cells, OHCs lack a significant afferent innervation and, instead, receive a rich efferent innervation from medial olivocochlear (MOC) efferent neurons. Activation of the MOC has been shown to exert a considerable suppressive effect over OHC activity. The precise function of these efferent tracts in auditory behavior, however, is the matter of considerable debate. The most frequent functions assigned to the MOC tracts are to protect the cochlea from traumatic damage associated with intense sound and to aid the detection of signals in noise. While considerable evidence shows that interruption of MOC activity exacerbates damage due to high-level sound exposure, the well characterized MOC physiology and evolutionary studies do not support such a role. Instead, a MOC protective effect is well explained as being a byproduct of the suppressive nature of MOC action on OHC mechanical behavior. A role in the enhancement of signals in noise backgrounds, on the other hand, is well supported by (1) an extensive physiological literature (2) examination of naturally occurring environmental acoustic conditions (3) recent data from multiple laboratories showing that the MOC plays a significant role in auditory selective attention by suppressing the response to unattended or ignored stimuli. This presentation will argue that, based on the extant literature combining the suppression of background noise through MOC-mediated rapid adaptation (RA) with the suppression of non-attended signals, in concert with the corticofugal pathways descending from the auditory cortex, the MOC system has one evolved function—to increase the signal-to-noise ratio, aiding in the detection of target signals. By contrast, the MOC system role in reducing noise damage and the effects of aging in the cochlea may well represent an exaptation, or evolutionary "spandrel".

Keywords: medial olivocochlear efferents, MOC, signal-to-noise ratio, protection from acoustic trauma, outer hair cells, OHC, corticofugal pathways, auditory attention

INTRODUCTION AND OVERVIEW

The exquisite sensitivity and frequency selectivity characteristic of the mammalian auditory system are consequences of the active mechanical behavior of cochlear outer hair cells (OHCs). Driven by the largest membrane potential in the body, OHCs increase the amplitude of the basilar membrane traveling wave by two to three orders of magnitude in response to sound. The main responses of OHCs are not thought to be communicated directly to the auditory CNS via afferent relays, but instead are reflected in the response of inner hair cells, and their rich primary afferent innervation, through the resulting mechanical disturbances in the Organ of Corti and subtectorial fluids.

OHCs, for their part, are under the control of a complex descending innervation, originating from medial olivary complex in the brainstem. These medial olivocochlear (MOC) neurons can be subdivided into ipsilaterally-activated "crossed" MOC, and the contralaterally-activated "uncrossed" MOC neurons (Warr, 1992). Additionally, corticofugal pathways descend from auditory cortex to the olivary complex, and influence OHC sensitivity through MOC connections (Khalfa et al., 2001; Perrot et al., 2006; Delano et al., 2007; Schofield, 2010). Activation of the MOC in any form, by ipsilateral or contralateral sound, by electrical stimulation of either subgroup or the auditory cortex or through manipulations of attention, reduces OHC motility through a shunting of the receptor current (Rabbitt et al., 2009); reductions in auditory activity are then observed at all levels within the afferent pathways.

There remains considerable discussion concerning the role of the MOC system in hearing (cf., Kirk and Smith, 2003; Robles and Delano, 2008; Robertson, 2009; Guinan, 2010). Different

functions have been proposed, with protection from noise trauma (cf., Rajan, 1988; Kujawa and Liberman, 1997; Maison et al., 2013) and the enhancement of target signals in noise (c.f., Winslow and Sachs, 1987, 1988; Kawase and Liberman, 1993; Kirk and Smith, 2003; Andéol et al., 2011) being most frequently mentioned. Here we will argue, as we have done previously (Kirk and Smith, 2003), that a meaningful discussion of *the* role of the MOC must first separate what the MOC *can be made to do*, from what it *does do*—which functions are supported by the MOC's physiologic characteristics and by consideration of the evolutionary forces involved in shaping them. The important reasons for making this distinction lay in the resulting experimental questions and stimulus paradigms used to study the system. For example, literature searches on google scholar with search terms of "medial olivocochlear" AND "acoustic trauma" (in title and abstract) yielded approximately 6 times more published research reports than searching for "medial olivocochlear" AND "signal-to-noise", "signals in noise" and related terms combined for recent years of 2005–2015. This suggests that authors have recently focused more on MOC protection against acoustic trauma, which—as we argue here—is likely an epiphenomenon (Kirk and Smith, 2003; Robertson, 2009; Maison et al., 2013; Liberman et al., 2014), compared with the role of the MOC in the detection of signals in noise—arguably the biological role of the system.

We approach this review from an evolutionary biological perspective because the role of the MOC must be rooted in physical conditions within naturally occurring acoustic environments and how those interact with an animal's phenotype to determine survival. In the case of the MOC, the conditions must necessarily be universal because of the near ubiquity of the MOC across the class Mammalia. There are many studies showing that interruption of MOC function exacerbates noise-induced trauma, and we suggest that this result is a real, predictable outcome of the suppressive nature of the MOC on cochlear mechanics. Yet, the demonstration of an MOC "protective" effect requires sound pressure levels (SPL) that are extremely rare, or do not occur at all, in natural acoustic environments. This effect may thus be regarded an exaptation or evolutionary "spandrel" in the sense proposed by Gould (1997).[1]

In this review, we use our earlier paper, Kirk and Smith (2003), as a starting point, and include important new data to present a single, unitary model of the biological role of the MOC system. Many of the older, specific studies mentioned here are described in more detail in Kirk and Smith (2003). Complete references for those studies can also be found in that work but, for the sake of brevity, we have not included an extensive list here. In that paper, we reviewed the extant data describing naturally-occurring acoustic environments, combined with a cladistic analysis that suggests that MOC-innervated OHCs are a general mammalian characteristic, to argue that the environmental pressures are insufficient to account for the widespread presence of the MOC. In making our arguments concerning the evolved role of the MOC in hearing, we will account for all of the different MOC subgroups, ipsilaterally- and contralaterally-activated efferents, as well as the corticofugal pathway (i.e., why the MOC is functionally connected with the auditory cortex), in a single, critical function. The conclusions we draw here, that the MOC has a single function, namely to increase the signal to noise ratio for target signals, is supported by a large literature.

DISTRIBUTION OF MOC WITHIN MAMMALS

With the exception of three species (the microchiropteran bats Hipposideros and Rhinolophus, and the blind mole rat, Spalax Ehrenbergi), the auditory end organ of all mammals is innervated by descending, efferent neurons (see Kirk and Smith, 2003 for review). MOC systems occur in four orders of placental mammals (Primates, Chiroptera, Carnivora, Rodentia) and two orders of marsupials (Dasyuromorphia and Didelphimorphia). This suggests that the MOC system is a general feature of the mammalian auditory system, which is likely to have emerged no later than at the time of divergence between marsupial and placental mammals, ca. 173 million years ago. Among mammals for which the anatomy has been described, 21 of 24 species possess cochlear OHCs that are innervated by MOC neurons. This wide distribution, across six orders and 16 families of mammals, suggests that evolutionary selection processes have favored the mammalian MOC system, despite pronounced inter-species differences in habitat and ecology.

NATURALLY-OCCURRING ACOUSTIC ENVIRONMENTS

Our review of the literature showed that the great majority of natural acoustic environments are characterized by relatively modest (<70 dB SPL) ambient noise levels (see Kirk and Smith, 2003). The literature described both biotic and abiotic noise under a wide range of environmental conditions (e.g., ground cover, vegetation, species assemblages, etc.). Primary sources of abiotic noise include wind, rain, and wave action; wind-generated noise has a characteristic spectrum, with the dominant power peaks present at frequencies below 200–500 Hz, and water-generated noise sources have similar low-frequency spectra with peaks that extend to higher frequencies, though at frequencies above 2.0 kHz, the energy present in any one particular frequency band does not exceed 20 dB SPL.

The most intense, naturally-occurring noise environments resulted from biotic causes, for example from the chorusing of insects, birds or frogs. During these events, the highest measured SPL reached approximately 92 dB SPL in an octave band centered at 2.0 kHz in a montane rainforest in Puerto

[1]Gould, with his collaborator R. C. Lewontin, applied the term "spandrel" to explain phenotypic traits that arise not because of their adaptive value, but as a consequence of other adaptations. In architecture, spandrels are any features, beit the triangular spaces over arched passageways in the Basilica di San Marco that inspired Gould and Lewontin, or the flat, rectangular spaces over a row of windows; the spandrels themselves were not the design feature, but are a consequence of, spaces "leftover" from design of the arches and, or windows. Regardless of how the spandrels have been adorned in the Basilica di San Marco, few would argue they themselves were designed specifically as artistic pieces. Gould and Lewontin likened architectural spandrels to evolutionary phenotypes that resulted, not because they have adaptive value, but as a consequence of the adaptive value of some related trait. Indeed, a spandrel might not confer adaptive value. Gould termed spandrels that conferred adaptive value "exaptations." Here we argue that the protective effect of MOC action is an exaptation resulting from the suppressive nature of MOC function.

Rico (Narins, 1982). It is important to point out that higher sound levels do occur under extreme conditions, such as with thunder or at the base of a waterfall, but are rare and discontinuously distributed in time and space. Some bat species also use vocalizations in echolocation that exceed 120–140 dB SPL, but these, too, are infrequent and outside the frequency range of all but a few mammals. Interestingly, of the known mammals lacking an MOC innervation of the ear, two species are microchiropteran bats (*Hipposiderous* and Rhinolophus).

MOC PROTECTION FROM NOISE TRAUMA

Our earlier survey of the existing MOC-noise trauma literature concluded that MOC-based protection was evident at SPLs of 100–105 dB SPL and higher; these acoustic conditions do not have an analog in nature. This literature continues to grow and, amongst the relevant, new studies, two have employed different approaches. First, Maison et al. (2013) exposed mice to a moderate-level, 84 dB SPL, noise for 1 week to produce acute, but not chronic threshold shifts in mice. Though the acoustic conditions used remain substantially outside those typically found in nature, the objective of their work was to study the role of both lateral and medial efferent tracts in reducing the effects noise-induced loss of Type I afferents. Prior to exposure, the mice underwent surgery, damaging or removing the lateral efferent tracts synapsing on primary afferents under the IHCs, or the MOC. The results of the study showed a relatively greater loss of primary afferents with the MOC lesions, likely due to the loss of OHC gain control during noise exposure.

Likewise, taking an entirely different approach, Liberman et al. (2014) showed for the first time that chronic lesion of the MOC can have damaging effects on the normal aging of the cochlea. In that study, the MOC system was surgically lesioned in CBA/CaJ mice, then left for 39 weeks to experience normal, low-level (∼40–70 dB SPL) ambient noise within the animal facility. At 45 weeks of age, the resulting effect of lack of MOC feedback was an accelerated, age-related decline in brainstem responses and a decrease in afferent synapses below inner hair cells, suggesting the MOC functions to aid in normal cochlear aging.

There are, however, complications in interpreting these interesting, new data as evidence of the protective effect of the MOC. Analysis of mouse mitochondrial DNA shows that most in-bred mouse strains have descended from the same wild *Mus musculus domesticus* female (Zheng et al., 2014). In the wild, the ancestral strain, the house mouse, reaches sexual maturity at 4–6 weeks, has a reproductive life of 5–7 months, and longevity estimates range from 3 months to between 7 and 9 months, rarely lives beyond 1 year (Latham and Mason, 2004). This is in stark contrast to the longevity of in-bred strains, which can live for >2–3 years in the laboratory.[2] The question remains, then, whether the presence of the MOC can alter the normal aging pattern given the reproductive biology of wild mice. It is important to note that, while the literature does not support an evolved MOC protective mechanism, this does in no way minimizes the importance of deliberate manipulation of the MOC as an interventional strategy to reduce acoustic trauma. Clearly, more research is needed to better understand this phenomenon and how it might be exploited.

[2]jaxmice.jax.org

DETECTION OF SIGNALS IN NOISE

As we pointed out above, given the wide distribution of the MOC within Mammalia, the environmental acoustic conditions that have acted to maintain the system must be nearly universal. Clearly, extreme, traumatic sound levels do not meet this requirement. Alternatively, our review shows that low-level noise, both exogenous (wind and water) and endogenous (heart, myogenic, respiratory, gnathosonic, etc.), are universal. In the presence of this low-level, broadband noise, then, the ear is tasked with essential behaviors such as identifying predator and prey (e.g., sound localization), as well as communicating. It shares these tasks with the other sensory systems, and – not surprisingly- these other systems have evolved to possess similar mechanisms to address the problem of signal and noise: During waking hours, human beings are exposed to a dense and complex stream of stimuli, engaging all sensory domains. Because cognitive systems are limited in their ability to process this wealth of sensory data, mechanisms for selection of a subset of this information are needed, and these mechanisms are studied in the Psychology and Neuroscience laboratories using selective attention tasks. Across sensory modalities, one core theme in theories of selective attention has been that of amplifying certain features or aspects of the sensory signal that are relevant for behavior, while suppressing others. This emphasis on the signal-to-noise ratio in sensory signaling is evident in competition (Desimone, 1996) and normalization (Reynolds and Heeger, 2009) theories of visual selective attention, as well as in models of auditory cortical re-tuning towards behaviorally relevant auditory frequencies (Weinberger, 2004). Across, modalities, physical stimulus characteristics and experience-based, low-level amplification mechanisms in the brain provide signals to facilitate sensory cortical processing regions based on stimulus salience, in a bottom-up fashion. In addition, top-down projections into sensory systems serve to enhance relevant signals and/or suppress unwanted information, that is, the noise.

A number of reviews (cf., Robles and Delano, 2008; Robertson, 2009; Guinan, 2010) have detailed the numerous studies, both physiological and behavioral, showing the importance of MOC action in reducing the effects of noise, and increasing the signal-to-noise ratio for target signals (cf., Nieder and Nieder, 1970; Winslow and Sachs, 1987, 1988; Kawase and Liberman, 1993; May and McQuone, 1995; Andéol et al., 2011). How this is accomplished in the auditory system was explained by Liberman et al. (1996), when they demonstrated that the MOC was responsible for the rapid adaptation (RA) seen in OHCs. RA, with a time constant in the range of 50–100 ms, reduces OHC responses to sustained stimulation, and is relatively larger with binaural, compared with monaural sound owing to the inclusion of both crossed and uncrossed MOC subgroups in the response. Given that ambient background noises tend to be longer in duration, or effectively continuous, while biologically-important signals are brief or transient, the MOC suppresses responding

to the noise alone and increases the signal-to-noise ratio for the target.

While MOC-mediated RA is a function of a low-level reflex loop, ending with crossed MOC fibers terminating on OHCs, important new findings suggest that corticofugal neurons, descending from the auditory cortex to the medial olivary complex, put the MOC system and, as a consequence, the OHCs, under cognitive control. A growing literature suggests that selective attention tasks produce alterations in peripheral auditory system function (Puel et al., 1988; Dai et al., 1991; Meric and Collet, 1992, 1994; Giard et al., 1994; Strickland and Viemeister, 1995; Maison et al., 2001; Delano et al., 2007; Srinivasan et al., 2012). As a whole, these studies show that representation in the auditory CNS of attended signals is relatively larger than ignored signals, owing to an apparent suppression of unattended sounds. Delano et al. (2007) showed conclusively that this effect resulted from MOC fibers terminating on OHCs. Delano et al. measured both the auditory nerve compound action potential (CAP) and cochlear microphonic (CM) response to auditory signals in chinchillas during visual and auditory tasks. They reported that CAPs recorded during visual discrimination tasks were smaller than, were suppressed compared with, CAPs recorded during auditory discrimination. Importantly, they also found that the CM response increased during the visual task, indicative of an MOC modulation of OHC membrane conductance resulting in a decrease in OHC gain (Mountain, 1980).

The function played by the so-called "uncrossed" MOC tract connecting the two ears in auditory signal processing is less well understood. When sound is played to the contralateral ear, these efferent neurons suppress responding in the opposite ear. Recent work by de Boer and Thornton (2007) has provided data suggesting that the uncrossed MOC is also under cognitive control. They showed that that shifts in the focus of attention may alter the ability of contralateral noise to suppress click-evoked otoacoustic emissions.

A study by our laboratory (Srinivasan et al., 2014) also supported that the uncrossed MOC has an important function in selective attention. We presented the same, brief tones simultaneously to both ears, with the overall duration of the tones varied in each ear. We compared the amplitude of DPOAEs recorded in one ear, as we instructed the subjects to count the shorter tones presented to the (1) ipsilateral or (2) contralateral ear, or (3) to ignore both ears and respond to subtle changes in a visual grating stimulus. DPOAE amplitude varied significantly with shifts in intermodal attention and, more importantly, when the focus of attention was shifted from one ear to the other. These data suggest that, like the corticofugal-crossed MOC tracts, the uncrossed MOC is under higher-level attentive control and can function to reduce the salience of ignored signals as a way of increasing the detectability of target signals.

THE ROLE OF MOC: INCREASING THE SIGNAL-TO-NOISE RATIO

Out of necessity, most physiological studies, including those of the MOC, focus on how systems function within tightly controlled experimental conditions. As such, infrequent consideration is paid to the selective variables that may have been involved in the evolution of the system. From an evolutionary biology perspective, "function" is an imprecise term, and refers to the myriad roles that may be played by a system in a variety of contexts. In order to define the biological role played by a system, we must first identify whether or not the stimulus conditions necessary to evoke a specific function are routinely found in nature. Clearly, MOC protection from noise trauma fails in this regard, as the necessary extreme noise conditions simply do not exist. Alternatively, given the wealth of data, and recent reports of the benefits of MOC feedback in reducing the deleterious effects of aging on the cochlea, MOC effects may very well represent an important exaptation, or evolutionary spandrel (Gould, 1997).

As described above, RA in OHCs is mediated by the MOC (Liberman et al., 1996). Thus, we considered DPOAE RA to relatively long-duration tones an ideal measure to characterize the role of the MOC in auditory selective attention in human listeners—the presence of RA in our data ensures that we are measuring MOC function (Bassim et al., 2003; Smith et al., 2012; Srinivasan et al., 2012, 2014). Initially, we hypothesized that changes in DPOAEs produced by shifts in the focus of attention would be observed as decreases in the slope of the RA function. Instead, what we have repeatedly observed across a number of different manipulations of attention, are *parallel* shifts in the absolute *level* of the DPOAE adaptation contour (Smith et al., 2012; Srinivasan et al., 2012, 2014). This effect is illustrated in schematic form in **Figure 1**.

That the MOC-controlled slope of the adaptation contour is unaffected by shifts in attention, and the entire function shifts only in absolute level, makes clear that two different, *concurrent* MOC processes are evident in the results; RA, which is entirely unaffected by attention, and a change in the gain of the cochlear amplifier to optimize the sensitivity of the cochlea, which is affected by the demands of the attention task. Both of the MOC phenomena observed in our data achieve the same result—increasing the signal to noise ratio for target signals via a reduction in responding to background noise; in the case of attention effects on cochlear gain, noise is defined as an unattended signal. By contrast, RA is a fundamental property of all sensory systems. It serves to decrease responding to sustained or repeated stimulation, preventing saturation and allowing for responses to new, transient stimuli. Because environmental noises, such as wind and water, are relatively long lasting, MOC RA suppresses the representation of these sounds at the level of the OHC, increasing the salience of new signals.

In studies of attention at the cortical or behavioral level, the effects of attending to an auditory signal are most typically observed as increases in the amplitude of the attended signal, compared with when that same signal is ignored (cf., Woldorff et al., 1987; Johnson and Zatorre, 2005; Kauramäki et al., 2007). Our DPOAE contours, on the other hand, are reduced in overall amplitude when listeners attend to the primaries (**Figure 1**; Smith et al., 2012; Srinivasan et al., 2012, 2014). We have explained this apparent paradox as being a consequence

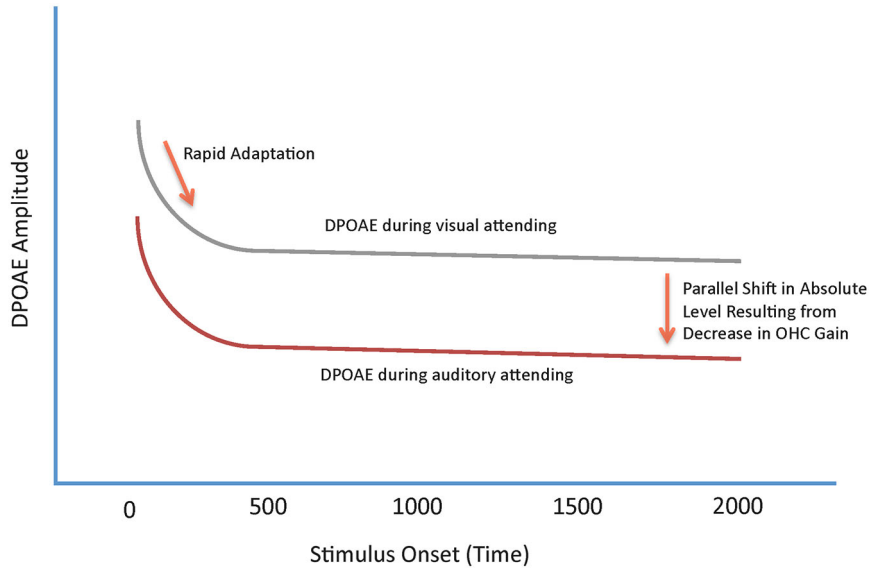

FIGURE 1 | Schematic summary of the effects of shifts in attention on DPOAE adaptation contours. The two contours represent the amplitude of the DPOAE as a function of time from primary tone onset. The upper, gray contour, represents a DPOAE contour measured during a visual gradient discrimination task. The lower, red, contour represents a DPOAE measured during an auditory attending task. Both contours show a rapid decrease in overall level following stimulus onset produced by rapid adaptation (RA). DPOAEs measured during visual attending tasks are, on average, higher in overall level compared with DPOAEs measured during auditory attending tasks. The difference in DPOAE contours between the two functions is observed as a parallel shift in overall amplitude.

of the subjects' attending to the primaries and, with the actual DPOAE being present in a different critical band, the DPOAE is suppressed by MOCs. Recent unpublished work in our laboratories measuring shifts in DP microstructure across different attended and unattended frequency bandwidths supports this notion (Srinivasan et al., unpublished). A similar effect has also been observed numerous times in psychophysical studies: For instance, in a simple threshold task where listeners are instructed to detect a specific frequency signal, thresholds for an unexpected tonal frequency are increased, and detection accuracy is decreased, with tonotopic distance from the expected frequency (cf., Dai et al., 1991; Strickland and Viemeister, 1995). Scharf et al. (1997) have demonstrated that this difference was reduced, or lost in patients with vestibular neuroectomy, where the MOC tracts to an ear are lesioned. This attentive process, like MOC neurons, is tuned and allows the listener to focus attention on one particular voice, or sound, at the exclusion of ignored sounds. This attentive tuning likely underlies the oft-mentioned "cocktail party" effect.

SUMMARY AND CONCLUSIONS

Our review argues that the biological role of the MOC system in hearing is to increase the signal-to-noise ratio for transient signals that are relevant for guiding behavior. This function results from two known processes that function concurrently, RA and selective attention, which both function to suppress environmental as well as task-irrelevant "noise". This role is well supported by the extant physiological literature and describes functions of all MOC tracts into the ear, including their control by corticofugal neurons descending from auditory cortex. We argue that the environmental noise literature does not support that the MOC have evolved to protect the ear from acoustic trauma. We instead suggest that this noise-protective function might represent an evolutionary byproduct with beneficial consequences for the organism.

ACKNOWLEDGMENTS

The authors are indebted to Professor E. Christopher Kirk, for encouraging us to remember Darwin in our work. Our thinking on the mechanisms of noise trauma has also benefited from Drs. Rick Davis, Colleen LePrell and Ed Lobarinas. This work was funded in part by NIH grants R01MH097320 and R01MH084932 to Andreas Keil.

REFERENCES

Andéol, G., Guillaume, A., Michel, C., Save, S., Pellieux, L., and Moulin, A. (2011). Auditory efferents facilitate sound localization in noise in humans. *J. Neurosci.* 31, 6759–6763. doi: 10.1523/JNEUROSCI.0248-11.2011

Bassim, M. K., Miller, R. L., Buss, E., and Smith, D. W. (2003). Rapid adaptation of the 2f1–f2 DPOAE in humans: binaural and contralateral stimulation effects. *Hear. Res.* 182, 140–152. doi: 10.1016/s0378-5955(03)00190-4

Dai, H. P., Scharf, B., and Buus, S. (1991). Effective attenuation of signals in noise under focused attention. *J. Acoust. Soc. Am.* 89, 2837–2842. doi: 10.1121/1.400721

de Boer, J., and Thornton, A. R. D. (2007). Effect of subject task on contralateral suppression of click evoked otoacoustic emissions. *Hear. Res.* 233, 117–123. doi: 10.1016/j.heares.2007.08.002

Delano, P. H., Elgueda, D., Hamame, C. M., and Robles, L. (2007). Selective attention to visual stimuli reduces cochlear sensitivity in chinchillas. *J. Neurosci.* 27, 4146–4153. doi: 10.1523/jneurosci.3702-06.2007

Desimone, R. (1996). Neural mechanisms for visual memory and their role in attention. *Proc. Natl. Acad. Sci. U S A* 93, 13494–13499. doi: 10.1073/pnas.93.24.13494

Giard, M. H., Collet, L., Bouchet, P., and Pernier, J. (1994). Auditory selective attention in the human cochlea. *Brain Res.* 633, 353–356. doi: 10.1016/0006-8993(94)91561-x

Gould, S. J. (1997). The exaptive excellence of spandrels as a term and prototype. *Proc. Natl. Acad. Sci. U S A* 94, 10750–10755. doi: 10.1073/pnas.94.20.10750

Guinan, J. J. Jr. (2010). Cochlear efferent innervation and function. *Curr. Opin. Otolaryngol. Head Neck Surg.* 18, 447–453. doi: 10.1097/MOO.0b013e32833e05d6

Johnson, J. A., and Zatorre, R. J. (2005). Attention to simultaneous unrelated auditory and visual events: behavioral and neural correlates. *Cereb. Cortex* 15, 1609–1620. doi: 10.1093/cercor/bhi039

Kauramäki, J., Jääskeläinen, I. P., and Sams, M. (2007). Selective attention increases both gain and feature selectivity of the human auditory cortex. *PLoS One* 2:e909. doi: 10.1371/journal.pone.0000909

Kawase, T., and Liberman, M. C. (1993). Antimasking effects of the olivocochlear reflex. I. Enhancement of compound action potentials to masked tones. *J. Neurophysiol.* 70, 2519–2532.

Khalfa, S., Bougeard, R., Morand, N., Veuillet, E., Isnard, J., Guenot, M., et al. (2001). Evidence of peripheral auditory activity modulation by the auditory cortex in humans. *Neuroscience* 104, 347–358. doi: 10.1016/s0306-4522(01)00072-0

Kirk, E. C., and Smith, D. W. (2003). Protection from acoustic trauma in *not* a primary function of the medial olivocochlear efferent system. *J. Assoc. Res. Otolaryngol.* 4, 445–465. doi: 10.1007/s10162-002-3013-y

Kujawa, S. G., and Liberman, M. C. (1997). Conditioning-related protection from acoustic injury: effects of chronic de-efferentation and sham surgery. *J. Neurophysiol.* 78, 3095–3106.

Latham, N., and Mason, G. (2004). From house mouse to mouse house: the behavioural biology of free-living *Mus musculus* and its implications in the laboratory. *Appl. Anim. Behav. Sci.* 86, 261–289. doi: 10.1016/j.applanim.2004.02.006

Liberman, M. C., Liberman, L. D., and Maison, S. F. (2014). Efferent feedback slows cochlear aging. *J. Neurosci.* 34, 4599–4607. doi: 10.1523/JNEUROSCI.4923-13.2014

Liberman, M. C., Puria, S., and Guinan, J. J. Jr. (1996). The ipsilaterally evoked olivocochlear reflex causes rapid adaptation of the 2f1–f2 distortion product otoacoustic emission. *J. Acoust. Soc. Am.* 99, 3572–3584. doi: 10.1121/1.414956

Maison, S., Micheyl, C., and Collet, L. (2001). Influence of focused auditory attention on cochlear activity in humans. *Psychophysiology* 38, 35–40. doi: 10.1111/1469-8986.3810035

Maison, S. F., Usubuchi, H., and Liberman, M. C. (2013). Efferent feedback minimizes cochlear neuropathy from moderate noise exposure. *J. Neurosci.* 33, 5542–5552. doi: 10.1523/JNEUROSCI.5027-12.2013

May, B. J., and McQuone, S. J. (1995). Effects of bilateral olivocochlear lesions on pure-tone intensity discrimination in cats. *Aud. Neurosci.* 1, 385–400.

Meric, C., and Collet, L. (1992). Visual attention and evoked otoacoustic emissions: a slight but real effect. *Int. J. Psychophysiol.* 12, 233–235. doi: 10.1016/0167-8760(92)90061-f

Meric, C., and Collet, L. (1994). Differential effects of visual attention on spontaneous and evoked otoacoustic emissions. *Int. J. Psychophysiol.* 17, 281–289. doi: 10.1016/0167-8760(94)90070-1

Mountain, D. C. (1980). Changes in endolymphatic potential and crossed olivocochlear bundle stimulations alter cochlear mechanics. *Science* 210, 71–72. doi: 10.1126/science.7414321

Narins, P. M. (1982). Effects of masking noise on evoked calling in the Puerto Rican coqui (Anura: Leptodactylidae). *J. Comp. Physiol. A* 147, 439–446. doi: 10.1007/bf00612008

Nieder, P. C., and Nieder, I. (1970). Crossed olivocochlear bundle: electrical stimulation enhances masked neural responses to loud clicks. *Brain Res.* 21, 135–137. doi: 10.1016/0006-8993(70)90029-6

Perrot, X., Ryvlin, P., Isnard, J., Guénot, M., Catenoix, H., Fischer, C., et al. (2006). Evidence for corticofugal modulation of peripheral auditory activity in humans. *Cereb. Cortex* 16, 941–948. doi: 10.1093/cercor/bhj035

Puel, J. L., Bonfils, P., and Pujol, R. (1988). Selective attention modifies the active micromechanical properties of the cochlea. *Brain Res.* 447, 380–383. doi: 10.1016/0006-8993(88)91144-4

Rabbitt, R. D., Clifford, S., Breneman, K. D., Farrell, B., and Brownell, W. E. (2009). Power efficiency of outer hair cell somatic electromotility. *PLoS Comput. Biol.* 5:e1000444. doi: 10.1371/journal.pcbi.1000444

Rajan, R. (1988). Effect of electrical stimulation of the crossed olivocochlear bundle on temporary threshold shifts in auditory sensitivity. I. Dependence on electrical stimulation parameters. *J. Neurophysiol.* 60, 549–568.

Reynolds, J. H., and Heeger, D. J. (2009). The normalization model of attention. *Neuron* 61, 168–185. doi: 10.1016/j.neuron.2009.01.002

Robertson, D. (2009). Centrifugal control in mammalian hearing. *Clin. Exp. Pharmacol. Physiol.* 36, 603–611. doi: 10.1111/j.1440-1681.2009.05185.x

Robles, L., and Delano, P. H. (2008). "Efferent system," in *The Senses: A Comprehensive Reference*, eds P. Dallos and D. Oertel (London: Academic Press), 413–445.

Scharf, B., Magnan, J., and Chay, A. (1997). On the role of the olivocochlear bundle in hearing: 16 case studies. *Hear. Res.* 103, 101–122. doi: 10.1016/s0378-5955(96)00168-2

Schofield, B. R. (2010). "Structural organization of the descending auditory pathway," in *The Oxford Handbook of Auditory Science: The Auditory Brain*, eds A. Rees and A. R. Palmer (New York: Oxford University Press), 43–64.

Smith, D. W., Aouad, R. K., and Keil, A. (2012). Cognitive task demands modulate the sensitivity of the human cochlea. *Front. Psychol.* 3:30. doi: 10.3389/fpsyg.2012.00030

Srinivasan, S., Keil, A., Osbourne, A. F., Cerwonka, C., Wong, J., Rieger, B. L., et al. (2014). Interaural attention modulates outer hair cell function. *Eur. J. Neurosci.* 40, 3785–3792. doi: 10.1111/ejn.12746

Srinivasan, S., Keil, A., Stratis, K., Woodruff Carr, K. L., and Smith, D. W. (2012). Effects of cross-modal selective attention on the sensory periphery: cochlear sensitivity is altered by selective attention. *Neuroscience* 223, 325–332. doi: 10.1016/j.neuroscience.2012.07.062

Strickland, E. A., and Viemeister, N. F. (1995). An attempt to find psychophysical evidence for efferent action in humans. *Abstr. Midwinter Res. Meet Assoc. Res. Otolaryngol.* 173.

Warr, W. B. (1992). "Organization of olivocochlear efferent systems in mammals," in *The Mammalian Auditory Pathway: Neuroanatomy*, eds D. B. Webster, A. N. Popper and R. R. Fay (New York: Springer-Verlag), 410–448.

Weinberger, N. M. (2004). Specific long-term memory traces in primary auditory cortex. *Nat. Rev. Neurosci.* 5, 279–290. doi: 10.1038/nrn1366

Winslow, R. L., and Sachs, M. B. (1987). Effect of electrical stimulation of the crossed olivocochlear bundle on auditory nerve response to tones in noise. *J. Neurophysiol.* 57, 1002–1021.

Winslow, R. L., and Sachs, M. B. (1988). Single tone intensity discrimination based on auditory-nerve responses in backgrounds of quiet, noise and with stimulation of the crossed olivocochlear bundle. *Hear. Res.* 35, 165–189. doi: 10.1016/0378-5955(88)90116-5

Woldorff, M. G., Hansen, J. C., and Hillyard, S. A. (1987). "Evidence for effects of selective attention in the mid-latency range of the human auditory event-related potential," in *Current Trends in Event Related Potential Research (EEG Suppl 40)*, eds R. Jr. Johnson, J. W. Rohrbaugh and R. Parasuraman (Amsterdam, Netherlands: Elsevier Science Publishers), 146–154.

Zheng, J., Chena, Y., Deng, F., Huang, R., Petersen, F., Ibrahim, S., et al. (2014). mtDNA sequence, phylogeny and evolution of laboratory mice. *Mitochondrion* 17, 126–131. doi: 10.1016/j.mito.2014.07.006

Conflict of Interest Statement: The authors declare that the research was conducted in the absence of any commercial or financial relationships that could be construed as a potential conflict of interest.

Received: 15 December 2014; accepted: 23 January 2015; published online: 25 February 2015.

*Citation: Smith DW and Keil A (2015) The biological role of the medial olivocochlear efferents in hearing: separating evolved function from exaptation. Front. Syst. Neurosci. **9**:12. doi: 10.3389/fnsys.2015.00012*

This article was submitted to the journal Frontiers in Systems Neuroscience.

frontiers in Systems Neuroscience

MINI REVIEW
published: 22 June 2015
doi: 10.3389/fnsys.2015.00094

The olivocochlear system and protection from acoustic trauma: a mini literature review

*Adrian Fuente**

Faculté de médecine, École d'orthophonie et d'audiologie, Université de Montréal, Montréal, QC, Canada

Large intersubject variability in the susceptibility to noise-induced hearing loss (NIHL) is known to occur in both humans and animals. It has been suggested that the olivocochlear system (OCS) plays a significant role in protecting the cochlea from exposure to high levels of noise. A mini literature review about the scientific evidence from animal and human studies about the association between the function of the OCS and susceptibility to NIHL was carried out. Animal data consistently show that de-efferented ears exhibit larger temporary threshold shift (TTS) and permanent threshold shift (PTS) than efferented ears. Data from human studies do not consistently show a correlation between the strength of the OCS function and amount of TTS. Further research on human subjects is required to determine how the OCS function could be used to predict susceptibility to NIHL in individual subjects.

OPEN ACCESS

Edited by:
Paul Hinckley Delano, Universidad de Chile, Chile

Reviewed by:
David W. Smith, University of Florida, USA
Amanda Lauer, Johns Hopkins University School of Medicine, USA

***Correspondence:**
Adrian Fuente, Faculté de médecine, École d'orthophonie et d'audiologie, Université de Montréal, C.P. 6128, succ. Centre-ville, Montréal, H3C 3J7, QC, Canada
adrian.fuente@umontreal.ca

Received: *30 January 2015*
Accepted: *02 June 2015*
Published: *22 June 2015*

Citation:
Fuente A (2015) The olivocochlear system and protection from acoustic trauma: a mini literature review. Front. Syst. Neurosci. 9:94. doi: 10.3389/fnsys.2015.00094

Keywords: noise, hearing loss, temporary threshold shift (TTS), permanent threshold shift (PTS), efferent auditory system, olivocochlear bundle, noise-induced hearing loss (NIHL)

Introduction

Noise-induced hearing loss (NIHL) is one of the most prevalent work-related health conditions around the world. Currently, in the United States alone, around 26 million people (15 percent of the population between 20 and 69 years) have hearing loss that may have been caused by exposure to noise at work or in leisure activities (National Institute on Deafness and other Communication Disorders (NIDCD), 2014). Large intersubject variability in susceptibility to NIHL is known to occur (Cody and Robertson, 1983). However, the mechanisms underlying such differences are poorly understood. It has been extensively suggested that the olivocochlear system (OCS), initially described by Rasmussen (1946, 1953), function may relate with susceptibility to NIHL. The OCS of the mammalian inner ear consists of two subdivisions, medial system (MOCS) and lateral system (LOCS). The MOCS has its origin in medially located superior olivary complex and controls cochlear function through synaptic contacts on outer hair cells (OHCs) from the ipsilateral and contralateral brainstem. The LOCS system, which originates in the lateral superior olive, is comprised of unmyelinated neurons that mainly project to the ipsilateral cochlea ending on type I auditory nerve fibers under inner hair cells (Warr and Guinan, 1979). The aim of this manuscript was to review the scientific evidence about the association between the OCS function and susceptibility to NIHL.

Methodology

A literature search was performed using the Web of Science Database. The strategy to find suitable articles for this review was the use of a single but well inclusive term for all research

studies that have investigated the OCS. The single term used was "olivocochlear". A total of 1, 168 entries were obtained using this term within the "topic" option of the Web of Science Database. As this mini literature review aimed to investigate research studies about the association between the OCS and protection from NIHL, all entries previously obtained were examined by reading the title of the article and the key words. Articles were included if they presented with the following key words: NIHL, acoustic trauma, acoustic injury, temporary threshold shift (TTS), permanent threshold shift (PTS), susceptibility, hearing loss. A total of 109 articles were initially selected. As the search strategy was still too broad, all abstracts (n = 109) were reviewed in order to determine whether they were suitable for the aim of this mini review. Both animal and human studies were included in this review. After reading the abstracts of such studies, a total of 52 articles were included, and thus the full articles were accessed. Most of the articles not included in this review were eliminated because they were not exploring a possible association between the OCS and NIHL. In addition, some studies were excluded as they were reviews or conference presentations, or because the full article was not found (n = 2).

Animal Studies: OCS and Protection for Acoustic Trauma

Initially, Trahiotis and Elliott (1970) did not find a significant difference in TTS between cats that had a section of the OCS and who were exposed to a broadband noise of 107 dB SPL during 10 min, and a control group of cats. However, more than 10 years later Handrock and Zeisberg (1982) demonstrated that guinea pigs with transection of the OCS presented with significantly lower and longer N1 amplitude as compared to control group animals after a noise exposure of 125 dB for 30 min. Similarly, Rajan and Johnstone (1983) reported that TTS from a high-frequency tone (10 kHz at 103 dB SPL for 1 min) can be decreased by contralateral stimulation or contralateral cochlear destruction in guinea pigs. The authors suggested that this reduction was the effect of the OCS. In a follow-up study, Rajan (1988a,b) found that electrical stimulation of the crossed OCS reduced the amount of TTS, as measured through compound action potential (CAP), after noise exposure in animals. In addition, the administration of strychnine could eliminate the reduction in TTS. Yamasoba and Dolan (1997) suggested that chronic strychnine administration into the cochlea inactivates the medial efferent fibers without changing hearing threshold and that the medial efferent fibers help to protect against PTS following noise exposure. In a follow-up study (Yamasoba and Dolan, 1998), using noise conditioning along with sectioning of the OCS, the authors concluded that although the OCS acts to attenuate NIHL, it may not be necessary for the acquired resistance to NIHL.

Liberman (1991) in a group of cats with sectioned middle-ear muscles did not find a significant association between OCS function and protection for acoustic injury. It is important to note, that in Liberman experiment, cats were binaurally exposed to a 6 kHz tone at 100 dB during 10 min. Further studies from (Rajan, 1989, 1990, 1995a,b, 1996, 2000, 2001a,b,c, 2003, 2005, 2007; Rajan and Johnstone, 1989) have then demonstrated that the OCS protective effect in animals depends on variables such as intensity and frequency of the noise, presence of hearing loss in the contralateral ear and whether the noise is presented monaurally or binaurally which leads to a differentiated pattern of stimulation of the uncrossed and crossed OC pathways.

Liberman and Gao (1995) investigated PTS between guinea pigs with an OCS that was surgically de-efferented and sham-operated animals. Animals were exposed to a narrow-band noise centered at 10 kHz for 2 h at a level of 109 or 112 dB. CAP, hair cell loss and stereocilia condition after noise exposure were investigated. Significant differences between surgically de-efferented and sham-operated animals were found only for CAP responses in those animals exposed at 112 dB. The authors concluded that the OCS may play a protective role for the extreme basal region of the cochlea. Reiter and Liberman (1995) proposed that the OCS protection relates to "slow" effects of OC activation rather than "fast" effects. The authors mentioned that the peak effect of the former is in frequency regions affected by 10-kHz exposures and when continuous OC stimulation is maintained for 1–2 min.

In the study carried out by Zheng et al. (1997a) OCS fibers in chinchillas were completely sectioned and then the animals were exposed to a 105 dB SPL broadband noise for 6 h. OHC function was explored through distortion product otoacoustic emissions (DPOAEs, 1.2–9.6 kHz) and cochlear microphonics (CM, 1–8 kHz). As a result of de-efferentation, the CM was decreased but DPOAEs were unchanged in de-efferented ears as compared with efferented control and sham-operated ears. Following noise exposure, the ears that were de-efferented showed significantly more depression for DPOAE input/output functions and greater decrement of CM amplitude. Differences between de-efferented and efferent-innervated ears were evident across all frequencies. However, OHC damage reflected by cytocochleogram was minimal in both efferented and de-efferented ears. The authors indicated that cochlear de-efferentation decreases the CM in chinchillas and increases the ear's susceptibility to NIHL. In addition, they claimed that de-efferentation increases susceptibility at low frequencies as well as high frequencies. Similarly, in another animal study from the same group of researchers (Zheng et al., 1997b), it was found that de-efferented ears showed substantially more TTS, greater PTS and greater OHC damage as compared with efferent ears. Subsequently, Zheng et al. (2000) investigated the effect of de-efferentation of the OCS in animals exposed to impulse noise. No significant differences between efferented and de-efferented ears were observed for TTS (colliculus evoked potentials, CEP). However, 20 days after noise exposure values for CEP returned to pre noise exposure values in the efferented ears remaining significantly depressed in de-efferented ears. The amount of loss of OHC after noise exposure was not significant between efferented and de-efferented ears.

Zennaro et al. (1998) measured DPOAE with contralateral noise in order to obtain the attenuation in DPOAE amplitudes in guinea pigs. The animals were then exposed to a 2 kHz

tone of 87 dB for 40 min, obtaining DPOAEs after this exposure (TTS). No association between the attenuation effect measured before noise exposure and the susceptibility to TTS was found. However, Maison and Liberman (2000) showed that the amount of suppression of OAEs was inversely correlated with the degree of hearing loss induced after noise exposure in a group of experimental animals.

Finally, it has been suggested that lateral OC fibers modulate cochlear nerve excitability protecting the cochlea from neural damage in acute acoustic injury (Darrow et al., 2007).

Noise Conditioning Effect in Animal Studies [with or Without Sectioning the Olivocochlear Bundle (OCB)]

Brown et al. (1998) based on their study suggested that MOCS neurons show long-term plasticity in acoustic responsiveness that is dependent on their acoustic history. Thus, noise conditioning may have an effect on the strength of the OCS reflex. Patuzzi and Thompson (1991) measured the changes in neural and microphonic sensitivity in the basal turn of the guinea-pig cochlea produced by a 10 kHz, 115 dB SPL sound presented for 60 and 150 s. The drops in neural and microphonic sensitivity observed after overstimulation were highly correlated. The presentation of a non-traumatizing pure-tone to the contralateral ear (10 kHz, 80 dB SPL) during acoustic overstimulation reduced the amount of acoustic trauma. Transection of the OCS abolished the protective effect of the contralateral sound and significantly reduced the variability in the data. Canlon and Fransson (1995) investigated guinea pigs that were sound conditioned to a low-level, long-term pure tone stimulus (1 kHz, 81 dB SPL, 24 days) before exposure to a traumatic noise (1 kHz, 105 dB SPL, 72 h). Auditory brainstem response (ABR) thresholds and DPOAEs were obtained. The effect of a traumatic exposure (1 kHz, 105 dB SPL, 72 h) on a control group and a sound conditioned group (1 kHz, 81 dB SPL, 24 days) was determined. The amplitude of DPOAEs for the control group was reduced at all tested frequencies. The sound conditioned group showed increases in DPOAE amplitude with increases in the intensity of the primaries for all tested frequencies and statistically significant reductions from the pre-exposure values were not found. In addition, traumatic noise exposure affected nearly 100% of the OHCs at around 14 mm from the round window. The sound conditioned group showed a significantly less (50%) OHC loss than the control group. In another study, Canlon et al. (1999) demonstrated that after noise conditioning, the medial OC efferent terminals were protected. However, Kujawa and Liberman (1997), based on the results of their study suggested that conditioning-related protection may arise from a generalized stress response, which can be elicited by noise exposure, brain surgery, or a variety of other means. In another study, Kujawa and Liberman (1999) found that guinea pigs that were daily conditioned (6 h per day) with an octave-band noise at 85 dB SPL presented a reduction of PTS after a traumatic exposure to the same noise band at 109 dB SPL for 4 h. These results were observed for CAP and DPOAEs. In addition, the conditioning effect also enhanced the olivocochlear reflex strength, as measured through DPOAEs. However, different results were obtained by Peng et al. (2007) who observed that DPOAE amplitudes (1–3 kHz) increased after long-term noise conditioning along with a reduction in the olivocochlear reflex strength. Using a different approach, Attanasio et al. (1999) investigated the association between the OCS and the progressive threshold shift reduction when repeated exposures to the same sound were presented. A group of guinea pigs was de-efferented and then implanted with permanent electrodes for electrocochleographic measurements. Ten days after the operation the animals were exposed to an octave-band noise, centered at 4 kHz, at 85-dB SPL, for 10 consecutive days, 6 h on/18 h off. The hearing threshold was registered before and at the end of each exposure session. Complete recovery from TS in the control ear began after 4 days of exposure, whereas in the de-efferented ear hearing loss increased to day 7 (55 dB), with only a partial reduction (45 dB) beyond 10 days of exposure.

Human Studies

Tachibana et al. (1992) demonstrated that transcutaneous electrostimulation (TE) around the ear reduced the TTS in a group of volunteers. One of the interpretations by the authors was that TE stimulated the OCS. However, a previous study (Collet et al., 1991) in human subjects exposed to noise did not find a correlation between TTS and the amount of TEOAE efferent suppression. Some years later, Scharf et al. (1994) reported a case study of a subject who underwent vestibular neurotomy for Ménière's disease. Hearing thresholds (1–4 kHz) using the Békésy tracking method were obtained before and after a 15-minute exposure to a continuous 1 kHz tone at 90 dB SPL. TTS were similar between the operated and unoperated ear, and even a trend of less TTS in the operated ear as compared to the unoperated ear was found. However, Engdahl (1996) in a group of 8 subjects found a positive correlation between DPOAE (2–4 kHz) amplitude change after noise exposure (a third-octave band noise of 102 dB SPL centered at 2 kHz for 10 min) and the amount of contralateral suppression of DPOAE.

Veuillet et al. (2001) studied the association between the function of the OCS and recovery of hearing level after noise exposure. Thirty-six military subjects with acoustic trauma following impulse noise (shooting) were selected. All subjects included in the study developed a unilateral hearing loss in the range of 25–70 dB from 4 to 8 kHz. Pure-tone audiometry was obtained at three different times, being the first one within the first 72 h after noise exposure and then 3 and 30 days after the initial evaluation. In addition, spontaneous OAEs (SOAES) and TEOAEs with and without contralateral suppression were obtained on these three different times. There was no significant correlation between NIHL at 4, 6 and 8 kHz measured 72 h after noise exposure and the strength of the OCS function. However, a significant correlation between audiometric threshold improvement, obtained on the third evaluation session

(30 days after noise exposure), and contralateral TEOAE suppression was obtained. However, Wagner et al. (2005) did not find a correlation between the amount of contralateral suppression and individual TTS in a group of human subjects. Similarly, Shupak et al. (2007) did not find an association between baseline medial OC reflex strength and pure-tone thresholds after 2 years of noise exposure in a cohort of 135 noise-exposed workers. In addition, other human studies have not found a significant correlation between DPOAE efferent suppression and shifts in pure-tone thresholds or shifts in DPOAE levels after occupational noise exposure of one workday (Müller and Janssen, 2008) or after 3 h of discotheque music (Müller et al., 2010). Similarly, Hannah et al. (2014) found that the amount of TTS was not predicted from TEOAE efferent suppression amplitudes in a group of 28 subjects who listened music with an MP3 player during 1 h, at an individually determined loud listening level.

Recently, Wolpert et al. (2014) studied a group of subjects (n = 40) who were exposed to a 60-min. broadband noise at 94 dB SPL. DPOAE with and without contralateral acoustic stimulation using two paradigms was obtained. One of them was through the investigation of the growth function of DPOAE (input/output function) and the other one was through a fine structure analysis of DPOAE. Hearing thresholds were obtained before and after noise exposure. TTS for the purposes of analyses was calculated as the maximum postnoise threshold change found across all frequencies in both ears. Results showed a statistically significant inverse correlation between contralateral suppression as measured through the growth function paradigm, and the amount of TTS. No significant correlation between TTS and contralateral suppression, as obtained through the fine structure analysis, was found.

Finally, an association between noise exposure and the strength of the OC function has been investigated in humans. Sliwinska-Kowalska and Kotylo (2002) have shown that workers occupationally exposed to noise presented with significant lower DPOAE efferent suppression than non-exposed control subjects. Similarly, Peng et al. (2010) found that young adults users of personal listening devices had lower although not statistically significant DPOAE efferent suppression amplitudes than non-users of personal listening devices.

Discussion

A number of animal studies have shown that the ear can be protected from sound over-exposure by activating the OCS. However, data from human studies is equivocal in demonstrating the protective role of the OCS against noise exposure. Further research in human subjects is needed to determine how OCS function can be applied to determine susceptibility to NIHL.

A question about how the OCS may have evolved to be associated with the protection against noise trauma remains. Christopher Kirk and Smith (2003) pointed out that while sustained sources of broadband noise are found in nearly all natural acoustic environments, frequency-averaged ambient noise levels in these environments rarely exceed 70 dB SPL. In this regard, new studies have shown that the OCS may still be associated with a protective effect in the presence of "non-traumatic" sounds. Maison et al. (2013) exposed animals to an 84-dB sound during 1 week. Animals were de-efferented in various degrees. The authors found that the noise caused minimal acute threshold shift and no chronic shifts in animals with normal efferent feedback. However, in de-efferented animals, they observed a cochlear neuropathy with up to 40% loss of cochlear nerve synapses with corresponding declines in ABR responses. In addition, recent studies have also found that declines in OCS may relate with and/or precede age-related hearing loss. Zhu et al. (2007) obtained DPOAE amplitudes and contralateral suppression of DPOAEs in C57 mouse from 6 to 40 weeks of age. The authors found that the contralateral suppression of DPOAEs declines quickly and precedes peripheral age-related hearing loss. Similar results have been found by Liberman et al. (2014) who found that the loss of efferent feedback in experimental animals, who were not acoustically overexposed, accelerated age-related amplitude reduction in cochlear neural responses and increased the loss of synapses between hair cells and the terminals of cochlear nerve fibers. With this new evidence showing the protective effect of the OCS without the presence of loud sound exposure, the role of the OCS for the protection from acoustic injury should be re-defined. As pointed out by Smith and Keil (2015), the noise-protective function of the OCS might represent an evolutionary byproduct with beneficial consequences for the organism.

References

Attanasio, G., Barbara, M., Buongiomo, G., Cordier, A., Mafera, B., Piccoli, F., et al. (1999). Protective effect of the cochlear efferent system during noise exposure. *Ann. N Y Acad. Sci.* 884, 361–367. doi: 10.1111/j.1749-6632.1999.tb08654.x

Brown, M. C., Kujawa, S. G., and Liberman, M. C. (1998). Single olivocochlear neurons in the guinea pig. II. Response plasticity due to noise conditioning. *J. Neurophysiol.* 79, 3088–3097.

Canlon, B., and Fransson, A. (1995). Morphological and functional preservation of the outer hair-cells from noise trauma by sound conditioning. *Hear. Res.* 84, 112–124. doi: 10.1016/0378-5955(95)00020-5

Canlon, B., Fransson, A., and Viberg, A. (1999). Medial olivocochlear efferent terminals are protected by sound conditioning. *Brain Res.* 850, 253–260. doi: 10.1016/s0006-8993(99)02091-0

Christopher Kirk, E., and Smith, D. W. (2003). Protection from acoustic trauma is not a primary function of the medial olivocochlear efferent system. *J. Assoc. Res. Otolaryngol.* 4, 445–465. doi: 10.1007/s10162-002-3013-y

Cody, A. R., and Robertson, D. (1983). Variability of noise-induced damage in the guinea pig cochlea: electrophysiological and morphological correlates after strictly controlled exposures. *Hear. Res.* 9, 55–70. doi: 10.1016/0378-5955(83)90134-x

Collet, L., Morgon, A., Veuillet, E., and Gartner, M. (1991). Noise and medial olivocochlear system in humans. *Acta Otolaryngol.* 111, 231–233. doi: 10.3109/00016489109137380

Darrow, K. N., Maison, S. F., and Liberman, M. C. (2007). Selective removal of lateral olivocochlear efferents increases vulnerability to acute acoustic injury. *J. Neurophysiol.* 97, 1775–1785. doi: 10.1152/jn.00955.2006

Engdahl, B. (1996). Effects of noise and exercise on distortion product otoacustic emissions. *Hear. Res.* 93, 72–82. doi: 10.1016/0378-5955(95)00197-2

Handrock, M., and Zeisberg, J. (1982). The influence of the effect system on adaptation, temporary and permanent threshold shift. *Arch. Otorhinolaryngol.* 234, 191–195. doi: 10.1007/bf00453630

Hannah, K., Ingeborg, D., Leen, M., Annelies, B., Birgit, P., Freya, S., et al. (2014). Evaluation of the olivocochlear efferent reflex strength in the susceptibility to temporary hearing deterioration after music exposure in young adults. *Noise Health* 16, 108–115. doi: 10.4103/1463-1741.132094

Kujawa, S. G., and Liberman, M. C. (1997). Conditioning-related protection from acoustic injury: effects of chronic deefferentation and sham surgery. *J. Neurophysiol.* 78, 3095–3106.

Kujawa, S. G., and Liberman, M. C. (1999). Long-term sound conditioning enhances cochlear sensitivity. *J. Neurophysiol.* 82, 863–873.

Liberman, M. C. (1991). The olivocochlear efferent bundle and susceptibility of the inner-ear to acoustic injury. *J. Neurophysiol.* 65, 123–132.

Liberman, M. C., and Gao, W. Y. (1995). Chronic cochlear de-efferentation and susceptibility to permanent acoustic injury. *Hear. Res.* 90, 158–168. doi: 10.1016/0378-5955(95)00160-2

Liberman, M. C., Liberman, L. D., and Maison, S. F. (2014). Efferent feedback slows cochlear aging. *J. Neurosci.* 34, 4599–4607. doi: 10.1523/jneurosci.4923-13.2014

Maison, S. F., and Liberman, M. C. (2000). Predicting vulnerability to acoustic injury with a noninvasive assay of olivocochlear reflex strength. *J. Neurosci.* 20, 4701–4707.

Maison, S. F., Usubuchi, H., and Liberman, M. C. (2013). Efferent feedback minimizes cochlear neuropathy from moderate noise exposure. *J. Neurosci.* 33, 5542–5552. doi: 10.1523/jneurosci.5027-12.2013

Müller, J., Dietrich, S., and Janssen, T. (2010). Impact of three hours of discotheque music on pure-tone thresholds and distortion product otoacoustic emissions. *J. Acoust. Soc. Am.* 128, 1853–1869. doi: 10.1121/1.3479535

Müller, J., and Janssen, T. (2008). Impact of occupational noise on pure-tone threshold and distortion product otacoustic emissions after one workday. *Hear. Res.* 246, 9–22. doi: 10.1016/j.heares.2008.09.005

National Institute on Deafness and other Communication Disorders (NIDCD). (2014). Noise-induced hearing loss. Available online at: http://www.nidcd.nih.gov/health/hearing/pages/noise.aspx Accessed on 22 December 2014.

Patuzzi, R. B., and Thompson, M. L. (1991). Cochlear efferent neurons and protection against acoustic trauma: protection of outer hair cell receptor current and interanimal variability. *Hear. Res.* 54, 45–58. doi: 10.1016/0378-5955(91)90135-v

Peng, J. H., Tao, Z. Z., and Huang, Z. W. (2007). Log-term sound conditioning increases distortion product otoacoustic emission amplitudes and decreases olivocochlear efferent reflex strength. *Neuroreport* 18, 1167–1170. doi: 10.1097/wnr.0b013e32820049a8

Peng, J. H., Wang, J. B., and Chen, J. H. (2010). Recreational noise exposure decreases olivocochlear efferent reflex strength in young adults. *J. Otolaryngol. Head Neck Surg.* 39, 426–432. doi: 10.2310/7070.2010.090220

Rajan, R. (1988a). Effect of electrical stimulation of the crossed olivocochlear bundle on temporary threshold shifts in auditory sensitivity. I. Dependence on electrical stimulation parameters. *J. Neurophysiol.* 60, 549–568.

Rajan, R. (1988b). Effect of electrical stimulation of the crossed olivocochlear bundle on temporary threshold shifts in auditory sensitivity. II. Dependence on the level of temporary threshold shifts. *J. Neurophysiol.* 60, 569–579.

Rajan, R. (1989). Tonic activity of the crossed olivocochlear bundle in guinea pigs with idiopathic losses in auditory sensitivity. *Hear. Res.* 39, 299–308. doi: 10.1016/0378-5955(89)90049-x

Rajan, R. (1990). The effect of upper pontine transections on normal cochlear responses and on the protective effects of contralateral acoustic stimulation in barbiturate-anesthetized normal-hearing guinea-pigs. *Hear. Res.* 45, 137–144. doi: 10.1016/0378-5955(90)90189-v

Rajan, R. (1995a). Involvement of cochlear efferent pathways in protective effects elicited with binaural loud sound exposure in cats. *J. Neurophysiol.* 74, 582–597.

Rajan, R. (1995b). Frequency and loss dependence of the protective effects of the olivocochlear pathways in cats. *J. Neurophysiol.* 74, 598–615.

Rajan, R. (1996). Additivity of loud-sound-induced threshold losses in the cat under conditions of active or inactive cochlear efferent-mediated protection. *J. Neurophysiol.* 75, 1601–1618.

Rajan, R. (2000). Centrifugal pathways protect hearing sensitivity at the cochlea in noisy environments that exacerbate the damage induced by loud sound. *J. Neurosci.* 20, 6684–6693.

Rajan, R. (2001a). Unilateral hearing losses alter loud sound-induced temporary threshold shifts and efferent effects in the normal-hearing ear. *J. Neurophysiol.* 85, 1257–1269.

Rajan, R. (2001b). Noise priming and the effects of different cochlear centrifugal pathways on loud-sound-induced hearing loss. *J. Neurophysiol.* 86, 1277–1288.

Rajan, R. (2001c). Cochlear outer-hair-cell efferents and complex-sound-induced hearing loss: protective and opposing effects. *J. Neurophysiol.* 86, 3073–3076.

Rajan, R. (2003). Crossed and uncrossed olivocochlear pathways exacerbate temporary shifts in hearing sensitivity after narrow band sound trauma in normal ears of animals with unilateral hearing impairment. *Audiol. Neurootol.* 8, 250–262. doi: 10.1159/000071997

Rajan, R. (2005). Contextual modulation of olivocochlear pathway effects on loud sound-induced cochlear hearing desensitization. *J. Neurophysiol.* 93, 1977–1988. doi: 10.1152/jn.00848.2004

Rajan, R. (2007). Bandwidth dependency of cochlear centrifugal pathways in modulating hearing desensitization caused by loud sound. *Neuroscience* 147, 1103–1113. doi: 10.1016/j.neuroscience.2007.05.017

Rajan, R., and Johnstone, B. M. (1983). Crossed cochlear influences on monaural temporary threshold shifts. *Hear. Res.* 9, 279–294. doi: 10.1016/0378-5955(83)90032-1

Rajan, R., and Johnstone, B. M. (1989). Contralateral cochlear destruction mediates protection from monoaural loud sound exposures through the crossed olivocochlear bundle. *Hear. Res.* 39, 263–277. doi: 10.1016/0378-5955(89)90046-4

Rasmussen, G. L. (1946). The olivary peduncle and other fiber projections of the superior olivary complex. *J. Comp. Neurol.* 84, 141–219. doi: 10.1002/cne.900840204

Rasmussen, G. L. (1953). Further observations of the efferent cochlear bundle. *J. Comp. Neurol.* 99, 61–74. doi: 10.1002/cne.900990105

Reiter, E. R., and Liberman, M. C. (1995). Efferent-mediated protection from acoustic overexposure—relation to slow effects of olivocochlear stimulation. *J. Neurophysiol.* 73, 506–514.

Scharf, B., Magnan, J., Collet, L., Ulmer, E., and Chays, A. (1994). On the role of the olivocochlear bundle in hearing: a case study. *Hear. Res.* 75, 11–26. doi: 10.1016/0378-5955(94)90051-5

Shupak, A., Tai, D., Shakoni, Z., Oren, M., Ravid, A., and Pratt, H. (2007). Otoacoustic emissions in early noise-induced hearing loss. *Otol. Neurotol.* 28, 745–752. doi: 10.1097/mao.0b013e3180a726c9

Sliwinska-Kowalska, M., and Kotylo, P. (2002). Occupational exposure to noise decreases optoacoustic. Emission efferent suppression. *Int. J. Audiol.* 41, 113–119. doi: 10.3109/14992020209090401

Smith, D. W., and Keil, A. (2015). The biological role of the medial olivocochlear efferents in hearing: separating evolved function from exaptation. *Front. Syst. Neurosci.* 9:12. doi: 10.3389/fnsys.2015.00012

Tachibana, M., Kiyoshita, Y., Senuma, H., Nakanishi, H., and Sasaki, K. (1992). Effect of transcutaneous electrostimulation on noise-induced temporary threshold shift. *Acta Otolaryngol.* 112, 595–598. doi: 10.3109/00016489209137446

Trahiotis, C., and Elliott, D. N. (1970). Behavioral investigation of some possible effects of sectioning the crossed olivocochlear bundle. *J. Acoust. Soc. Am.* 47, 592–596. doi: 10.1121/1.1911934

Veuillet, E., Martin, V., Suc, B., Vesson, J. F., Morgon, A., and Collet, L. (2001). Otoacoustic emissions and medial olivocochlear suppression during auditory recovery from acoustic trauma in humans. *Acta Otolaryngol.* 121, 278–283. doi: 10.1080/000164801300043848

Wagner, W., Heppelmann, G., Kuehn, M., Tisch, M., Vonthein, R., and Zenner, H. P. (2005). Olivocochear activity and temporary threshold shift-susceptibility in humans. *Laryngoscope* 115, 2021–2028. doi: 10.1097/01.mlg.0000181463.16591.a7

Warr, W. B., and Guinan, J. J. Jr. (1979). Efferent innervation of the organ of corti: two separate systems. *Brain Res.* 173, 152–155. doi: 10.1016/0006-8993(79)91104-1

Wolpert, S., Heyd, A., and Wagner, W. (2014). Assessment of the noise-protective action of the olivocochlear efferents in humans. *Audiol. Neurootol.* 19, 31–40. doi: 10.1159/000354913

Yamasoba, T., and Dolan, D. F. (1997). Chronic strychnine administration into the cochlea potentiates permanent threshold shift following noise exposure. *Hear. Res.* 112, 13–20. doi: 10.1016/s0378-5955(97)00092-0

Yamasoba, T., and Dolan, D. F. (1998). The medial cochlear efferent system does not appear to contribute to the development of acquired resistance to acoustic trauma. *Hear. Res.* 120, 143–151. doi: 10.1016/s0378-5955(98)00054-9

Zennaro, O., Erre, J. P., Aran, J. M., and Dauman, R. (1998). Short-term effectivemess of medical efferents does not predict susceptibility to temporary threshold shift in the guinea pig. *Acta Otolaryngol.* 118, 681–684. doi: 10.1080/00016489850183179

Zheng, X. Y., Henderson, D., Hu, B. H., Ding, D. L., and McFadden, S. L. (1997a). The influence of the cochlear efferent system on chronic acoustic trauma. *Hear. Res.* 107, 147–159. doi: 10.1016/s0378-5955(97)00031-2

Zheng, X. Y., Henderson, D., McFadden, S. L., and Hu, B. H. (1997b). The role of the cochlear efferent system in acquired resistance to noise-induced hearing loss. *Hear. Res.* 104, 191–203. doi: 10.1016/s0378-5955(96)00187-6

Zheng, X. Y., McFadden, S. L., Ding, D. L., and Henderson, D. (2000). Cochlear de-efferentation and impulse noise-induced acoustic trauma in the chinchilla. *Hear. Res.* 144, 187–195. doi: 10.1016/s0378-5955(00)00065-4

Zhu, X. X., Vasilyeva, O. N., Kim, S., Jacobson, M., Romney, J., Waterman, M. S., et al. (2007). Auditory efferent feedback system deficits precede age-related hearing loss: contralateral suppression of otoacoustic emissions in mice. *J. Comp. Neurol.* 503, 593–604. doi: 10.1002/cne.21402

Conflict of Interest Statement: The author declares that the research was conducted in the absence of any commercial or financial relationships that could be construed as a potential conflict of interest.

frontiers in Systems Neuroscience

MINI REVIEW
published: 30 September 2015
doi: 10.3389/fnsys.2015.00134

Corticofugal modulation of peripheral auditory responses

Gonzalo Terreros[1] *and Paul H. Delano*[1,2]*

[1] *Programa de Fisiología y Biofísica, ICBM, Facultad de Medicina, Universidad de Chile, Santiago, Chile,* [2] *Departamento de Otorrinolaringología, Hospital Clínico de la Universidad de Chile, Santiago, Chile*

The auditory efferent system originates in the auditory cortex and projects to the medial geniculate body (MGB), inferior colliculus (IC), cochlear nucleus (CN) and superior olivary complex (SOC) reaching the cochlea through olivocochlear (OC) fibers. This unique neuronal network is organized in several afferent-efferent feedback loops including: the (i) colliculo-thalamic-cortico-collicular; (ii) cortico-(collicular)-OC; and (iii) cortico-(collicular)-CN pathways. Recent experiments demonstrate that blocking ongoing auditory-cortex activity with pharmacological and physical methods modulates the amplitude of cochlear potentials. In addition, auditory-cortex microstimulation independently modulates cochlear sensitivity and the strength of the OC reflex. In this mini-review, anatomical and physiological evidence supporting the presence of a functional efferent network from the auditory cortex to the cochlear receptor is presented. Special emphasis is given to the corticofugal effects on initial auditory processing, that is, on CN, auditory nerve and cochlear responses. A working model of three parallel pathways from the auditory cortex to the cochlea and auditory nerve is proposed.

Keywords: auditory efferent, olivocochlear, top-down, neural network, descending projections, corticofugal

OPEN ACCESS

Edited by:
Jonathan B. Fritz,
University of Maryland, USA

Reviewed by:
Shihab Shamma,
University of Maryland, USA
Jun Yan,
University of Calgary, Canada

***Correspondence:**
Paul H. Delano,
Programa de Fisiología y Biofísica,
ICBM, Facultad de Medicina,
Universidad de Chile,
Independencia 1027,
Santiago 8380453, Chile
pdelano@med.uchile.cl

Received: *29 April 2015*
Accepted: *15 September 2015*
Published: *30 September 2015*

Citation:
Terreros G and Delano PH (2015) Corticofugal modulation of peripheral auditory responses. Front. Syst. Neurosci. 9:134. doi: 10.3389/fnsys.2015.00134

Introduction

Since the first description of the crossed and uncrossed olivocochlear (OC) bundles by Rasmussen (1946, 1960), these brainstem pathways have been considered as the auditory efferent system itself, and the terms "*olivocochlear*" and "*auditory efferent*" have been frequently used as synonyms. However, several lines of neuroanatomical evidence demonstrate the presence of an efferent network originated in the auditory cortex that reaches the cochlear receptor through OC neurons (Feliciano et al., 1995; Mulders and Robertson, 2000). This network comprises descending projections from the auditory cortex to the medial geniculate body (MGB), inferior colliculus (IC), cochlear nucleus (CN) and superior olivary complex (SOC) that form multiple feedback loops, including the: (i) colliculo-thalamic-cortico-collicular; (ii) cortico-(collicular)-OC; and (iii) cortico-(collicular)-CN pathways (Saldaña et al., 1996; Robles and Delano, 2008; Xiong et al., 2009; Malmierca and Ryugo, 2011; Schofield, 2011).

The functionality of the corticofugal pathways to OC neurons has been proven by recent evidence demonstrating that auditory cortex activity can modulate afferent responses even at the level of sensory transduction (Xiao and Suga, 2002; León et al., 2012). Several functions have been attributed to these corticofugal effects on cochlear responses, including selective attention (Oatman, 1971), modulation of afferent inputs during wake/sleep cycle (Velluti et al., 1989) and antimasking of acoustic signals in noise background (Nieder and Nieder, 1970). It is important to highlight that any efferent modulation of the most peripheral structures of the auditory pathway—the auditory nerve and cochlear hair cells—must be mediated by the OC system.

In this mini-review, anatomical and physiological evidence supporting the presence of a functional efferent network from the auditory cortex to the cochlear receptor are presented. Special emphasis is given to the corticofugal effects on CN, auditory nerve and cochlear responses produced by auditory cortex manipulations. A working model of three parallel pathways from the auditory cortex to the cochlea and auditory nerve is proposed.

The Olivocochlear System: the Final and Mandatory Pathway from the Central Nervous System to the Cochlear Receptor

The OC system comprises medial (MOC) and lateral (LOC) olivocochlear neurons located in the SOC (Warr and Guinan, 1979). MOC neurons have thick and myelinated axons that are mainly directed towards outer hair cells (OHC) of the contralateral cochlea, while LOC neurons possess thin and unmyelinated fibers that make synapses with ipsilateral auditory nerve dendrites just beneath cochlear inner hair cells (Guinan, 1996). Similarly to alpha-motor neurons, MOC neurons release acetylcholine as their main neurotransmitter, and activate nicotinic receptors comprised by five α9/α10 subunits located in OHCs (Elgoyhen et al., 1994, 2001). On the other hand, several neurotransmitters and neuromodulators are known to be released by LOC neurons, including acetylcholine, GABA, dopamine, dynorphines, encephalin, and CGRP (Eybalin, 1993). Importantly, for the central nervous system, MOC neurons are the final and mandatory pathway to regulate the mechanical vibrations of the basilar membrane, acting as individual motor units along the cochlear partition (LePage, 1989; Murugasu and Russell, 1996; Cooper and Guinan, 2003). Therefore, the OC system is fundamental in the functioning of the efferent network, as all cortical or subcortical modulations of cochlear and auditory nerve responses must be transmitted through MOC or LOC synapses.

The OC function can be evaluated through a brainstem reflex that is activated by ipsilateral or contralateral auditory stimulation (Buño, 1978; Liberman, 1989). The neural circuit of this reflex is constituted by auditory nerve fibers, CN neurons, and crossed or uncrossed MOC fibers (de Venecia et al., 2005). The ipsilateral MOC reflex pathway comprises a double crossing, including the afferent pathway from the CN and the crossed MOC fibers, while the contralateral MOC reflex comprises only one crossing in the ascending pathway and the uncrossed MOC fibers. There is also anatomical evidence showing differences in the cochlear innervation patterns of crossed and uncrossed MOC fibers (Brown, 2014), which is in agreement with physiological data obtained in humans, that suggest different functions for the crossed and uncrossed MOC reflex (Lilaonitkul and Guinan, 2009). In addition, indirect LOC stimulation through IC descending pathways modulates the amplitude of auditory nerve responses (Groff and Liberman, 2003). Therefore, the OC system can modulate OHC and auditory nerve responses through three different pathways: (i) the crossed; (ii) uncrossed MOC fibers; and (iii) LOC neurons.

Descending Projections from the Auditory Cortex to the Medial Geniculate Body

Among the auditory subcortical nuclei, the MGB receives the largest number of cortical descending projections from pyramidal neurons located in layers V and VI of the auditory cortex, forming tonotopic feedback loops between the primary auditory cortex and ventral MGB (Bartlett et al., 2000; Winer et al., 2001; Winer, 2006; Winer and Lee, 2007). Physiological studies demonstrate that the auditory cortex modulates MGB responses (Ryugo and Weinberger, 1976; Villa et al., 1991; Zhang and Suga, 2000; Antunes and Malmierca, 2011), and that this modulation is different for ventral and medial MGB neurons (Tang et al., 2012). The electrical microstimulation of the auditory cortex produced sharply tuned effects in the ventral MGB, while suppressive and broad-band effects were obtained in the medial MGB. However, whether the corticofugal modulation of thalamic neurons affects OC activity is unknown. Importantly, as there is no anatomical evidence of direct descending connections from MGB to OC neurons, any possible thalamic modulation of OC activity should be produced indirectly through the colliculo-thalamic-cortico-collicular loop.

Descending Projections from the Auditory Cortex to the Inferior Colliculus, Superior Olivary Complex and Cochlear Nucleus

The IC is a key structure of the ascending and descending auditory pathways (Huffman and Henson, 1990). Direct descending projections from the auditory cortices to the IC are mainly originated in layer V of the primary fields, and in a lesser extent from layer VI (Faye-Lund, 1985; Doucet et al., 2003). Most of the cortico-collicular fibers are glutamatergic (Feliciano and Potashner, 1995) and are directed to the ipsilateral IC, but there are also fibers directed to the contralateral IC (Bajo et al., 2007; Nakamoto et al., 2013a,b). Although the majority of cortico-collicular descending projections are directed to the IC cortices, a small subset reaches the central nucleus of the IC, which is the main ascending and tonotopic structure of this nucleus (Saldaña et al., 1996; Bajo and Moore, 2005). In agreement with these neuroanatomical findings, physiological evidence demonstrates a tonotopic modulation of the central nucleus of the IC by auditory cortex microstimulation (Yan and Suga, 1998; Yan et al., 2005). In addition, IC responses to sound intensity (Yan and Ehret, 2002), duration (Ma and Suga, 2001) and location (Zhou and Jen, 2005) are also modulated by the auditory cortex. More comprehensive reviews about the corticofugal effects on IC responses can be found elsewhere (Anderson and Malmierca, 2013; Bajo and King, 2013; Malmierca et al., 2015).

The SOC and the CN are also direct targets of cortical descending projections, mainly from primary auditory cortex, but also from ventral and rostral secondary fields (Weedman and Ryugo, 1996a,b; Doucet et al., 2002). Moreover, Mulders and Robertson showed evidence of the presence of synaptic connections between cortical descending axons and MOC neurons (Mulders and Robertson, 2000). There is also evidence

of indirect connections between the auditory cortex and SOC through IC synapses (Thompson and Thompson, 1993; Vetter et al., 1993). Despite these neuroanatomical findings, there is still no physiological evidence of how the auditory cortex modulates the activity of SOC neurons. Regarding connections from the auditory cortex to the CN, Schofield and colleagues have demonstrated that the dorsal and ventral CN receive direct projections from the auditory cortex, as well as indirect projections, passing through the IC or the SOC (Schofield and Cant, 1999; Schofield and Coomes, 2005; Schofield et al., 2006). In summary, descending projections from the auditory cortex to the IC, SOC and CN create multiple feedback loops that can modulate cochlear responses through OC neurons (**Figure 1**).

Corticofugal Effects on Cochlear Nucleus

The first evidence of a feedback control of CN responses by the central nervous system was found several decades ago in physiological experiments performed in awake and behaving cats (Hernández-Peón et al., 1956; Dewson et al., 1966). Hernández-Peón et al. (1956) found a reduction in the evoked potentials recorded from the CN in cats while receiving stimuli of other sensory modalities. Later, Dewson et al. (1966) showed that auditory cortex ablations modified the evoked responses of the CN. These pioneer studies suggested the presence of corticofugal pathways from the auditory cortex to the CN that were discovered several decades later (Weedman and Ryugo, 1996a,b; Schofield and Coomes, 2005, 2006).

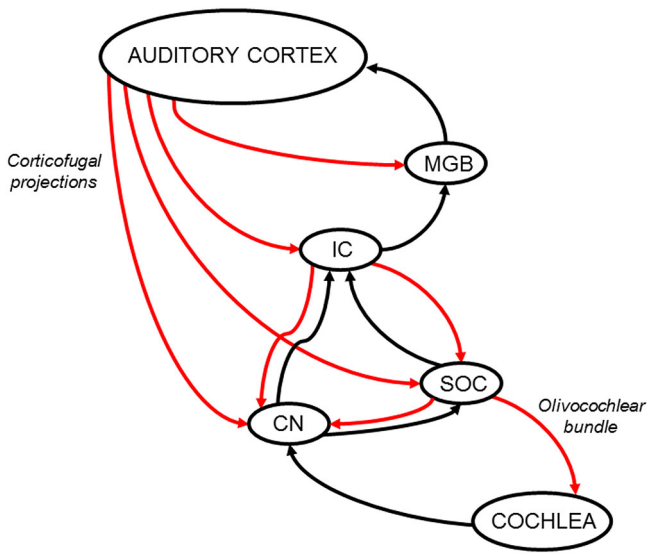

FIGURE 1 | Schematic diagram of the auditory efferent network. Ascending and descending pathways are depicted in black and red arrows respectively. A simplified model of the auditory efferent system is presented. Corticofugal projections from the auditory cortex to the inferior colliculus (IC) and medial geniculate body (MGB) and afferent connections from the IC and MGB to the auditory cortex form a "top loop" within this network (colliculo-thalamic-cortico-collicular loop, Xiong et al., 2009). Bottom loops are constituted by auditory-cortex descending projections to the CN (cortico-(collicular)-cochlear nucleus loop) and SOC (cortico-(collicular)-olivocochlear loop), which are connected to the cochlear receptor by the OC bundle. Note, the relevant position of the IC in the interaction between top and bottom loops. In addition, it is important to highlight that cortical modulations of cochlear responses, can modify IC responses through ascending connections to the CN and IC, meaning that the interaction between the top and bottom loops is bidirectional. CN: cochlear nucleus; IC: inferior colliculus; MGB: medial geniculate body; SOC: superior olivary complex.

The functionality of these pathways has been recently confirmed by studying the effects of electrical microstimulation of the auditory cortex in the contralateral CN of mice (Luo et al., 2008). These authors found that focal stimulation of a specific area of the auditory cortex increased the magnitudes and shortened the latencies of the responses of ventral CN neurons that had similar characteristic frequencies to the stimulated cortical site, while opposite effects were observed for CN neurons with other characteristic frequencies (Luo et al., 2008). Moreover, they found similar results in the ipsilateral ventral CN (Liu et al., 2010) and in the dorsal CN (Kong et al., 2014). These physiological studies are illustrative of a general characteristic of the efferent system: the frequency selectivity of corticofugal projections, which has also been obtained activating the descending pathways to the MGB, IC and cochlea (Suga and Ma, 2003).

Corticofugal Effects on Auditory-Nerve and Cochlear Responses

Only a few physiological studies have assessed the corticofugal effects of auditory cortex manipulations on the most peripheral auditory structures, including, auditory nerve responses (León et al., 2012; Dragicevic et al., 2015), cochlear electrical responses (Xiao and Suga, 2002; León et al., 2012; Dragicevic et al., 2015) and otoacoustic emissions (OAE; Khalfa et al., 2001; Perrot et al., 2006). In a seminal work, Xiao and Suga (2002) demonstrated that the auditory cortex activity modulates the amplitude and frequency tuning of cochlear microphonics (CM) responses near the echolocalizing frequency of the mustached bat (61 kHz). In addition, corticofugal effects on cochlear responses have been found in human patients with epilepsy refractory to pharmacological treatment. In these patients, cortical resection of the temporal superior gyrus produced a bilateral reduction of the MOC reflex that was more pronounced in the ear contralateral to the resected auditory cortex (Khalfa et al., 2001). Moreover, electrical microstimulation of the auditory cortex by means of a chronic intra-cerebral multielectrode array produced a significant reduction of OAE, while there was no change under stimulation of non-auditory cortical areas (Perrot et al., 2006).

A recent work by León et al. (2012) extended the findings of the corticofugal effects observed in bats and humans to the chinchilla. In this work the spontaneous activity of the auditory cortex was inactivated by two methods: cortical cooling with cryoloops and lidocaine microinjections. The combined experimental approaches and the adequate control of the cochlear temperature ruled out the possibility of a direct cooling of the cochlea by the cortical cryoloops, as it has

been suggested in guinea pigs by Coomber et al. (2011). Both types of cortical manipulations produced changes in the amplitudes of auditory-nerve compound action potentials (CAP) and CM responses (León et al., 2012). Although these effects were diverse, the most common pattern was a concomitant reduction in the amplitudes of CAP and CM responses. The electrical stimulation of the crossed MOC fibers at the floor of the fourth ventricle produces a decrease in CAP amplitudes and a simultaneous increase of CM responses (Gifford and Guinan, 1987). Therefore, the parallel changes of CAP and CM amplitudes observed in chinchillas after auditory cortex inactivation suggest a concomitant modulation of MOC and LOC neurons, as the latter system can only affect CAP but not CM responses (Groff and Liberman, 2003). León et al. (2012) proposed that the ongoing activity of the auditory cortex regulates cochlear sensitivity through parallel pathways to the cochlear receptor. However, whether these corticofugal effects were affecting the functioning of the OC reflex circuit remained unknown.

In a recent study, Dragicevic et al. (2015) used auditory cortex microstimulation in chinchillas to demonstrate that in addition to the corticofugal modulation of cochlear sensitivity on CAP and CM responses, the auditory cortex also modulates the strength of the contralateral OC reflex on CAP but not on CM responses. In agreement with neuroanatomical data, the largest corticofugal effects were obtained in auditory cortices with short latency responses (<15 ms), which correspond to primary auditory fields. Moreover, these two types of corticofugal modulations: (i) on cochlear sensitivity; and (ii) on the OC reflex strength were not correlated, suggesting the presence of at least two functionally different descending pathways to the crossed and uncrossed MOC neurons, and possibly a third pathway to LOC neurons (**Figure 2**). Some functional consequences of the corticofugal effects on the strength of the OC reflex could be the finding of stronger reflexes in awake than in anesthetized animals (Guitton et al., 2004; Chambers et al., 2012; Aedo et al., 2015), and the diminishing of tinnitus perception during stimulation of the auditory cortex in human patients (Fenoy et al., 2006; Fregni et al., 2006).

The model of three parallel descending pathways from the auditory cortex, is also supported by the presence of different types of projecting neurons, including regular and burst spiking pyramidal neurons from layer V (Hefti and Smith, 2000), and neurons from layer VI (Winer et al., 2001). Moreover, the differential corticofugal effects obtained with different microstimulation rates: 5 Hz to modulate IC and MGB responses (Suga and Ma, 2003) and 32–33 Hz to modulate SOC activity (Xiao and Suga, 2002; Dragicevic et al., 2015), suggest different activation thresholds for cortical neurons projecting to these subcortical nuclei.

Functional Role of the Auditory Efferent System

Different functions can be assigned to the different loops formed in the auditory efferent pathways. Functions mainly depending on the OC brainstem circuit are protection to acoustic trauma (Maison and Liberman, 2000) and balance of interaural cochlear sensitivity (Darrow et al., 2006), while neural plasticity during learning of behaviorally relevant auditory tasks has been attributed to the colliculo-thalamic-cortico-collicular loop (Xiong et al., 2009; Bajo et al., 2010). A top-down frequency filter needed in different behavioral situations can be proposed as the general function for the cortico-olivocochlear circuit, including selective attention to auditory or visual stimuli (Delano et al., 2007; Smith et al., 2012), regulation of afferent responses during wake/sleep cycle (Velluti et al., 1989; Froehlich et al., 1993), and antimasking of auditory stimuli in a noisy environment (Kawase and Liberman, 1993). As there is increasing evidence of the modulation of cochlear responses during selective attention, this putative function of the corticofugal system is discussed next.

Selective Attention to Visual or Auditory Stimuli

Since the early experiments performed in cats by Hernández-Peón et al. (1956), the auditory efferent system has been proposed to function as a top-down filter of peripheral auditory responses during attention. To address this proposal, two types of attentional paradigms have been used: (i) attention to visual stimuli using irrelevant auditory distractors (Oatman, 1971; Delano et al., 2007), in which all peripheral auditory responses at all frequencies should be suppressed through the efferent system; and (ii) attention to auditory targets of specific frequency (Smith et al., 2012; Srinivasan et al., 2012), in which the peripheral auditory responses near the target frequency would be enhanced while other frequencies would be suppressed by the efferent system.

CAP reductions in response to click and tone auditory distractors during selective attention to visual stimuli have been obtained in cats and chinchillas (Oatman, 1971; Delano et al., 2007). In the latter work, CM increases concomitant to CAP reductions were obtained during visual attention, suggesting that these attentional effects were indeed produced by activation of MOC neurons, as the electrical stimulation of MOC fibers produces CAP reductions with simultaneous CM increases (Elgueda et al., 2011).

Contradictory results have been obtained in visual attention tasks with auditory distractors in humans. For instance, Puel et al. (1988) showed that click-evoked OAE were reduced in 13 out of 16 evaluated subjects during visual attention (1.25 dB in average). Similarly, Wittekindt et al. (2014) showed that during periods of visual attention to Gabor patches, there was a reduction in the amplitude of distortion product otoacoustic emissions (DPOAE). On the other hand, Smith and colleagues (Smith et al., 2012; Srinivasan et al., 2012), found a DPOAE increase during selective attention to visual stimuli, but a DPOAE reduction during auditory attention to the DPOAE primary tones (f_1 and f_2). These opposite results could be explained by the differential generating mechanisms of click-evoked OAE with that of DPOAEs (Shera and Guinan, 1999). Importantly, in the work of Smith et al. (2012), subjects attended to the primary tones (f_1 and f_2) that generate the DPOAEs, but measurements were

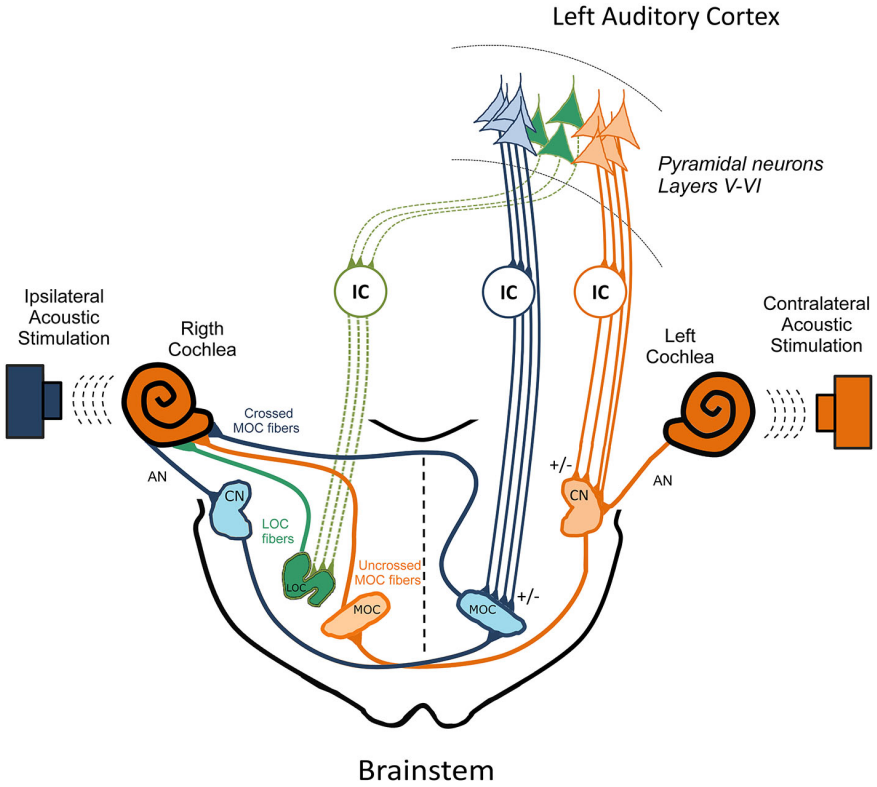

FIGURE 2 | The three pathways model for the cortico-collicular-olivocochlear and cochlear nucleus circuits. In order to simplify this model, the colliculo-thalamic-cortico-collicular loop has been omitted. In addition, only efferent pathways from the left auditory cortex to the right cochlea are presented. Three OC pathways are directed to the right cochlear receptor and auditory nerve, which are depicted in color green, orange and blue corresponding to the: (i) right LOC fibers; (ii) right uncrossed MOC; and (iii) left crossed MOC neurons respectively. Ipsilateral acoustic stimulation of the right cochlea activates right AN, right CN neurons that send projections to the contralateral MOC. In turn, left crossed MOC neurons modulate right cochlear responses (blue brainstem pathways), constituting the ipsilateral OC reflex. On the other hand, contralateral acoustic stimulation of the left cochlea activates, left AN, left CN neurons that send projections to the right uncrossed MOC fibers, which modulate right cochlear responses (orange brainstem pathways), constituting the contralateral OC reflex that connects both ears. This model proposes that the descending pathways from the left auditory cortex directed to the left IC and to the left CN (orange corticofugal pathways) modulate the contralateral OC reflex, by regulating the activity of the left CN and right uncrossed MOC neurons. On the other hand, descending pathways directed to the left IC and left MOC (blue corticofugal pathways) regulate crossed MOC activity, which is involved in the ipsilateral OC reflex. Finally, corticofugal pathways to the contralateral IC (green corticofugal pathways) could regulate right LOC neurons, modulating the activity of right AN fibers. The +/− signs represent possible excitatory and inhibitory pathways. Modified from Dragicevic et al. (2015) with permission. AN: auditory nerve; CN: cochlear nucleus; LOC: lateral olivocochlear; MOC: medial olivocochlear; IC: inferior colliculus.

obtained from a distant location in the cochlear partition at the $2f_1–f_2$ frequency. Future experiments should clarify whether the corticofugal effects are different if the subject attention is directed to the primary tones (f_1 and f_2) or to the DPOAE frequency ($2f_1–f_2$).

Both ears are connected through the uncrossed MOC pathway that is activated by contralateral sounds (de Venecia et al., 2005). Notably, differential effects of interaural attention through uncrossed MOC fibers have been found in human studies (de Boer and Thornton, 2007; Srinivasan et al., 2014). Srinivasan et al. (2014) found that alternating auditory attention between the two ears modifies the strength of corticofugal effects on DPOAEs responses, suggesting that attention can independently modulate crossed and uncrossed MOC neurons. These findings are in agreement with the results obtained by Dragicevic et al. (2015) and support the model proposed in this article (**Figure 2**).

Concluding Remarks

In summary, here we reviewed the growing anatomical and physiological evidence supporting the presence of an efferent network from auditory cortex to OC neurons. Cortical descending effects on CN, auditory nerve and cochlear responses are proposed to be produced by three parallel pathways from auditory cortex to the crossed and uncrossed MOC neurons and to LOC neurons. These connections are probably activated during selective attention, learning induced plasticity and other cognitive functions.

Acknowledgments

Supported by FONDECYT 3130635 and Fundación Guillermo Puelma. We thank Professor Luis Robles for his valuable comments.

References

Aedo, C., Tapia, E., Pavez, E., Elgueda, D., Delano, P. H., and Robles, L. (2015). Stronger efferent suppression of cochlear neural potentials by contralateral acoustic stimulation in awake than in anesthetized chinchilla. *Front. Syst. Neurosci.* 9:21. doi: 10.3389/fnsys.2015.00021

Anderson, L. A., and Malmierca, M. S. (2013). The effect of auditory cortex deactivation on stimulus-specific adaptation in the inferior colliculus of the rat. *Eur. J. Neurosci.* 37, 52–62. doi: 10.1111/ejn.12018

Antunes, F. M., and Malmierca, M. S. (2011). Effect of auditory cortex deactivation on stimulus-specific adaptation in the medial geniculate body. *J. Neurosci.* 31, 17306–17316. doi: 10.1523/jneurosci.1915-11.2011

Bajo, V. M., and King, A. J. (2013). Cortical modulation of auditory processing in the midbrain. *Front. Neural Circuits* 6:114. doi: 10.3389/fncir.2012.00114

Bajo, V. M., and Moore, D. R. (2005). Descending projections from the auditory cortex to the inferior colliculus in the gerbil, Meriones unguiculatus. *J. Comp. Neurol.* 486, 101–116. doi: 10.1002/cne.20542

Bajo, V. M., Nodal, F. R., Bizley, J. K., Moore, D. R., and King, A. J. (2007). The ferret auditory cortex: descending projections to the inferior colliculus. *Cereb. Cortex* 17, 475–491. doi: 10.1093/cercor/bhj164

Bajo, V. M., Nodal, F. R., Moore, D. R., and King, A. J. (2010). The descending corticocollicular pathway mediates learning-induced auditory plasticity. *Nat. Neurosci.* 13, 253–260. doi: 10.1038/nn.2466

Bartlett, E. L., Stark, J. M., Guillery, R. W., and Smith, P. H. (2000). Comparison of the fine structure of cortical and collicular terminals in the rat medial geniculate body. *Neuroscience* 100, 811–828. doi: 10.1016/s0306-4522(00)00340-7

Brown, M. C. (2014). Single-unit labeling of medial olivocochlear neurons: the cochlear frequency map for efferent axons. *J. Neurophysiol.* 111, 2177–2186. doi: 10.1152/jn.00045.2014

Buño, W. Jr. (1978). Auditory nerve fiber activity influenced by contralateral ear sound stimulation. *Exp. Neurol.* 59, 62–74. doi: 10.1016/0014-4886(78)90201-7

Chambers, A. R., Hancock, K. E., Maison, S. F., Liberman, M. C., and Polley, D. B. (2012). Sound-evoked olivocochlear activation in unanesthetized mice. *J. Assoc. Res. Otolaryngol.* 13, 209–217. doi: 10.1007/s10162-011-0306-z

Coomber, B., Edwards, D., Jones, S. J., Shackleton, T. M., Goldschmidt, J., Wallace, M. N., et al. (2011). Cortical inactivation by cooling in small animals. *Front. Syst. Neurosci.* 5:53. doi: 10.3389/fnsys.2011.00053

Cooper, N. P., and Guinan, J. J. Jr. (2003). Separate mechanical processes underlie fast and slow effects of medial olivocochlear efferent activity. *J. Physiol.* 548, 307–312. doi: 10.1111/j.1469-7793.2003.00307.x

Darrow, K. N., Maison, S. F., and Liberman, M. C. (2006). Cochlear efferent feedback balances interaural sensitivity. *Nat. Neurosci.* 9, 1474–1476. doi: 10.1038/nn1807

de Boer, J., and Thornton, A. R. (2007). Effect of subject task on contralateral suppression of click evoked otoacoustic emissions. *Hear Res.* 233, 117–123. doi: 10.1016/j.heares.2007.08.002

Delano, P. H., Elgueda, D., Hamame, C. M., and Robles, L. (2007). Selective attention to visual stimuli reduces cochlear sensitivity in chinchillas. *J. Neurosci.* 27, 4146–4153. doi: 10.1523/jneurosci.3702-06.2007

de Venecia, R. K., Liberman, M. C., Guinan, J. J. Jr., and Brown, M. C. (2005). Medial olivocochlear reflex interneurons are located in the posteroventral cochlear nucleus: a kainic acid lesion study in guinea pigs. *J. Comp. Neurol.* 487, 345–360. doi: 10.1002/cne.20550

Dewson, J. H. III, Nobel, K. W., and Pribram, K. H. (1966). Corticofugal influence at cochlear nucleus of the cat: some effects of ablation of insular-temporal cortex. *Brain Res.* 2, 151–159. doi: 10.1016/0006-8993(66)90020-5

Doucet, J. R., Molavi, D. L., and Ryugo, D. K. (2003). The source of corticocollicular and corticobulbar projections in area Te1 of the rat. *Exp. Brain Res.* 153, 461–466. doi: 10.1007/s00221-003-1604-4

Doucet, J. R., Rose, L., and Ryugo, D. K. (2002). The cellular origin of corticofugal projections to the superior olivary complex in the rat. *Brain Res.* 925, 28–41. doi: 10.1016/s0006-8993(01)03248-6

Dragicevic, C. D., Aedo, C., León, A., Bowen, M., Jara, N., Terreros, G., et al. (2015). The olivocochlear reflex strength and cochlear sensitivity are independently modulated by auditory cortex microstimulation. *J. Assoc. Res. Otolaryngol.* 16, 223–240. doi: 10.1007/s10162-015-0509-9

Elgoyhen, A. B., Johnson, D. S., Boulter, J., Vetter, D. E., and Heinemann, S. (1994). Alpha 9: an acetylcholine receptor with novel pharmacological properties expressed in rat cochlear hair cells. *Cell* 79, 705–715. doi: 10.1016/0092-8674(94)90555-x

Elgoyhen, A. B., Vetter, D. E., Katz, E., Rothlin, C. V., Heinemann, S. F., and Boulter, J. (2001). Alpha10: a determinant of nicotinic cholinergic receptor function in mammalian vestibular and cochlear mechanosensory hair cells. *Proc. Natl. Acad. Sci. U S A* 98, 3501–3506. doi: 10.1073/pnas.051622798

Elgueda, D., Delano, P. H., and Robles, L. (2011). Effects of electrical stimulation of olivocochlear fibers in cochlear potentials in the chinchilla. *J. Assoc. Res. Otolaryngol.* 12, 317–327. doi: 10.1007/s10162-011-0260-9

Eybalin, M. (1993). Neurotransmitters and neuromodulators of the mammalian cochlea. *Physiol. Rev.* 73, 309–373.

Faye-Lund, H. (1985). The neocortical projection to the inferior colliculus in the albino rat. *Anat. Embryol. (Berl).* 173, 53–170. doi: 10.1007/bf00707304

Feliciano, M., and Potashner, S. J. (1995). Evidence for a glutamatergic pathway from the guinea pig auditory cortex to the inferior colliculus. *J. Neurochem.* 65, 1348–1357. doi: 10.1046/j.1471-4159.1995.65031348.x

Feliciano, M., Saldaña, E., and Mugnaini, E. (1995). Direct projections from the rat primary auditory neocortex to nucleus sagulum, paralemniscal regions, superior olivary complex and cochlear nuclei. *Aud. Neurosci.* 1, 287–308.

Fenoy, A. J., Severson, M. A., Volkov, I. O., Brugge, J. F., and Howard, M. A. 3rd (2006). Hearing suppression induced by electrical stimulation of human AC. *Brain Res.* 1118, 75–83. doi: 10.1016/j.brainres.2006.08.013

Fregni, F., Marcondes, R., Boggio, P. S., Marcolin, M. A., Rigonatti, S. P., Sanchez, G., et al. (2006). Transient tinnitus suppression induced by repetitive transcranial magnetic stimulation and transcranial direct current stimulation. *Eur. J. Neurol.* 13, 996–1001. doi: 10.1111/j.1468-1331.2006.01414.x

Froehlich, P., Collet, L., Valatx, J. L., and Morgon, A. (1993). Sleep and active cochlear micromechanical properties in human subjects. *Hear. Res.* 66, 1–7. doi: 10.1016/0378-5955(93)90254-x

Gifford, M. L., and Guinan, J. J. Jr. (1987). Effects of electrical stimulation of medial olivocochlear neurons on ipsilateral and contralateral cochlear responses. *Hear. Res.* 29, 179–194. doi: 10.1016/0378-5955(87)90166-3

Groff, J. A., and Liberman, M. C. (2003). Modulation of cochlear afferent response by the lateral olivocochlear system: activation via electrical stimulation of the inferior colliculus. *J. Neurophysiol.* 90, 3178–3200. doi: 10.1152/jn.00537.2003

Guinan, J. J. Jr. (1996). "Physiology of olivocochlear efferents," in *The Cochlea*, eds P. Dallos, A. Popper, and R. Fay (New York: Springer), 435–502.

Guitton, M. J., Avan, P., Puel, J. L., and Bonfils, P. (2004). Medial olivocochlear efferent activity in awake guinea pigs. *Neuroreport* 15, 1379–1382. doi: 10.1097/01.wnr.0000131672.15566.64

Hefti, B. J., and Smith, P. H. (2000). Anatomy, physiology and synaptic responses of rat layer V auditory cortical cells and effects of intracellular GABA(A) blockade. *J. Neurophysiol.* 83, 2626–2638.

Hernández-Peón, R., Scherrer, H., and Jouvet, M. (1956). Modification of electric activity in cochlear nucleus during attention in unanesthetized cats. *Science* 123, 331–332. doi: 10.1126/science.123.3191.331

Huffman, R. F., and Henson, O. W. Jr. (1990). The descending auditory pathway and acousticomotor systems: connections with the inferior colliculus. *Brain Res. Brain Res. Rev.* 15, 295–323. doi: 10.1016/0165-0173(90)90005-9

Kawase, T., and Liberman, M. C. (1993). Antimasking effects of the olivocochlear reflex. I. Enhancement of compound action potentials to masked tones. *J. Neurophysiol.* 70, 2519–2532.

Khalfa, S., Bougeard, R., Morand, N., Veuillet, E., Isnard, J., Guenot, M., et al. (2001). Evidence of peripheral auditory activity modulation by the auditory cortex in humans. *Neuroscience* 104, 347–358. doi: 10.1016/s0306-4522(01)00072-0

Kong, L., Xiong, C., Li, L., and Yan, J. (2014). Frequency-specific corticofugal modulation of the dorsal cochlear nucleus in mice. *Front. Syst. Neurosci.* 8:125. doi: 10.3389/fnsys.2014.00125

León, A., Elgueda, D., Silva, M. A., Hamamé, C. M., and Delano, P. H. (2012). Auditory cortex basal activity modulates cochlear responses in chinchillas. *PLoS One* 7:e36203. doi: 10.1371/journal.pone.0036203

LePage, E. L. (1989). Functional role of the olivo-cochlear bundle: a motor unit control system in the mammalian cochlea. *Hear Res.* 38, 177–198. doi: 10.1016/0378-5955(89)90064-6

Liberman, M. C. (1989). Rapid assessment of sound-evoked olivocochlear feedback: suppression of compound action potentials by contralateral sound. *Hear Res.* 38, 47–56. doi: 10.1016/0378-5955(89)90127-5

Lilaonitkul, W., and Guinan, J. J. Jr. (2009). Human medial olivocochlear reflex: effects as functions of contralateral, ipsilateral and bilateral elicitor bandwidths. *J. Assoc. Res. Otolaryngol.* 10, 459–470. doi: 10.1007/s10162-009-0163-1

Liu, X., Yan, Y., Wang, Y., and Yan, J. (2010). Corticofugal modulation of initial neural processing of sound information from the ipsilateral ear in the mouse. *PLoS One* 5:e14038. doi: 10.1371/journal.pone.0014038

Luo, F., Wang, Q., Kashani, A., and Yan, J. (2008). Corticofugal modulation of initial sound processing in the brain. *J. Neurosci.* 28, 11615–11621. doi: 10.1523/jneurosci.3972-08.2008

Ma, X., and Suga, N. (2001). Corticofugal modulation of duration-tuned neurons in the midbrain auditory nucleus in bats. *Proc. Natl. Acad. Sci. U S A* 98, 14060–14065. doi: 10.1073/pnas.241517098

Maison, S. F., and Liberman, M. C. (2000). Predicting vulnerability to acoustic injury with a noninvasive assay of olivocochlear reflex strength. *J. Neurosci.* 20, 4701–4707.

Malmierca, M. S., Anderson, L. A., and Antunes, F. M. (2015). The cortical modulation of stimulus-specific adaptation in the auditory midbrain and thalamus: a potential neuronal correlate for predictive coding. *Front. Syst. Neurosci.* 9:19. doi: 10.3389/fnsys.2015.00019

Malmierca, M. S., and Ryugo, D. K. (2011). "Descending connections of the auditory cortex to the midbrain and the brainstem," in *The AC*, eds J. A. Winer and C. E. Schreiner (New York: Springer Press), 189–208.

Mulders, W. H., and Robertson, D. (2000). Evidence for direct cortical innervation of medial olivocochlear neurones in rats. *Hear. Res.* 144, 65–72. doi: 10.1016/s0378-5955(00)00046-0

Murugasu, E., and Russell, I. J. (1996). The effect of efferent stimulation on basilar membrane displacement in the basal turn of the guinea pig cochlea. *J. Neurosci.* 16, 325–332.

Nakamoto, K. T., Mellott, J. G., Killius, J., Storey-Workley, M. E., Sowick, C. S., and Schofield, B. R. (2013a). Ultrastructural examination of the corticocollicular pathway in the guinea pig: a study using electron microscopy, neural tracers and GABA immunocytochemistry. *Front. Neuroanat.* 7:13. doi: 10.3389/fnana.2013.00013

Nakamoto, K. T., Sowick, C. S., and Schofield, B. R. (2013b). Auditory cortical axons contact commissural cells throughout the guinea pig inferior colliculus. *Hear. Res.* 306, 131–144. doi: 10.1016/j.heares.2013.10.003

Nieder, P., and Nieder, I. (1970). Antimasking effect of crossed olivocochlear bundle stimulation with loud clicks in guinea pig. *Exp. Neurol.* 28, 179–188. doi: 10.1016/0014-4886(70)90172-x

Oatman, L. C. (1971). Role of visual attention on auditory evoked potentials in unanesthetized cats. *Exp. Neurol.* 32, 341–356. doi: 10.1016/0014-4886(71)90003-3

Perrot, X., Ryvlin, P., Isnard, J., Guénot, M., Catenoix, H., Fischer, C., et al. (2006). Evidence for corticofugal modulation of peripheral auditory activity in humans. *Cereb. Cortex* 16, 941–948. doi: 10.1093/cercor/bhj035

Puel, J. L., Bonfils, P., and Pujol, R. (1988). Selective attention modifies the active micromechanical properties of the cochlea. *Brain Res.* 447, 380–383. doi: 10.1016/0006-8993(88)91144-4

Rasmussen, G. L. (1946). The olivary peduncle and other fiber projections of the superior olivary complex. *J. Comp. Neurol.* 84, 141–219. doi: 10.1002/cne.900840204

Rasmussen, G. L. (1960). "Efferent fibers of the cochlear nerve and cochlear nucleus," in *Neural Mechanisms of the Auditory and Vestibular Systems*, ed G. L. Rasmussen and W. F. Windle (Springfield, IL: Thomas), 105–115.

Robles, L., and Delano, P. H. (2008). "Efferent system," in *The Senses: A Comprehensive Reference*, eds P. Dallos and D. Oertel (London, UK: Academic Press), 413–445.

Ryugo, D. K., and Weinberger, N. M. (1976). Corticofugal modulation of the medial geniculate body. *Exp. Neurol.* 51, 377–391. doi: 10.1016/0014-4886(76)90262-4

Saldaña, E., Feliciano, M., and Mugnaini, E. (1996). Distribution of descending projections from primary auditory neocortex to inferior colliculus mimics the topography of intracollicular projections. *J. Comp. Neurol.* 371, 15–40. doi: 10.1002/(sici)1096-9861(19960715)371:1<15::aid-cne2>3.0.co;2-o

Schofield, B. R. (2011). "Central descending auditory pathways," in *Auditory and Vestibular Efferents*, eds D. K. Ryugo, A. N. Popper, and R. R. Fay (New York, NY: Springer-Verlag), 261–290.

Schofield, B. R., and Cant, N. B. (1999). Descending auditory pathways: projections from the inferior colliculus contact superior olivary cells that project bilaterally to the cochlear nuclei. *J. Comp. Neurol.* 409, 210–223. doi: 10.1002/(sici)1096-9861(19990628)409:2<210::aid-cne3>3.0.co;2-a

Schofield, B. R., and Coomes, D. L. (2005). Auditory cortical projections to the cochlear nucleus in guinea pigs. *Hear. Res.* 199, 89–102. doi: 10.1016/j.heares.2004.08.003

Schofield, B. R., and Coomes, D. L. (2006). Pathways from auditory cortex to the cochlear nucleus in guinea pigs. *Hear. Res.* 216–217, 81–89. doi: 10.1016/j.heares.2006.01.004

Schofield, B. R., Coomes, D. L., and Schofield, R. M. (2006). Cells in auditory cortex that project to the cochlear nucleus in guinea pigs. *J. Assoc. Res. Otolaryngol.* 7, 95–109. doi: 10.1007/s10162-005-0025-4

Shera, C. A., and Guinan, J. J. Jr. (1999). Evoked otoacoustic emissions arise by two fundamentally different mechanisms: a taxonomy for mammalian OAEs. *J. Acoust. Soc. Am.* 105, 782–798. doi: 10.1121/1.426948

Smith, D. W., Aouad, R. K., and Keil, A. (2012). Cognitive task demands modulate the sensitivity of the human cochlea. *Front. Psychol.* 3:30. doi: 10.3389/fpsyg.2012.00030

Srinivasan, S., Keil, A., Stratis, K., Osborne, A. F., Cerwonka, C., Wong, J., et al. (2014). Interaural attention modulates outer hair cell function. *Eur. J. Neurosci.* 40, 3785–3792. doi: 10.1111/ejn.12746

Srinivasan, S., Keil, A., Stratis, K., Woodruff, K. L., and Smith, D. W. (2012). Effects of cross-modal selective attention on the sensory periphery: cochlear sensitivity is altered by selective attention. *Neuroscience* 223, 325–332. doi: 10.1016/j.neuroscience.2012.07.062

Suga, N., and Ma, X. (2003). Multiparametric corticofugal modulation and plasticity in the auditory system. *Nat. Rev. Neurosci.* 4, 783–794. doi: 10.1038/nrn1222

Tang, J., Yang, W., and Suga, N. (2012). Modulation of thalamic auditory neurons by the primary auditory cortex. *J. Neurophysiol.* 108, 935–942. doi: 10.1152/jn.00251.2012

Thompson, A. M., and Thompson, G. C. (1993). Relationship of descending inferior colliculus projections to olivocochlear neurons. *J. Comp. Neurol.* 335, 402–412. doi: 10.1002/cne.903350309

Velluti, R., Pedemonte, M., and García-Austt, E. (1989). Correlative changes of auditory nerve and microphonic potentials throughout sleep. *Hear. Res.* 39, 203–208. doi: 10.1016/0378-5955(89)90091-9

Vetter, D. E., Saldaña, E., and Mugnaini, E. (1993). Input from the inferior colliculus to medial olivocochlear neurons in the rat: a double label study with PHA-L and cholera toxin. *Hear. Res.* 70, 173–186. doi: 10.1016/0378-5955(93)90156-u

Villa, A. E., Rouiller, E. M., Simm, G. M., Zurita, P., de Ribaupierre, Y., and de Ribaupierre, F. (1991). Corticofugal modulation of the information processing in the auditory thalamus of the cat. *Exp. Brain Res.* 86, 506–517. doi: 10.1007/bf00230524

Warr, W. B., and Guinan, J. J. Jr. (1979). Efferent innervation of the organ of corti: two separate systems. *Brain Res.* 173, 152–155. doi: 10.1016/0006-8993(79)91104-1

Weedman, D. L., and Ryugo, D. K. (1996a). Pyramidal cells in primary auditory cortex project to cochlear nucleus in rat. *Brain Res.* 706, 97–102. doi: 10.1016/0006-8993(95)01201-x

Weedman, D. L., and Ryugo, D. K. (1996b). Projections from auditory cortex to the cochlear nucleus in rats: synapses on granule cell dendrites. *J. Comp. Neurol.* 371, 311–324. doi: 10.1002/(sici)1096-9861(19960722)371:2<311::aid-cne10>3.0.co;2-v

Winer, J. A. (2006). Decoding the auditory corticofugal systems. *Hear. Res.* 212, 1–8. doi: 10.1016/j.heares.2005.06.014

Winer, J. A., Diehl, J. J., and Larue, D. T. (2001). Projections of auditory cortex to the medial geniculate body of the cat. *J. Comp. Neurol.* 430, 27–55. doi: 10.1002/1096-9861(20010129)430:1<27::aid-cne1013>3.0.co;2-8

Winer, J. A., and Lee, C. C. (2007). The distributed auditory cortex. *Hear. Res.* 229, 3–13. doi: 10.1016/j.heares.2007.01.017

Wittekindt, A., Kaiser, J., and Abel, C. (2014). Attentional modulation of the inner ear: a combined otoacoustic emission and EEG study. *J. Neurosci.* 34, 9995–10002. doi: 10.1523/JNEUROSCI.4861-13.2014

Xiao, Z., and Suga, N. (2002). Modulation of cochlear hair cells by the auditory cortex in the mustached bat. *Nat. Neurosci.* 5, 57–63. doi: 10.1038/nn786

Xiong, Y., Zhang, Y., and Yan, J. (2009). The neurobiology of sound-specific auditory plasticity: a core neural circuit. *Neurosci. Biobehav. Rev.* 33, 1178–1184. doi: 10.1016/j.neubiorev.2008.10.006

Yan, J., and Ehret, G. (2002). Corticofugal modulation of midbrain sound processing in the house mouse. *Eur. J. Neurosci.* 16, 119–128. doi: 10.1046/j.1460-9568.2002.02046.x

Yan, J., Zhang, Y., and Ehret, G. (2005). Corticofugal shaping of frequency tuning curves in the central nucleus of the inferior colliculus of mice. *J. Neurophysiol.* 93, 71–83. doi: 10.1152/jn.00348.2004

Yan, W., and Suga, N. (1998). Corticofugal modulation of the midbrain frequency map in the bat auditory system. *Nat. Neurosci.* 1, 54–58. doi: 10.1038/255

Zhang, Y., and Suga, N. (2000). Modulation of responses and frequency tuning of thalamic and collicular neurons by cortical activation in mustached bats. *J. Neurophysiol.* 84, 325–333.

Zhou, X., and Jen, P. H. (2005). Corticofugal modulation of directional sensitivity in the midbrain of the big brown bat, Eptesicus fuscus. *Hear. Res.* 203, 201–215. doi: 10.1016/j.heares.2004.12.008

Conflict of Interest Statement: The authors declare that the research was conducted in the absence of any commercial or financial relationships that could be construed as a potential conflict of interest.

frontiers in
SYSTEMS NEUROSCIENCE

ORIGINAL RESEARCH ARTICLE
published: 06 October 2014
doi: 10.3389/fnsys.2014.00188

Descending projections from auditory cortex to excitatory and inhibitory cells in the nucleus of the brachium of the inferior colliculus

Jeffrey G. Mellott[1], Martha E. Bickford[2] and Brett R. Schofield[1]*

[1] *Department of Anatomy and Neurobiology, Northeast Ohio Medical University, Rootstown, OH USA*
[2] *Department of Anatomical Sciences and Neurobiology, University of Louisville, Louisville, KY USA*

Edited by:
Paul Hinckley Delano, Universidad de Chile, Chile

Reviewed by:
Victoria M. Bajo Lorenzana, University of Oxford, UK
Jorge Mpodozis, Universidad de Chile, Chile

***Correspondence:**
Brett R. Schofield, Department of Anatomy and Neurobiology, Northeast Ohio Medical University, 4209 State Route 44, PO Box 95, Rootstown, OH 44272, USA
e-mail: bschofie@neomed.edu

Descending projections from the auditory cortex (AC) terminate in subcortical auditory centers from the medial geniculate nucleus (MG) to the cochlear nucleus, allowing the AC to modulate the processing of acoustic information at many levels of the auditory system. The nucleus of the brachium of the inferior colliculus (NBIC) is a large midbrain auditory nucleus that is a target of these descending cortical projections. The NBIC is a source of several auditory projections, including an ascending projection to the MG. This ascending projection appears to originate from both excitatory and inhibitory NBIC cells, but whether the cortical projections contact either of these cell groups is unknown. In this study, we first combined retrograde tracing and immunochemistry for glutamic acid decarboxylase (GAD, a marker of GABAergic cells) to identify GABAergic and non-GABAergic NBIC projections to the MG. Our first result is that GAD-immunopositive cells constitute ~17% of the NBIC to MG projection. We then used anterograde labeling and electron microscopy to examine the AC projection to the NBIC. Our second result is that cortical boutons in the NBIC form synapses with round vesicles and asymmetric synapses, consistent with excitatory effects. Finally, we combined fluorescent anterograde labeling of corticofugal axons with immunochemistry and retrograde labeling of NBIC cells that project to the MG. These final results suggest first that AC axons contact both GAD-negative and GAD-positive NBIC cells and, second, that some of cortically-contacted cells project to the MG. Overall, the results imply that corticofugal projections can modulate both excitatory and inhibitory ascending projections from the NBIC to the auditory thalamus.

Keywords: medial geniculate nucleus, ascending, GABA, corticofugal, modulation

INTRODUCTION

The discovery of extensive projections from the auditory cortex (AC) to brainstem auditory nuclei below the inferior colliculus (IC) (Feliciano et al., 1995) substantially broadened our view of the corticofugal system (reviewed by Schofield, 2010, 2011; Malmierca and Ryugo, 2011). Corticofugal projections terminate in auditory centers from the medial geniculate nucleus (MG) to the cochlear nucleus, presumably allowing the AC to modulate processing of acoustic information at many levels of the auditory system. Physiological studies have implicated these cortical projections in a wide range of functions, including the tuning of cells for a variety of stimulus parameters (e.g., frequency, amplitude, duration; Popelár et al., 2003; Suga, 2008; Xiong et al., 2009; He and Yu, 2010), stimulus-specific adaptation and sensitivity to pitch and spatial cues (Jen et al., 1998; Nakamoto et al., 2008, 2010; Anderson and Malmierca, 2013) and adaptation to changing spatial cues (Bajo et al., 2010). Identification of the subcortical circuits contacted by cortical axons is an important step for understanding the mechanisms of corticofugal effects and characterizing their broader functions.

The present study focuses on a subcortical area, the nucleus of the brachium of the inferior colliculus (NBIC), that has been largely ignored in recent examinations of the corticofugal system. The NBIC is a large midbrain auditory nucleus associated with a prominent fiber tract, the brachium of the IC. This brachium contains the axons of IC cells that project to the MG as well as many descending axons that originate in AC and travel to the IC (Diamond et al., 1969; Saldaña et al., 1996). The fiber tract extends from the lateral part of the IC rostrally through the lateral midbrain tegmentum to reach the caudal end of the MG. A large number of cells are distributed along this pathway; many cells are concentrated in the medial part of the fiber tract, although the latter, fiber-rich area contains a substantial number of neurons (e.g., Kudo et al., 1984; Morest and Oliver, 1984; King et al., 1998).

Abbreviations: 4, trochlear nucleus; AQ, cerebral aqueduct; FB, Fast Blue; FG, FluoroGold; GAD, glutamic acid decarboxylase; GB, green beads; IC, inferior colliculus; MG, medial geniculate body; MGd, dorsal division of medial geniculate; MGm, medial division of medial geniculate; MGsg, supragenicular division of medial geniculate; MGv, ventral division of medial geniculate; mlf, medial longitudinal fasciculus; NBIC, nucleus of the brachium of the inferior colliculus; PAG, periaqueductal gray; PBG, parabigeminal nucleus; ps, pseudosylvian sulcus; RB, red beads; s, shell of MG; SC, superior colliculus; SN, substantia nigra.

The NBIC has been implicated in a variety of functions, including orienting responses, auditory attention and multimodal processing. These functions are served by inputs to the NBIC from numerous auditory centers, most notably the IC and the AC, and substantial projections from the NBIC to the MG and the superior colliculus (Calford and Aitkin, 1983; Kudo et al., 1984; LeDoux et al., 1985; Thiele et al., 1996; Jiang et al., 1997; King et al., 1998). NBIC cells respond to acoustic stimuli and can be sensitive to azimuth and elevation cues that are used for sound localization (Aitkin and Jones, 1992; Schnupp and King, 1997; Slee and Young, 2013). The NBIC receives input from somatosensory and visual nuclei, and appears to play a role in integration of multiple sensory modalities (Berkley et al., 1980; Flink et al., 1983; Itoh et al., 1984; Wiberg and Blomqvist, 1984; Redgrave et al., 1987; Doubell et al., 2000). The multimodal nature of NBIC is reflected in its projections to the medial geniculate nucleus, where NBIC axons terminate primarily in the medial, dorsal and suprageniculate subdivisions (i.e., outside the ventral MG, the main relay for lemniscal information; Calford and Aitkin, 1983; Kudo et al., 1984). These subdivisions are part of the extralemniscal pathway and include cells with multimodal responses. They may be particularly important for detecting change and analyzing stimulus context (discussed in Anderson and Linden, 2011).

Glutamate and GABA are the major effectors of ascending auditory inputs to the MG. Electrical stimulation of the brachium of the IC produces excitation and inhibition of MG cells that can be eliminated by pharmacological blockade of glutamate and GABA receptors in the MG (Peruzzi et al., 1997; Bartlett and Smith, 1999, 2002; Smith et al., 2007). Anatomical studies have identified GABAergic and non-GABAergic projections to the MG from the IC in several species (cats: Winer et al., 1996; rats: Peruzzi et al., 1997; guinea pigs: Mellott et al., 2014). A GABAergic projection from the NBIC to the MG has also been identified, but thus far has been described only in rats (Peruzzi et al., 1997). In the first part of the present study, we document a GABAergic projection from the NBIC to the MG in guinea pigs.

The NBIC is also a target of descending projections from the AC (Diamond et al., 1969; Andersen et al., 1980). These projections originate from a wide span of cortical areas, including primary AC (Saldaña et al., 1996; Budinger et al., 2006) as well as other AC areas (Winer et al., 1998; Kimura et al., 2004). To our knowledge, there are no studies comparing relative strengths of projections to NBIC from different cortical areas, but the studies cited above (based on anterograde tracing or degeneration) clearly indicate projections from areas believed to have distinct functions (e.g., primary vs. non-primary areas). Whether the cortical projections contact NBIC cells that project to the MG is unknown. In the second part of the present study, we describe evidence that auditory cortical axons terminate on cells in the NBIC and that the targets include GABAergic and non-GABAergic cells that project to the MG. These results imply that auditory corticofugal projections could activate, or modulate, both excitatory and inhibitory ascending projections from the NBIC to the auditory thalamus.

MATERIALS AND METHODS

All procedures were conducted in accordance with the Institutional Animal Care and Use Committee and NIH guidelines. Results are described from 15 adult pigmented guinea pigs (Elm Hill Labs; Chelmsford, MA, USA) of either gender weighing 317–1058 g. Efforts were made to minimize the number of animals and their suffering.

SURGERY

Each animal was anesthetized with halothane or isoflurane (4–5% for induction, 1.75–3% for maintenance) in oxygen. The head was shaved and disinfected with Betadine (Purdue Products L.P., Stamford, CT, USA). Atropine sulfate (0.08 mg/kg i.m.) was given to minimize respiratory secretions and Ketofen (ketoprofen, 3 mg/kg i.m.; Henry Schein, Melville, NY 11747, USA) was given for post-operative pain management. Ophthalmic ointment (Moisture Eyes PM, Bausch & Lomb, Rochester, NY, USA) was applied to each eye to protect the cornea. The animal's head was positioned in a stereotaxic frame. Body temperature was maintained with a feedback-controlled heating pad. Sterile instruments and aseptic techniques were used for all surgical procedures. An incision was made in the scalp and the surrounding skin was injected with Marcaine (0.25% bupivacaine with epinephrine 1:200,000; Hospira, Inc., Lake Forest, IL, USA), a long-lasting local anesthetic. A craniotomy was made over the desired target coordinates using a dental drill. In animals that received tracer deposits in multiple areas (left and right MG or an MG and the AC), all deposits were done during a single surgery. Following tracer injections, Gelfoam (Harvard Apparatus, Holliston, MA, USA) was placed in the craniotomy and the scalp was sutured. The animal was then removed from the stereotaxic frame and placed in a clean cage. The animal was monitored until it could walk, eat and drink without difficulty.

TRACERS

Five fluorescent tracers were used for retrograde labeling of NBIC cells from the MG: red fluorescent RetroBeads ("red beads," Luma-Fluor, Inc., Naples, FL, USA; injected without dilution); green fluorescent RetroBeads ("green beads," LumaFluor; injected without dilution); Fast Blue (FB, 5% in water; EMS-Chemie GmbH, Gross Umstadt, Germany), FluoroGold (4% in sterile water; FluoroChrome, Inc., Englewood, CO, USA) and fluorescein dextran (FD, 10% in saline, 10 k molecular weight; Invitrogen, Carlsbad, CA, USA) mixed in equal proportion with 4% FG (FG/FD). The use of this variety of tracers provides numerous advantages not available with a single tracer. All the tracers used in the present study are known to be sensitive retrograde markers (Schofield et al., 2007; Schofield, 2008). In addition, FB and FG diffuse readily, facilitating large injections and attempts to maximize the spread of injections to include as much of the target as possible. In contrast, red or green beads show very limited diffusion. This facilitates very small injections that are still informative because of the high sensitivity of the beads. The dextrans are less sensitive as retrograde tracers (in many pathways they label fewer cells than other tracers with a similar injection size), but often provide the most extensive labeling of dendrites. The extent of dendritic labeling varies with the pathway

(e.g., Schofield and Cant, 1996; Bajo and Moore, 2005; Schofield et al., 2006), but still provides some of the best opportunities for identifying contacts between labeled cells and labeled axons (e.g., Coomes Peterson and Schofield, 2007). Stereotaxic coordinates were used to target specific MG subdivisions. Large injections were made with a microsyringe (1 μl; Hamilton, Reno, NV, USA) (**Table 1**). Each syringe was dedicated to a single tracer or specific mixture. Small injections were made with a micropipette (tip inside diameter 25 μm) attached to a Nanoliter Injector (World Precision Instruments, Sarasota, FL, USA).

Fluorescent dextrans have proven to be superb anterograde tracers for labeling AC axons extending to subcortical sites in guinea pigs (cochlear nucleus: Schofield and Coomes, 2005a,b; IC: Nakamoto et al., 2013a,b; superior olivary complex: Coomes and Schofield, 2004; pontomesencephalic tegmentum: Schofield and Motts, 2009). FD and FluoroRuby (FR; tetramethylrhodamine dextran, 10 k molecular weight, 10% in sterile saline) were used for anterograde tracing from the AC. Each tracer was injected with a 1 μl Hamilton microsyringe dedicated to use with that tracer. Tracer was deposited into the left AC of 5 of the animals with MG injections (**Table 1**). Two additional animals received injections of tracer into the AC for subsequent analysis with electron microscopy (**Table 1**). In all cases, tracer was deposited in a grid-like array (9–32 deposit sites) centered on core auditory fields using the pseudosylvian sulcus as a surface landmark (primary AC and the dorsocaudal field; see Wallace et al., 2000, 2002). Volumes of 0.1–0.2 μl were deposited at each site for a total volume of 2.4–6.4 μl in a given animal.

PERFUSION AND TISSUE PROCESSING

Light microscopy

Five to twenty days after surgery, the animal was deeply anesthetized with isoflurane and perfused transcardially with Tyrode's solution (a bicarbonate-buffered Ringer's solution; http://en.wikipedia.org/wiki/Tyrode's_solution), followed by 250 ml of 4% paraformaldehyde in 0.1 M phosphate buffer, pH 7.4 and then 250 ml of the same fixative with 10% sucrose. The brain was removed from the skull and stored at 4°C in fixative with 25–30% sucrose. The following day the cerebellum was removed and the cerebral cortex was separated from the brainstem and thalamus (separating the tissue simplifies processing and minimizes the amount of immunochemical reagents needed for staining and, in relevant cases, for electron microscopy). The brainstem was further trimmed with transverse cuts at the rostral end of the thalamus and posterior to the superior olive. Each piece of tissue was frozen and cut on a sliding microtome into sections 40 or 50 μm thick that were collected serially in six sets. The cortex was cut in the transverse plane; the brainstem/thalamus was cut in transverse, sagittal or horizontal planes.

One series of brainstem sections was split into rostral and caudal sets so that sections through the thalamus could be stained

Table 1 | Injections into the MG or AC.

Case	MG injections							AC injections			
	Side	Tracer	Total volume	MGv	MGd	MGsg	MGm	Side	Tracer	No. of deposit sites	Total volume (μl)
GP636	R	FG	0.05 μl	x	x	x	x				
GP640	L	RB	0.4 μl	x	x	x	x				
GP640	R	FB	0.08 μl	x	x	x	x				
GP689	L	RB	69 nl			(x)	x				
GP689	R	GB	69 nl				x				
GP692	L	FG	0.05 μl	x	x	x	x				
GP693	L	RB	46 nl		x						
GP695	L	RB	27.6 nl	x							
GP696	L	RB	27.6 nl			x					
GP698	L	RB	18.4 nl			x					
GP718	L	FG	0.05 μl		x			L	FR	9	2.4
GP719	L	FG	0.05 μl	x				L	FR	12	3.2
GP721	L	FG	0.08 μl	x	x	x	x	L	FR	15	4.0
GP722	L	FG/FD	0.08 μl			x	x	L	FR	15	3.6
GP726	L	FG	0.08 μl	x	x			L	FR	17	4.6
GP363*								L	FD	32	6.4
GP391*								L	FR	5	0.9

*Summary of injection parameters and distribution of deposit sites for tracer injections. Fluorescent tracers were deposited into left (L) or right (R) medial geniculate nuclei (MG) and/or into the left auditory cortex (AC). Total volume = volume of tracer deposited within the target on the indicated side. Volumes indicated in nanoliters (nl) represent injections made with a Nanoliter Injector (see text); volumes indicated in microliters (μl) were made with a 1 μl microsyringe or, for some injections into the AC, with a 10 μl microsyringe. For each MG injection, the subdivisions that were included in the deposit sites are indicated: "x" indicates substantial deposit within the subdivision, "(x)" indicates only minor encroachment of the tracer into that subdivision. An empty space indicates no significant spread of tracer into that subdivision. In Case GP692, the tracer spread medial and ventral to the MGm; none of the other cases had significant tracer spread outside the MG. FB, Fast Blue; FG, FluoroGold; FG/FD, 1:1 mixture of FG and fluorescein dextran; GB, green beads; RB, red beads. *, animals that were analyzed with electron microscopy.*

for cytochrome oxidase activity to identify MG subdivisions (Anderson et al., 2007) and sections through the midbrain could be stained with antibodies to brain nitric oxide synthase (**Table 2**) to identify IC subdivisions (Coote and Rees, 2008) and facilitate identification of NBIC borders (personal observations). One or more additional series of sections were stained to identify putative GABAergic cells with antibodies to glutamic acid decarboxylase (GAD) (Nakamoto et al., 2013c). Briefly, the sections were pretreated with normal goat serum to limit non-specific labeling, then exposed (1–2 days at 4°C) to mouse anti-GAD polyclonal antibody (**Table 2**). The sections were treated with 1% biotinylated goat anti-mouse antibody and labeled with streptavidin conjugated to a fluorescent marker (AlexaFluor 488). In some cases with cortical injections, synaptic sites were stained in one series of sections by treatment with antibodies to synapsin 1 (**Table 2**), a synaptic marker. Specificity of the anti-synapsin 1 antibody was established by western blot (Abcam). The marker was visualized with goat anti-rabbit secondary antibody conjugated to AlexaFluor 750 (**Table 2**). For some series, NeuroTrace 435/455 Fluorescent Nissl Stain (Cat # N21479; Molecular Probes, www.lifetechnologies.com) was used as a Nissl counterstain. Stained sections were mounted on gelatin-coated slides, allowed to dry and coverslipped with DPX (www.sigmaaldrich.com).

In animals that received cortical injections, sections through AC were examined to ensure that the tracer did not penetrate the underlying white matter or deeper brain structures. All cases had extensive labeling of cells in the MG, confirming injection into the AC.

Processing for electron microscopy

Two animals that received tracer injections into the AC were processed for electron microscopy as described previously (Nakamoto et al., 2013b). Briefly, the animals were perfused after 11–18 days as described above except that the fixative was 2% glutaraldehyde plus 2% paraformaldehyde in 0.1 M phosphate buffer. The brain was stored in the fixative overnight and then sectioned on a Vibrotome (50 μm thick sections) in the sagittal plane. Tracer was revealed with biotinylated antibodies to fluorescein or rhodamine (**Table 2**) and streptavidin peroxidase, which was then used to precipitate diaminobenzidine (DAB). Some of the reacted sections were mounted on glass slides, counterstained for Nissl substance, and covered for light microscopic examination. A subset of sections with labeled axons were post-fixed in 2% osmium tetroxide, dehydrated in alcohols and embedded in Durcupan (Electron Microscopy Sciences, Fort Washington, PA, USA) between sheets of Aclar Embedding Film (Ted Pella, Inc. Redding, CA, USA). These sheets were examined in a light microscope and areas of the NBIC that contained labeled axons were trimmed out and mounted on a blank resin block. Ultrathin sections (silver-gold interference) were cut with a Leica UC6 ultramicrotome, collected on 300 mesh nickel grids and stained with antibodies to GABA to reveal GABAergic neurons (described in detail in Coomes et al., 2002). Briefly, grids holding thin sections were placed on rabbit anti-GABA antibodies (**Table 2**) overnight, then marked with secondary antibodies linked to 15 nm gold particles (**Table 2**). Sections were stained with 1% uranyl acetate and, in some cases, lead citrate.

DATA ANALYSIS

Light microscopy—brightfield and wide-field fluorescence

Cytoarchitecture and injection sites. The location and extent of each MG injection site was determined by comparison of the tracer deposit with borders of MG subdivisions identified in sections stained for cytochrome oxidase (Anderson et al., 2007).

Table 2 | List of main reagents used for immunochemistry.

	Host	Conjugated to	Working dilution	Source*	Catalog number
PRIMARY ANTIBODY					
Anti-bNOS	Mouse		1:1000	Sigma	N2280
Anti-GABA	Rabbit		1:500–1:1000	Sigma	A2052
Anti-GAD67	Mouse		1:100–1:1000	Millipore	MAB5406
Anti-synapsin 1	Rabbit		1:500–1:1000	Abcam	Ab8
Anti-fluorescein	Goat	Biotin	1:1000	Vector	BA-0601
Anti-rhodamine	Goat	Biotin	1:1000	Vector	BA-0605
SECONDARY ANTIBODY					
Anti-Mouse	Goat	Biotin	1:100	Vector	BA-9200
Anti-Rabbit	Goat	AF750	1:100	Invitrogen	A21039
Anti-Rabbit	Goat	15 nm gold	1:25	Ted Pella	15727
TAG					
Streptavidin		AF488	1:100	Invitrogen	S-11223
Streptavidin		AF647	1:100	Invitrogen	S-21374
Streptavidin		Peroxidase	1:100	Jackson	016-030-084

Abbreviations: bNOS, brain nitric oxide synthase; GAD, glutamic acid decarboxylase; AF488, AF647, AF750: AlexaFluor fluorescent marker excited maximally by wavelength indicated by the number (in nm).

**Sources: Abcam, www.abcam.com; Jackson ImmunoResearch, www.jacksonimmuno.com; Invitrogen, www.lifetechnologies.com; Millipore, www.millipore.com; Sigma, www.sigmaaldrich.com; Ted Pella, www.tedpella.com; Vector, www.vectorlabs.com.*

Injections into the cortex were examined to confirm that they were located in the AC (i.e., in temporal cortex between pseudosylvian and rhinal sulci; cf. Wallace et al., 2000, 2002) and did not extend into the subcortical white matter or other structures. The NBIC was identified by comparison with descriptions in cat (Kudo et al., 1984; Morest and Oliver, 1984) and ferret (King et al., 1998). Identification of the borders of the NBIC with the IC and with the MG were facilitated by both the bNOS and the GAD immunochemistry (see Results).

Immunochemistry. Immunostaining revealed GAD-immunoreactive (GAD+) cells and boutons in the NBIC. Immunopositive cells were labeled intensely and were readily distinguished from immunonegative cells. The GAD immunostain was also readily visible in tracer-labeled cells, making it straightforward to distinguish GAD+ vs. GAD-negative staining in the retrogradely labeled cells. Results from 8 injections (3 large and 5 small) that had robust immunostaining were used for quantitative analysis. Labeled cells in the NBIC were plotted with a Neurolucida reconstruction system (MBF Bioscience, Williston, VT, USA) attached to a Zeiss Axioplan II microscope (Carl Zeiss MicroImaging, Inc., Thornwood, NY, USA). For each case, every labeled cell was plotted in an evenly spaced series of sections (usually every sixth section) through the NBIC ipsilateral to the tracer deposit.

In some cases, the anti-GAD staining did not fully penetrate the tissue, resulting in a central layer in the section where GAD staining was absent. Data from these cases were plotted with the Neurolucida system and a 63× objective (NA = 1.4), with special attention to focusing on the center of the soma when plotting the symbol for a particular cell. This approach provides sufficient resolution in the z plane (section depth) to allow filtering of the data by depth. After the data were plotted, the X, Y, and Z coordinates of all markers from each subdivision of each tissue section were exported from Neurolucida to Microsoft Excel and sorted based on the Z coordinate. The depth of penetration of the GAD labeling was assessed under the 63× objective to determine the range of depths (measured from each surface of the section) where GAD staining was robust. This yielded 2 zones of data from each section (1 associated with each surface), and a central zone that was stained poorly or not at all with GAD. All markers in the central zone were excluded from further analyses. (Note: the central zone is typically 10–15 μm thick, given that the sections, which were cut at 40 or 50 μm thick, are usually 20–25 μm thick once dehydrated and coverslipped for microscopy).

In order to assess the relationship of cortical synapses to NBIC cells in our light microscopic experiments, we examine tracer-labeled cortical boutons in tissue stained with antibodies to the presynaptic synaptic marker synapsin 1. We counted double-labeled boutons across the NBIC in two sagittal sections, thus including samples from a wide rostro-caudal and medio-lateral expanse of the NBIC. The tissue was examined at high magnification (63× oil objective, NA = 1.4) to allow careful assessment of colocalization between the tracer label and the anti-synapsin label. In addition, analysis was limited to a region near the surface of the section where synapsin staining was robust. Our goal was to assess the proportion of likely cortical synapses that were associated with NBIC somas vs. those located in the neuropil, and thus likely to contact dendrites of the NBIC cells. By selecting only double-labeled boutons, we avoided false negative staining that could have arisen from incomplete penetration of the anti-synapsin immunochemicals. Given these constraints, all double-labeled boutons in the stained zone near the top surface of each tissue section were counted. This yielded 455 boutons. The boutons were classified as "perisomatic" if they appeared to be in close apposition to a NeuroTrace-labeled soma.

Structured illumination fluorescence microscopy

High resolution imaging of fluorescent structures was accomplished with structured illumination microscopy (Apotome 2 system) on a Zeiss AxioImager Z2 (www.zeiss.com/microscopy) controlled by Neurolucida software (version 11.03, MBF Bioscience). Most often, optical sections were collected at a spacing of 0.2 μm, over a total depth of 4–6 μm, although finer spacing and greater depths were employed as necessary. The system is equipped with a metal halide illuminator (X-Cite 120Q, Lumen Dynamics, www.ldgi.com) allowing for fluorescence analysis throughout the visible spectrum and in several infrared channels (excitation at 647 or 750 nm).

Electron microscopy

Ultrastructure was analyzed with two electron microscopes (EM). One EM is a JEOL JEM 100S transmission electron microscope with which areas of interest were photographed at 15,000–40,000 magnification with high-resolution film (Kodak SO-163; Kodak, Rochester, NY, USA). The negatives were scanned at 1200–2000 pixels/inch (ScanMaker 800, Microtek, Santa Fe Springs, CA, USA) to produce digital images. A second EM is a Phillips CM10 equipped with a digital camera for direct capture of digital images. Synapses were identified by the presence of vesicles in the presynaptic profile, a clear synaptic cleft and the presence of a postsynaptic density. Tracer-labeled profiles were readily identified by the presence of DAB precipitate. GABA-positive (GABA+) profiles were easily distinguished from GABA-negative profiles by a distinct difference in the density of overlying gold particles (Nakamoto et al., 2013a). GABA immunostaining was also readily distinguished from the DAB label (Nakamoto et al., 2013b).

FIGURE PRODUCTION

Plots showing the distribution of labeled cells were created with Neurolucida software (MBF Bioscience, Williston, VT, USA) and refined with Adobe Illustrator (Adobe Systems, Inc., San Jose, CA, USA). Photomicrographs were captured using either a Zeiss AxioImager Z1 fluorescence microscope and AxioCam HRm or HRc cameras (Zeiss) controlled by AxioVision Software (version 4.6, Zeiss) or with structured illumination microscopy on the AxioImager Z2 as described above. Final images were produced by selecting the relevant optical sections from the stack and creating a maximum projection image (Neurolucida 11.03 software). Electron micrographs were assembled from the digital files. For both light and electron micrographs, Adobe Photoshop (Version CS3 or CS6, Adobe Systems) was used to add labels, crop images, erase background around tissue sections and to colorize

monochrome images. Contrast levels were adjusted globally by adjusting levels or curves.

RESULTS

IDENTIFICATION OF THE NBIC IN GUINEA PIGS

The NBIC in guinea pigs was identified by comparison with descriptions in cats, ferrets and rats (Kudo et al., 1984; Schnupp and King, 1997; Paxinos and Watson, 1998). The rostral end, where the NBIC abuts the MG, and the caudal end, where the NBIC abuts the IClc, can be difficult to delineate in standard Nissl stains. We report here that bNOS and GAD immunostaining are particularly helpful in these areas. At the caudal end, the NBIC has less intense bNOS staining and less intense GAD staining than the IClc, allowing the structures to be distinguished. The rostral borders were particularly enhanced by the anti-GAD staining. The MG in guinea pigs is nearly devoid of GABAergic cells (Arcelli et al., 1997). GABAergic cells are present throughout the NBIC, distinguishing it from the MG. GAD+ puncta (i.e., boutons) also differ, being much more numerous in the MG than in the NBIC.

NBIC PROJECTIONS TO THE MG

Figure 1 shows a representative example of a large injection of FluoroGold (FG) into the right MG. This injection included parts of all 4 major subdivisions (ventral, dorsal, medial, and suprageniculate) as well as the MG shell. The injection did not spread to the caudal border of the MG, and completely missed the caudal end of the MGm, which abuts the NBIC. We conclude that the injection did not encroach directly on the NBIC. Retrogradely labeled cells were very numerous in many regions, including the ipsilateral and contralateral IC and many subcollicular auditory nuclei previously described as sources of input to the MG (Anderson et al., 2006; Schofield et al., 2014a,b) and in the NBIC. The following description is limited to label in the NBIC. As described above, the NBIC consists of a concentration of cells located medial to the main bundle of inferior brachium fibers and cells located among these fibers. Following tracer injections in the MG, labeled cells were quite numerous within the large nuclear region and scattered in smaller numbers within the fiber tract. The majority of labeled cells in the NBIC were located ipsilateral to the injection site, although a few labeled cells were present contralaterally.

A proportion of the retrogradely labeled cells were immunopositive for GAD (GAD+) (**Figure 2**), while the remaining cells were GAD-negative. The two cell types were intermingled, with no obvious relationship to the location of the injection site within the MG. Although negative staining can be difficult to interpret, retrogradely labeled immunonegative cells were often located near GAD+ cells (e.g., **Figures 2A,B**). Such a result suggests that the immunonegative cell was in fact non-GABAergic, and not unlabeled because of incomplete immunostaining. **Figure 3** shows a plot of the labeled cells in the right NBIC following a large injection of Fast Blue into the right MG. Labeled cells were located throughout the rostro-caudal length of the NBIC, extending from the caudal end of the nucleus where it abuts the lateral cortex of the IC to the rostral end at the level of the MG. The majority of cells, however, were concentrated between these two extremes, i.e., in transverse sections with a prominent superior colliculus. GAD+ retrogradely-labeled

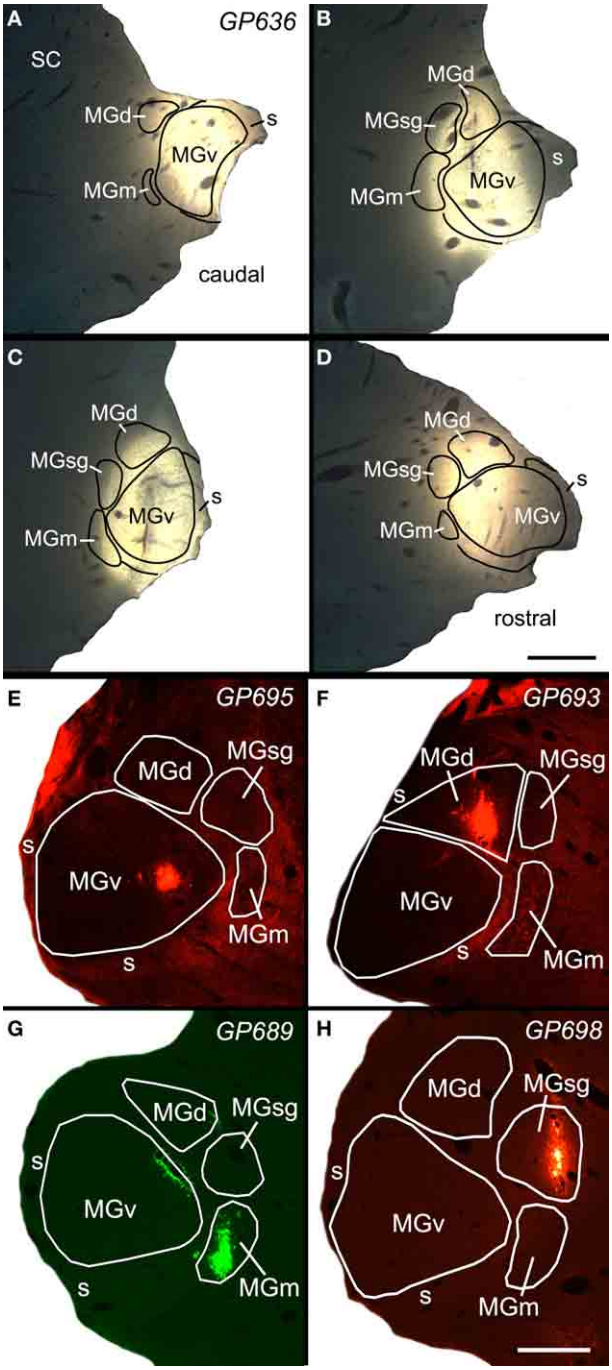

FIGURE 1 | Photomicrographs of a representative large injection site (A–D) and 4 small injection sites (E–H) in the medial geniculate nucleus (MG). (A–D) Series of transverse sections through the MG showing a large injection of FluoroGold that involved all MG subdivisions. Sections are arranged from caudal to rostral. Scale bar in D = 1 mm. **(E)** Small injection of red beads confined to the ventral subdivision of the MG (MGv). **(F)** Small injection of red beads confined to the dorsal subdivision of MG (MGd). **(G)** Small injection of green beads into the medial subdivision of the MG (MGm). Additional green fluorescence is seen around the margins of a blood vessel along the dorsomedial border of the ventral MG (v); this represents spread of beads that does not result in retrogradely labeled cells. This injection was into the right MG; the image has been reversed left

(Continued)

FIGURE 1 | Continued
to right to facilitate comparisons with the other small injections. **(H)** Small injection of red beads into the supragenic ulate MG (sg). Scale bar in H = 0.5 mm and applies to **(E–H)**. Transverse sections; dorsal is up; lateral is to the left in **(A–D)**, and to the right in **(E–H)**. Panels **(A–D)** were previously published in Mellott et al. (2014); panel **(G)** was previously published in Schofield et al. (2014b).

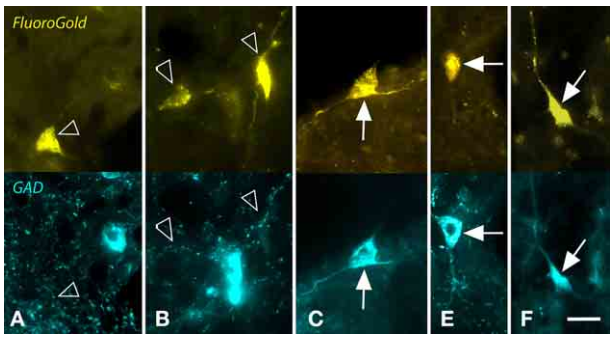

FIGURE 2 | Photomicrographs showing examples of GAD-negative and GAD+ cells in the nucleus of the brachium of the inferior colliculus that were retrogradely labeled by a large injection of FluoroGold (FG) into the ipsilateral medial geniculate nucleus. For each panel, the upper image shows cells labeled with FG and the lower image shows the same region visualized for GAD immunoreactivity. **(A,B)** Examples of FG-labeled cells (open arrows) that were GAD-negative. In both panels, nearby cells were robustly labeled for GAD (blue cells). **(C–F)** Examples of FG-labeled cells (solid arrows) that were also GAD+. Scale bar = 20 μm. **A,C–E**: GP636; **B**: GP721.

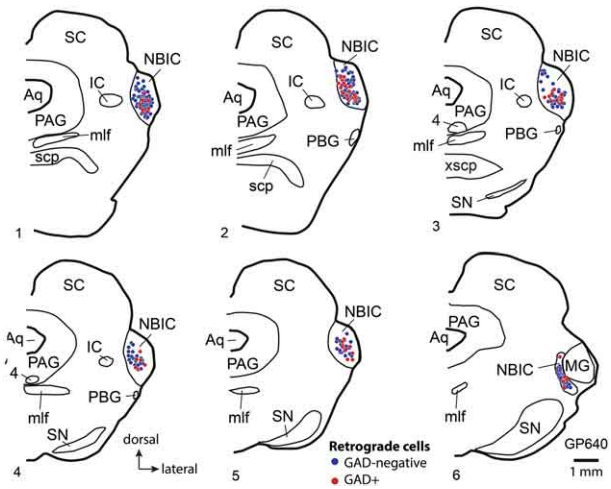

FIGURE 3 | Plots showing the distribution of labeled cells in transverse sections through the right nucleus of the brachium of the inferior colliculus (NBIC) after a large injection of Fast Blue (FB) into the right MG. Each symbol represents one retrogradely-labeled cell. Symbol color indicates whether the FB-labeled cell was GAD-negative (blue circle) or GAD+ (red circle). Sections are numbered from rostral to caudal and are spaced 300 μm apart. See list for abbreviations.

cells (red symbols in **Figure 3**) were located throughout the rostro-caudal extent of the NBIC.

The proportion of retrogradely labeled NBIC cells that were GAD+ was quantified from 3 experiments with large injections into the MG (**Table 3**, top panel). On average, 17% of the retrogradely labeled cells were GAD+. The values ranged from 14 to 21% across the 3 experiments (490 cells counted). Some of the variability may reflect the 3 different retrograde tracers (FB, FG, and RB) but a second possibility is that the projections (GABAergic or otherwise) do not terminate evenly across the MG subdivisions. Analysis of results from 7 experiments with small injections support this latter interpretation. Two injections confined to the MGv (GP695, GP719) produced almost no labeled cells in the NBIC and were not analyzed further. Five additional injections labeled enough cells in the NBIC to warrant quantification (**Table 3**, bottom panel) Injections into the MGm resulted in 13–14% GAD+ retrograde cells, whereas injections into the MGsg resulted in only 2–4% GAD+ retrograde cells. Injections into the MGd labeled an intermediate amount (9% of retrograde cells were GAD+).

AUDITORY CORTICAL PROJECTIONS TO NBIC

Multiple areas of the AC project to the NBIC (Saldaña et al., 1996; Winer et al., 1998; Kimura et al., 2004; Budinger et al., 2006), so we injected anterograde tracer at multiple sites across temporal cortex. **Figure 4A** shows a representative injection site of FR into the left AC. The deposits typically spanned multiple cortical layers, including layers V and VI, but did not extend below layer VI into the white matter. Tangentially, the deposit sites spanned a wide region of temporal cortex, including regions adjacent to the pseudosylvian sulcus, a surface landmark near the border between A1 and adjacent auditory belt areas S ("small area") and dorsorostral belt (cf. Wallace et al., 2000, 2002). We conclude that the injection sites labeled corticofugal axons originating from multiple subdivisions of the AC, including primary AC (A1) and (across cases) varying amounts of the surrounding auditory areas. Labeled axons and boutons were present in large numbers in numerous subcortical nuclei, including the ipsilateral MG, ipsilateral and contralateral IC and other brainstem nuclei as described in previous studies (e.g., Feliciano et al., 1995; Coomes and Schofield, 2004; Coomes Peterson and Schofield, 2007; Schofield and Motts, 2009). The present report focuses on labeled axons in the NBIC.

On the side ipsilateral to the cortical injection, the brachium of the IC (i.e., the fiber pathway itself) contained many labeled axons (**Figure 4B**). No labeled axons were found in the contralateral NBIC, so the remaining discussions are limited to the ipsilateral NBIC. Many of the axons labeled in the ipsilateral NBIC presumably continue on to the IC, one of the most prominent targets of corticofugal projections. Nonetheless, labeled axons also give rise to boutons within the brachium, including terminal boutons as well as en passant boutons. Some of these axons arose from collateral branches of axons that continued caudally (perhaps to reach the IC). It was not possible to determine if some axons terminate in the NBIC without additional branching. While it is typical for boutons to represent presynaptic sites, the presence of synapses within the NBIC was of particular concern given the large number of passing axons. We first labeled synaptic sites with antibodies

Table 3 | Percentage of retrogradely labeled NBIC cells that are GAD-immunopositive (GAD+).

Case	Tracer	# Sections	MG subdivisions	Retro only	Retro-GAD+	% GAD+
LARGE INJECTIONS						
GP636 R	FG	3	all	85	14	14%
GP640 L	RB	7	all	92	18	16%
GP640 R	FB	7	all	221	60	21%
Totals				398	92	
Averages				133	31	17%
SMALL INJECTIONS						
GP689 L	RB	4	MGm/sg	49	7	13%
GP689 R	GB	4	MGm	66	11	14%
GP696 L	RB	5	MGsg	52	1	2%
GP698 L	RB	6	MGsg	94	4	4%
GP718 L	FG	5	MGd	103	10	9%
Totals				364	33	
Averages				73	7	8%

*Summary of GAD+ and GAD-negative ("Retro only") labeled cells in the NBIC after large injections of retrograde tracer into the MG (upper panel) or small injections into 1 or 2 MG subdivisions. Note that 2 animals with injections confined to the MGv were included for study (see **Table 1**), but had so few labeled cells in the NBIC that they were not included in the quantitative analysis. "Case" indicates the experiment number and the side of the tracer injection. # sections, number of sections in which retrogradely labeled cells were counted. Note that cells were counted only at depths within the sections that were well-stained with the GAD immunomarker (see Materials and Methods). Retro only, number of cells that were labeled with the retrograde tracer and were GAD-immunonegative. "Retro-GAD+" = number of cells that were retrogradely labeled and were also GAD-positive. "% GAD+" = percentage of retrogradely labeled cells that were GAD, calculated as the number of Retro GAD/(Retro only + Retro-GAD). FB, Fast Blue; FG, FluoroGold; RB, red beads.*

to synapsin 1, a molecule involved in linking synaptic vesicles to the cytoskeleton and thus concentrated in presynaptic terminals. **Figures 4C,D** show examples of FR-labeled boutons that also show punctate labeling with synapsin 1. The penetration of the anti-synapsin was rather limited, so only a portion of the tissue near the surface could be analyzed. Nonetheless, double-labeled boutons were readily observed. The majority of such boutons (88%; 399/455 boutons analyzed) were located in the neuropil, presumably to contact dendrites of NBIC cells (**Figures 4C,D**, yellow arrowheads). We also observed double-labeled boutons (12%) in apparent contact with NBIC cell bodies (**Figures 4C,D**, white arrowheads).

To further establish the presence of cortical synapses, we used electron microscopy to examine NBIC tissue in animals in which AC axons were labeled with FR and subsequently made electron dense with diaminobenzidine (DAB). GABAergic neurons were also labeled with antibodies to GABA. The latter staining was visualized with immunogold particles that are readily distinguished from the DAB label that identified the cortical boutons. **Figure 5** shows examples of DAB-labeled cortical boutons forming synapses on dendrites in the NBIC. The results confirm that cortical axons form synapses with NBIC cells. The cortical boutons were generally small, with profile diameters on the order of 0.5–1.0 μm (**Figure 5**). Prominent postsynaptic densities, indicating asymmetric synapses, ranged from 0.25 to 0.5 μm in length and could be straight or curved (concave toward the bouton) (**Figure 5**). The synaptic vesicles were round and very numerous, often filling much of the presynaptic profile. Our small sample of synapses contacted dendrites (**Figure 5**), which is consistent with our light microscopic data showing a majority of cortical boutons ending in the NBIC neuropil. While GABA+ profiles were sometimes in close proximity to the cortical boutons (**Figures 5C,D**), the postsynaptic profiles of the cortical boutons were GABA-negative. A larger sample size would be needed to characterize contacts on NBIC somas and GABAergic cells.

AUDITORY CORTICAL PROJECTIONS TO NBIC CELLS THAT PROJECT TO THE MG

As described in the Introduction, the NBIC projects to numerous targets. Our final question concerned the projections of the NBIC cells contacted by cortical axons. Specifically, we asked whether any of the cortically-targeted NBIC cells project to the MG We addressed this question with structured illumination fluorescence microscopy and a combination of anterograde labeling of auditory cortical axons, retrograde labeling of NBIC cells that project to the MG, and immunostaining with anti-GAD to label GABAergic cells. Every case with successful labeling of both anterograde and retrograde pathways provided evidence for cortical contacts onto NBIC-MG cells. **Figures 6A–D** show examples of cortical boutons in contact with GAD-negative NBIC cells labeled by retrograde transport of FluoroGold from the MG. The cortical axons appeared to contact both somas and proximal dendrites. Other FR-labeled cortical boutons appeared to contact GAD-positive NBIC cells that project to the MG (**Figures 6E–H**). Once again, the boutons appeared to contact both somas and proximal dendrites. In addition, there were many labeled cortical boutons located in the neuropil without any obvious association with retrogradely labeled cells. The retrograde tracers rarely labeled the dendrites extensively, so it is possible that cortical boutons also contact the distal dendrites of NBIC cells that project to the MG. However, it is also possible that these boutons contact NBIC cells that were not labeled by the tracer either because the injection did not fill the entire MG or because the contacted cells project to some other target (e.g., the superior colliculus, a prominent target of NBIC projections).

DISCUSSION

The present results demonstrate a projection from the NBIC to the MG in guinea pigs that originates from both GAD+ and GAD-negative cells. The GAD+ cells constitute ∼17% of the projecting population. Below, we discuss evidence that the GAD-negative NBIC cells are likely to be glutamatergic. Our data also demonstrate a projection from the AC to the NBIC similar to that described in numerous species (cat: Diamond et al., 1969; rat: Saldaña et al., 1996; Kimura et al., 2004; gerbil: Budinger et al., 2006). We identify cortical synapses in the NBIC and provide evidence that cortical axons contact both GABAergic and non-GABAergic (presumably glutamatergic) NBIC cells that project

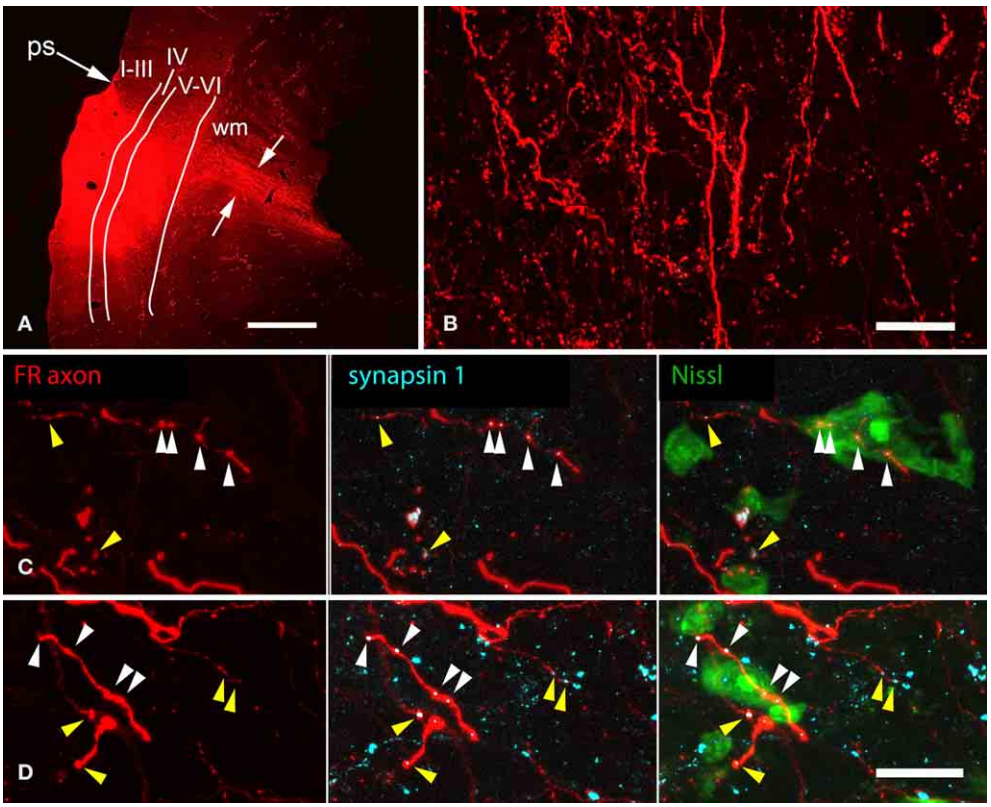

FIGURE 4 | Photomicrographs showing representative results after an injection of FluoroRuby (FR) into the left auditory cortex. (A) Transverse section showing part of a large deposit of FR into the left auditory cortex. The deposit site (bright red area) was confined to the cortical layers (indicated by Roman numerals); FR-labeled axons (between white arrows) are seen extending into the subcortical white matter (wm). GP724. ps, pseudosylvian sulcus. Dorsal is up; lateral is to the left. Scale bar = 1 mm. **(B)** FR-labeled axons in the nucleus of the brachium of the inferior colliculus (NBIC) after the injection shown in panel **(A)** labeled axons as well as many boutons are visible. Sagittal section. Scale bar = 20 μm. Structured illumination image stack; maximum projection image. **(C,D)** Structured illumination fluorescence images showing FR-labeled boutons (red) in the NBIC that are also immunoreactive for the synaptic marker synapsin 1 (imaged with AlexaFluor 647 and colorized cyan). Each row shows a single area visualized for FR (all panels), synapsin 1 (cyan, middle and right panels) and Neurotrace (a Nissl stain, colorized green, right panel). Many swellings on the FR-labeled axons were immunopositive for synapsin 1; some of these were closely apposed to labeled somas (white arrowheads), whereas other synapsin 1-positive, FR labeled boutons were located in the neuropil (yellow arrowheads), between Nissl-stained cells (presumably forming synapses with unlabeled dendrites). GP724. Sagittal sections. Scale bar = 20 μm.

to the MG. These results suggest that corticofugal projections can modulate activity in both excitatory and inhibitory ascending projections from the NBIC to the auditory thalamus.

TECHNICAL CONSIDERATIONS

Tracer injections

In addition to dense projections to the MG, the NBIC projects to some surrounding nuclei (e.g., subparafascicular nucleus) as well-more rostral thalamic nuclei (e.g., paraventricular nucleus, Kudo et al., 1984). The course of NBIC axons to these extra-MG targets is not clear, so we cannot rule out the possibility that some of the retrogradely labeled cells in the present paper send axons to terminate in these other areas. Such labeling would be most likely in cases with large injections, where the microsyringe needle causes damage that could lead to labeling fibers of passage. However, all our findings were confirmed in cases with small injections made with micropipettes. This approach is much less likely to label fibers of passage, so we conclude that the majority of cells labeled in the present cases project to the MG.

Injections of tracer into the AC were designed to maximize labeling of corticofugal axons and thus the opportunities for finding connections with the retrogradely labeled NBIC cells. The injections appeared to be completely confined to AC (as described by Wallace et al., 2000, 2002), but we are unable to distinguish contributions from different cortical areas. Studies in cats and rats suggest that multiple AC areas project to the NBIC (Diamond et al., 1969; Andersen et al., 1980; Saldaña et al., 1996; Kimura et al., 2004), and one might predict that projections from different areas serve different functions. Future studies will be needed to examine this issue.

Immunostaining and quantification

The anti-GAD antibody used for light microscopy in the present study has been verified previously in guinea pigs and is likely to have labeled the majority of GABAergic cells and few if any other cells (Nakamoto et al., 2013c). The staining was robust in that immunopositive cells were readily distinguished from immunonegative cells. As described in Materials and Methods

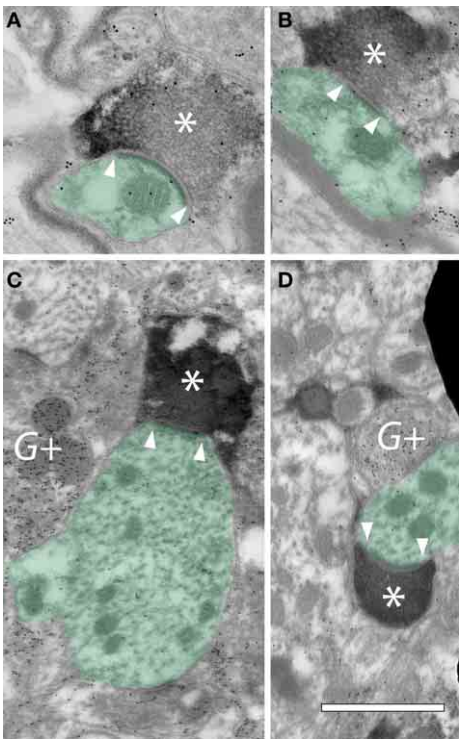

FIGURE 5 | Electron micrographs showing FR-labeled cortical boutons forming synapses in the ipsilateral nucleus of the brachium of the inferior colliculus (NBIC). (A–D) Cortical boutons (*) are filled with DAB precipitate resulting from transport of FluoroRuby. Internal structures in the boutons were obscured by the DAB precipitate, but round synaptic vesicles could often appear negatively stained within the profiles. Postsynaptic densities were typically prominent (located between the white arrowheads). The postsynaptic targets of these cortical boutons were dendrites (green shading). Post-embedding immunogold staining was used to identify GABAergic profiles, indicated by gold particles (small black dots) (G+). GP363. Scale bar = 1 μm.

(Section Light microscopy—brightfield and wide-field fluorescence), our quantitative analyses were limited to tissue depths that had robust immunostaining. We conclude that false negative staining, in which retrogradely-labeled GABAergic cells were unstained by the immunomarker, is unlikely to have affected our results substantially. The anti-GABA antibody used for EM has also been validated in guinea pigs (Nakamoto et al., 2013a) and is likely to have labeled the majority of GABAergic profiles.

The percentage of retrogradely labeled cells that were GAD+ varied across cases. To some extent this can be related to MG subdivision, but there may also be differences due to the tracers. The percentages after small injections (2–14%) never reached as high values as those obtained after large injections (14–21%). It is possible that GABAergic NBIC projections are particularly dense to small parts of the MG that were included in our large injection sites but not our small injections. A second possibility is that the GABAergic cells are less efficiently labeled by the tracers (perhaps they have fewer axonal terminals than the glutamatergic cells) and thus are less well-labeled by smaller injections. While we cannot rule out such issues, the values of 13–14% for the GABAergic component of projections to the MGm is quite close to the values reached in 2 of the 3 large injections (14, 16, and 21%; see **Table 3**).

The other antibodies used here have been characterized previously. We used concentrations of antibodies that we have optimized empirically for guinea pigs and for the current fixation protocol, so we expect false negatives and/or false positives to be minimal. The use of bNOS was limited to cytoarchitectural analysis; our results matched those published in guinea pigs (Coote and Rees, 2008) and are unlikely to have affected our conclusions. Anti-fluorescein and anti-rhodamine staining was absent when applied to tissue that did not have tracer injections, so we are unlikely to have any substantial artifactual staining with these antibodies. The synapsin antibody was validated by Western blot (by the manufacturer). As described in the Results, the penetration of this antibody was limited so false negatives would be prominent in deeper parts of the sections. We avoided this area by restricting our analysis of synapsin staining to tissue near the cut surfaces (where staining was prominent).

Limitations of light and electron microscopy

Light microscopy with fluorescent markers allows us to survey a large area of tissue while visualizing multiple markers, but is limited in its ability to identify synaptic contacts. The latter issue is addressed by electron microscopy (EM), but technical requirements of EM limit the number of distinguishable labels and the amount of tissue that can be analyzed in a reasonable time. By combining the two approaches, we obtained several types of information regarding the projection of the AC to the NBIC. Our results with light microscopy provide strong evidence for cortical synapses in the NBIC. The electron microscopy results support this conclusion. Our small sample of synapses analyzed with EM did not reveal GABAergic targets of AC boutons. While we did not quantify the GAD+ vs. GAD-negative targets in our light microscopy data, the proportion of apparent targets that were GAD+ were clearly a minority. In fact, our retrograde tracing showed that a minority (21% or less) of the NBIC-MG cells are GAD+, so cortical boutons would have to be highly biased toward GABAergic cells for them to represent a large proportion of the targets. We conclude that AC boutons are likely to contact NBIC GABAergic cells but that the frequency of such contacts is too low to have been revealed in our small EM sample. Fluorescence microscopy also facilitates multi-labeling experiments. Our triple-label experiments, combining anterograde and retrograde tracing with immunochemistry, suggest that some of the NBIC cells contacted by AC axons project to the MG, and that this includes both GABAergic and non-GABAergic cells. Future experiments with triple labeling adapted for EM will be needed to confirm cortical synapses with NBIC GABAergic cells as well as cortical synapses on MG-projecting NBIC cells.

FUNCTIONAL IMPLICATIONS

Physiology of NBIC-MG projections

In vitro experiments demonstrate that electrical stimulation of the brachium of the IC leads to both excitation and inhibition of MG cells (e.g., Hu et al., 1994; Peruzzi et al., 1997; Bartlett and Smith, 1999; Smith et al., 2007). The results of such experiments

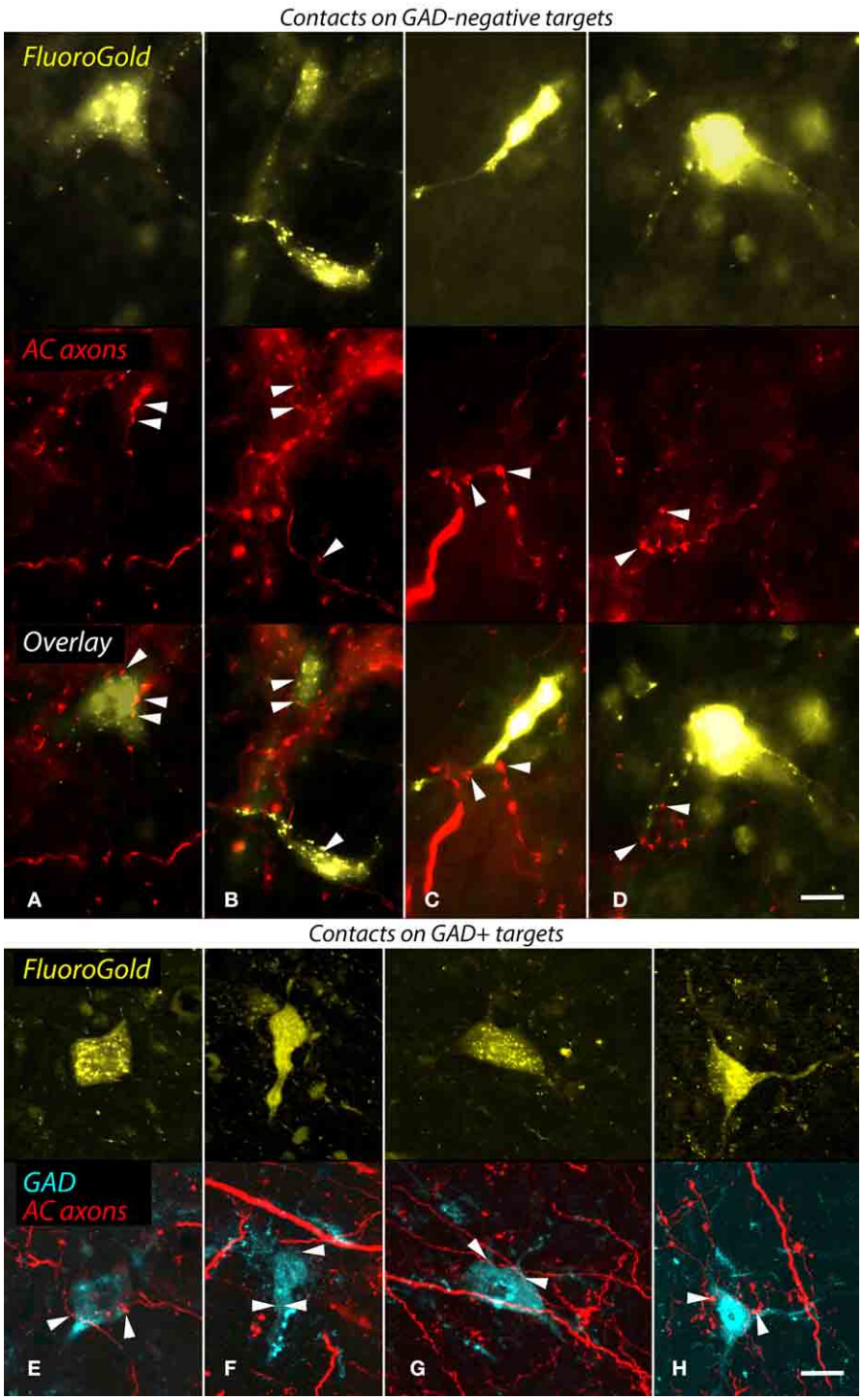

FIGURE 6 | Structured illumination fluorescence micrographs showing FluoroGold (FG)-labeled GAD-negative and GAD+ cells in the nucleus of the brachium of the inferior colliculus (NBIC) that project to the medial geniculate nucleus (MG) and appear to receive synaptic inputs from FluoroRuby (FR)-labeled auditory cortical (AC) axons. (A–D) Cortical contacts on GAD-negative cells. In each column, the top image shows NBIC cells labeled by an injection of FG into the ipsilateral MG. The middle panel shows the same area visualized for axons labeled by an injection of FR into the ipsilateral AC. The bottom panel shows an overlay of the images, with labeled AC boutons (arrowheads) in close apposition to FG-labeled cell bodies **(A,B)** or proximal dendrites **(C,D)**. The cells in **(B,D)** were labeled by an injection restricted to the dorsal MG (MGd; GP718); the cell in **(A)** was labeled by a large injection into all MG subdivisions (GP721), and the cell in **(C)** was labeled by an injection into the dorsal and ventral MG (MGd, MGv; GP726). Scale bar = 10 μm. **(E–H)** Apparent AC contacts onto GAD+ NBIC cells. The upper images in each column show FG-labeled NBIC cells after FG injections into all MG subdivisions (**E,G,H**; GP721) or an injection into the

(Continued)

FIGURE 6 | Continued
medial (MGm) and suprageniculate (MGsg) (**F**; GP722). The lower panel in each column shows the overlaid images from the same area depicting GAD immunostaining (colorized cyan) and FR-labeled cortical axons (red). All four FG-labeled cells are also GAD-immunoreactive (GAD+). In addition, FR-labeled boutons are in apparent contact (arrowheads) with the somas or proximal dendrites of each labeled cell. Structured illumination fluorescence; "maximum projection" images from image stacks (optical section thickness = 0.2 μm). Scale bar = 10 μm.

are generally interpreted in terms of activating IC inputs to the MG, but it seems likely that NBIC projections to the MG are also stimulated, either by direct stimulation of the NBIC cells or by stimulation of the NBIC axons that intermingle with IC axons in the brachium as the brachium nears the MG (Kudo and Niimi, 1980; Kudo et al., 1984). The effects of brachial stimulation on MG cells are blocked by antagonists of GABA and glutamate, indicating that the ascending fibers in the brachium use these two transmitters. It is likely, then, that the non-GABAergic cells in the present study are glutamatergic and that the NBIC, like the IC, provides both glutamatergic and GABAergic ascending inputs to the MG.

A previous study identified GAD-positive cells in NBIC that project to the MG in rats (Peruzzi et al., 1997). The present study identified a higher percentage of GABAergic cells (17 vs. 10%), but in both species the GABAergic cells form a minority of the projection. How this inhibition is integrated with other projections to the MG remains to be determined. Using *in vivo* intracellular recording in guinea pigs, Yu et al. (2004) showed that acoustic stimulation could elicit excitation and inhibition in MG cells. Some cells showed a combination of excitation and inhibition, while others showed only excitation or only inhibition. While the source of the inhibition could not be specified (the MG receives ascending GABAergic inputs from the IC as well as from the NBIC), the data indicate that inhibitory inputs can be driven by acoustic stimuli and may dominate the responses of some MG cells in some instances. Smith and colleagues have used *in vitro* recording to investigate the ascending excitation and inhibition to the MG (Bartlett and Smith, 1999; Smith et al., 2006, 2007). By electrically stimulating the brachium of the IC, they distinguished populations of MG cells that receive only excitatory inputs, only inhibitory inputs or convergent excitatory and inhibitory inputs. The populations show different integrative properties suggesting different functions in hearing. The authors suggested that early inhibition could prevent responses to later excitatory inputs (thus gating the responses of MG cells) whereas later inhibition could alter the onset/sustained nature of responses or modify response selectivity for temporal properties of a stimulus. Thus, both *in vivo* and *in vitro* recordings suggest that ascending inhibitory inputs could play important, and multiple, roles in the responses of MG cells.

NBIC projections in general

The functions of NBIC projections to the MG remain elusive. NBIC has been studied more for its connections with the SC and a role in orientating responses (e.g., Redgrave et al., 1987; King et al., 1998; Doubell et al., 2000). NBIC cells can show tuning for spatial cues and direction of movement (Aitkin and Jones, 1992; Schnupp and King, 1997; Slee and Young, 2013). It is not known if the same NBIC cells project to the SC and the MG, but it appears reasonable to expect that NBIC projections to the MG may play a role in spatial hearing, orientation and, perhaps, auditory attention.

Further insights may be gained by considering the subdivisions of MG that are targeted by NBIC axons. NBIC projects to the extralemniscal MG, largely avoiding the MGv but terminating widely to include MGd, MGm, and MGsg as well as surrounding areas (and several intralaminar nuclei of the thalamus) (present data; Kudo et al., 1984). These areas serve numerous functions. Anderson and Linden (2011) suggested a role in detecting stimulus change and analyzing stimulus context. Numerous studies have associated these areas with behavioral cueing, whereby auditory or other sensory inputs can be associated with positive or negative reinforcement (reviewed by Hu, 2003). Projections from these areas to the amygdala appear critical for such associations (LeDoux et al., 1985). Finally, these areas of the MG also project to the basal ganglia and may support orienting responses or could be involved in sensory gating and selection among multiple stimuli. One or more of these functions might be considered for the NBIC.

AC PROJECTIONS TO NBIC

Projections to the NBIC originate from primary AC, the suprasylvian fringe (in cats) and the posterodorsal area (in rats) (Diamond et al., 1969; Andersen et al., 1980; Saldaña et al., 1996; Winer et al., 1998; Kimura et al., 2004; Budinger et al., 2006). The laminar origins of these projections are unknown. Saldaña et al. (1996) described boutons in the NBIC arising from branches of corticocollicular axons. Corticocollicular projections arise from layer V and, to a lesser extent, from layer VI (Schofield, 2009), suggesting that these layers are the source(s) of projections to NBIC.

Round synaptic vesicles and asymmetric synaptic junctions (present data) suggest that the cortical projections to NBIC are excitatory. The present data suggest that both GABAergic and non-GABAergic NBIC cells are contacted by AC axons. If these cells can be driven by the AC inputs, then the corticofugal system could elicit both excitation and inhibition in the targets of the NBIC cells. Such a dual effect has been attributed to AC projections to the IC, where physiological studies have identified direct excitation of collicular cells as well as indirect inhibition (and excitation) of collicular cells following stimulation of the AC (Mitani et al., 1983). These effects have been attributed to AC axons forming excitatory synapses with glutamatergic and GABAergic collicular cells that, once activated by the cortical inputs, subsequently excite or inhibit other collicular cells via local axon collaterals (discussed in Nakamoto et al., 2013b). NBIC cells appear to have local axons in addition to extrinsic projections (Ramón y Cajal, 1995), so cortical inputs may affect NBIC cells directly and via local connections.

CORTICOFUGAL PROJECTIONS AND SUBCORTICAL AUDITORY CIRCUITS

The corticofugal system has been implicated in the selectivity of subcortical cells for specific stimulus parameters and the plastic retuning of responses according to stimulus salience or altered sensory input (e.g., Jen et al., 1998; Popelár et al., 2003; Nakamoto et al., 2008, 2010; Suga, 2008; Xiong et al., 2009; Bajo et al., 2010; He and Yu, 2010; Anderson and Malmierca, 2013). Many studies have focused on projections to the IC or the MG, but corticofugal effects have been observed from the thalamus to the cochlea. Together, the cortical effects allow the auditory system as a whole to respond more effectively to stimuli of particular significance and to adapt to changes in sensory input. The circuitry that underlies these functions includes direct AC projections to the subcortical auditory structures as well as cortical connections with modulatory systems that affect all levels of the auditory pathway (e.g., Metherate, 2011; Schofield et al., 2011).

Many nuclei targeted by AC projections are themselves a source of projections to numerous places, so a key step for understanding the functions of AC projections to a given target is to identify the projections of targeted cells. Projections to the IC, for example, appear to contact multiple pathways, including ascending pathways to the MG (Coomes Peterson and Schofield, 2007), descending pathways to the CN (Schofield and Coomes, 2006), commissural pathways between the two colliculi (Nakamoto et al., 2013c) and intrinsic connections within the IC (Jen et al., 2001). Such pathways establish feedback loops that allow the AC to modulate its own input as well as multi-neuronal descending chains that extend the functional reach of the AC projections. Cortical projections to other targets may have more limited range. AC projections to the superior olivary complex contact some cells that project to the IC (Coomes Peterson and Schofield, 2007) and other cells that project to the cochlea (Mulders and Robertson, 2000), thereby affecting both ascending and descending pathways from the superior olive. However, not all output pathways from the superior olive are targeted by the AC; the medial superior olivary nucleus, a major source of binaural inputs to the IC, receives virtually no AC inputs. The cochlear nucleus is another area where AC projections contact only a subset of the potential targets. AC axons contact granule cells (whose projections are contained entirely within the cochlear nucleus) as well as cells that project to the IC (Weedman et al., 1996; Jacomme et al., 2003; Schofield and Coomes, 2005b). There is no evidence for cortical inputs to octopus cells, spherical bushy cells or globular bushy cells of the cochlear nucleus, suggesting that the output pathways from these cells are relatively insulated from cortical inputs. While many questions remain, the available evidence demonstrates that AC projections are in a position to have direct influence on selected brainstem circuits and thus to affect some auditory functions more than others.

The NBIC, despite being identified many years ago as a target of AC projections, has yet to be incorporated into a broad overview of the corticofugal system. The issue is relevant because of the wide array of projections from the NBIC, including ascending projections to the MG, to other thalamic nuclei and to the superior colliculus as well as descending projections to the IC (Kudo et al., 1983, 1984; King et al., 1998; Senatorov and Hu, 2002). Which of these output pathways from the NBIC are under direct influence by AC inputs? The present study provides a first step in identifying the ascending projections from the NBIC to the MG as a likely target of AC projections. This ascending projection comprises a large, presumably excitatory component and a smaller GABAergic component; both of these components appear to be contacted by cortical axons. Thus, the corticofugal projections are in a position to modify ascending excitatory and inhibitory projections from the NBIC to the thalamus. As suggested above, NBIC functions could involve sensory gating, selective attention or orienting responses and likely include integration across sensory systems. Identifying the roles of AC projections in such functions remain to be determined, and will require more information about the specific areas of the AC that project to the NBIC, the cell types that give rise to these projections, and the conditions under which these projections are active.

AUTHOR CONTRIBUTIONS

Brett R. Schofield and Jeffrey G. Mellott designed and performed the experiments and analyzed data. Jeffrey G. Mellott and Martha E. Bickford performed the electron microscopy and analyzed the data. Brett R. Schofield wrote the paper with input from the other authors.

ACKNOWLEDGMENTS

Supported by NIH R01DC004391, F32DC012450, and R01EY016155. We gratefully acknowledge technical assistance from Colleen Sowick and Megan Storey-Workley. Special thanks to Nichole Foster for valuable comments on an early draft of the manuscript.

REFERENCES

Aitkin, L., and Jones, R. (1992). Azimuthal processing in the posterior auditory thalamus of cats. *Neurosci. Lett.* 142, 81–84.

Andersen, R. A., Snyder, R. L., and Merzenich, M. M. (1980). The topographic organization of corticocollicular projections from physiologically identified loci in the AI, AII, and anterior auditory cortical fields of the cat. *J. Comp. Neurol.* 191, 479–494.

Anderson, L. A., and Linden, J. F. (2011). Physiological differences between histologically defined subdivisions in the mouse auditory thalamus. *Hear Res* 274, 48–60. doi: 10.1016/j.heares.2010.12.016

Anderson, L. A., and Malmierca, M. S. (2013). The effect of auditory cortex deactivation on stimulus-specific adaptation in the inferior colliculus of the rat. *Eur. J. Neurosci.* 37, 52–62. doi: 10.1111/ejn.12018

Anderson, L. A., Malmierca, M. S., Wallace, M. N., and Palmer, A. R. (2006). Evidence for a direct, short latency projection from the dorsal cochlear nucleus to the auditory thalamus in the guinea pig. *Eur. J. Neurosci.* 24, 491–498. doi: 10.1111/j.1460-9568.2006.04930.x

Anderson, L. A., Wallace, M. N., and Palmer, A. R. (2007). Identification of subdivisions in the medial geniculate body of the guinea pig. *Hear. Res.* 228, 156–167. doi: 10.1016/j.heares.2007.02.005

Arcelli, P., Frassoni, C., Regondi, M. C., De Biasi, S., and Spreafico, R. (1997). GABAergic neurons in mammalian thalamus: a marker of thalamic complexity? *Brain Res. Bull.* 42, 27–37.

Bajo, V. M., and Moore, D. R. (2005). Descending projections from the auditory cortex to the inferior colliculus in the gerbil, *Meriones unguiculatus*. *J. Comp. Neurol.* 486, 101–116. doi: 10.1002/cne.20542

Bajo, V. M., Nodal, F. R., Moore, D. R., and King, A. J. (2010). The descending corticocollicular pathway mediates learning-induced auditory plasticity. *Nat. Neurosci.* 13, 253–260. doi: 10.1038/nn.2466

Bartlett, E. L., and Smith, P. H. (1999). Anatomic, intrinsic, and synaptic properties of dorsal and ventral division neurons in rat medial geniculate body. *J. Neurophysiol.* 81, 1999–2016.

Bartlett, E. L., and Smith, P. H. (2002). Effects of paired-pulse and repetitive stimulation on neurons in the rat medial geniculate body. *Neuroscience* 113, 957–974. doi: 10.1016/S0306-4522(02)00240-3

Berkley, K. J., Blomqvist, A., Pelt, A., and Flink, R. (1980). Differences in the collateralization of neuronal projections from the dorsal column nuclei and lateral cervical nucleus to the thalamus and tectum in the cat: an anatomical study using two different double-labeling techniques. *Brain Res.* 202, 273–290.

Budinger, E., Heil, P., Hess, A., and Scheich, H. (2006). Multisensory processing via early cortical stages: connections of the primary auditory cortical field with other sensory systems. *Neuroscience* 143, 1065–1083. doi: 10.1016/j.neuroscience.2006.08.035

Calford, M. B., and Aitkin, L. M. (1983). Ascending projections to the medial geniculate body of the cat: evidence for multiple, parallel auditory pathways through thalamus. *J. Neurosci.* 3, 2365–2380.

Coomes, D. L., Bickford, M. E., and Schofield, B. R. (2002). GABAergic circuitry in the dorsal division of the cat medial geniculate nucleus. *J. Comp. Neurol.* 453, 45–56. doi: 10.1002/cne.10387

Coomes, D. L., and Schofield, B. R. (2004). Projections from the auditory cortex to the superior olivary complex in guinea pigs. *Eur. J. Neurosci.* 19, 2188–2200. doi: 10.1111/j.0953-816X.2004.03317.x

Coomes Peterson, D., and Schofield, B. R. (2007). Projections from auditory cortex contact ascending pathways that originate in the superior olive and inferior colliculus. *Hear. Res.* 232, 67–77. doi: 10.1016/j.heares.2007.06.009

Coote, E. J., and Rees, A. (2008). The distribution of nitric oxide synthase in the inferior colliculus of guinea pig. *Neuroscience* 154, 218–225. doi: 10.1016/j.neuroscience.2008.02.030

Diamond, I. T., Jones, E. G., and Powell, T. P. S. (1969). The projection of the auditory cortex on the diencephalon and brain stem in the cat. *Brain Res.* 15, 305–340.

Doubell, T. P., Baron, J., Skaliora, I., and King, A. J. (2000). Topographical projection from the superior colliculus to the nucleus of the brachium of the inferior colliculus in the ferret: convergence of visual and auditory information. *Eur. J. Neurosci.* 12, 4290–4308. doi: 10.1111/j.1460-9568.2000.01337.x

Feliciano, M., Saldaña, E., and Mugnaini, E. (1995). Direct projections from the rat primary auditory neocortex to nucleus sagulum, paralemniscal regions, superior olivary complex and cochlear nuclei. *Auditory Neurosci.* 1, 287–308.

Flink, R., Wiberg, M., and Blomqvist, A. (1983). The termination in the mesencephalon of fibres from the lateral cervical nucleus. an anatomical study in the cat. *Brain Res.* 259, 11–20.

He, J., and Yu, Y. (2010). "Role of descending control in the auditory pathway," in *The Oxford Handbook of Auditory Neuroscience*, Vol. 2, The Auditory Brain eds A. Rees and A. R. Palmer (Oxford: Oxford University Press), 247–268.

Hu, B. (2003). Functional organization of lemniscal and nonlemniscal auditory thalamus. *Exp. Brain Res.* 153, 543–549. doi: 10.1007/s00221-003-1611-5

Hu, B., Senatorov, V., and Mooney, D. (1994). Lemniscal and non-lemniscal synaptic transmission in rat auditory thalamus. *J. Physiol.* 479, 217–231.

Itoh, K., Kaneko, T., Kudo, M., and Mizuno, N. (1984). The intercollicular region in the cat: a possible relay in the parallel somatosensory pathways from the dorsal column nuclei to the posterior complex of the thalamus. *Brain Res.* 308, 166–171.

Jacomme, A. V., Nodal, F. R., Bajo, V. M., Manunta, Y., Edeline, J. M., Babalian, A., et al. (2003). The projection from auditory cortex to cochlear nucleus in guinea pigs: an *in vivo* anatomical and *in vitro* electrophysiological study. *Exp. Brain Res.* 153, 467–476. doi: 10.1007/s00221-003-1606-2

Jen, P. H., Chen, Q. C., and Sun, X. D. (1998). Corticofugal regulation of auditory sensitivity in the bat inferior colliculus. *J. Comp. Physiol. A* 183, 683–697.

Jen, P. H., Sun, X., and Chen, Q. C. (2001). An electrophysiological study of neural pathways for corticofugally inhibited neurons in the central nucleus of the inferior colliculus of the big brown bat, *Eptesicus fuscus*. *Exp. Brain Res.* 137, 292–302. doi: 10.1007/s002210000637

Jiang, Z. D., Moore, D. R., and King, A. J. (1997). Sources of subcortical projections to the superior colliculus in the ferret. *Brain Res.* 755, 279–292.

Kimura, A., Donishi, T., Okamoto, K., and Tamai, Y. (2004). Efferent connections of "posterodorsal" auditory area in the rat cortex: implications for auditory spatial processing. *Neuroscience* 128, 399–419. doi: 10.1016/j.neuroscience.2004.07.010

King, A. J., Jiang, Z. D., and Moore, D. R. (1998). Auditory brainstem projections to the ferret superior colliculus: anatomical contribution to the neural coding of sound azimuth. *J. Comp. Neurol.* 390, 342–365.

Kudo, M., Itoh, K., Kawamura, S., and Mizuno, N. (1983). Direct projections to the pretectum and the midbrain reticular formation from auditory relay nuclei in the lower brainstem of the cat. *Brain Res.* 288, 13–19.

Kudo, M., and Niimi, K. (1980). Ascending projections of the inferior colliculus in the cat: an autoradiographic study. *J. Comp. Neurol.* 191, 545–556.

Kudo, M., Tashiro, T., Higo, S., Matsuyama, T., and Kawamura, S. (1984). Ascending projections from the nucleus of the brachium of the inferior colliculus in the cat. *Exp. Brain Res.* 54, 203–211.

LeDoux, J. E., Ruggiero, D. A., and Reis, D. J. (1985). Projections to the subcortical forebrain from anatomically defined regions of the medial geniculate body in the rat. *J. Comp. Neurol.* 242, 182–213.

Malmierca, M. S., and Ryugo, D. K. (2011). "Descending connections of auditory cortex to the midbrain and brain stem," in *The Auditory Cortex*, eds J. A. Winer and C. E. Schreiner (New York, NY: Springer Science+Business Media), 189–208.

Mellott, J. G., Foster, N. L., Nakamoto, K. T., Motts, S. D., and Schofield, B. R. (2014). Distribution of GABAergic cells in the inferior colliculus that project to the thalamus. *Front. Neuroanat.* 8:17. doi: 10.3389/fnana.2014.00017

Metherate, R. (2011). Functional connectivity and cholinergic modulation in auditory cortex. *Neurosci. Biobehav. Rev.* 35, 2058–2063. doi: 10.1016/j.neubiorev.2010.11.010

Mitani, A., Shimokouchi, M., and Nomura, S. (1983). Effects of stimulation of the primary auditory cortex upon colliculogeniculate neurons in the inferior colliculus of the cat. *Neurosci. Lett.* 42, 185–189.

Morest, D. K., and Oliver, D. L. (1984). The neuronal architecture of the inferior colliculus in the cat: defining the functional anatomy of the auditory midbrain. *J. Comp. Neurol.* 222, 209–236.

Mulders, W. H., and Robertson, D. (2000). Evidence for direct cortical innervation of medial olivocochlear neurones in rats. *Hear. Res.* 144, 65–72. doi: 10.1016/S0378-5955(00)00046-0

Nakamoto, K. T., Jones, S. J., and Palmer, A. R. (2008). Descending projections from auditory cortex modulate sensitivity in the midbrain to cues for spatial position. *J. Neurophysiol.* 99, 2347–2356. doi: 10.1152/jn.01326.2007

Nakamoto, K. T., Mellott, J. G., Killius, J., Storey-Workley, M. E., Sowick, C. S., and Schofield, B. R. (2013a). Analysis of excitatory synapses in the guinea pig inferior colliculus: a study using electron microscopy and GABA immunocytochemistry. *Neuroscience* 237, 170–183. doi: 10.1016/j.neuroscience.2013.01.061

Nakamoto, K. T., Mellott, J. G., Killius, J., Storey-Workley, M. E., Sowick, C. S., and Schofield, B. R. (2013b). Ultrastructural examination of the corticocollicular pathway in the guinea pig: a study using electron microscopy, neural tracers, and GABA immunocytochemistry. *Front. Neuroanat.* 7:13. doi: 10.3389/fnana.2013.00013

Nakamoto, K. T., Shackleton, T. M., and Palmer, A. R. (2010). Responses in the inferior colliculus of the guinea pig to concurrent harmonic series and the effect of inactivation of descending controls. *J. Neurophysiol.* 103, 2050–2061. doi: 10.1152/jn.00451.2009

Nakamoto, K. T., Sowick, C. S., and Schofield, B. R. (2013c). Auditory cortical axons contact commissural cells throughout the guinea pig inferior colliculus. *Hear. Res.* 306, 131–144. doi: 10.1016/j.heares.2013.10.003

Paxinos, G., and Watson, C. (1998). *The Rat Brain in Stereotaxic Coordinates*. 4th Edn. San Diego, CA: Academic Press.

Peruzzi, D., Bartlett, E., Smith, P. H., and Oliver, D. L. (1997). A monosynaptic GABAergic input from the inferior colliculus to the medial geniculate body in rat. *J. Neurosci.* 17, 3766–3777.

Popelár, J., Nwabueze-Ogbo, F. C., and Syka, J. (2003). Changes in neuronal activity of the inferior colliculus in rat after temporal inactivation of the auditory cortex. *Physiol. Res.* 52, 615–628.

Ramón y Cajal, S. (1995). *Histology of the Nervous System of Man and Vertebrates*, Vol. 2 (translated from the French edition, 1911). New York, NY: Oxford University Press.

Redgrave, P., Mitchell, I. J., and Dean, P. (1987). Descending projections from the superior colliculus in rat: a study using orthograde transport of wheat germ-agglutinin conjugated horseradish peroxidase. *Exp. Brain Res.* 68, 147–167.

Saldaña, E., Feliciano, M., and Mugnaini, E. (1996). Distribution of descending projections from primary auditory neocortex to inferior colliculus mimics the topography of intracollicular projections. *J. Comp. Neurol.* 371, 15–40.

Schnupp, J. W. H., and King, A. J. (1997). Coding for auditory space in the nucleus of the brachium of the inferior colliculus in the ferret. *J. Neurophysiol.* 78, 2717–2731.

Schofield, B. R. (2008). Retrograde axonal tracing with fluorescent markers. *Curr Protoc Neurosci Chapter* 1:Unit 1 17. doi: 10.1002/0471142301.ns0117s43

Schofield, B. R. (2009). Projections to the inferior colliculus from layer VI cells of auditory cortex. *Neuroscience* 159, 246–258. doi: 10.1016/j.neuroscience.2008.11.013

Schofield, B. R. (2010). "Structural organization of the descending auditory pathway," in *The Oxford Handbook of Auditory Neuroscience* Vol.2, The Auditory Brain, eds A. Rees and A. R. Palmer (Oxford: Oxford University Press), 43–64

Schofield, B. R. (2011). "Central descending auditory pathways," in *Springer Handbook of Auditory Research*, Vol.15, Auditory and Vestibular Efferents, eds D. K. Ryugo, A. N. Popper, and R. R. Fay (New York, NY: Springer-Verlag), 261–290.

Schofield, B. R., and Cant, N. B. (1996). Origins and targets of commissural connections between the cochlear nuclei in guinea pigs. *J. Comp. Neurol.* 375, 128–146.

Schofield, B. R., and Coomes, D. L. (2005a). Auditory cortical projections to the cochlear nucleus in guinea pigs. *Hear. Res.* 199, 89–102. doi: 10.1016/j.heares.2004.08.003

Schofield, B. R., and Coomes, D. L. (2005b). Projections from auditory cortex contact cells in the cochlear nucleus that project to the inferior colliculus. *Hear. Res.* 206, 3–11. doi: 10.1016/j.heares.2005.03.005

Schofield, B. R., and Coomes, D. L. (2006). Pathways from auditory cortex to the cochlear nucleus in guinea pigs. *Hear. Res.* 216-217, 81–89. doi: 10.1016/j.heares.2006.01.004

Schofield, B. R., Coomes, D. L., and Schofield, R. M. (2006). Cells in auditory cortex that project to the cochlear nucleus in guinea pigs. *J. Assoc Res Otolaryngol* 7:95–109. doi: 10.1007/s10162-005-0025-4

Schofield, B. R., Mellott, J. G., and Motts, S. D. (2014a). Subcollicular projections to the auditory thalamus and collateral projections to the inferior colliculus. *Front. Neuroanat.* 8:16. doi: 10.3389/fnana.2014.00070

Schofield, B. R., and Motts, S. D. (2009). Projections from auditory cortex to cholinergic cells in the midbrain tegmentum of guinea pigs. *Brain Res. Bull.* 80, 163–170. doi: 10.1016/j.brainresbull.2009.06.015

Schofield, B. R., Motts, S. D., and Mellott, J. G. (2011). Cholinergic cells of the pontomesencephalic tegmentum: connections with auditory structures from cochlear nucleus to cortex. *Hear. Res.* 279, 85–95. doi: 10.1016/j.heares.2010.12.019

Schofield, B. R., Motts, S. D., Mellott, J. G., and Foster, N. L. (2014b). Projections from the dorsal and ventral cochlear nuclei to the medial geniculate body. *Front. Neuroanat.* 8, 10. doi: 10.3389/fnana.2014.00010

Schofield, B. R., Schofield, R. M., Sorensen, K. A., and Motts, S. D. (2007). On the use of retrograde tracers for identification of axon collaterals with multiple fluorescent retrograde tracers. *Neuroscience* 146, 773–783. doi: 10.1016/j.neuroscience.2007.02.026

Senatorov, V. V., and Hu, B. (2002). Extracortical descending projections to the rat inferior colliculus. *Neuroscience* 115, 243–250. doi: 10.1016/S0306-4522(02)00316-0

Slee, S. J., and Young, E. D. (2013). Linear processing of interaural level difference underlies spatial tuning in the nucleus of the brachium of the inferior colliculus. *J. Neurosci.* 33, 3891–3904. doi: 10.1523/JNEUROSCI.3437-12.2013

Smith, P. H., Bartlett, E. L., and Kowalkowski, A. (2006). Unique combination of anatomy and physiology in cells of the rat paralaminar thalamic nuclei adjacent to the medial geniculate body. *J. Comp. Neurol.* 496, 314–334. doi: 10.1002/cne.20913

Smith, P. H., Bartlett, E. L., and Kowalkowski, A. (2007). Cortical and collicular inputs to cells in the rat paralaminar thalamic nuclei adjacent to the medial geniculate body. *J. Neurophysiol.* 98, 681–695. doi: 10.1152/jn.00235.2007

Suga, N. (2008). Role of corticofugal feedback in hearing. *J. Comp. Physiol. A* 194, 169–183. doi: 10.1007/s00359-007-0274-2

Thiele, A., Rubsamen, R., and Hoffmann, K.-P. (1996). Anatomical and physiological investigation of auditory input to the superior colliculus of the echolocating megachiropteran bat *Rousettus aegyptiacus*. *Exp. Brain Res.* 112, 223–236.

Wallace, M. N., Rutkowski, R. G., and Palmer, A. R. (2000). Identification and localisation of auditory areas in guinea pig cortex. *Exp. Brain Res.* 132, 445–456. doi: 10.1007/s002210000362

Wallace, M. N., Rutkowski, R. G., and Palmer, A. R. (2002). Interconnections of auditory areas in the guinea pig neocortex. *Exp. Brain Res.* 143, 106–119. doi: 10.1007/s00221-001-0973-9

Weedman, D. L., Pongstaporn, T., and Ryugo, D. K. (1996). Ultrastructural study of the granule cell domain of the cochlear nucleus in rats: mossy fiber endings and their targets. *J. Comp. Neurol.* 369, 345–360.

Wiberg, M., and Blomqvist, A. (1984). The projection to the mesencephalon from the dorsal column nuclei. an anatomical study in the cat. *Brain Res.* 311, 225–244.

Winer, J. A., Larue, D. T., Diehl, J. J., and Hefti, B. J. (1998). Auditory cortical projections to the cat inferior colliculus. *J. Comp. Neurol.* 400, 147–174.

Winer, J. A., Saint Marie, R. L., Larue, D. T., and Oliver, D. L. (1996). GABAergic feedforward projections from the inferior colliculus to the medial geniculate body. *Proc. Natl. Acad. Sci. U.S.A.* 93, 8005–8010.

Xiong, Y., Zhang, Y., and Yan, J. (2009). The neurobiology of sound-specific auditory plasticity: a core neural circuit. *Neurosci. Biobehav. Rev.* 33, 1178–1184. doi: 10.1016/j.neubiorev.2008.10.006

Yu, Y. Q., Xiong, Y., Chan, Y. S., and He, J. (2004). *In vivo* intracellular responses of the medial geniculate neurones to acoustic stimuli in anaesthetized guinea pigs. *J. Physiol.* 560, 191–205. doi: 10.1113/jphysiol.2004.067678

Conflict of Interest Statement: The authors declare that the research was conducted in the absence of any commercial or financial relationships that could be construed as a potential conflict of interest.

Received: 10 August 2014; accepted: 16 September 2014; published online: 06 October 2014.

Citation: Mellott JG, Bickford ME and Schofield BR (2014) Descending projections from auditory cortex to excitatory and inhibitory cells in the nucleus of the brachium of the inferior colliculus. Front. Syst. Neurosci. ***8****:188. doi: 10.3389/fnsys.2014.00188*

This article was submitted to the journal Frontiers in Systems Neuroscience.

frontiers in
SYSTEMS NEUROSCIENCE

REVIEW ARTICLE
published: 09 March 2015
doi: 10.3389/fnsys.2015.00019

The cortical modulation of stimulus-specific adaptation in the auditory midbrain and thalamus: a potential neuronal correlate for predictive coding

Manuel S. Malmierca[1,2]*, Lucy A. Anderson[1†] and Flora M. Antunes[1†]

[1] *Auditory Neuroscience Laboratory, Institute of Neuroscience of Castilla y León (INCyL), University of Salamanca, Salamanca, Spain*
[2] *Faculty of Medicine, Department of Cell Biology and Pathology, University of Salamanca, Salamanca, Spain*

Edited by:
Paul Hinckley Delano, Universidad de Chile, Chile

Reviewed by:
Kyle T. Nakamoto, Northeast Ohio Medical University, USA
Daniel Llano, University of Illinois at Urbana-Champaign, USA

****Correspondence:***
Manuel S. Malmierca, Auditory Neuroscience Laboratory, Institute of Neuroscience of Castilla y León (INCyL), University of Salamanca, C Pintor Fernando Gallego 1, 37007 Salamanca, Spain
e-mail: msm@usal.es

[†] These authors have contributed equally to this work.

To follow an ever-changing auditory scene, the auditory brain is continuously creating a representation of the past to form expectations about the future. Unexpected events will produce an error in the predictions that should "trigger" the network's response. Indeed, neurons in the auditory midbrain, thalamus and cortex, respond to rarely occurring sounds while adapting to frequently repeated ones, i.e., they exhibit stimulus specific adaptation (SSA). SSA cannot be explained solely by intrinsic membrane properties, but likely involves the participation of the network. Thus, SSA is envisaged as a high order form of adaptation that requires the influence of cortical areas. However, present research supports the hypothesis that SSA, at least in its simplest form (i.e., to frequency deviants), can be transmitted in a bottom-up manner through the auditory pathway. Here, we briefly review the underlying neuroanatomy of the corticofugal projections before discussing state of the art studies which demonstrate that SSA present in the medial geniculate body (MGB) and inferior colliculus (IC) is not inherited from the cortex but can be modulated by the cortex via the corticofugal pathways. By modulating the gain of neurons in the thalamus and midbrain, the auditory cortex (AC) would refine SSA subcortically, preventing irrelevant information from reaching the cortex.

Keywords: auditory, IC, MGB, SSA, MMN, corticofugal projections, cooling technique, predictive coding

INTRODUCTION

Sounds seldom occur in isolation and we are constantly swamped with a cacophony of sounds that impinge on our ears at every instant, therefore, an essential operation of the brain is to detect rare and potentially important stimuli while ignoring irrelevant ambient backgrounds (Ranganath and Rainer, 2003; Kaya and Elhilali, 2014). Since we are living in a dynamic and permanently changing world, to organize the auditory scene the brain needs to "*adapt*" and efficiently respond to changes in the stimulus incidence and context. Adaptation is an omnipresent property of neurons in the auditory system, however, most types of adaptation previously described in the literature are governed by activity-dependent mechanisms operating at the level of the neuron's output rather than its input, such as those dependent on the history of the stimulation (Calford and Semple, 1995; Brosch and Schreiner, 1997; Ingham and McAlpine, 2004; Furukawa et al., 2005; Gutfreund and Knudsen, 2006; Gutfreund, 2012). The so-called stimulus-specific adaptation (SSA) is a higher level of adaptation which results from adaptation to a specific stimulus, rather than from the intrinsic properties of the neuron (Ulanovsky et al., 2003, 2004). Neurons showing SSA adapt to frequently occurring stimuli (standards) yet respond strongly to rare stimuli (deviants) (Dragoi et al., 2000; Ulanovsky et al., 2003; Katz et al., 2006; Reches and Gutfreund, 2008; Anderson et al., 2009; Malmierca et al., 2009, 2014; von der Behrens et al., 2009; Antunes et al., 2010; Pérez-González and Malmierca, 2012, 2014; Escera and Malmierca, 2014; Nelken, 2014). Such deviant stimuli, i.e., those that are novel in time and space, are perceptually advantaged and give rise to psychophysical effects such as attention capture (Tiitinen et al., 1994) or pop-outs (Diliberto et al., 2000). However, in order to ascertain that a specific stimulus is novel, there must be a neuronal network capable of comparing current and previous stimuli, as shown by the computational studies of Abbott et al. (1997) and Eytan et al. (2003). Thus, at the neuronal level, neurons showing SSA must integrate sensory information to create a predictive model of the world, enabling them to adapt to commonly occurring stimuli and respond more strongly to novel features in the environment. In other words, the neuron's previous experience determines its future sensitivity, which suggests SSA may be a basic mechanism underlying predictive coding (Friston, 2005; Baldeweg, 2006; Bar, 2007; Winkler et al., 2009; Bendixen et al., 2012). Moreover, previous studies have also suggested that SSA could be linked to auditory memory, recognition of acoustic objects and auditory scene analysis (Nelken, 2004; Winkler et al., 2009).

In the auditory brain, SSA occurs in the midbrain (inferior colliculus, IC), thalamus (medial geniculate body, MGB) and cortex (Kraus et al., 1994; King et al., 1995; Ulanovsky et al., 2003, 2004; Pérez-González et al., 2005; Reches and Gutfreund,

2008; Anderson et al., 2009; Malmierca et al., 2009, 2014; von der Behrens et al., 2009; Yu et al., 2009; Antunes et al., 2010; Reches et al., 2010; Taaseh et al., 2011; Zhao et al., 2011; Patel et al., 2012; Pérez-González and Malmierca, 2012, 2014; Hershenhoren et al., 2014; Nelken, 2014). Evidence for SSA in the brainstem has not been extensively investigated; however neurons within the cochlear nucleus do not appear to exhibit SSA in response to similar paradigms that would elicit SSA in the midbrain (Ayala et al., 2013). SSA is strong in the non-lemniscal subcortical regions of the IC and MGB (Anderson et al., 2009; Malmierca et al., 2009; Antunes et al., 2010), but the primary auditory cortex (A1) is the first lemniscal station where SSA seems to be widespread and strong (Ulanovsky et al., 2003). Thus, SSA was originally suggested to emerge in the auditory cortex (AC) as a high order feature of sensory processing that would be transmitted to subcortical nuclei in a top-down fashion (Nelken and Ulanovsky, 2007). Indeed, it is well known that a remarkable feature of the thalamus is the massive set of corticofugal projections that it receives (**Figure 1**). In the MGB, these projections outnumber the ascending projections by a factor of 10 (Winer et al., 2001; Kimura et al., 2003, 2005, 2007; Winer, 2006; Winer and Lee, 2007; Ojima and Rouiller, 2011) and strongly modulate the responses of MGB neurons (Ryugo and Weinberger, 1976; Villa et al., 1991, 1999; He et al., 2002; He, 2003a,b; Palmer et al., 2007). Similarly, the IC in the midbrain also receives a significant corticofugal projection (Saldaña et al., 1996; Bajo et al., 2007; Stebbings et al., 2014) which although not as heavy and dense as the MGB, has been demonstrated to have a strong influence on the collicular neuronal responses (Yan and Suga, 1998; Jen et al., 2001; Yan and Ehret, 2001, 2002; Jen and Zhou, 2003; Yan et al., 2005; Nakamoto et al., 2008, 2010; Markovitz et al., 2013; **Figures 1**, **2**).

Here, we will focus on the effect of the descending cortical projections on SSA at the level of the MGB and IC (**Figures 2–4**). By disentangling the effect of cortical influence on subcortical SSA we endeavor to gain a better understanding of the neuronal circuitry underlying this property. We begin with a brief introduction to the descending *cortico-collicular* and *cortico-thalamic* projections before detailing our recent studies using cortical-cooling to study the effect of reversibly deactivating the AC on SSA in the IC and MGB.

THE DESCENDING PATHWAY FROM THE AUDITORY CORTEX TO THE THALAMUS AND MIDBRAIN

In parallel to the ascending auditory pathways, there are stepwise, descending projections from the AC to the organ of Corti (Malmierca and Ryugo, 2011; Malmierca, 2015). Although these corticofugal pathways have been known since the end of the 19th century (Held, 1893), a renaissance in their study was triggered by the description of the olivocochlear bundle in 1946 by Rasmussen (1946, 1953). The AC projects to a wide range of subcortical targets in the auditory pathway (Winer, 2006; Winer and Lee, 2007), the largest of which are to the MGB (auditory thalamus; **Figure 1**) and the IC (midbrain; **Figure 1**).

The *cortico-thalamic system* (**Figure 1**) is the heaviest projection of the corticofugal network, not only in the descending auditory system, but of the whole brain, comparable only to the corticospinal tract (Winer et al., 2001; Winer, 2006; Malmierca and Ryugo, 2011). The cortico-thalamic system forms a reciprocal connection between the cortex and the thalamus, with a large-scale topographical overlap in the spatial territories of thalamocortical cells and corticothalamic axonal terminals (Winer, 2006, but see Llano and Sherman, 2008). Most terminal boutons arising from the AC and terminating in the MGB are small ($\sim$0.5 μm^2 in diameter) and most likely originate from the pyramidal neurons of layer VI (Bartlett et al., 2000), but a few very large boutons (>2 μm^2) also occur and are thought to originate from neurons in layer V (Rouiller and Welker, 1991, 2000; Shi and Cassell, 1997; Bartlett et al., 2000). These large corticothalamic terminals tend to form complexes with the dendrites partially surrounded by astrocytic processes (Bartlett et al., 2000). Sherman and Guillery (1998) proposed the notion of "drivers" and "modulators" of thalamic neurons in the visual and somatosensory thalamus; this hypothesis has since been applied to the auditory system (Llano and Sherman, 2008). According to this theory, type I terminals play a modulatory role in the first-order thalamic nuclei, such as the ventral subdivision of the MGB (MGV). Thus, the corticothalamic inputs converge with ascending inputs on thalamic neurons such that the ascending inputs drive the thalamic neurons, and the cortical inputs modulate them. In contrast, in "higher order" thalamic nuclei, such as the dorsal subdivision of the MGB (MGD), the "driver" inputs arise from the large type II axons and terminals originating from the AC, and interact with ascending input from the IC.

The major corticofugal projections are glutamatergic (Potashner et al., 1988) suggesting an excitatory function. The AC also projects to the auditory sector of the reticular thalamic nucleus, which in turns projects to the MGB (Rouiller and Welker, 1991, 2000; Bartlett et al., 2000) thus, providing the MGB with an inhibitory influence (Bartlett et al., 2000). Therefore, the corticofugal projection may play a key role in modulating the MGB responses to sound through a direct excitatory pathway and/or an indirect inhibitory pathway. Physiological studies based on electrical stimulation or cooling of the AC have confirmed the excitatory and inhibitory effects of the AC on MGB neurons (Ryugo and Weinberger, 1976; He, 1997, 2003a,b; He et al., 2002; Yu et al., 2004).

The *cortico-collicular system* (**Figure 1**) on the other hand, is made of projections that originate in the AC, bypass the MGB and terminate in the IC (Faye-Lund, 1985; Herbert et al., 1991; Saldaña et al., 1996; Winer et al., 1998; Doucet et al., 2003; Bajo and Moore, 2005; Bajo et al., 2007). Most of these studies have shown a topographic (tonotopic) organization of these projections arising from the primary AC (A1), such that the low frequency regions of A1 project to the dorsolateral region of the IC and the high frequency region of A1 projects to the ventromedial region of the IC. The projections originate bilaterally in multiple cortical areas (reviewed by Winer, 2005); however, the projections originating from A1 constitute the heaviest projection. Projections to the IC also originate from

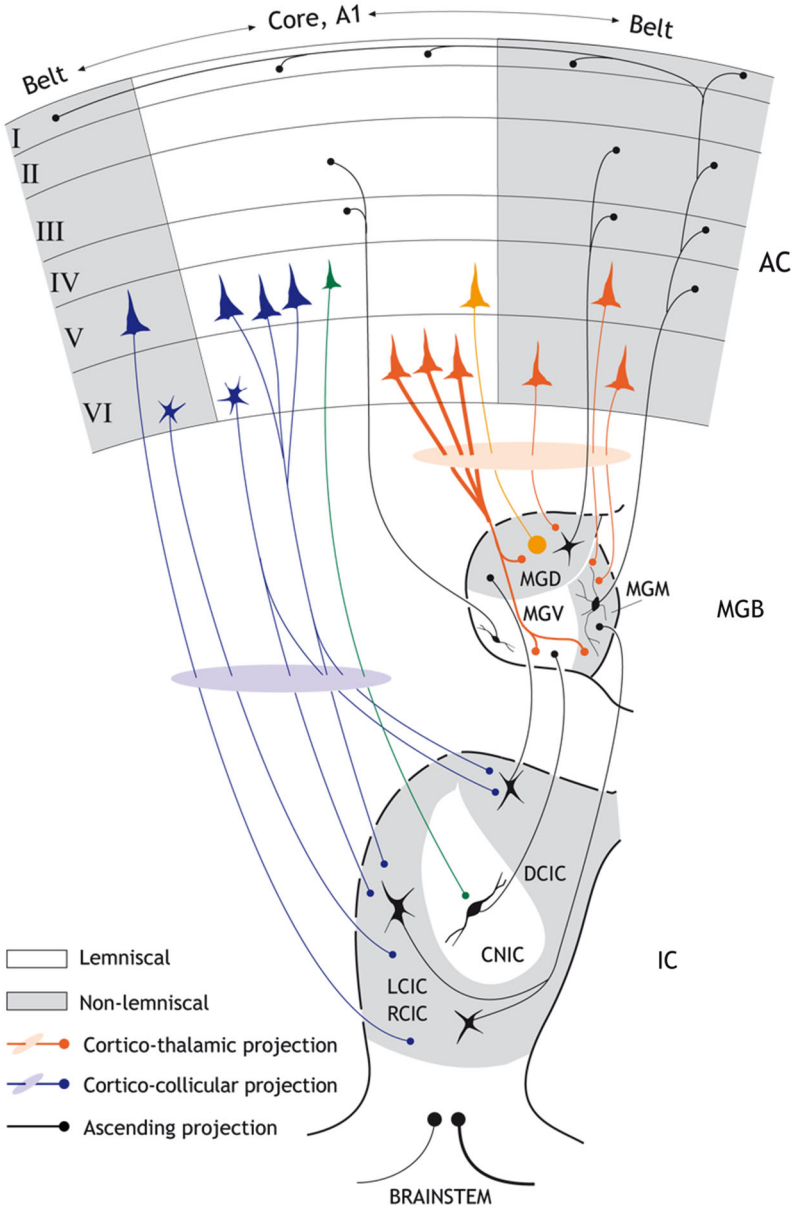

FIGURE 1 | Schematic diagram showing the major anatomical subdivisions of the IC, MGB and AC that illustrates the ascending and descending pathways from the midbrain up to the cortex and back. Non-lemniscal (belt) divisions are highlighted as gray areas. Black connections indicate ascending projections; while red connections indicate major cortico-thalamic connections and purple connections major cortico-collicular projections. Strong SSA is mainly restricted to "*non-lemniscal*" regions of the IC and MGB, but is found in the "*lemniscal*" or core A1. The major cortico-collicular projections emerge from pyramidal neurons in layer V (but a few small neurons deep in layer VI also contribute to this pathway and project predominantly to the collicular cortices). The larger pyramidal neurons from layer V project to the cortical regions of the IC while the smaller pyramidal neurons from layer V project to the CNIC (green). By contrast, the major cortico-thalamic projections emerge from pyramidal neurons in layer VI (but a few pyramidal neurons from layer V also contribute to this pathway). Most terminal boutons arising from the AC and terminating in the MGB are small (~0.5 μm^2 in diameter) and most likely originate from the pyramidal neurons of layer VI. Some cortico-thalamic terminals boutons arise from layer V (orange) and are very large (>2 μm^2). There are also interactions between the core and belt areas of the AC (horizontal black arrows). The connections between the reticular thalamic nucleus, MGB and AC as well as the contralateral corticofugal projections are not shown for simplicity. Abbreviations: A1, primary auditory cortex; AC auditory cortex; CNIC, central nucleus of the inferior colliculus; DCIC, dorsal cortex of the inferior colliculus; LCIC, RCIC; lateral and rostral cortex of the inferior colliculus; MGD; dorsal division of the medial geniculate body; MGM; medial division of the medial geniculate body; MGV; ventral division of the medial geniculate body.

non-primary areas. These latter projections are more variable and less dense than those arising from A1 (Herbert et al., 1991; Bajo et al., 2007). The projections from A1 target the collicular cortices (dorsal, lateral and rostral cortex of the IC; DCIC,

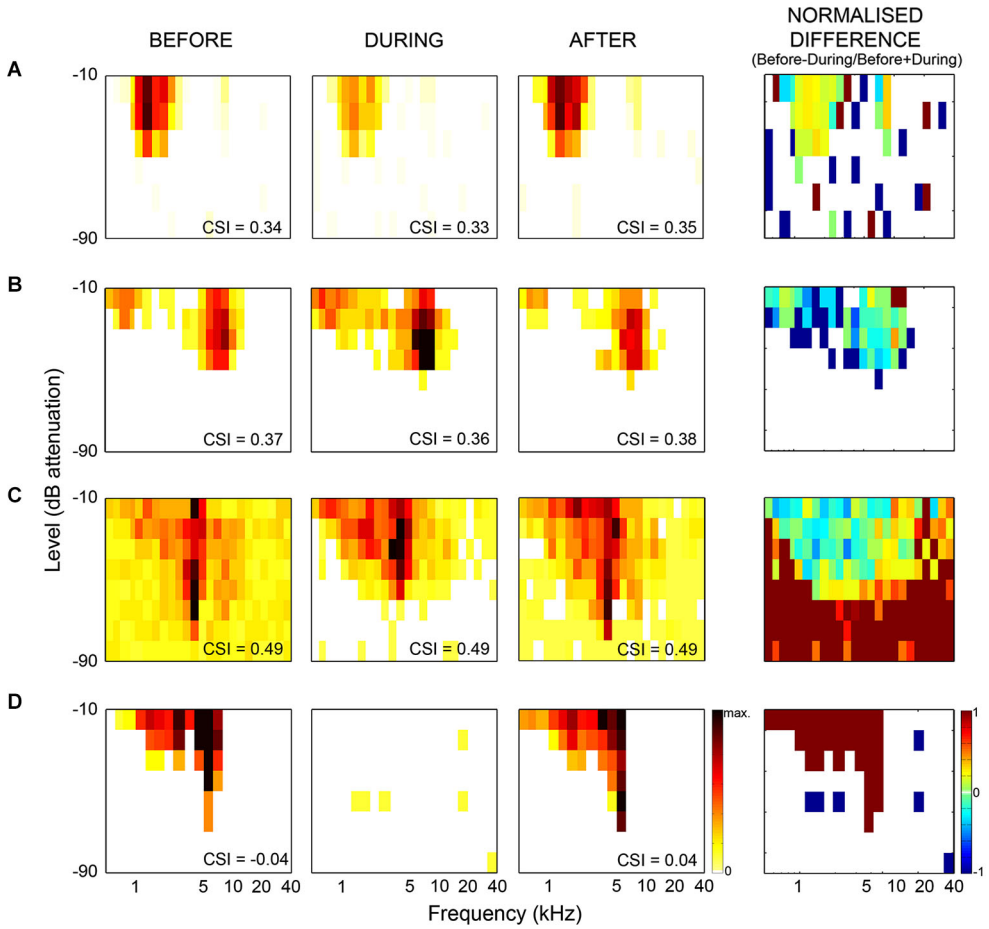

FIGURE 2 | Examples of frequency response areas in the inferior colliculus recorded from neurons which showed no change in SSA during cooling. The CSI index quantifies the level of SSA, and was calculated as CSI = [d(f1) + d(f2) − s(f1) +s(f2)] / [d(f1) + d(f2) + s(f1) + s(f2)], where d(fi) and s(fi) were responses (in spike counts/stimulus) to either frequency fi when it was deviant or standard, respectively. The CSI index was maintained, but there were significant changes in firing rate, spontaneous activity and latencies of the neurons. **(A)** example showing decreased firing rate during cooling. **(B)** increased firing rate during cooling. **(C)** example showing decreased spontaneous rate, increased threshold and increased firing within the frequency response area (FRA) during cooling. **(D)** example which ceased firing during cooling. First column shows FRA before cooling, second column shows FRA during cooling, third column shows FRA after cooling. Firing rate indicated by color bar to right of "After" FRA in **(D)**. The min-max firing rate range is the same across each neuron for all conditions, although varies between neurons. The fourth column shows the normalized difference in FRA (before-during/before+during), difference in firing indicated by color bar to right of difference plot in **(D)** (cool colors = −1, hot colors = 1, no firing = white). Redrawn and modified from Anderson and Malmierca (2013).

LCIC, and RCIC respectively) bilaterally, with the ipsilateral projection being most dense. The central nucleus of the IC also receives a weak, yet significant projection (Saldaña et al., 1996; Winer et al., 1998; Bajo et al., 2007; Nakamoto et al., 2013a,b); the projection to the central nucleus of the IC differs not only in the density of terminal boutons (which is always lower for the central nucleus), but also in their morphology, having, on average, thinner axons and smaller boutons than those terminating in the collicular cortices (Saldaña et al., 1996; Bajo et al., 2007).

The cortico-collicular projections originate primarily in layer V, and to a lesser extent in layer VI (Wong and Kelly, 1981; Games and Winer, 1988; Winer and Prieto, 2001; Doucet et al., 2003; Bajo and Moore, 2005; Bajo et al., 2007; Bajo and King, 2013; Stebbings et al., 2014). More detailed studies have shown that neurons from layer V include pyramidal cells, but those from layer VI are of unknown type except that they are described as "small labeled neurons deep in layer VI" (Bajo and Moore, 2005; Bajo and King, 2013). The largest population of these pyramidal neurons projects to the ipsilateral IC, and a smaller population projects to the contralateral IC or bilaterally to both ICs. Moreover, it seems that the larger pyramidal neurons from layer V project to the cortical regions of the IC while the smaller pyramidal neurons project to the central nucleus. Layer VI neurons seem to project primarily to the collicular cortices (Schofield, 2009). Furthermore, the pyramidal neurons involved in the descending pathway to the IC may correspond to intrinsic bursting neurons (Hefti and Smith, 2000; Slater et al., 2013).

The corticocofugal projection to the IC is glutamatergic (Feliciano and Potashner, 1995), thus the AC may modulate the processing of sounds in the IC either directly, or through the activation of local inhibitory connections within the IC. In this respect, it is worth mentioning that Mitani et al. (1983) found IPSPs in IC neurons after AC stimulation, and Nakamoto et al. (2013a,b) found a very small percentage of corticocollicular targets that were GABAergic IC neurons. These studies suggest that polysynaptic network mechanisms are necessary to achieve local inhibition in the IC after AC stimulation.

THE EFFECT OF THE CORTICOFUGAL PROJECTIONS ON THALAMIC SSA

The AC has been shown to modulate several features of auditory processing in all subcortical regions including the MGB. For example, studies based on electrical stimulation of the AC have shown that the AC can facilitate or suppress responses in the MGB (He, 2003a,b). Furthermore, earlier studies using reversible AC deactivation (Ryugo and Weinberger, 1976; Villa et al., 1991) confirmed that the responses of many MGB neurons are under the control of the AC, thus it would not be surprising that the AC might influence SSA. A simple and elegant way to test this issue is to reversibly deactivate the cortex using the cooling technique (e.g., Lomber, 1999; Lomber et al., 1999, 2007; Lomber and Malhotra, 2008; Nakamoto et al., 2008, 2010; Carrasco and Lomber, 2009a,b, 2010; Coomber et al., 2011). Using this technique, we reversibly deactivated the AC to silence its neurons and the ipsilateral descending projections to the MGB (Antunes and Malmierca, 2011, 2014) in order to analyze what effect the AC exerts on the SSA exhibited by auditory thalamic neurons. Using an oddball stimulus designed to elicit SSA to frequencies (Ulanovsky et al., 2003, 2004; Malmierca et al., 2009; Antunes et al., 2010), we recorded single neuron responses throughout the MGB before, during and after reversibly deactivating the AC by cooling (Antunes and Malmierca, 2011, 2014).

Our results demonstrate that some general properties of the MGB responses were significantly modified during the period of cortical deactivation (such as frequency response maps, spontaneous activity, latency, etc. **Figure 2** shows similar effects observed in the IC). This confirms the MGB receives strong cortical modulation (like other thalamic and subcortical nuclei) through the corticofugal pathway, as demonstrated in previous studies of the auditory (Ryugo and Weinberger, 1976; Villa et al., 1991, 1999; Bajo et al., 1995; Yu et al., 2004; Luo et al., 2008; Liu et al., 2010), visual (Sillito et al., 1994; Rushmore et al., 2005) and somatosensory systems (Ghosh et al., 1994). However, remarkably, despite changes in basic neuronal activity in the MGB during the period of AC deactivation, SSA levels and its dynamics over time were mostly unaffected (**Figures 3**, **4**; Antunes and Malmierca, 2011, 2014).

The AC modulates the firing rate of MGB neurons in a gain control manner (**Figures 4C,D**), affecting the responses to all stimuli in the stimulation paradigm similarly. This "unspecific" control of the AC over the firing rate of MGB neurons did not significantly change the SSA sensitivity (quantified by a ratio of driven rates) of the majority of MGB neurons (46 of 48 neurons). Only two of the 48 neurons showed a significant reduction in SSA during AC deactivation, but these neurons still retained significant levels of SSA. Both neurons drastically increased their firing rates during AC deactivation to both stimuli, decreasing the ratio between the standard and the deviant (and therefore their SSA), as in the "iceberg effect" (Carandini and Ferster, 2000; Isaacson and Scanziani, 2011; Katzner et al., 2011. **Figure 5** illustrates the "iceberg effect" mediated by GABAergic inhibition in IC neurons). These two neurons were the exception in the MGB population, where the gain changes imposed by the cortex were significant but not strong enough to cause an iceberg effect able to significantly change the level of SSA. These findings demonstrated that SSA in the MGB is neither simply inherited from the AC, nor fully generated in the first instance at the level of the AC.

Although SSA was only weakly affected by cortical deactivation, this study found an interesting relationship between SSA and the changes imposed by the AC. The gain exerted by the AC varies significantly with the level of SSA exhibited by the MGB neurons such that the facilitation exerted by the AC on MGB neurons decreases as the SSA increases (**Figures 4C,D**). This relationship is not dependent on the anatomical subdivision to which the MGB neurons belong, but only on their level of SSA. Hence, the AC facilitates neurons with no or low SSA, diminishing this facilitatory effect as the SSA increases. Some highly adapting neurons were even suppressed by the AC. So, although SSA in the MGB is not driven by the AC, there is an active communication between the thalamus and the cortex that is moderated according to the SSA of the individual thalamic neurons. The lack of correlation between the firing rate changes and the subdivision suggests that it is the degree of SSA rather than the localization within one or the other of the subdivisions that determines the modulatory effect of the AC on the MGB.

Although there was no significant statistical effect of subdivision on the firing rate changes, the majority of non-adapting neurons from the lemniscal MGV, a subdivision strongly driven by the corticofugal modulation originating from layer VI of A1, were mainly facilitated by the AC, as demonstrated in previous studies using AC electrical stimulation (He et al., 2002; He, 2003a,b; Yu et al., 2004). This facilitation can be achieved by direct excitation from the AC and/or by a release of inhibitory inputs from IC neurons via TRN inhibition on these inhibitory inputs. Through modulating non-adapting neurons in such a way the AC is not only facilitating the responses to the deviant stimulus but also to the standard stimulus. Therefore, we can speculate that the AC can reinforce frequently occurring signals and may contribute to a subcortical repetition enhancement effect, a phenomenon known to occur in humans to complex stimulation (Skoe and Kraus, 2010a,b). In this manner, the incoming stream is constantly being monitored, even when the stimulus is physically invariant and attention is directed elsewhere, creating predictable patterns and expectations (Winkler et al., 2009; Skoe and Kraus, 2010a,b; Skoe et al., 2013, 2014). By contrast, Antunes and Malmierca demonstrated that some high adapting neurons (i.e., CSI > 0.5) from the non-lemniscal MGB received a

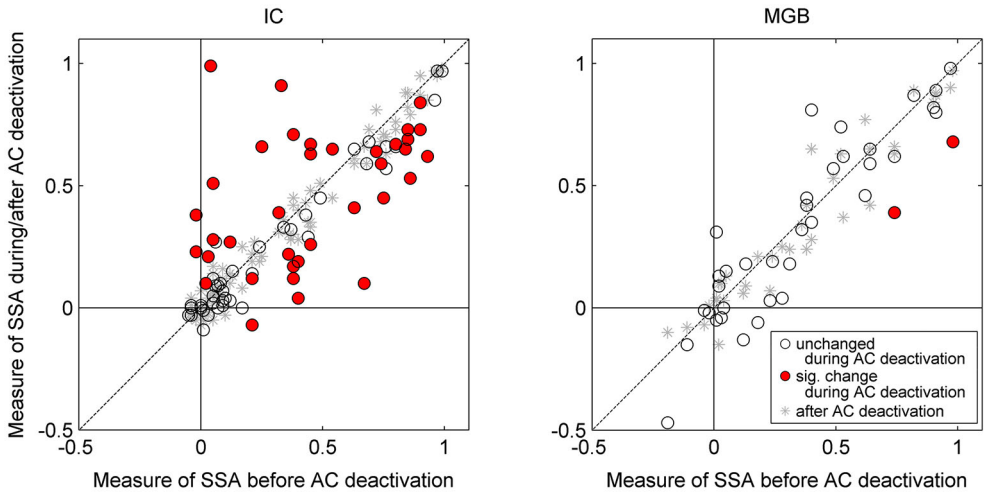

FIGURE 3 | Scatterplots for IC neurons (left panel) and MGB neurons (right panel) of CSI before cooling vs. CSI during cooling (circles) and after cooling (asterisks). Red circles indicate those neurons which show a significant change with cooling, whereas those with open circles indicate a non-significant change. All neurons included in the analyses returned to their previous CSI values after cooling (all asterisks lay along the line of equality for before vs. after cooling condition). Auditory cortical deactivation could have one of three effects on the SSA sensitivity of IC neurons; CSI values either showed no change, or a significant decrease or increase. By contrast, CSI values in the MGB were unchanged during cortical cooling (with the exception of two neurons which showed a significant decrease in SSA). Data plotted from Antunes and Malmierca (2011), and Anderson and Malmierca (2013).

suppressive influence from the corticofugal pathway, presumably resulting from the strong corticofugal inhibitory effects on the non-lemniscal MGB via the TRN (Villa and Abeles, 1990; He, 2003a,b; Yu et al., 2004). Such inhibitory modulation can switch off the non-lemniscal MGB and indeed, it has been suggested as a way to functionally prepare the AC for sole processing of auditory information (Yu et al., 2004), since the non-lemniscal MGB is involved in multisensory integration (Doron et al., 2002).

Antunes and Malmierca (2011) showed that the possible inhibition driven by the corticofugal pathway did not underlie SSA in the MGB neurons, since the neurons maintained SSA during AC deactivation. Hence, if inhibition plays a role in SSA, as has been suggested in previous studies (Eytan et al., 2003; Yu et al., 2009; Richardson et al., 2011; Duque et al., 2014), other pathways should be involved, such as those coming from the IC (Peruzzi et al., 1997), the TRN-MGB connections themselves (Yu et al., 2009), as well as non-AC inputs to the TRN from basal forebrain (Hallanger and Wainer, 1988; Asanuma and Porter, 1990; Bickford et al., 1994), amygdala (Zikopoulos and Barbas, 2012), prefrontal cortex (Zikopoulos and Barbas, 2006), and GABAergic inputs from zona incerta (Cavdar et al., 2006). It may be that in the highly adaptive neurons, the suppressive effect exerted by the corticofugal pathway on the general responses of the neuron helps to increase the contrast between the standard and the deviant, as in the "iceberg effect" (Carandini and Ferster, 2000; Isaacson and Scanziani, 2011; Katzner et al., 2011. **Figure 5** illustrates the "iceberg effect" mediated by GABAergic inhibition in IC neurons). This would help the AC to focus on processing the information encoded in the deviant stimulus, by reducing the responses still evoked by the commonly repeated one. It could be that the AC, together with the TRN, participates in a modulatory mechanism for a balance between excitation and inhibition that, by reducing the firing rate of the neuron, increases the contrast between the standard and the deviant, and therefore increases SSA sensitivity (**Figure 5**). In the same line, the fact that the highly adapting neurons receive less facilitatory influence from the cortex leads to a low discharge rate of these neurons, consequently augmenting the contrast between the standard and the deviant, thus increasing SSA. Indeed, highly adapting neurons in the MGB show lower discharge rates than non-adapting neurons (Antunes et al., 2010).

A subset of neurons had their acoustic responsiveness eliminated with cortical deactivation (four in the MGD, two in the MGV; the other was not histologically localized). These data are in agreement with the drivers and modulators hypothesis proposed by Sherman and Guillery (1998). The main corticofugal projections to the MGB arise from layer VI neurons, whose terminals are mostly small and modulatory (Rouiller and Welker, 1991, 2000; Ojima, 1994; Bajo et al., 1995; Bartlett et al., 2000; Ojima and Rouiller, 2011). In addition, a few pyramidal neurons from layer V with large terminal boutons of the driver type project to the MGD and MGV subdivisions (Rouiller and Welker, 1991, 2000; Ojima, 1994; Bajo et al., 1995; Bartlett et al., 2000; Ojima and Rouiller, 2011). The seven neurons that ceased firing during AC cooling had nonexistent or very low levels of SSA, agreeing with our main result that SSA in the MGB is not inherited from the AC.

THE EFFECT OF THE CORTICOFUGAL PROJECTIONS ON COLLICULAR SSA

As previously mentioned, it has long been known that the IC receives descending projections from the AC, and therefore the

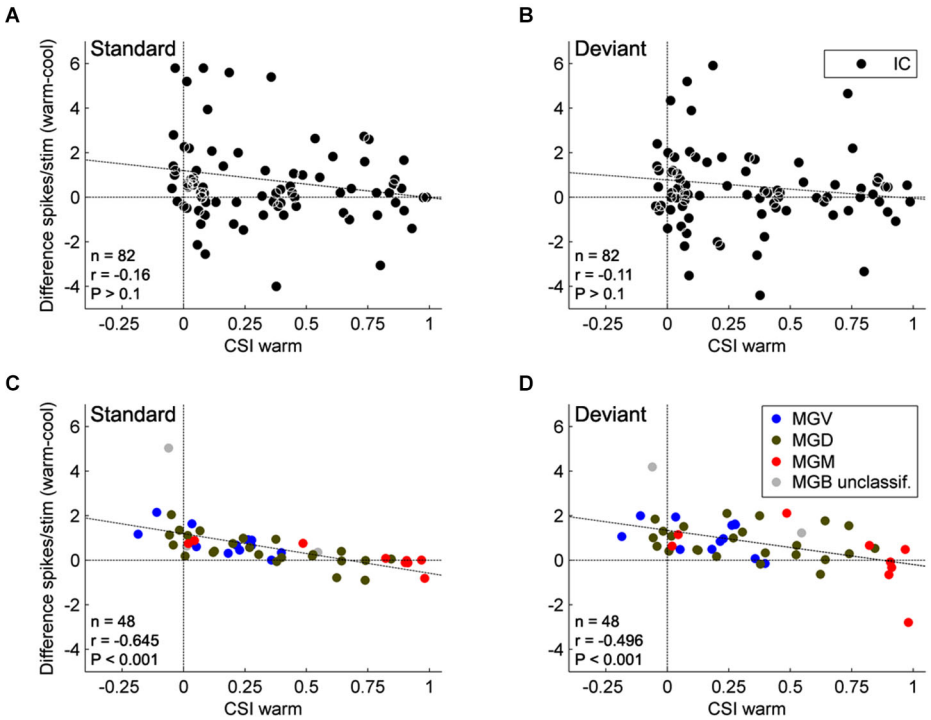

FIGURE 4 | Effect of AC deactivation on the firing rate of IC and MGB neurons. Scatterplots of the CSI (warm condition) vs. the difference in firing rate between the warm and cool conditions (spikes/stimulus difference) in response to standard (**A**, IC; **C**, MGB), and deviant stimuli (**B**, IC; **D**, MGB), for each neuron. Black dots represent neurons in the IC (**A,B**; ***n* = 82**), while blue, green, and red dots represent the neurons that were localized to the ventral ($n = 12$), dorsal ($n = 24$), and medial ($n = 9$) subdivisions of the MGB, respectively (total $n = 45$, neurons that were localized to one of the three MGB subdivisions). Positive values indicate a reduction in firing rate with AC deactivation; and negative values an increment (above and below the horizontal line at the origin, respectively). Note that no correlation is shown for the IC neurons, while MGB neurons show a significant negative correlation. These data suggest that the gain exerted by the AC on MGB neurons depends on the level of SSA that the MGB neurons show. There was no effect of subdivision nor was there an interaction between condition and subdivision ($n = 45$, Two-way repeated measures ANOVA, for the responses to the deviants: $F_{(1,42)} = 21.95$, $P < 0.001$, main effect of condition; $F_{(2,42)} = 2.96$, $P = 0.06$, main effect of subdivision; and $F_{(2,42)} = 0.12$, $P = 0.89$, interaction; Two way repeated measures ANOVA, for the responses to the standards: $F_{(1,42)} = 22.88$, $P < 0.001$, main effect of condition; $F_{(2,42)} = 2.89$, $P = 0.07$, main effect of subdivision; and $F_{(2,42)} = 1.06$, $P = 0.36$, interaction). Data plotted from Antunes and Malmierca (2011), and Anderson and Malmierca (2013).

responses of these IC neurons could be influenced by cortical activity (Saldaña et al., 1996; Winer et al., 1998; Malmierca and Ryugo, 2011). Although the corticocollicular projection terminates more densely on the cortical regions of the IC (Saldaña et al., 1996; Winer et al., 1998), these corticocollicular projections can also target the central nucleus directly, albeit less densely. The corticocollicular projections are excitatory (Feliciano and Potashner, 1995), however, the excitatory and inhibitory intra- and intercollicular projections (Hernandez et al., 2006) may also propagate this cortical feedback throughout the entire IC (Malmierca et al., 2005). Therefore, the corticocollicular projection may result in either an excitatory or inhibitory effect on neurons throughout the entire IC. Indeed, previous studies have demonstrated that many IC properties, even in the central nucleus of the IC, are controlled by the AC (Yan and Suga, 1998; Jen et al., 2001; Jen and Zhou, 2003; Yan et al., 2005; Nakamoto et al., 2008; Markovitz et al., 2013). Moreover, neurons showing SSA in the IC (Malmierca et al., 2009; Duque et al., 2012; Ayala and Malmierca, 2013; Ayala et al., 2013) may be under the modulation of the AC. Thus, we studied the effects of non-focal, reversible deactivation of the ipsilateral AC on the response of IC neurons that showed SSA (Anderson and Malmierca, 2013) using the same cortical cooling technique and experimental parameters as used for the MGB study (Antunes and Malmierca, 2011). As expected, the results demonstrated that the changes in the basic response properties of the IC neurons were widespread and strong in the majority of IC neurons (**Figure 2**). However, changes in SSA sensitivity were less common, with only about half of the neurons recorded showing a significant change in their SSA, while the other half remained unchanged (**Figure 3**). Thus, the effect of AC deactivation on the IC was in agreement with the MGB study (Antunes and Malmierca, 2011, 2014) for approximately half the IC neurons recorded, i.e., cortical deactivation caused a modulation in the discharge rate of MGB neurons which affected responses to both standard and deviant stimuli proportionally. However, the other 50% of IC neurons recorded showed disproportionate changes in the discharge

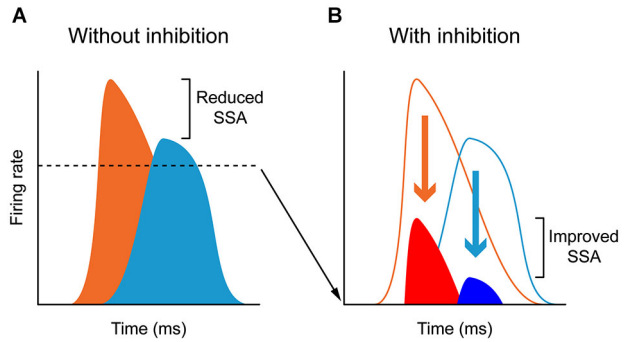

FIGURE 5 | Inhibition and "iceberg effect": In the absence of inhibition **(A)**, neurons respond to deviants (orange) and standards (light blue) with high firing rates and thus the deviant to standard ratio is small. By contrast, $GABA_A$- mediated inhibition reduces the responses to both deviants (red) and standards (dark blue) acting as in the "iceberg effect", thus increasing the deviant to standard ratio and enhancing SSA **(B)**. For more details, see Pérez-González et al. (2012).

rate to either the standard or the deviant stimulus, resulting in significant changes in SSA sensitivity which could either decrease (34% of recorded IC population) or increase (18%) (**Figure 3**).

This change in SSA could indicate the occurrence of a gain control modulation similar to that produced by the action of $GABA_A$ mediated inhibition in the IC (**Figure 5**; Pérez-González et al., 2012), similar to that described in the visual cortex and compatible with the "iceberg effect" (Carandini and Ferster, 2000; Isaacson and Scanziani, 2011). Under normal conditions, the corticocollicular projections may activate intrinsic GABAergic neurons in the IC. AC deactivation will lead to subsequent increase in the activity of those neurons usually under an inhibitory influence, augmenting the ratio between the standard and deviant stimulus. The iceberg effect may potentially contribute to a significant change in SSA in either direction as a simple shift in the neuron's spike output threshold could produce large changes in the ratio of responses to standard or deviant. However, during AC deactivation there were a few instances of dramatic changes in SSA sensitivity (for example see Figure 7 in Anderson and Malmierca (2013)), which suggests that in these cases the AC may take a more active role in response generation rather than merely adjusting the gain of IC responses.

In contrast to the MGB neurons, in the IC there was no relation between the changes imposed by the AC and the SSA exhibited by the neurons (**Figures 4A,B**). This is another important difference between the effect of the AC on the MGB and IC. However, this would not be totally unexpected since the corticofugal projection to the MGB and the IC arises mostly from different neuronal types located in different auditory cortical layers (**Figure 1**; layer V projects to IC, and layer VI to MGB; Bajo et al., 2010; Malmierca and Ryugo, 2011). Single neurons that target both the IC and MGB have not been identified (**Figure 1**; Wong and Kelly, 1981; Coomes and Schofield, 2004; Bajo and King, 2013).

A SYNTHESIS ON THE CORTICAL PROCESSING IN THE MODULATION OF SUBCORTICAL SSA

Our findings taken together demonstrate that the AC and the corticofugal pathway provides a gating or gain-control mechanism (Villa et al., 1991; He, 1997, 2003a,b; Yu et al., 2004) that indirectly modulates SSA and its dynamics in the MGB and IC neurons, rather than directly creating and transmitting this property to these auditory thalamic and midbrain nuclei. Previous studies of the auditory system support the hypothesis that SSA can be generated and driven in a bottom-up fashion, and then enhanced and modulated at the cortical level. For example, ascending sensory information is processed in parallel within the auditory system, with information from the thalamus arriving simultaneously and independently to multiple cortical areas (Imaizumi et al., 2004; Lee and Winer, 2008; Carrasco and Lomber, 2009a,b). This ascending information is then modulated by intracortical connections (Carrasco and Lomber, 2009a,b), as well as by cortico-thalamo-cortical loop projections (Bajo et al., 1995; Winer et al., 1999; Llano and Sherman, 2008). Such cortico-thalamo-cortical projections, also demonstrated in the somatosensory system (Theyel et al., 2010), are particularly interesting since they allow interconnections between the lemniscal and the non-lemniscal auditory nuclei (Bajo et al., 1995; Winer et al., 1999; Llano and Sherman, 2008). Moreover, there may even be the opportunity for intracortical interactions between the non-lemniscal and lemniscal AC fields, or indeed from the non-lemnical subcortical nuclei to the lemniscal AC. A recent study has demonstrated a bidirectional information flow from the non-lemniscal AC to the lemniscal AC (Carrasco and Lomber, 2010), therefore, the fact that A1 is the first lemniscal station in which SSA is widespread and strong (Ulanovsky et al., 2003) may result from this cortico-thalamo-cortical route, followed by a unidirectional flow of information from the secondary to the A1 (Carrasco and Lomber, 2009a,b). The thalamo-cortical projection from the medial subdivision of the MGB (MGM) to A1 is also a candidate causing an enhancement of SSA in A1 (Malmierca et al., 2002; Kimura et al., 2003; Anderson et al., 2006).

The feedback driven modulation of the subcortical nuclei that includes the MGB and IC would likely influence the transfer of ascending input to the AC (Villa et al., 1991; Luo et al., 2008), as well as the corticocortical processing itself, as demonstrated in other sensory systems (Sillito et al., 2006; Theyel et al., 2010). Recent studies suggest that the corticofugal system can participate in a gain control process that leads to improved coding of salient stimuli, and possibly underlies auditory attention (He, 2003a,b) and learning-induced plasticity mechanisms (Bajo et al., 2010; Skoe et al., 2013). Conversely, the increased coupling of cortical and thalamic activity may amplify the effectiveness of a particular feature of the external sensory input, allowing its detection and binding to higher cognitive processing (Villa et al., 1999). Our results are consistent with the role of the corticofugal pathway in scaling the sensitivity of MGB and IC neurons to its driving inputs by controlling their gain. SSA would therefore be generated in a bottom-up fashion, as a pre-attentive gating involved in reducing sensory input to behaviorally relevant aspects.

The differential influence of the descending cortical projection on SSA in IC and MGB may reflect a method of statistical refinement in the process of bottom-up transmission based on the suggestion that there is a redundancy reduction throughout successive levels (Schwartz and Simoncelli, 2001; Chechik et al., 2006). For example, previous measurements of information content and stimulus-induced redundancy from neurons in the IC, MGB and primary AC in response to natural stimuli, suggest stimulus identity was reduced in the AC and MGB neurons compared to those in IC (Chechik et al., 2006). Thus, redundancy reduction may be a generic organizing principle of neural systems, and a potential role for the descending cortical projection would be to make gross changes at the lowest possible level of the pathway. Therefore, if SSA to frequency deviants is generated in the IC (and/or below) the greatest AC modulation will be at this lowest level, and then as SSA is propagated up the auditory pathway (MGB) it would only require minor modifications. Since the rat IC contains about 350,000 neurons while MGB only 65,000 (i.e., less than 20% of the total of IC neurons; Kulesza et al., 2002) individual neurons in the MGB will be integrating over more inputs than individual IC neurons, and hence, the role of the MGB neurons may be to combine the adaptive properties received across a range of inputs, rather than generate SSA de-novo which would subsequently require greater cortical intervention.

STIMULUS-SPECIFIC ADAPTATION, MISMATCH NEGATIVITY AND PREDICTIVE CODING: THE INTERACTION BETWEEN BOTTOM-UP AND TOP-DOWN PROCESSING

The mismatch negativity (MMN) is an evoked scalp potential elicited by rare events embedded in a series of frequently repeating events (Näätänen et al., 1978). Since SSA is a decrease, or even a total cessation, in the response of a single neuron to a repeated stimulus, which recovers on the presentation of another, new stimulus (Ulanovsky et al., 2003), it resembles in many aspects the phenomenon of MMN, and it has been proposed to be a precursor to the generation of deviance detection (Nelken and Ulanovsky, 2007; Malmierca et al., 2014).

In MMN paradigms, short term predictive representations of environmental regularities are thought to be formed based on the observed likelihood of frequently repeating events (standard). Implicitly learned statistical regularities serve as a basis to automatically detect rare events (deviant) which do not match predictions. Recent modeling studies (Lieder et al., 2013) suggested that the MMN reflects approximate Bayesian learning of sensory regularities, and that the MMN-generating process adjusts a probabilistic model of the environment according to mismatch responses (prediction errors). Thus, the *MMN response is now widely considered as a perceptual prediction error signal* (Friston, 2005; Garrido et al., 2008, 2009; den Ouden et al., 2012), which can be considered a member of a family of prediction errors, which include perceptual, higher cognitive, and motivational prediction errors (**Figure 6**).

The MMN response is widely considered as a perceptual prediction error signal (Friston, 2005; Winkler, 2007; Garrido et al., 2008, 2009; den Ouden et al., 2012; Winkler et al., 2012; Fishman, 2014) that results from the comparison between the actual sensory input and a memory trace so-called prediction encoded in top-down activity (Rao and Ballard, 1999; Yuille and Kersten, 2006). A prediction error would arise when there is a mismatch between the predicted and the actual sensory input (**Figure 6**). According to the hierarchical predictive coding framework, veridical prediction is supported by neural processes

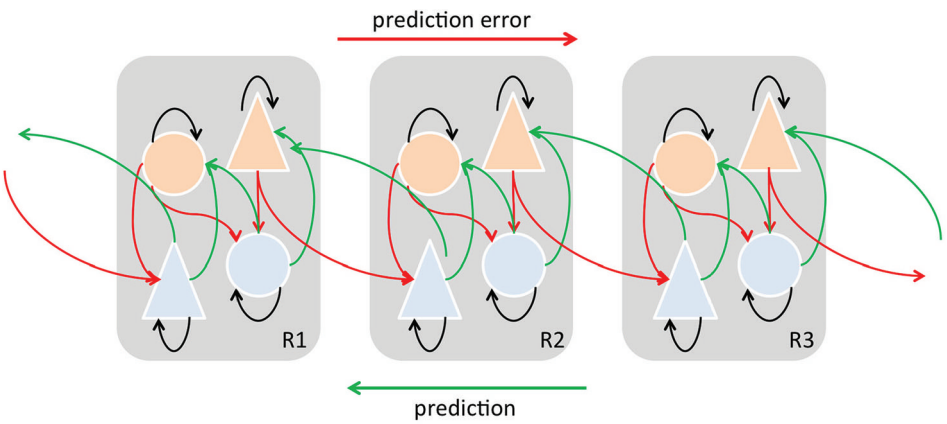

FIGURE 6 | Simplified schematic diagram detailing the neuronal architectures that might encode a density on the states of a hierarchical dynamic model of predictive coding by Friston (2005, 2009). State units are in light blue and error-units in orange. This shows the speculative cells of origin of forward driving connections that convey prediction error from a lower area to a higher area and the backward connections that construct predictions. These predictions try to explain prediction error in lower levels. In this scheme, the sources of forward and backward connections are superficial and deep pyramidal cells, respectively. In the original model by Friston (2005, 2009) subcortical regions may contribute to the model as well. "Predictions" and "prediction errors" are sent and received from each level in the hierarchy. Feed-forward signals conveying prediction errors originate in superficial layers and terminate in deep (infragranular) layers of their targets, are mediated by GABA and fast AMPA receptor kinetics and associated with gamma-band oscillations. On the other hand, feedback signals conveying predictions originate in deep layers and project to superficial layers, are mediated by slow NMDA receptor kinetics and associated with beta-band oscillations Adapted and modified from Friston (2005, 2009), Seth et al. (2012).

optimizing probabilistic representations of the causes of sensory inputs (**Figure 6**; Friston, 2010). SSA as an adaptation process may in its own way improve the neural coding efficiency by reducing the response to potentially redundant information (in a similar manner to redundancy reduction as suggested by Chechik et al., 2006). Moreover, as we have reviewed previously, there are plenty of opportunities for a continuous interaction between the top-down flow of predictions and bottom-up flow of prediction errors to enable a continual updating and optimizing of the internal sensory representation. We do not currently know the detailed organization of the inputs received by those subcortical neurons showing significant SSA, but the fact that auditory cortical inputs project more densely to those areas populated by neurons showing SSA, especially in the IC (but also in the MGB), suggests neurons showing SSA may be key players in the integration of descending information with the incoming information from lower areas. Thus, when a prediction error occurs the lower areas would return the ensuing prediction error by means of forward connections and the corticofugal projections would drive the neuronal activity along different neuronal stages to adjust and update the sensory representation (Winkler et al., 2009). The top-down adjustment would be through direct or indirect inputs which in turn would project back to higher auditory centers (**Figure 6**). Also, it is important to highlight that the sensory representation requires fast *on-line* adjustments on the neuronal activity. In agreement with this, the corticofugal modulation on IC neurons has been demonstrated to exert short-term plastic reorganization in the frequency domain (i.e, Suga and Ma, 2003) and on SSA responses (Anderson and Malmierca, 2013). For example, as previously demonstrated, the cortical cells projecting to the IC arise mainly from pyramidal neurons in layer V (Games and Winer, 1988; Winer and Prieto, 2001; Doucet et al., 2003; Malmierca and Ryugo, 2011) and use glutamate as neurotransmitter (Feliciano and Potashner, 1995). Since predictive coding is based on NMDA-dependent synaptic plasticity and its regulation by other neuromodulators (Friston, 2005), future pharmacological studies will undoubtedly help to disentangle which role synaptic plasticity plays that may underlie the neurobiological mechanisms of MMN as well as the SSA responses.

CONCLUDING REMARKS

In summary, here we have reviewed the neuronal and anatomical basis that may underlie SSA, MMN and predictive coding. The corticofugal projections arising from the AC may be much more important than previously estimated since they may play a key role linking these fields to the concept of mental models (Craik, 1943; Bendixen et al., 2012), allowing us to foresee the consequences of a given action and enabling us to prepare for future events, such as the rain that is to be expected, or the bad mood of our partner or boss. Thus, consciously or unconsciously we can then take appropriate action to prevent undesirable and unpleasant consequences, e.g., getting wet by the rain, or even change the future, e.g., to take proactive action to ensure the bad mood of our partner or supervisor will not occur. These examples illustrate that behavior is optimized when we can predict the dimensions of a stimulus (Kotz et al., 2014). This is the basis of the huge flexibility underlying our interactions with our physical and social environment.

ACKNOWLEDGMENTS

Financial support was provided by the Spanish MINECO (BFU2013-43608-P) and JCYL (SA343U14) to MSM.

REFERENCES

Abbott, L. F., Varela, J. A., Sen, K., and Nelson, S. B. (1997). Synaptic depression and cortical gain control. *Science* 275, 220–224. doi: 10.1126/science.275.5297.221

Anderson, L. A., Christianson, G. B., and Linden, J. F. (2009). Stimulus-specific adaptation occurs in the auditory thalamus. *J. Neurosci.* 29, 7359–7363. doi: 10.1523/JNEUROSCI.0793-09.2009

Anderson, L. A., and Malmierca, M. S. (2013). The effect of auditory cortex deactivation on stimulus-specific adaptation in the inferior colliculus of the rat. *Eur. J. Neurosci.* 37, 52–62. doi: 10.1111/ejn.12018

Anderson, L. A., Malmierca, M. S., Wallace, M. N., and Palmer, A. R. (2006). Evidence for a direct, short latency projection from the dorsal cochlear nucleus to the auditory thalamus in the guinea pig. *Eur. J. Neurosci.* 24, 491–498. doi: 10.1111/j.1460-9568.2006.04930.x

Antunes, F. M., and Malmierca, M. S. (2011). Effect of auditory cortex deactivation on stimulus-specific adaptation in the medial geniculate body. *J. Neurosci.* 31, 17306–17316. doi: 10.1523/JNEUROSCI.1915-11.2011

Antunes, F. M., and Malmierca, M. S. (2014). An overview of stimulus-specific adaptation in the auditory thalamus. *Brain Topogr.* 27, 480–499. doi: 10.1007/s10548-013-0342-6

Antunes, F. M., Nelken, I., Covey, E., and Malmierca, M. S. (2010). Stimulus-specific adaptation in the auditory thalamus of the anesthetized rat. *PLoS One* 5:e14071. doi: 10.1371/journal.pone.0014071

Asanuma, C., and Porter, L. L. (1990). Light and electron microscopic evidence for a GABAergic projection from the caudal basal forebrain to the thalamic reticular nucleus in rats. *J. Comp. Neurol.* 302, 159–172. doi: 10.1002/cne.903020112

Ayala, Y. A., and Malmierca, M. S. (2013). Stimulus-specific adaptation and deviance detection in the inferior colliculus. *Front. Neural Circuits* 6:89. doi: 10.3389/fncir.2012.00089

Ayala, Y. A., Pérez-González, D., Duque, D., Nelken, I., and Malmierca, M. S. (2013). Frequency discrimination and stimulus deviance in the inferior colliculus and cochlear nucleus. *Front. Neural Circuits* 6:119. doi: 10.3389/fncir.2012.00119

Bajo, V. M., and King, A. J. (2013). Cortical modulation of auditory processing in the midbrain. *Front. Neural Circuits* 6:114. doi: 10.3389/fncir.2012.00114

Bajo, V. M., and Moore, D. R. (2005). Descending projections from the auditory cortex to the inferior colliculus in the gerbil, Meriones unguiculatus. *J. Comp. Neurol.* 486, 101–116. doi: 10.1002/cne.20542

Bajo, V. M., Nodal, F. R., Bizley, J. K., Moore, D. R., and King, A. J. (2007). The ferret auditory cortex: descending projections to the inferior colliculus. *Cereb. Cortex* 17, 475–491. doi: 10.1093/cercor/bhj164

Bajo, V. M., Nodal, F. R., Moore, D. R., and King, A. J. (2010). The descending corticocollicular pathway mediates learning-induced auditory plasticity. *Nat. Neurosci.* 13, 253–260. doi: 10.1038/nn.2466

Bajo, V. M., Rouiller, E. M., Welker, E., Clarke, S., Villa, A. E., de Ribaupierre, Y., et al. (1995). Morphology and spatial distribution of corticothalamic terminals originating from the cat auditory cortex. *Hear. Res.* 83, 161–174. doi: 10.1016/0378-5955(94)00199-z

Baldeweg, T. (2006). Repetition effects to sounds: evidence for predictive coding in the auditory system. *Trends Cogn. Sci.* 10, 93–94. doi: 10.1016/j.tics.2006.01.010

Bar, M. (2007). The proactive brain: using analogies and associations to generate predictions. *Trends Cogn. Sci.* 11, 280–289. doi: 10.1016/j.tics.2007.05.005

Bartlett, E. L., Stark, J. M., Guillery, R. W., and Smith, P. H. (2000). Comparison of the fine structure of cortical and collicular terminals in the rat medial geniculate body. *Neuroscience* 100, 811–828. doi: 10.1016/s0306-4522(00)00340-7

Bendixen, A., Schröger, E., Ritter, W., and Winkler, I. (2012). Regularity extraction from non-adjacent sounds. *Front. Psychol.* 3:143. doi: 10.3389/fpsyg.2012.00143

Bickford, M. E., Günlük, A. E., Van Horn, S. C., and Sherman, S. M. (1994). GABAergic projection from the basal forebrain to the visual sector of the thalamic reticular nucleus in the cat. *J. Comp. Neurol.* 348, 481–510. doi: 10.1002/cne.903480402

Brosch, M., and Schreiner, C. E. (1997). Timecourseof forward masking tuning curves in cat primary auditory cortex. *J. Neurophysiol.* 77, 923–943.

Calford, M. B., and Semple, M. N. (1995). Monaural inhibition in cat auditorycortex. *J. Neurophysiol.* 73, 1876–1891.

Carandini, M., and Ferster, D. (2000). Membrane potential and firing rate in cat primary visual cortex. *J. Neurosci.* 20, 470–484.

Carrasco, A., and Lomber, S. G. (2009a). Differential modulatory influences between primary auditory cortex and the anterior auditory field. *J. Neurosci.* 29, 8350–8362. doi: 10.1523/JNEUROSCI.6001-08.2009

Carrasco, A., and Lomber, S. G. (2009b). Evidence for hierarchical processing in cat auditory cortex: nonreciprocal influence of primary auditory cortex on the posterior auditory field. *J. Neurosci.* 29, 14323–14333. doi: 10.1523/JNEUROSCI.2905-09.2009

Carrasco, A., and Lomber, S. G. (2010). Reciprocal modulatory influences between tonotopic and non-tonotopic cortical fields in the cat. *J. Neurosci.* 30, 1476–1487. doi: 10.1523/JNEUROSCI.5708-09.2009

Cavdar, S., Ona, T. F., Cakmak, Y. O., Saka, E., Yananli, H. R., and Aker, R. (2006). Connections of the zona incerta to the reticular nucleus of the thalamus in the rat. *J. Anat.* 209, 251–258. doi: 10.1111/j.1469-7580.2006.00600.x

Chechik, G., Anderson, M. J., Bar-Yosef, O., Young, E. D., Tishby, N., and Nelken, I. (2006). Reduction of information redundancy in the ascending auditory pathway. *Neuron* 51, 359–368. doi: 10.1016/j.neuron.2006.06.030

Coomber, B., Edwards, D., Jones, S., Shackleton, T., Goldschmidt, J. R., Wallace, M., et al. (2011). Cortical inactivation by cooling in small animals. *Front. Syst. Neurosci.* 5:53. doi: 10.3389/fnsys.2011.00053

Coomes, D. L., and Schofield, B. R. (2004). Projections from the auditory cortex to the superior olivary complex in guinea pigs. *Eur. J. Neurosci.* 19, 2188–2200. doi: 10.1111/j.0953-816x.2004.03317.x

Craik, K. J. W. (1943). *The Nature of Explanation.* Cambridge Eng: University Press.

den Ouden, H. E. M., Kok, P., and de Lange, F. P. (2012). How prediction errors shape perception, attention and motivation. *Front. Psychol.* 3:548. doi: 10.3389/fpsyg.2012.00548

Diliberto, K. A., Altarriba, J., and Neill, W. T. (2000). Novel popout and familiar popout in a brightness discrimination task. *Percept. Psychophys.* 62, 1494–1500. doi: 10.3758/bf03212149

Doron, N. N., Ledoux, J. E., and Semple, M. N. (2002). Redefining the tonotopic core of rat auditory cortex: physiological evidence for a posterior field. *J. Comp. Neurol.* 453, 345–360. doi: 10.1002/cne.10412

Doucet, J. R., Molavi, D. L., and Ryugo, D. K. (2003). The source of corticocollicular and corticobulbar projections in area Te1 of the rat. *Exp. Brain Res.* 153, 461–466. doi: 10.1007/s00221-003-1604-4

Dragoi, V., Sharma, J., and Sur, M. (2000). Adaptation-induced plasticity of orientation tuning in adult visual cortex. *Neuron* 28, 287–298. doi: 10.1016/s0896-6273(00)00103-3

Duque, D., Malmierca, M. S., and Caspary, D. M. (2014). Modulation of stimulus-specific adaptation by GABAA receptor activation or blockade in the medial geniculate body of the anesthetized rat. *J. Physiol.* 592, 729–743. doi: 10.1113/jphysiol.2013.261941

Duque, D., Pérez-González, D., Ayala, Y. A., Palmer, A. R., and Malmierca, M. S. (2012). Topographic distribution, frequency and intensity dependence of stimulus-specific adaptation in the inferior colliculus of the rat. *J. Neurosci.* 32, 17762–17774. doi: 10.1523/JNEUROSCI.3190-12.2012

Escera, C., and Malmierca, M. S. (2014). The auditory novelty system: an attempt to integrate human and animal research. *Psychophysiology* 51, 111–123. doi: 10.1111/psyp.12156

Eytan, D., Brenner, N., and Marom, S. (2003). Selective adaptation in networks of cortical neurons. *J. Neurosci.* 23, 9349–9356.

Faye-Lund, H. (1985). The neocortical projection to the inferior colliculus in the albino rat. *Anat. Embryol. (Berl)* 173, 53–70. doi: 10.1007/bf00707304

Feliciano, M., and Potashner, S. J. (1995). Evidence for a glutamatergic pathway from the guinea pig auditory cortex to the inferior colliculus. *J. Neurochem.* 65, 1348–1357. doi: 10.1046/j.1471-4159.1995.65031348.x

Fishman, Y. I. (2014). The mechanisms and meaning of the mismatch negativity. *Brain Topogr.* 27, 500–526. doi: 10.1007/s10548-013-0337-3

Friston, K. (2005). A theory of cortical responses. *Philos. Trans. R. Soc. Lond. B Biol. Sci.* 360, 815–836. doi: 10.1098/rstb.2005.1622

Friston, K. (2009). The free-energy principle: a rough guide to the brain? *Trends Cogn. Sci.* 13, 293–301. doi: 10.1016/j.tics.2009.04.005

Friston, K. (2010). The free-energy principle: a unified brain theory? *Nat. Rev. Neurosci.* 11, 127–138. doi: 10.1038/nrn2787

Furukawa, S., Maki, K., Kashino, M., and Riquimaroux, H. (2005). Dependency of the interaural phase difference sensitivities of inferior collic-ular neurons on a preceding tone and its implications in neural population coding. *J. Neurophysiol.* 93, 3313–3326. doi: 10.1152/jn.01219.2004

Games, K. D., and Winer, J. A. (1988). Layer V in rat auditory cortex: projections to the inferior colliculus and contralateral cortex. *Hear. Res.* 34, 1–25. doi: 10.1016/0378-5955(88)90047-0

Garrido, M., Friston, K., Kiebel, S., Stephan, K., Baldeweg, T., and Kilner, J. M. (2008). The functional anatomy of the MMN: a DCM study of the roving paradigm. *Neuroimage* 42, 936–944. doi: 10.1016/j.neuroimage.2008.05.018

Garrido, M., Kilner, J., Stephan, K., and Friston, K. (2009). The mismatch negativity: a review of underlying mechanisms. *Clin. Neurophysiol.* 120, 453–463. doi: 10.1016/j.clinph.2008.11.029

Ghosh, S., Murray, G. M., Turman, A. B., and Rowe, M. J. (1994). Corticothalamic influences on transmission of tactile information in the ventroposterolateral thalamus of the cat: effect of reversible inactivation of somatosensory cortical areas I and II. *Exp. Brain Res.* 100, 276–286. doi: 10.1007/bf00227197

Gutfreund, Y. (2012). Stimulus-specific adaptation, habituation and change detection in the gaze control system. *Biol. Cybern.* 106, 657–668. doi: 10.1007/s00422-012-0497-3

Gutfreund, Y., and Knudsen, E. I. (2006). Adaptation in the auditory space map of the barn owl. *J. Neurophysiol.* 96, 813–825. doi: 10.1152/jn.01144.2005

Hallanger, A. E., and Wainer, B. H. (1988). Ultrastructure of ChAT-immunoreactive synaptic terminals in the thalamic reticular nucleus of the rat. *J. Comp. Neurol.* 278, 486–497. doi: 10.1002/cne.902780403

He, J. (1997). Modulatory effects of regional cortical activation on the onset responses of the cat medial geniculate neurons. *J. Neurophysiol.* 77, 896–908.

He, J. (2003a). Corticofugal modulation of the auditory thalamus. *Exp. Brain Res.* 153, 579–590. doi: 10.1007/s00221-003-1680-5

He, J. (2003b). Corticofugal modulation on both ON and OFF responses in the nonlemniscal auditory thalamus of the guinea pig. *J. Neurophysiol.* 89, 367–381. doi: 10.1152/jn.00593.2002

He, J., Yu, Y. Q., Xiong, Y., Hashikawa, T., and Chan, Y. S. (2002). Modulatory effect of cortical activation on the lemniscal auditory thalamus of the Guinea pig. *J. Neurophysiol.* 88, 1040–1050.

Hefti, B. J., and Smith, P. H. (2000). Anatomy, physiology and synaptic responses of rat layer V auditory cortical cells and effects of intracellular GABA(A) blockade. *J. Neurophysiol.* 83, 2626–2638.

Held, H. (1893). Die centralem Bahnen des nervus acusticus bei der Katz. *Arch. Anat. Abtheil.* 15, 190–271.

Herbert, H., Aschoff, A., and Ostwald, J. (1991). Topography of projections from the auditory cortex to the inferior colliculus in the rat. *J. Comp. Neurol.* 304, 103–122. doi: 10.1002/cne.903040108

Hernandez, O., Rees, A., and Malmierca, M. S. (2006). A GABAergic component in the commissure of the inferior colliculus in rat. *Neuroreport* 17, 1611–1614. doi: 10.1097/01.wnr.0000236857.70715.be

Hershenhoren, I., Taaseh, N., Antunes, F. M., and Nelken, I. (2014). Intracellular correlates of stimulus-specific adaptation. *J. Neurosci.* 34, 3303–3319. doi: 10.1523/JNEUROSCI.2166-13.2014

Imaizumi, K., Priebe, N. J., Crum, P. A., Bedenbaugh, P. H., Cheung, S. W., and Schreiner, C. E. (2004). Modular functional organization of cat anterior auditory field. *J. Neurophysiol.* 92, 444–457. doi: 10.1152/jn.01173.2003

Ingham, N. J., and McAlpine, D. (2004). Spike-frequency adaptation in the inferior colliculus. *J. Neurophysiol.* 91, 632–645. doi: 10.1152/jn.00779.2003

Isaacson, J. S., and Scanziani, M. (2011). How inhibition shapes cortical activity. *Neuron* 72, 231–243. doi: 10.1016/j.neuron.2011.09.027

Jen, P. H., Sun, X., and Chen, Q. C. (2001). An electrophysiological study of neural pathways for corticofugally inhibited neurons in the central nucleus of the inferior colliculus of the big brown bat, Eptesicus fuscus. *Exp. Brain Res.* 137, 292–302. doi: 10.1007/s002210000637

Jen, P. H., and Zhou, X. (2003). Corticofugal modulation of amplitude domain processing in the midbrain of the big brown bat, Eptesicus fuscus. *Hear. Res.* 184, 91–106. doi: 10.1016/s0378-5955(03)00237-5

Katz, Y., Heiss, J. E., and Lampl, I. (2006). Cross-whisker adaptation of neurons in the rat barrel cortex. *J. Neurosci.* 26, 13363–13372. doi: 10.1523/jneurosci.4056-06.2006

Katzner, S., Busse, L., and Carandini, M. (2011). GABAa inhibition controls response gain in visual cortex. *J. Neurosci.* 31, 5931–5941. doi: 10.1523/JNEUROSCI.5753-10.2011

Kaya, E. M., and Elhilali, M. (2014). Investigating bottom-up auditory attention. *Front. Hum. Neurosci.* 8:327. doi: 10.3389/fnhum.2014.00327

Kimura, A., Donishi, T., Okamoto, K., Imbe, H., and Tamai, Y. (2007). Efferent connections of the ventral auditory area in the rat cortex: implications for auditory processing related to emotion. *Eur. J. Neurosci.* 25, 2819–2834. doi: 10.1111/j.1460-9568.2007.05519.x

Kimura, A., Donishi, T., Okamoto, K., and Tamai, Y. (2005). Topography of projections from the primary and non-primary auditory cortical areas to the medial geniculate body and thalamic reticular nucleus in the rat. *Neuroscience* 135, 1325–1342. doi: 10.1016/j.neuroscience.2005.06.089

Kimura, A., Donishi, T., Sakoda, T., Hazama, M., and Tamai, Y. (2003). Auditory thalamic nuclei projections to the temporal cortex in the rat. *Neuroscience* 117, 1003–1016. doi: 10.1016/s0306-4522(02)00949-1

King, C., McGee, T., Rubel, E. W., Nicol, T., and Kraus, N. (1995). Acoustic features and acoustic changes are represented by different central pathways. *Hear. Res.* 85, 45–52. doi: 10.1016/0378-5955(95)00028-3

Kotz, S. A., Stockert, A., and Schwartze, M. (2014). Cerebellum, temporal predictability and the updating of a mental model. *Philos. Trans. R. Soc. Lond. B Biol. Sci.* 369:20130403. doi: 10.1098/rstb.2013.0403

Kraus, N., McGee, T., Littman, T., Nicol, T., and King, C. (1994). Nonprimary auditory thalamic representation of acoustic change. *J. Neurophysiol.* 72, 1270–1277.

Kulesza, R. J., Viñuela, A., Saldaña, E., and Berrebi, A. S. (2002). Unbiased stereological estimates of neuron number in subcortical auditory nuclei of the rat. *Hear. Res.* 168, 12–24. doi: 10.1016/s0378-5955(02)00374-x

Lee, C. C., and Winer, J. A. (2008). Connections of cat auditory cortex: I. Thalamocortical system. *J. Comp. Neurol.* 507, 1879–1900. doi: 10.1002/cne.21611

Lieder, F., Stephan, K. E., Daunizeau, J., Garrido, M. I., and Friston, K. J. (2013). A neurocomputational model of the mismatch negativity. *PLoS Comput. Biol.* 9:e1003288. doi: 10.1371/journal.pcbi.1003288

Liu, X., Yan, Y., Wang, Y., and Yan, J. (2010). Corticofugal modulation of initial neural processing of sound information from the ipsilateral ear in the mouse. *PLoS One* 5:e14038. doi: 10.1371/journal.pone.0014038

Llano, D. A., and Sherman, S. M. (2008). Evidence for nonreciprocal organization of the mouse auditory thalamocortical-corticothalamic projection systems. *J. Comp. Neurol.* 507, 1209–1227. doi: 10.1002/cne.21602

Lomber, S. G. (1999). The advantages and limitations of permanent or reversible deactivation techniques in the assessment of neural function. *J. Neurosci. Methods* 86, 109–117. doi: 10.1016/s0165-0270(98)00160-5

Lomber, S. G., and Malhotra, S. (2008). Double dissociation of 'what' and 'where' processing in auditory cortex. *Nat. Neurosci.* 11, 609–616. doi: 10.1038/nn.2108

Lomber, S. G., Malhotra, S., and Hall, A. J. (2007). Functional specialization in non-primary auditory cortex of the cat: areal and laminar contributions to sound localization. *Hear. Res.* 229, 31–45. doi: 10.1016/j.heares.2007.01.013

Lomber, S. G., Payne, B. R., and Horel, J. A. (1999). The cryoloop: an adaptable reversible cooling deactivation method for behavioural or electrophysiological assessment of neural function. *J. Neurosci. Methods* 86, 179–194. doi: 10.1016/s0165-0270(98)00165-4

Luo, F., Wang, Q., Kashani, A., and Yan, J. (2008). Corticofugal modulation of initial sound processing in the brain. *J. Neurosci.* 28, 11615–11621. doi: 10.1523/JNEUROSCI.3972-08.2008

Malmierca, M. S. (2015). "Auditory system," in *The Rat Nervous System*, 4th Edn. ed G. Paxinos (Amsterdam: Academic Press).

Malmierca, M. S., Cristaudo, S., Pérez-González, D., and Covey, E. (2009). Stimulus-specific adaptation in the inferior colliculus of the anesthetized rat. *J. Neurosci.* 29, 5483–5493. doi: 10.1523/JNEUROSCI.4153-08.2009

Malmierca, M. S., Hernández, O., and Rees, A. (2005). Intercollicular commissural projections modulate neuronal responses in the inferior colliculus. *Eur. J. Neurosci.* 21, 2701–2710. doi: 10.1111/j.1460-9568.2005.04103.x

Malmierca, M. S., Merchán, M. A., Henkel, C. K., and Oliver, D. L. (2002). Direct projections from cochlear nuclear complex to auditory thalamus in the rat. *J. Neurosci.* 22, 10891–10897.

Malmierca, M. S., and Ryugo, D. K. (2011). "Descending connections of auditory cortex to the midbrain and brainstem," in *The Auditory Cortex*, eds J. A. Winer and C. E. Schreiner (New York, NY: Springer), 189–208.

Malmierca, M. S., Sanchez-Vives, M. V., Escera, C., and Bendixen, A. (2014). Neuronal adaptation, novelty detection and regularity encoding in audition. *Front. Syst. Neurosci.* 8:111. doi: 10.3389/fnsys.2014.00111

Markovitz, C. D., Tang, T. T., and Lim, H. H. (2013). Tonotopic and localized pathways from primary auditory cortex to the central nucleus of the inferior colliculus. *Front. Neural Circuits* 7:77. doi: 10.3389/fncir.2013.00077

Mitani, A., Shimokouchi, M., and Nomura, S. (1983). Effects of stimulation of the primary auditory cortex upon colliculogeniculate neurons in the inferior colliculus of the cat. *Neurosci. Lett.* 42, 185–189. doi: 10.1016/0304-3940(83)90404-4

Näätänen, R., Gaillard, A. W., and Mäntysalo, S. (1978). Early selective-attention effect on evoked potential reinterpreted. *Acta Psychol. (Amst)* 42, 313–329. doi: 10.1016/0001-6918(78)90006-9

Nakamoto, K. T., Jones, S. J., and Palmer, A. R. (2008). Descending projections from auditory cortex modulate sensitivity in the midbrain to cues for spatial position. *J. Neurophysiol.* 99, 2347–2356. doi: 10.1152/jn.01326.2007

Nakamoto, K. T., Mellott, J. G., Killius, J., Storey-Workley, M. E., Sowick, C. S., and Schofield, B. R. (2013a). Ultrastructural examination of the corticocollicular pathway in the guinea pig: a study using electron microscopy, neural tracers and GABA immunocytochemistry. *Front. Neuroanat.* 7:13. doi: 10.3389/fnana.2013.00013

Nakamoto, K. T., Mellott, J. G., Killius, J., Storey-Workley, M. E., Sowick, C. S., and Schofield, B. R. (2013b). Analysis of excitatory synapses in the guinea pig inferior colliculus: a study using electron microscopy and GABA immunocytochemistry. *Neuroscience* 237, 170–183. doi: 10.1016/j.neuroscience.2013.01.061

Nakamoto, K. T., Shackleton, T. M., and Palmer, A. R. (2010). Responses in the inferior colliculus of the guinea pig to concurrent harmonic series and the effect of inactivation of descending controls. *J. Neurophysiol.* 103, 2050–2061. doi: 10.1152/jn.00451.2009

Nelken, I. (2004). Processing of complex stimuli and natural scenes in the auditory cortex. *Curr. Opin. Neurobiol.* 14, 474–480. doi: 10.1016/j.conb.2004.06.005

Nelken, I. (2014). Stimulus-specific adaptation and deviance detection in the auditory system: experiments and models. *Biol. Cybern.* 108, 655–663. doi: 10.1007/s00422-014-0585-7

Nelken, I., and Ulanovsky, N. (2007). Mismatch negativity and stimulus-specific adaptation in animal models. *J. Psychophysiol.* 21, 214–223. doi: 10.1027/0269-8803.21.34.214

Ojima, H. (1994). Terminal morphology and distribution of corticothalamic fibers originating from layers 5 and 6 of cat primary auditory cortex. *Cereb. Cortex* 4, 646–663. doi: 10.1093/cercor/4.6.646

Ojima, H., and Rouiller, E. M. (2011). "Auditory cortical projections to the medial geniculate body," in *The Auditory Cortex*, eds J. A. Winer and C. E. Schreiner (New York: Springer), 171–188.

Palmer, A. R., Hall, D. A., Sumner, C., Barrett, D. J., Jones, S., Nakamoto, K., et al. (2007). Some investigations into non-passive listening. *Hear. Res.* 229, 148–157. doi: 10.1016/j.heares.2006.12.007

Patel, C. R., Redhead, C., Cervi, A. L., and Zhang, H. (2012). Neural sensitivity to novel sounds in the rat's dorsal cortex of the inferior colliculus as revealed by evoked local field potentials. *Hear. Res.* 286, 41–54. doi: 10.1016/j.heares.2012.02.007

Pérez-González, D., Hernández, O., Covey, E., and Malmierca, M. S. (2012). $GABA_A$-mediated inhibition modulates stimulus-specific adaptation in the inferior colliculus. *PLoS One* 7:e34297. doi: 10.1371/journal.pone.0034297

Pérez-González, D., and Malmierca, M. S. (2012). Variability of the time course of stimulus-specific adaptation in the inferior colliculus. *Front. Neural Circuits* 6:107. doi: 10.3389/fncir.2012.00107

Pérez-González, D., and Malmierca, M. S. (2014). Adaptation in the auditory system: an overview. *Front. Integr. Neurosci.* 8:19. doi: 10.3389/fnint.2014.00019

Pérez-González, D., Malmierca, M. S., and Covey, E. (2005). Novelty detector neurons in the mammalian auditory midbrain. *Eur. J. Neurosci.* 22, 2879–2885. doi: 10.1111/j.1460-9568.2005.04472.x

Peruzzi, D., Bartlett, E., Smith, P. H., and Oliver, D. L. (1997). A monosynaptic GABAergic input from the inferior colliculus to the medial geniculate body in rat. *J. Neurosci.* 17, 3766–3777.

Potashner, S. J., Dymczyk, L., and Deangelis, M. M. (1988). D-aspartate uptake and release in the guinea pig spinal cord after partial ablation of the cerebral cortex. *J. Neurochem.* 50, 103–111. doi: 10.1111/j.1471-4159.1988.tb13236.x

Ranganath, C., and Rainer, G. (2003). Neural mechanisms for detecting and remembering novel events. *Nat. Rev. Neurosci.* 4, 193–202. doi: 10.1038/nrn1052

Rao, R. P., and Ballard, D. H. (1999). Predictive coding in the visual cortex: a functional interpretation of some extra-classical receptive-field effects. *Nat. Neurosci.* 2, 79–87. doi: 10.1038/4580

Rasmussen, G. L. (1946). The olivary peduncle and other fiber projections of the superior olivary complex. *J. Comp. Neurol.* 84, 141–219. doi: 10.1002/cne.900840204

Rasmussen, G. L. (1953). Further obsevations of the efferent cochlear bundle. *J. Comp. Neurol.* 99, 61–74. doi: 10.1002/cne.900990105

Reches, A., and Gutfreund, Y. (2008). Stimulus-specific adaptations in the gaze control system of the barn owl. *J. Neurosci.* 28, 1523–1533. doi: 10.1523/JNEUROSCI.3785-07.2008

Reches, A., Netser, S., and Gutfreund, Y. (2010). Interactions between stimulus-specific adaptation and visual auditory integration in the forebrain of the barn owl. *J. Neurosci.* 30, 6991–6998. doi: 10.1523/JNEUROSCI.5723-09.2010

Richardson, B. D., Ling, L. L., Uteshev, V. V., and Caspary, D. M. (2011). Extrasynaptic GABA(A) receptors and tonic inhibition in rat auditory thalamus. *PLoS One* 6:e16508. doi: 10.1371/journal.pone.0016508

Rouiller, E. M., and Welker, E. (1991). Morphology of corticothalamic terminals arising from the auditory cortex of the rat: a Phaseolus vulgaris-leucoagglutinin (PHA-L) tracing study. *Hear. Res.* 56, 179–190. doi: 10.1016/0378-5955(91)90168-9

Rouiller, E. M., and Welker, E. (2000). A comparative analysis of the morphology of corticothalamic projections in mammals. *Brain Res. Bull.* 53, 727–741. doi: 10.1016/s0361-9230(00)00364-6

Rushmore, R. J., Payne, B. R., and Lomber, S. G. (2005). Functional impact of primary visual cortex deactivation on subcortical target structures in the thalamus and midbrain. *J. Comp. Neurol.* 488, 414–426. doi: 10.1002/cne.20597

Ryugo, D. K., and Weinberger, N. M. (1976). Corticofugal modulation of the medial geniculate body. *Exp. Neurol.* 51, 377–391. doi: 10.1016/0014-4886(76)90262-4

Saldaña, E., Feliciano, M., and Mugnaini, E. (1996). Distribution of descending projections from primary auditory neocortex to inferior colliculus mimics the topography of intracollicular projections. *J. Comp. Neurol.* 371, 15–40. doi: 10.1002/(sici)1096-9861(19960715)371:1<15::aid-cne2>3.0.co;2-o

Schofield, B. R. (2009). Projections to the inferior colliculus from layer VI cells of auditory cortex. *Neuroscience* 159, 246–258. doi: 10.1016/j.neuroscience.2008.11.013

Schwartz, O., and Simoncelli, E. P. (2001). Natural signal statistics and sensory gain control. *Nat. Neurosci.* 4, 819–825. doi: 10.1038/90526

Seth, A. K., Suzuki, K., and Critchley, H. D. (2012). An interoceptive predictive coding model of conscious presence. *Front. Psychol.* 2:395. doi: 10.3389/fpsyg.2011.00395

Sherman, S. M., and Guillery, R. W. (1998). On the actions that one nerve cell can have on another: distinguishing "drivers" from "modulators". *Proc. Natl. Acad. Sci. U S A* 95, 7121–7126. doi: 10.1073/pnas.95.12.7121

Shi, C. J., and Cassell, M. D. (1997). Cortical, thalamic and amygdaloid projections of rat temporal cortex. *J. Comp. Neurol.* 382, 153–175. doi: 10.1002/(sici)1096-9861(19970602)382:2<153::aid-cne2>3.3.co;2-#

Sillito, A. M., Cudeiro, J., and Jones, H. E. (2006). Always returning: feedback and sensory processing in visual cortex and thalamus. *Trends Neurosci.* 29, 307–316. doi: 10.1016/j.tins.2006.05.001

Sillito, A. M., Jones, H. E., Gerstein, G. L., and West, D. C. (1994). Feature-linked synchronization of thalamic relay cell firing induced by feedback from the visual cortex. *Nature* 369, 479–482. doi: 10.1038/369479a0

Skoe, E., Chandrasekaran, B., Spitzer, E. R., Wong, P. C., and Kraus, N. (2014). Human brainstem plasticity: the interaction of stimulus probability and auditory learning. *Neurobiol. Learn. Mem.* 109, 82–93. doi: 10.1016/j.nlm.2013.11.011

Skoe, E., and Kraus, N. (2010a). Auditory brain stem response to complex sounds: a tutorial. *Ear Hear.* 31, 302–324. doi: 10.1097/AUD.0b013e3181cdb272

Skoe, E., and Kraus, N. (2010b). Hearing it again and again: on-line subcortical plasticity in humans. *PLoS One* 5:e13645. doi: 10.1371/journal.pone.0013645

Skoe, E., Krizman, J., Spitzer, E., and Kraus, N. (2013). The auditory brainstem is a barometer of rapid auditory learning. *Neuroscience* 243, 104–114. doi: 10.1016/j.neuroscience.2013.03.009

Slater, B. J., Willis, A. M., and Llano, D. A. (2013). Evidence for layer-specific differences in auditory corticocollicular neurons. *Neuroscience* 229, 144–154. doi: 10.1016/j.neuroscience.2012.10.053

Stebbings, K. A., Lesicko, A. M., and Llano, D. A. (2014). The auditory corticocollicular system: molecular and circuit-level considerations. *Hear. Res.* 314, 51–59. doi: 10.1016/j.heares.2014.05.004

Suga, N., and Ma, X. (2003). Multiparametric corticofugal modulation and plasticity in the auditory system. *Nat. Rev. Neurosci.* 4, 783–794. doi: 10.1038/nrn1222

Taaseh, N., Yaron, A., and Nelken, I. (2011). Stimulus-specific adaptation and deviance detection in the rat auditory cortex. *PLoS One* 6:e23369. doi: 10.1371/journal.pone.0023369

Theyel, B. B., Llano, D. A., and Sherman, S. M. (2010). The corticothalamocortical circuit drives higher-order cortex in the mouse. *Nat. Neurosci.* 13, 84–88. doi: 10.1038/nn.2449

Tiitinen, H., May, P., Reinikainen, K., and Näätänen, R. (1994). Attentive novelty detection in humans is governed by pre-attentive sensory memory. *Nature* 372, 90–92. doi: 10.1038/372090a0

Ulanovsky, N., Las, L., Farkas, D., and Nelken, I. (2004). Multiple time scales of adaptation in auditory cortex neurons. *J. Neurosci.* 24, 10440–10453. doi: 10.1523/jneurosci.1905-04.2004

Ulanovsky, N., Las, L., and Nelken, I. (2003). Processing of low-probability sounds by cortical neurons. *Nat. Neurosci.* 6, 391–398. doi: 10.1038/nn1032

Villa, A. E., and Abeles, M. (1990). Evidence for spatiotemporal firing patterns within the auditory thalamus of the cat. *Brain Res.* 509, 325–327. doi: 10.1016/0006-8993(90)90558-s

Villa, A. E., Rouiller, E. M., Simm, G. M., Zurita, P., de Ribaupierre, Y., and de Ribaupierre, F. (1991). Corticofugal modulation of the information processing in the auditory thalamus of the cat. *Exp. Brain Res.* 86, 506–517. doi: 10.1007/bf00230524

Villa, A. E., Tetko, I. V., Dutoit, P., De Ribaupierre, Y., and De Ribaupierre, F. (1999). Corticofugal modulation of functional connectivity within the auditory thalamus of rat, guinea pig and cat revealed by cooling deactivation. *J. Neurosci. Methods* 86, 161–178. doi: 10.1016/s0165-0270(98)00164-2

von der Behrens, W., Bäuerle, P., Kössl, M., and Gaese, B. H. (2009). Correlating stimulus-specific adaptation of cortical neurons and local field potentials in the awake rat. *J. Neurosci.* 29, 13837–13849. doi: 10.1523/JNEUROSCI.3475-09.2009

Winer, J. A. (2005). "Three systems of descending projections to the inferior colliculus," in *The Inferior Colliculus*, eds J. A. Winer and C. E. Schreiner (New York: Springer), 231–247.

Winer, J. A. (2006). Decoding the auditory corticofugal systems. *Hear. Res.* 212, 1–8. doi: 10.1016/j.heares.2005.06.014

Winer, J. A., Diehl, J. J., and Larue, D. T. (2001). Projections of auditory cortex to the medial geniculate body of the cat. *J. Comp. Neurol.* 430, 27–55. doi: 10.1002/1096-9861(20010129)430:1<27::aid-cne1013>3.3.co;2-#

Winer, J. A., Larue, D. T., Diehl, J. J., and Hefti, B. J. (1998). Auditory cortical projections to the cat inferior colliculus. *J. Comp. Neurol.* 400, 147–174. doi: 10.1002/(sici)1096-9861(19981019)400:2<147::aid-cne1>3.3.co;2-v

Winer, J. A., and Lee, C. C. (2007). The distributed auditory cortex. *Hear. Res.* 229, 3–13. doi: 10.1016/j.heares.2007.01.017

Winer, J. A., and Prieto, J. J. (2001). Layer V in cat primary auditory cortex (AI): cellular architecture and identification of projection neurons. *J. Comp. Neurol.* 434, 379–412. doi: 10.1002/cne.1183

Winer, J. A., Sally, S. L., Larue, D. T., and Kelly, J. B. (1999). Origins of medial geniculate body projections to physiologically defined zones of rat primary auditory cortex. *Hear. Res.* 130, 42–61. doi: 10.1016/s0378-5955(98)00217-2

Winkler, I. (2007). Interpreting the mismatch negativity. *J. Psychophysiol.* 21, 147–163. doi: 10.1027/0269-8803.21.34.147

Winkler, I., Denham, S. L., Mill, R., Bőhm, T. M., and Bendixen, A. (2012). Multistability in auditory stream segregation: a predictive coding view. *Philos. Trans. R. Soc. Lond. B Biol. Sci.* 367, 1001–1012. doi: 10.1098/rstb.2011.0359

Winkler, I., Denham, S. L., and Nelken, I. (2009). Modeling the auditory scene: predictive regularity representations and perceptual objects. *Trends Cogn. Sci.* 13, 532–540. doi: 10.1016/j.tics.2009.09.003

Wong, D., and Kelly, J. P. (1981). Differentially projecting cells in individual layers of the auditory cortex:a double-labeling study. *Brain Res.* 230, 362–366. doi: 10.1016/0006-8993(81)90416-9

Yan, J., and Ehret, G. (2001). Corticofugal reorganization of the midbrain tonotopic map in mice. *Neuroreport* 12, 3313–3316. doi: 10.1097/00001756-200110290-00033

Yan, J., and Ehret, G. (2002). Corticofugal modulation of midbrain sound processing in the house mouse. *Eur. J. Neurosci.* 16, 119–128. doi: 10.1046/j.1460-9568.2002.02046.x

Yan, W., and Suga, N. (1998). Corticofugal modulation of the midbrain frequency map in the bat auditory system. *Nat. Neurosci.* 1, 54–58. doi: 10.1038/255

Yan, J., Zhang, Y., and Ehret, G. (2005). Corticofugal shaping of frequency tuning curves in the central nucleus of the inferior colliculus of mice. *J. Neurophysiol.* 93, 71–83. doi: 10.1152/jn.00348.2004

Yu, Y. Q., Xiong, Y., Chan, Y. S., and He, J. (2004). Corticofugal gating of auditory information in the thalamus: an in vivo intracellular recording study. *J. Neurosci.* 24, 3060–3069. doi: 10.1523/jneurosci.4897-03.2004

Yu, X. J., Xu, X. X., He, S., and He, J. (2009). Change detection by thalamic reticular neurons. *Nat. Neurosci.* 12, 1165–1170. doi: 10.1038/nn.2373

Yuille, A., and Kersten, D. (2006). Vision as Bayesian inference: analysis by synthesis? *Trends Cogn. Sci.* 10, 301–308. doi: 10.1016/j.tics.2006.05.002

Zhao, L., Liu, Y., Shen, L., Feng, L., and Hong, B. (2011). Stimulus-specific adaptation and its dynamics in the inferior colliculus of rat. *Neurosci.* 181, 163–174. doi: 10.1016/j.neuroscience.2011.01.060

Zikopoulos, B., and Barbas, H. (2006). Prefrontal projections to the thalamic reticular nucleus form a unique circuit for attentional mechanisms. *J. Neurosci.* 26, 7348–7361. doi: 10.1523/jneurosci.5511-05.2006

Zikopoulos, B., and Barbas, H. (2012). Pathways for emotions and attention converge on the thalamic reticular nucleus in primates. *J. Neurosci.* 32, 5338–5350. doi: 10.1523/JNEUROSCI.4793-11.2012

Conflict of Interest Statement: The authors declare that the research was conducted in the absence of any commercial or financial relationships that could be construed as a potential conflict of interest.

Received: 19 December 2014; accepted: 03 February 2015; published online: 09 March 2015.

Citation: Malmierca MS, Anderson LA and Antunes FM (2015) The cortical modulation of stimulus-specific adaptation in the auditory midbrain and thalamus: a potential neuronal correlate for predictive coding. Front. Syst. Neurosci. ***9****:19. doi: 10.3389/fnsys.2015.00019*

This article was submitted to the journal Frontiers in Systems Neuroscience.

frontiers in
SYSTEMS NEUROSCIENCE

ORIGINAL RESEARCH ARTICLE
published: 01 July 2014
doi: 10.3389/fnsys.2014.00125

Frequency-specific corticofugal modulation of the dorsal cochlear nucleus in mice

*Lingzhi Kong[1†], Colin Xiong[1†], Liang Li[2] and Jun Yan[1]**

[1] Department of Physiology and Pharmacology, Faculty of Medicine, Hotchkiss Brain Institute, University of Calgary, Calgary, AB, Canada
[2] Department of Psychology, Department of Machine Intelligence, Speech and Hearing Research Center, Key Laboratory on Machine Perception (Ministry of Education), PKU-IDG/McGovern Institute for Brain Research, Peking University, Beijing, China

Edited by:
Paul Hinckley Delano, Universidad de Chile, Chile

Reviewed by:
Manuel S. Malmierca, University of Salamanca, Spain
Xavier G. A. Perrot, Université Claude Bernard Lyon 1, France

***Correspondence:**
Jun Yan, Department of Physiology and Pharmacology, Faculty of Medicine, Hotchkiss Brain Institute, University of Calgary, 3330 Hospital Drive NW, Calgary, AB T2N 4N1, Canada
e-mail: juyan@ucalgary.ca

† These authors have contributed equally to this work.

The primary auditory cortex (AI) modulates the sound information processing in the lemniscal subcortical nuclei, including the anteroventral cochlear nucleus (AVCN), in a frequency-specific manner. The dorsal cochlear nucleus (DCN) is a non-lemniscal subcortical nucleus but it is tonotopically organized like the AVCN. However, it remains unclear how the AI modulates the sound information processing in the DCN. This study examined the impact of focal electrical stimulation of AI on the auditory responses of the DCN neurons in mice. We found that the electrical stimulation induced significant changes in the best frequency (BF) of DCN neurons. The changes in the BFs were highly specific to the BF differences between the stimulated AI neurons and the recorded DCN neurons. The DCN BFs shifted higher when the AI BFs were higher than the DCN BFs and the DCN BFs shifted lower when the AI BFs were lower than the DCN BFs. The DCN BFs showed no change when the AI and DCN BFs were similar. Moreover, the BF shifts were linearly correlated to the BF differences. Thus, our data suggest that corticofugal modulation of the DCN is also highly specific to frequency information, similar to the corticofugal modulation of the AVCN. The frequency-specificity of corticofugal modulation does not appear limited to the lemniscal ascending pathway.

Keywords: corticofugal modulation, primary auditory cortex, dorsal cochlear nucleus, frequency-specific modulation, lemniscal, non-lemniscal, neural plasticity

INTRODUCTION

Understanding the central processing of auditory information is incomplete without considering the descending systems. Morphologically, the auditory cortex sends a large number of descending fibers to the subcortical nuclei (corticofugal projections, Doucet et al., 2002, 2003; Coomes and Schofield, 2004), including the auditory thalamus (Roger and Arnault, 1989; Winer et al., 2001), inferior colliculus (Andersen et al., 1980; Faye-Lund, 1985; Coleman and Clerici, 1987; Herbert et al., 1991; Saldaña et al., 1996; Winer et al., 1998, 2002; Bajo and Moore, 2005; Coomes et al., 2005; Bajo et al., 2007; Peterson and Schofield, 2007; Markovitz et al., 2013) and cochlear nucleus (Weedman and Ryugo, 1996a,b; Jacomme et al., 2003; Schofield and Coomes, 2005a,b; Meltzer and Ryugo, 2006; Schofield et al., 2006). In addition, the corticofugal system implements a highly selective modulation of the physiological response in the subcortical nuclei (Yan and Suga, 1996, 1999; Ma and Suga, 2001a; Nakamoto et al., 2008; Bajo et al., 2010). In the frequency domain, focal activation of the primary auditory cortex (AI) shifts the receptive fields of neurons in the subcortical nuclei towards the best frequency (BF) of activated AI neurons and reorganizes the frequency maps of those subcortical nuclei including the ventral division of the medial geniculate body (MGBv; Zhang and Suga, 2000; Tang et al., 2012), the central nucleus of the inferior colliculus (ICc; Yan and Suga, 1998; Zhang and Suga, 2000; Yan et al., 2005; Yan and Ehret, 2001, 2002; Ma and Suga, 2001b, 2003) and even the anteroventral cochlear nucleus (AVCN; Luo et al., 2008; Liu et al., 2010).

Frequency-specific corticofugal modulation appears to be a feature of the lemniscal auditory pathway. Up to now, it has been exclusively observed in the lemniscal subcortical nuclei (MGBv, ICc and AVCN) and not in the non-lemniscal nuclei (Calford and Aitkin, 1983; Imig and Morel, 1983; Hu et al., 1994) including those found in the medial division of the medial geniculate body (MGBm) and the external nucleus of the inferior colliculus (ICx; Jen et al., 2001; Zhang and Suga, 2005; Wu and Yan, 2007; Tang et al., 2012). Given that the lemniscal auditory pathway is also characterized by a sharp tuning in sound frequency and a strict tonotopic projection (Calford, 1983; Rodrigues-Dageff et al., 1989; Redies and Brandner, 1991; Anderson and Linden, 2011), the question raised here is whether the frequency-specificity of corticofugal modulation is limited to the lemniscal system or dominated by the tonotopy regime of the central auditory system.

The dorsal cochlear nucleus (DCN) is tonotopically organized (Young et al., 1992; Luo et al., 2009). In contrast to the AVCN, the DCN receives inputs from both the auditory and somatosensory systems (Baizer et al., 2012), and projects to the ICx and MGBm (Malmierca et al., 2002). The DCN could therefore be a non-lemniscal nucleus because it is tightly associated to non-lemniscal

auditory system (Malmierca et al., 2002; Ryugo et al., 2003; Luo et al., 2012). In the present study, we examined the effects of focal electrical stimulation of the AI (ES_{AI}) on the auditory responses of the DCN neurons. Our data show that ES_{AI} induced a frequency-specific shift in the frequency tunings of the DCN neurons, similar to the modulation of the AVCN (Luo et al., 2008; Liu et al., 2010).

MATERIALS AND METHODS

C57 female mice, aged 4–7 weeks and weighing 14.6–20.7 g, were used in this study. All protocols and procedures were approved by the Animal Care Committee of the University of Calgary (protocol number: M04044). Animals were anesthetized with a mixture of ketamine (85 mg/kg, i.p., Bimeda-MTC Animal Health Inc., Canada) and xylazine (15 mg/kg, i.p., Bimeda-MTC Animal Health Inc.). The anesthetic level was maintained by additional doses of ketamine and xylazine, 17 mg/kg and 3 mg/kg respectively. Under anesthesia, the mouse's head was fixed in a custom-made head holder by rigidly clamping between the palate and nasal/frontal bones. The mouth bar was adjusted to align bregma and lambda of the skull in one horizontal plane. Once the mouse's head was positioned, the scalp was incised along the midline and subcutaneous tissue and muscle were removed to expose the skull. Two holes, 3 and 2 mm in diameter respectively, were drilled to expose the right cerebellum above the cochlear nucleus (5.6–6.5 mm posterior to bregma, 2.1–2.6 mm lateral to the midline) and the left AI (2.2–3.6 mm posterior to bregma, 4–4.5 mm lateral to the midline). After surgery, the animal was placed in a sound-proof chamber to record the response of DCN neurons before and after electrical stimulation of the auditory cortex (**Figure 1**). During all surgery and electrophysiological experiments, the animal's body temperature was maintained at a constant 37°C using a feedback-controlled heating pad.

ACOUSTIC STIMULATION

Tone bursts, 60-ms duration with 5-ms rise and fall times, were used as acoustic stimuli. They were digitally synthesized and converted into analog sinusoidal waves by an Enhanced Real-time Processor (RP2, Tucker-Davis Tech., Gainesville, FL, USA). The signals were then fed to a tweeter via a digital attenuator (PA5, Tucker-Davis Tech., Gainesville, FL, USA). The output amplitude of the tone bursts was expressed as dB SPL within 1 dB accuracy (reference 20 μPa). The tweeter was placed 45° to the right of and 13 cm away from the mouse's right ear. During calibration, the tweeter was driven by 20-volt sinusoidal peak-to-peak bursts without attenuation. It was calibrated at the right and left ear of the animal with a condenser microphone (Model 2520, Larson-Davis Laboratories, USA) and a microphone preamplifier (Model 2200C, Larson-Davis Laboratories, USA). Frequencies and intensities of tone bursts were varied either manually or automatically with software (BrainWare, Tucker-Davis Tech., Gainesville, FL, USA).

RECORDING AND ELECTRICAL STIMULATION OF THE AI

A tungsten electrode (~2 MΩ impedance, FHC, USA) was advanced perpendicular to the surface of the left auditory cortex. The electrode was initially connected to the preamplifier of the data acquisition system. Signals from the electrode were fed to a 16-channel preamplifier, amplified 10,000 times and filtered using a bandwidth of 0.3–10 kHz (RA16, Tucker-Davis Tech., Gainesville, FL, USA), and recorded with software (BrainWare, Tucker-Davis Tech., Gainesville, FL, USA). A pure tone with manual alternation of frequencies and amplitudes was continuously delivered once per second during the electrode penetration. Tone-evoked action potentials were frequently located at layers III/IV of the AI. The lowest amplitude (minimum threshold) and the corresponding frequency at which the neuron showed a response were determined by manual alternation of the tone frequency and amplitude. After 5 ~ 8 penetrations, a rough tonotopy of the AI and the intended location for stimulation of the AI were determined. Once the electrode was in position and the tone-evoked action potentials were observed again, the frequency tunings of the AI neurons were measured with a series of tone bursts at 10 dB above the MT and frequencies that varied from 3 to 40 kHz in 1 kHz steps. Tone stimuli were presented 15 times at each frequency. The frequency to which the neuron showed the largest response magnitude was defined as the BF of the AI neuron. The electrode was then disconnected from the recording system and reconnected to the output of a constant current isolator (A360, WPI Inc., Sarasata, FL) for the ES_{AI}. The electrode was advanced to a depth of about 700–800 μm below the brain surface to layer V of the AI where it was maintained for the duration of the experiment. This procedure ensured that the locations of the recording and stimulating sites were in the same AI cell column with the same BFs.

An indifferent electrode was placed on the brain surface just adjacent to the stimulating electrode. The negative pulses (monophasic, 0.1 ms, 500 nA constant current) were generated by a stimulator (Grass S88, Natus Neurology, West Warwick, RI) and a constant-current isolator (A360, WPI, Inc., Sarasata, FL, USA). The electrical pulses were synchronized with the offset of the tone bursts at BF and 20 dB above the MT of the cortical neurons. The combined acoustic from the tweeter and electric stimuli were respectively delivered in both ears (with a right predominance) and to the left AI at a rate of 4 Hz for 7 min; this stimulus paradigm was also used in our previous study (Yan and Ehret, 2002).

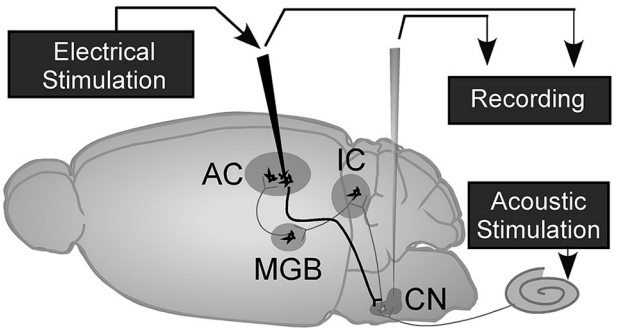

FIGURE 1 | A schematic of the mouse brain with recording and electrical stimulation sites (adapted from Luo et al., 2008). The corticofugal projection to DCN is indicated by a solid dark line. Auditory cortex, AC; medial geniculate body, MGB; inferior colliculus, IC; cochlear nucleus, CN.

DCN RECORDING

Two tungsten electrodes (∼2 MΩ impedance) were dorsoventrally positioned in the right cochlear nucleus. The space between the two electrodes was 100 μm. The location of the DCN was determined physiologically. A pure tone with manual alteration of its frequency and amplitude was continuously delivered once per second during electrode penetration. Tone-evoked responses were commonly observed at a depth of 2.5 mm below the surface of the cerebellum. Once the responses to the tone stimuli were observed, the minimum threshold and the corresponding frequency were measured by manually alternating the frequency and amplitude of the tone. The frequencies at the minimum threshold were measured for each 100-μm interval to map, in an approximate manner, the tonotopic organization along the dorsal-ventral axis. According to the three-dimensional tonotopy of the cochlear nucleus obtained from our previous study (Luo et al., 2009), the frequencies at the minimum threshold decreased dorsoventrally in the same frequency range for both the DCN and posteroventral cochlear nucleus (PVCN) neurons. Thus, the ventral boundary of the DCN was determined when the frequency at the minimum threshold increased as the electrode was advanced into the PVCN. The electrode was then withdrawn in ∼100-μm intervals until the action potential recordings stabilized. The minimum threshold and the corresponding frequency of the recorded DCN neuron were determined manually again, and the frequency tunings of the DCN neuron was also measured with the same procedure used for the AI neurons. These response curves of the DCN neurons served as control responses. The frequency to which the neuron showed the largest response magnitude was defined as the BF of the DCN neuron. A negative current of electrical pulses was then delivered to the AI for the micro-electrical stimulation of the AI neurons (4/s for 7 min). The response curves of DCN neurons were again recorded immediately after cortical stimulation and every 30 min until a recovery rate of at least 50% in the BF was obtained.

DATA PROCESSING

The tungsten electrode (∼2 MΩ impedance) often detected multiunit activities. Cluster cutting isolated and selected single-unit action potentials by examining eight parameters of the action potential waveform, i.e., peak, valley, spike height, spike width, peak time, valley time, and two user-defined voltages (Yan and Ehret, 2002; Yan et al., 2002). Single-unit responses to the series of tones were eventually displayed using post-stimulus time-cumulative (PSTC) histograms with a bin width of 1 ms. The BFs of the DCN neurons were compared before (pre-ES BF) and after (post-ES BF) the ES_{AI}. Since the ranges of upward and downward BF shifts were found to be similar, the BF shifts were expressed using a linear kHz scale (Sakai and Suga, 2001; Yan and Ehret, 2002). The changes in the BFs of DCN neurons were analyzed according to the differences in BFs between the recorded DCN neurons and the stimulated cortical neurons.

STATISTICAL ANALYSIS

Data were expressed as mean ± SD. The paired *t*-test (two-tailed) was used to compare the differences between groups of data. A *p*-value of <0.05 was considered to be statistically significant.

RESULTS

The effects of ES_{AI} were studied in 60 contralateral DCN neurons from 26 mice (2–4 neurons per mouse). The BFs of recorded DCN neurons ranged from 10 to 27 kHz and the BFs of stimulated cortical neurons ranged from 10 to 28 kHz. These values fell within the central range of mouse hearing (Zhang et al., 2005). Our data show that the AI significantly impacts the auditory response of the DCN neurons. The changes in the response properties of DCN neurons occurred within 30 min, peaked at 1.5 h, and recovered at 3 h after the ES_{AI}.

The ES_{AI} clearly changed the frequency tunings of the contralateral DCN neurons. **Figure 2** shows three different examples of DCN neurons modulated by ES_{AI}. In **Figure 2A**, the BFs of both cortical and DCN neurons were 11 kHz (matched). The auditory response of the DCN neuron increased after the ES_{AI} (facilitation) while the BF of the DCN neuron did not change. **Figure 2B** shows that the pre-ES BF of the DCN neuron was 21 kHz while the cortical neuron had a BF of 27 kHz (unmatched). The auditory response at the pre-ES BF (21 kHz, control) of the DCN neuron decreased after the ES_{AI} (inhibition). Hereafter, we use the "facilitation" and "inhibition" for simplicity. These terms represent the overall increase and decrease in neuronal activity without prejudging their underlying neurobiological mechanisms. However, the auditory response at 24 kHz (post-ES BF of DCN neuron) showed the largest increase. Both the facilitation and inhibition by ES_{AI} resulted in a BF shift of the DCN neuron from 21 to 24 kHz. In **Figure 2C**, the pre-ES BF (16 kHz) of the DCN neuron was higher than the BF (11 kHz) of the cortical neuron (unmatched). The BF of this DCN neuron shifted from 16 to 14 kHz after the ES_{AI}. Thus, the changes in the BF of the DCN neurons appear to be determined by the relationship between the BFs of the DCN and AI neurons: (1) the DCN BFs did not change when the BFs of the DCN neurons and those of the AI neurons were matched; and (2) the DCN BFs shifted towards the BFs of the AI neurons when the BFs of the DCN and AI neurons were unmatched.

We also analyzed the effect of ES_{AI} on the frequency tunings of all 60 DCN neurons. The DCN neurons were classified according to the difference between the BFs of the DCN neurons and AI neurons: (1) unmatched group (14 neurons, $BF_{DCN} \approx BF_{AI}$, **Figure 3**, open circles and open bar); (2) unmatched Group 1 (21 neurons, $BF_{DCN} - BF_{AI} < -1$ kHz, **Figure 3**, filled circles and filled bars); and (3) unmatched Group 2 (25 neurons, $BF_{DCN} - BF_{AI} > 1$ kHz, **Figure 3**, filled circles and filled bars). For the auditory response (spikes) at the pre-ES BF and 10 dB above the MT of DCN neurons (control), the response increased after the ES_{AI} for the matched group (**Figure 3A**, open circles) while it decreased for the unmatched group (**Figure 3A**, filled black circles). On average, the response of the matched group (**Figure 3B**, open bar) significantly increased by 9.95% ($p < 0.01$). In contrast, the response of the unmatched group (**Figure 3B**, filled black bars) significantly decreased by 6.71% ($p < 0.001$) for the unmatched Group 1 and 8.36% ($p < 0.001$) for the unmatched Group 2. For the auditory response (spikes) at the post-ES BF and 10 dB above the MT of DCN neurons, the response increased after ES_{AI} for the unmatched group (**Figure 3A**, filled gray circles). On average, the response

of the unmatched group (**Figure 3B**, filled gray bars) significantly increased by 12.25% ($p < 0.001$) for the unmatched Group 1 and 10.49% ($p < 0.001$) for the unmatched Group 2. Thus, the ES_{AI} remarkably inhibits the auditory response at the pre-ES BF of DCN neurons while it facilities the auditory response at the post-ES BF when the BFs of the DCN and AI neuron are unmatched.

Our results indicate that the shifts in DCN BFs appear to be associated with the BFs of stimulated cortical neurons. To clarify this issue, we further analyzed the correlation of the shifts in DCN BFs to the BFs of the stimulated AI neurons. It became apparent that the BF changes of DCN neurons were systematically associated with the differences in the BFs between the stimulated AI neurons and the recorded DCN neurons (**Figure 4A**). The shift in BFs was linearly correlated with the differences between the BFs of the AI and DCN neurons ($R^2 = 0.811$; $p < 0.01$). When the BFs of AI neurons were higher than the BFs of DCN neurons, cortical stimulation significantly increased the BFs of DCN neurons by 2.07 kHz ($p < 0.001$), and when BFs of cortical neurons were lower than the BFs of DCN neurons, cortical stimulation significantly decreased the BFs of DCN neurons by 2.77 kHz ($p < 0.001$) (**Figure 4B**, filled bars). When the BFs of AI neurons were the same as the BFs of DCN neurons (**Figure 4A**, open circles), cortical stimulation did not shift the BFs of DCN neurons (**Figure 4B**, open bar).

DISCUSSION

Our data clearly demonstrated that the auditory cortex modulated the auditory responses of the DCN neurons in a frequency-specific manner. The BF shifts of DCN neurons were significantly correlated to the differences in the BFs between the stimulated AI neurons and the recorded DCN neurons. Thus, the DCN and AVCN not only exhibit mirror-symmetrical tonotopic maps (Luo et al., 2009), but also share a similar pattern of corticofugal modulation (Luo et al., 2008; Liu et al., 2010). Therefore, the frequency-specificity of corticofugal modulation appears to be dominated by the tonotopy regime of the central auditory system. However, the AVCN and DCN belong to two distinct auditory pathways (lemniscal vs. non-lemniscal, respectively) with different anatomical and physiological properties (Calford and Aitkin, 1983; Imig and Morel, 1983; Hu et al., 1994). Given that the corticofugal modulation of AVCN re-shapes the high-fidelity representation of initial sound information and impacts the sound information that progresses upwards through the lemniscal pathway, what is the function of the corticofugal modulation of the DCN in the non-lemniscal pathway?

The non-lemniscal auditory pathway engages in functions complementary with those of the lemniscal auditory pathway including the integration of information within and across sensory modalities, detection of changes in ongoing stimuli and interestingly, tinnitus (Young et al., 1995; Malmierca et al., 2002; Ryugo et al., 2003; Luo et al., 2012). The hyperactivity of the DCN neurons is considered to be a physiological correlate of the somatosensory tinnitus (Kaltenbach and McCaslin, 1996; Zhang and Kaltenbach, 1998; Baizer et al., 2012), and the corticofugal feedbacks, via the frequency-specific enhancement of the tinnitus-related frequencies, could be partially responsible (Mulders and Robertson, 2009; Eggermont, 2012, 2013). Our findings demonstrate that the DCN is modulated by the AI in a frequency-specific manner, suggesting that the AI may contribute

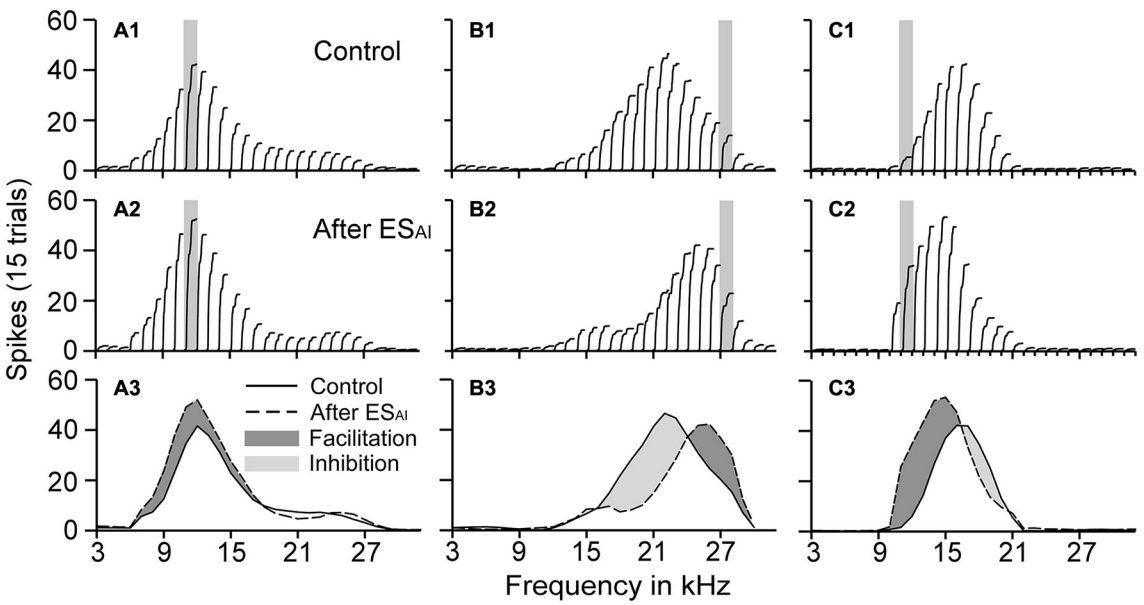

FIGURE 2 | Three examples illustrating the effects of the ES_{AI} on the frequency tunings of DCN neurons (A–C). The ES_{AI} did not change the BF but increased the auditory responses of the matched DCN neurons (A1, A2), while the BFs of the unmatched DCN neurons shifted towards the cortical BF (B1, B2 and C1, C2). The ES_{AI} caused facilitation (A3, B3, C3) and inhibition (B3, C3) of DCN auditory responses. The gray bars in the top two rows of panels represent the BFs of the stimulated cortical neurons. In the bottom row of panels, the dark gray area represents facilitation, whereas the light gray area represents inhibition.

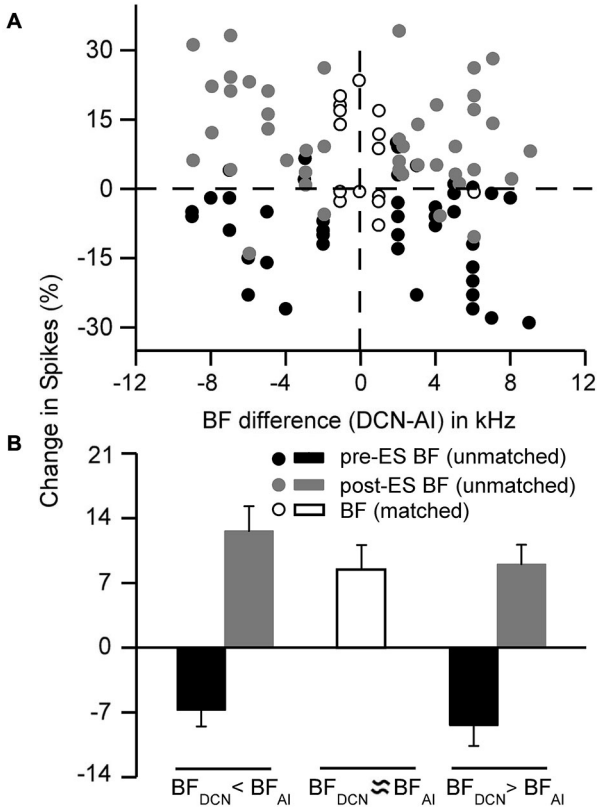

FIGURE 3 | Frequency-specific changes in the auditory responses (spikes) of DCN neurons after contralateral cortical stimulation. **(A)** The degree of change was different between the matched and unmatched DCN neurons. Filled black circles indicate responses at pre-ES BFs (Control); filled gray circles indicate responses at post-ES BFs, open circles indicate responses of neurons with matched BF. **(B)** The averaged response change after cortical stimulation. Filled black bars show averaged responses at pre-ES BFs (control); filled gray bars show averaged responses at post-ES BFs, open bar shows averaged response of neurons with matched BF. The error bars represent the SEM.

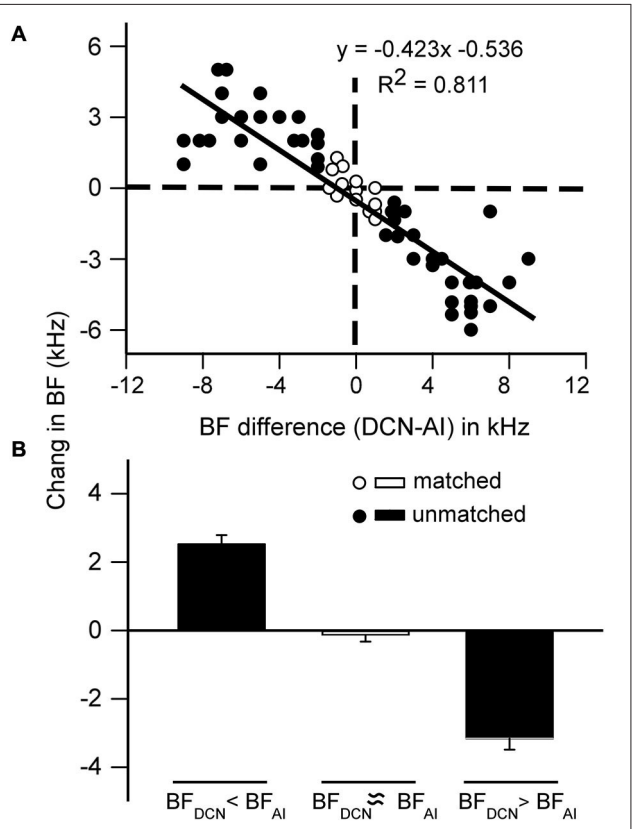

FIGURE 4 | Frequency-specific changes in the BF of DCN neurons after contralateral cortical stimulation. **(A)** The degree of change was systematically correlated to the BF difference between the AI and DCN neurons. Open circles, BF shift of neurons with matched BF; filled circles, BF shift of neurons with unmatched BF. **(B)** The averaged BF change after cortical stimulation. Open bar indicates the BF shift of neurons with matched BF; filled bars indicate the BF shift of neurons with unmatched BF. The error bars represent the SEM.

to the chronic form of tinnitus through its modulation of the DCN. The DCN is a relay for auditory information ascending from the periphery to the non-lemniscal pathway. Thus, the AI may also be involved in the other functions of the non-lemniscal pathway.

In addition to tonotopic organization and multisensory inputs, the DCN is a layered structure and consists of distinct cell types including the fusiform cells, giant cells, granule neurons and cartwheel cells (Mugnaini et al., 1980; Browner and Baruch, 1982; Webster and Trune, 1982; Ryugo and Willard, 1985; Willott et al., 1992; Willott, 2001). It has been shown *in vitro* studies that different types of neurons have different membrane properties and firing patterns (Hirsch and Oertel, 1988; Oertel and Wu, 1989; Zhang and Oertel, 1993a,b,c). It would be interesting to determine how the corticofugal modulation is associated with the layered structure and cell types of DCN.

Considering the multiple descending projections within the auditory system, the auditory cortex may modulate the DCN in a direct or indirect manner. The corticofugal projections to the DCN originate from large pyramidal neurons in layer V of the AI, and some fibers directly innervate fusiform cells in all layers of the DCN (Jacomme et al., 2003; Meltzer and Ryugo, 2006; Schofield and Coomes, 2005a,b). These fibers allow the cortical neurons to directly impact the activity of the principal DCN neurons. However, the majority of corticofugal fibers terminate in granule cell lamina between the DCN and the PVCN (Weedman and Ryugo, 1996a,b; Doucet et al., 2002, 2003). The cortical-dependent modulation of DCN neuronal activity through these fibers may involve intrinsic connections between granule cell lamina and the DCN as well as interconnections between the DCN and the ventral cochlear nucleus (Mugnaini et al., 1980; Snyder and Leake, 1988; Wickesberg and Oertel, 1988; Manis, 1989). Although the number of corticofugal fibers to the DCN is much lower than those to the granule cell lamina, we speculate that the highly specific corticofugal modulation is likely mediated by the corticofugal fibers directly projecting to DCN neurons. This is similar to our observations in the case of corticocollicular modulation. The corticocollicular projections mostly target the caudal cortex, dorsal cortex and lateral nucleus of the inferior colliculus, while the tonotopically-organized ICc only receives

sparse but tonotopic descending projections from the AI (Saldaña et al., 1996; Winer et al., 1998, 2002; Bajo and Moore, 2005; Bajo et al., 2007). Additionally, direct glutamatergic projections from the AI to the ICc are believed to be responsible for the frequency-specific corticofugal modulation of the ICc (Yan et al., 2005).

In sum, the AI modulates the neural responses in the DCN in a highly frequency-specific manner, similar to the corticofugal modulation of the AVCN. Thus, the frequency-specificity of corticofugal modulation does not appear limited to the lemniscal ascending pathway but dominated by the tonotopy regime of the auditory system. As the DCN receives many descending projections, their involvement in corticofugal modulation requires careful study.

ACKNOWLEDGMENTS

This work was supported by grants from the Natural Sciences and Engineering Research Council of Canada (Discovery Grant), the Campbell McLaurin Chair for Hearing Deficiencies, and Alberta Innovates—Health Solutions.

REFERENCES

Anderson, L. A., and Linden, J. F. (2011). Physiological differences between histologically defined subdivisions in the mouse auditory thalamus. *Hear. Res.* 274, 48–60. doi: 10.1016/j.heares.2010.12.016

Andersen, R. A., Snyder, R. L., and Merzenich, M. M. (1980). The topographic organization of corticocollicular projections from physiologically identified loci in the AI, AII and anterior auditory cortical fields of the cat. *J. Comp. Neurol.* 191, 479–494. doi: 10.1002/cne.901910310

Baizer, J. S., Manohar, S., Paolone, N. A., Weinstock, N., and Salvi, R. J. (2012). Understanding Tinnitus: the dorsal cochlear nucleus, organization and plasticity. *Brain Res.* 1485, 40–53. doi: 10.1016/j.brainres.2012.03.044

Bajo, V. M., and Moore, D. R. (2005). Descending projections from the auditory cortex to the inferior colliculus in the gerbil, Meriones unguiculatus. *J. Comp. Neurol.* 486, 101–116. doi: 10.1002/cne.20542

Bajo, V. M., Nodal, F. R., Bizley, J. K., Moore, D. R., and King, A. J. (2007). The ferret auditory cortex: descending projections to the inferior colliculus. *Cereb. Cortex* 17, 475–491. doi: 10.1093/cercor/bhj164

Bajo, V. M., Nodal, F. R., Moore, D. R., and King, A. J. (2010). The descending corticocollicular pathway mediates learning-induced auditory plasticity. *Nat. Neurosci.* 13, 253–260. doi: 10.1038/nn.2466

Browner, R. H., and Baruch, A. (1982). The cytoarchitecture of the dorsal cochlear nucleus in the 3-month- and 26-month-old C57BL/6 mouse: a Golgi impregnation study. *J. Comp. Neurol.* 211, 115–138. doi: 10.1002/cne.902110203

Calford, M. B. (1983). The parcellation of the medial geniculate body of the cat defined by the auditory response properties of single units. *J. Neurosci.* 3, 2350–2364.

Calford, M. B., and Aitkin, L. M. (1983). Ascending projections to the medial geniculate body of the cat: evidence for multiple, parallel auditory pathways through thalamus. *J. Neurosci.* 3, 2365–2380.

Coleman, J. R., and Clerici, W. J. (1987). Sources of projections to subdivisions of the inferior colliculus in the rat. *J. Comp. Neurol.* 262, 215–226. doi: 10.1002/cne.902620204

Coomes, D. L., and Schofield, B. R. (2004). Projections from the auditory cortex to the superior olivary complex in guinea pigs. *Eur. J. Neurosci.* 19, 2188–2200. doi: 10.1111/j.0953-816x.2004.03317.x

Coomes, D. L., Schofield, R. M., and Schofield, B. R. (2005). Unilateral and bilateral projections from cortical cells to the inferior colliculus in guinea pigs. *Brain Res.* 1042, 62–72. doi: 10.1016/j.brainres.2005.02.015

Doucet, J. R., Molavi, D. L., and Ryugo, D. K. (2003). The source of corticocollicular and corticobulbar projections in area Te1 of the rat. *Exp. Brain Res.* 153, 461–466. doi: 10.1007/s00221-003-1604-4

Doucet, J. R., Rose, L., and Ryugo, D. K. (2002). The cellular origin of corticofugal projections to the superior olivary complex in the rat. *Brain Res.* 925, 28–41. doi: 10.1016/s0006-8993(01)03248-6

Eggermont, J. J. (2012). *The Neuroscience of Tinnitus.* Oxford: Oxford University Press.

Eggermont, J. J. (2013). Hearing loss, hyperacusis, or Tinnitus: what is modeled in animal research? *Hear. Res.* 295, 140–149. doi: 10.1016/j.heares.2012.01.005

Faye-Lund, H. (1985). The neocortical projection to the inferior colliculus in the albino rat. *Anat. Embryol. (Berl)* 173, 53–70. doi: 10.1007/bf00707304

Herbert, H., Aschoff, A., and Ostwald, J. (1991). Topography of projections from the auditory cortex to the inferior colliculus in the rat. *J. Comp. Neurol.* 304, 103–122. doi: 10.1002/cne.903040108

Hirsch, J. A., and Oertel, D. (1988). Synaptic connections in the dorsal cochlear nucleus of mice, in vitro. *J. Physiol.* 396, 549–562.

Hu, B., Senatorov, V., and Mooney, D. (1994). Lemniscal and non-lemniscal synaptic transmission in rat auditory thalamus. *J. Physiol.* 479(Pt. 2), 217–231.

Imig, T. J., and Morel, A. (1983). Organization of the thalamocortical auditory system in the cat. *Annu. Rev. Neurosci.* 6, 95–120. doi: 10.1146/annurev.ne.06.030183.000523

Jacomme, A. V., Nodal, F. R., Bajo, V. M., Manunta, Y., Edeline, J. M., Babalian, A., et al. (2003). The projection from auditory cortex to cochlear nucleus in guinea pigs: an in vivo anatomical and in vitro electrophysiological study. *Exp. Brain Res.* 153, 467–476. doi: 10.1007/s00221-003-1606-2

Jen, P. H., Sun, X., and Chen, Q. C. (2001). An electrophysiological study of neural pathways for corticofugally inhibited neurons in the central nucleus of the inferior colliculus of the big brown bat, *Eptesicus fuscus*. *Exp. Brain Res.* 137, 292–302. doi: 10.1007/s002210000637

Kaltenbach, J. A., and McCaslin, D. L. (1996). Increases in spontaneous activity in the dorsal cochlear nucleus following exposure to high intensity sound: a possible neural correlate of Tinnitus. *Aud. Neurosci.* 3, 57–78.

Liu, X., Yan, Y., Wang, Y., and Yan, J. (2010). Corticofugal modulation of initial neural processing of sound information from the ipsilateral ear in the mouse. *PLoS One* 5:e14038. doi: 10.1371/journal.pone.0014038

Luo, F., Wang, Q., Farid, N., Liu, X., and Yan, J. (2009). Three-dimensional tonotopic organization of the C57 mouse cochlear nucleus. *Hear. Res.* 257, 75–82. doi: 10.1016/j.heares.2009.08.002

Luo, F., Wang, Q., Kashani, A., and Yan, J. (2008). Corticofugal modulation of initial sound processing in the brain. *J. Neurosci.* 28, 11615–11621. doi: 10.1523/JNEUROSCI.3972-08.2008

Luo, H., Zhang, X., Nation, J., Pace, E., Lepczyk, L., and Zhang, J. (2012). Tinnitus suppression by electrical stimulation of the rat dorsal cochlear nucleus. *Neurosci. Lett.* 522, 16–20. doi: 10.1016/j.neulet.2012.05.072

Ma, X., and Suga, N. (2001a). Corticofugal modulation of duration-tuned neurons in the midbrain auditory nucleus in bats. *Proc. Natl. Acad. Sci. U S A* 98, 14060–14065. doi: 10.1073/pnas.241517098

Ma, X., and Suga, N. (2001b). Plasticity of bat's central auditory system evoked by focal electric stimulation of auditory and/or somatosensory cortices. *J. Neurophysiol.* 85, 1078–1087.

Ma, X., and Suga, N. (2003). Augmentation of plasticity of the central auditory system by the basal forebrain and/or somatosensory cortex. *J. Neurophysiol.* 89, 90–103. doi: 10.1152/jn.00968.2001

Malmierca, M. S., Merchán, M. A., Henkel, C. K., and Oliver, D. L. (2002). Direct projections from cochlear nuclear complex to auditory thalamus in the rat. *J. Neurosci.* 22, 10891–10897.

Manis, P. B. (1989). Responses to parallel fiber stimulation in the guinea pig dorsal cochlear nucleus in vitro. *J. Neurophysiol.* 61, 149–161.

Markovitz, C. D., Tang, T. T., and Lim, H. H. (2013). Tonotopic and localized pathways from primary auditory cortex to the central nucleus of the inferior colliculus. *Front. Neural Circuits* 7:77. doi: 10.3389/fncir.2013.00077

Meltzer, N. E., and Ryugo, D. K. (2006). Projections from auditory cortex to cochlear nucleus: a comparative analysis of rat and mouse. *Anat. Rec. A Discov. Mol. Cell. Evol. Biol.* 288, 397–408. doi: 10.1002/ar.a.20300

Mugnaini, E., Warr, W. B., and Osen, K. K. (1980). Distribution and light microscopic features of granule cells in the cochlear nuclei of cat, rat and mouse. *J. Comp. Neurol.* 191, 581–606. doi: 10.1002/cne.901910406

Mulders, W. H. A. M., and Robertson, D. (2009). Hyperactivity in the auditory midbrain after acoustic trauma: dependence on cochlear activity. *Neuroscience* 164, 733–746. doi: 10.1016/j.neuroscience.2009.08.036

Nakamoto, K. T., Jones, S. J., and Palmer, A. R. (2008). Descending projections from auditory cortex modulate sensitivity in the midbrain to cues for spatial position. *J. Neurophysiol.* 99, 2347–2356. doi: 10.1152/jn.01326.2007

Oertel, D., and Wu, S. H. (1989). Morphology and physiology of cells in slice preparations of the dorsal cochlear nucleus of mice. *J. Comp. Neurol.* 283, 228–247. doi: 10.1002/cne.902830206

Peterson, D. C., and Schofield, B. R. (2007). Projections from auditory cortex contact ascending pathways that originate in the superior olive and inferior colliculus. *Hear. Res.* 232, 67–77. doi: 10.1016/j.heares.2007.06.009

Redies, H., and Brandner, S. (1991). Functional organisation of the auditory thalamus in the guinea pig. *Exp. Brain Res.* 86, 384–392. doi: 10.1007/bf00228962

Rodrigues-Dageff, C., Simm, G., de Ribaupierre, Y., Villa, A., de Ribaupierre, F., and Rouiller, E. M. (1989). Functional organisation of the ventral division of the medial geniculate body of the cat: evidence for a rostro-caudal gradient of response properties and cortical projections. *Hear. Res.* 39, 103–125. doi: 10.1016/0378-5955(89)90085-3

Roger, M., and Arnault, P. (1989). Anatomical study of the connections of the primary auditory area in the rat. *J. Comp. Neurol.* 287, 339–356. doi: 10.1002/cne.902870306

Ryugo, D. K., Haenggeli, C. A., and Doucet, J. R. (2003). Multimodal inputs to the granule cell domain of the cochlear nucleus. *Exp. Brain Res.* 153, 477–485. doi: 10.1007/s00221-003-1605-3

Ryugo, D. K., and Willard, F. H. (1985). The dorsal cochlear nucleus of the mouse: a light microscopic analysis of neurons that project to the inferior colliculus. *J. Comp. Neurol.* 242, 381–396. doi: 10.1002/cne.902420307

Sakai, M., and Suga, N. (2001). Plasticity of the cochleotopic (frequency) map in specialized and nonspecialized auditory cortices. *Proc. Natl. Acad. Sci. U S A* 98, 3507–3512. doi: 10.1073/pnas.061021698

Saldaña, E., Feliciano, M., and Mugnaini, E. (1996). Distribution of descending projections from primary auditory neocortex to inferior colliculus mimics the topography of intracollicular projections. *J. Comp. Neurol.* 371, 15–40. doi: 10.1002/(sici)1096-9861(19960715)371:1<15::aid-cne2>3.0.co;2-o

Schofield, B. R., and Coomes, D. L. (2005a). Auditory cortical projections to the cochlear nucleus in guinea pigs. *Hear. Res.* 199, 89–102. doi: 10.1016/j.heares.2004.08.003

Schofield, B. R., and Coomes, D. L. (2005b). Projections from auditory cortex contact cells in the cochlear nucleus that project to the inferior colliculus. *Hear. Res.* 206, 3–11. doi: 10.1016/j.heares.2005.03.005

Schofield, B. R., Coomes, D. L., and Schofield, R. M. (2006). Cells in auditory cortex that project to the cochlear nucleus in guinea pigs. *J. Assoc. Res. Otolaryngol.* 7, 95–109. doi: 10.1007/s10162-005-0025-4

Snyder, R. L., and Leake, P. A. (1988). Intrinsic connections within and between cochlear nucleus subdivisions in cat. *J. Comp. Neurol.* 278, 209–225. doi: 10.1002/cne.902780205

Tang, J., Yang, W., and Suga, N. (2012). Modulation of thalamic auditory neurons by the primary auditory cortex. *J. Neurophysiol.* 108, 935–942. doi: 10.1152/jn.00251.2012

Webster, D. B., and Trune, D. R. (1982). Cochlear nuclear complex of mice. *Am. J. Anat.* 163, 103–130. doi: 10.1002/aja.1001630202

Weedman, D. L., and Ryugo, D. K. (1996a). Projections from auditory cortex to the cochlear nucleus in rats: synapses on granule cell dendrites. *J. Comp. Neurol.* 371, 311–324. doi: 10.1002/(sici)1096-9861(19960722)371:2<311::aid-cne10>3.0.co;2-v

Weedman, D. L., and Ryugo, D. K. (1996b). Pyramidal cells in primary auditory cortex project to cochlear nucleus in rat. *Brain Res.* 706, 97–102. doi: 10.1016/0006-8993(95)01201-x

Wickesberg, R. E., and Oertel, D. (1988). Tonotopic projection from the dorsal to the anteroventral cochlear nucleus of mice. *J. Comp. Neurol.* 268, 389–399. doi: 10.1002/cne.902680308

Willott, J. F. (2001). *Handbook of Mouse Auditory Research.* Boca Raton, FL: CRC Press.

Willott, J. F., Bross, L. S., and McFadden, S. L. (1992). Morphology of the dorsal cochlear nucleus in C57BL/6J and CBA/J mice across the life span. *J. Comp. Neurol.* 321, 666–678. doi: 10.1002/cne.903210412

Winer, J. A., Chernock, M. L., Larue, D. T., and Cheung, S. W. (2002). Descending projections to the inferior colliculus from the posterior thalamus and the auditory cortex in rat, cat and monkey. *Hear. Res.* 168, 181–195. doi: 10.1016/S0378-5955(02)00489-6

Winer, J. A., Diehl, J. J., and Larue, D. T. (2001). Projections of auditory cortex to the medial geniculate body of the cat. *J. Comp. Neurol.* 430, 27–55. doi: 10.1002/1096-9861(20010129)430:1<27::aid-cne1013>3.0.co;2-8

Winer, J. A., Larue, D. T., Diehl, J. J., and Hefti, B. J. (1998). Auditory cortical projections to the cat inferior colliculus. *J. Comp. Neurol.* 400, 147–174. doi: 10.1002/(sici)1096-9861(19981019)400:2<147::aid-cne1>3.3.co;2-v

Wu, Y., and Yan, J. (2007). Modulation of the receptive fields ofmidbrain neurons elicited by thalamic electrical stimulation through corticofugal feedback. *J. Neurosci.* 27, 10651–10658. doi: 10.1523/jneurosci.1320-07.2007

Yan, J., and Ehret, G. (2001). Corticofugal reorganization of the midbrain tonotopic map in mice. *Neuroreport* 12, 3313–3316. doi: 10.1097/00001756-200110290-00033

Yan, J., and Ehret, G. (2002). Corticofugal modulation of midbrain sound processing in the house mouse. *Eur. J. Neurosci.* 16, 119–128. doi: 10.1046/j.1460-9568.2002.02046.x

Yan, J., and Suga, N. (1996). Corticofugal modulation of time-domain processing of biosonar information in bats. *Science* 273, 1100–1103. doi: 10.1126/science.273.5278.1100

Yan, J., and Suga, N. (1999). Corticofugal amplification of facilitative auditory responses of subcortical combination-sensitive neurons in the mustached bat. *J. Neurophysiol.* 81, 817–824.

Yan, J., Zhang, Y., and Ehret, G. (2005). Corticofugal shaping of frequency tuning curves in the central nucleus of the inferior colliculus of mice. *J. Neurophysiol.* 93, 71–83. doi: 10.1152/jn.00348.2004

Yan, J., Zhang, Y., Jia, Z., Taverna, F., McDonald, R., Muller, R., et al. (2002). Place-cell impairment in glutamate receptor 2 mutant mice. *J. Neurosci.* 22:RC204.

Yan, W., and Suga, N. (1998). Corticofugal modulation of the midbrain frequency map in the bat auditory system. *Nat. Neurosci.* 1, 54–58. doi: 10.1038/255

Young, E. D., Nelken, I., and Conley, R. A. (1995). Somatosensory effects on neurons in dorsal cochlear nucleus. *J. Neurophysiol.* 73, 743–765.

Young, E. D., Spirou, G. A., Rice, J. J., and Voigt, H. F. (1992). Neural organization and responses to complex stimuli in the dorsal cochlear nucleus. *Philos. Trans. R. Soc. Lond. B Biol. Sci.* 336, 407–413. doi: 10.1098/rstb.1992.0076

Zhang, J. S., and Kaltenbach, J. A. (1998). Increases in spontaneous activity in the dorsal cochlear nucleus of the rat following exposure to high-intensity sound. *Neurosci. Lett.* 250, 197–200. doi: 10.1016/s0304-3940(98)00482-0

Zhang, S., and Oertel, D. (1993a). Cartwheel and superficial stellate cells of the dorsal cochlear nucleus of mice: intracellular recordings in slices. *J. Neurophysiol.* 69, 1384–1397.

Zhang, S., and Oertel, D. (1993b). Giant cells of the dorsal cochlear nucleus of mice: intracellular recordings in slices. *J. Neurophysiol.* 69, 1398–1408.

Zhang, S., and Oertel, D. (1993c). Tuberculoventral cells of the dorsal cochlear nucleus of mice: intracellular recordings in slices. *J. Neurophysiol.* 69, 1409–1421.

Zhang, Y., and Suga, N. (2000). Modulation of responses and frequency tuning of thalamic and collicular neurons by cortical activation in mustached bats. *J. Neurophysiol.* 84, 325–333.

Zhang, Y., and Suga, N. (2005). Corticofugal feedback for collicular plasticity evoked by electric stimulation of the inferior colliculus. *J. Neurophysiol.* 94, 2676–2682. doi: 10.1152/jn.00549.2005

Zhang, Y., Hakes, J. J., Bonfield, S. P., and Yan, J. (2005). Corticofugal feedback for auditory midbrain plasticity elicited by tones and electrical stimulation of basal forebrain in mice. *Eur. J. Neurosci.* 22, 871–879. doi: 10.1111/j.1460-9568.2005.04276.x

Conflict of Interest Statement: The authors declare that the research was conducted in the absence of any commercial or financial relationships that could be construed as a potential conflict of interest.

Received: 18 May 2014; accepted: 16 June 2014; published online: 01 July 2014.
Citation: Kong L, Xiong C, Li L and Yan J (2014) Frequency-specific corticofugal modulation of the dorsal cochlear nucleus in mice. Front. Syst. Neurosci. ***8****:125. doi: 10.3389/fnsys.2014.00125*
This article was submitted to the journal Frontiers in Systems Neuroscience.

frontiers in
SYSTEMS NEUROSCIENCE

ORIGINAL RESEARCH ARTICLE
published: 20 January 2015
doi: 10.3389/fnsys.2014.00253

Acoustic input and efferent activity regulate the expression of molecules involved in cochlear micromechanics

Veronica Lamas[1], Juan C. Arévalo[1], José M. Juiz[2] and Miguel A. Merchán[1]*

[1] *Laboratory of Neurobiology of Hearing, Institute for Neuroscience of Castilla y Leon, University of Salamanca, Salamanca, Spain*
[2] *Facultad de Medicina de Albacete, Instituto de Investigación en Discapacidades Neurológicas (IDINE), Universidad de Castilla La Mancha, Albacete, Spain*

Edited by:
Paul Hinckley Delano, Universidad de Chile, Chile

Reviewed by:
Jiri Popelar, Institute of Experimental Medicine AS CR, Czech Republic
Maria Eugenia Gomez-Casati, INGEBI-CONICET Buenos aires, Argentina

***Correspondence:**
Miguel A. Merchán, Laboratory of Neurobiology of Hearing, Institute for Neuroscience of Castilla y Leon, University of Salamanca, Pintor Fernando Gallego 1, 37007 Salamanca, Spain
e-mail: merchan@usal.es

Electromotile activity in auditory outer hair cells (OHCs) is essential for sound amplification. It relies on the highly specialized membrane motor protein prestin, and its interactions with the cytoskeleton. It is believed that the expression of prestin and related molecules involved in OHC electromotility may be dynamically regulated by signals from the acoustic environment. However little is known about the nature of such signals and how they affect the expression of molecules involved in electromotility in OHCs. We show evidence that prestin oligomerization is regulated, both at short and relatively long term, by acoustic input and descending efferent activity originating in the cortex, likely acting in concert. Unilateral removal of the middle ear ossicular chain reduces levels of trimeric prestin, particularly in the cochlea from the side of the lesion, whereas monomeric and dimeric forms are maintained or even increased in particular in the contralateral side, as shown in Western blots. Unilateral removal of the auditory cortex (AC), which likely causes an imbalance in descending efferent activity on the cochlea, also reduces levels of trimeric and tetrameric forms of prestin in the side ipsilateral to the lesion, whereas in the contralateral side prestin remains unaffected, or even increased in the case of trimeric and tetrameric forms. As far as efferent inputs are concerned, unilateral ablation of the AC up-regulates the expression of α10 nicotinic Ach receptor (nAChR) transcripts in the cochlea, as shown by RT-Quantitative real-time PCR (qPCR). This suggests that homeostatic synaptic scaling mechanisms may be involved in dynamically regulating OHC electromotility by medial olivocochlear efferents. Limited, unbalanced efferent activity after unilateral AC removal, also affects prestin and β-actin mRNA levels. These findings support that the concerted action of acoustic and efferent inputs to the cochlea is needed to regulate the expression of major molecules involved in OHC electromotility, both at the transcriptional and posttranscriptional levels.

Keywords: prestin oligomerization, acetylcholine α10 receptors, auditory cortex ablation, conductive hearing loss, descending control

INTRODUCTION

Electromotility of outer hair cells (OHCs) in the organ of Corti is essential for active mechanical amplification of sound signals (Elgoyhen and Franchini, 2011). Somatic electromotility, i.e., the ability of OHCs to shorten or elongate in response to membrane voltage changes, depends on the unique properties of the membrane motor protein Prestin, whose voltage-dependent conformational changes are transferred to the actin cytoskeleton, a final effector of OHC micromechanical activation. The molecular structure of Prestin, its mechanisms and role in OHC electromotility, have been extensively studied (He et al., 2014). However, the complexity and extremely fast speed rates of operation of Prestin in particular and electromotility mechanisms in general, raise questions about regulation by incoming signals and possible adaptations to altered auditory input. There is some evidence that conductive hearing loss induces up-regulation of prestin mRNA (Mazurek et al., 2007; Yu et al., 2008; Yang et al., 2009). Up regulation of Prestin also has been reported after noise-induced hearing loss in preserved regions of the organ of Corti, consistent with compensatory mechanisms to stabilize thresholds and frequency discrimination (Xia et al., 2013).

Descending central feedback channeled through the efferent olivocochlear system is a major dynamic modulator of OHC electromotility and hence cochlear amplification (Elgoyhen and Franchini, 2011). Activity of medial olivocochlear cell (MOC) fibers acting on OHCs contributes to adapt cochlear gain by adjusting cochlear amplification. This effect is mediated by acetylcholine (Ach) released by MOC endings at the base of OHCs. Ach binds to a postsynaptic nicotinic Ach receptor (nAchR) assembled from α9 and α10 subunits whose activation hyperpolarizes OHCs. Ach-mediated hyperpolarization of OHCs has been linked to changes in axial electromotility amplitude and OHC compliance (He and Dallos, 1999, 2000).

Convergence of acoustic input and efferent connections on OHCs, raises the possibility that the expression of proteins involved in somatic electromotility is dynamically balanced by the interaction of signals from the acoustic environment and ongoing feedback from descending efferent inputs, primarily from MOC. To test this hypothesis, we compared the effects of a conductive unilateral hearing loss induced by removal of the ossicular chain (Sumner et al., 2005) with that of a partial deactivation of MOC activity by restricted ablation of the auditory cortex (AC). Previous work from our laboratory supports that in the rat AC restricted ablations induce a reversible deafness likely through descending, corticofugal control of MOC fibers (Lamas et al., 2013).

We tested changes in Prestin protein expression by Western blot after unilateral conductive hearing loss as a measure of regulation by acoustic input imbalance, and compared this with changes in Prestin protein expression after unilateral AC ablation. In parallel, because OHC electromotility regulation by MOC involves specialized cholinergic neurotransmission, we tested by qRT-PCR whether the expression of the alpha10 nAChR gene mRNA, a staple of cholinergic neurotransmission at the MOC-OHC synapse (Dallos et al., 1997; Maison et al., 2002, 2007; Batta et al., 2004; Vetter et al., 2007), changes along with the expression of Prestin and β-actin genes, as cell markers of the effects of MOC inactivation on OHC electromotility.

METHODS

This study was carried out in accordance with Spanish (Royal Decree 53/2013-Law 32/2007) and European Union (Directive 2010/63/EU) regulations on the care and use of animals in biomedical research.

Sixty eight young male Wistar rats weighing between 250–300 g were used in this study. One set of 12 animals was used in experiments of middle ear ossicle removal. Eight animals underwent surgical removal of the ossicular chain as described below, and were randomly assigned to one of two post-surgery day (PSD) survival groups, 7 PSD (n = 4) or 15 PSD (n = 4). The remaining animals were assigned to the normal control group (n = 4). For the cortical ablation experiments, a total of 49 animals were used. Forty-two underwent AC surgical removal, and were randomly assigned to one of three survival time groups: 1, 7 or 15 PSD (n = 14 for each PSD). The remaining 14 animals were used as normal controls.

SURGICAL PROCEDURES

The AC ablations were performed under deep anesthesia using a mixture of ketamine chlorhydrate (30 mg/kg Imalgene 1000, Rhone Méreuse, Lyon, France) and xylazine chlorhydrate (5 mg/Kg, Rompun, Bayer, Leverkusen, Germany), as previously described in Lamas et al. (2013). The animals were returned to their cages after the ablations, carefully monitoring post-surgery recovery. Once the corresponding lesion survival time was completed, animals were anesthetized with 0.1 ml of sodium Pentobarbitol injected intraperitoneally (ip), and decapitated in order to collect the brain and the cochleae. After this, brains were immersed in 4% p-formaldehyde whereas the cochleae were immediately frozen in liquid nitrogen for qRT-PCR or Western blotting, as described below in detail.

The middle ear ossicular chain removal was performed under the same anesthetic cocktail and conditions. The left external acoustic meatus was exposed under microscopy control. The eardrum was punctured with the aid of a needle and the ossicular chain removed by extraction with tweezers. After surgery, the presence of an intact footplate attached to the oval window was confirmed under the microscope. Animals were returned to their cages after the ablations, carefully monitoring the post-surgery recovery. Once the corresponding post lesional survival times were completed, animals were anesthetized with 0.1 ml sodium Pentobarbitol, ip, and decapitated in order to collect the cochleae.

Once collected the cochleae were immediately frozen in liquid nitrogen for Western blotting.

RNA EXTRACTION

To study expression of target mRNAs with qRT-PCR, total RNA was purified from the collected and homogenized cochleae using TRIZOL® (Gibco BRL, Gaithersburg, MD, USA) following the manufacturer's protocol and a column from an RNeasy mini kit (Qiagen, Valencia, CA, USA) according to manufacturer's instructions. RNA concentrations were determined using a NanoDrop ND-1000 spectrophotometer (NanoDrop Technologies Inc., Wilmington, USA). Each RNA sample was assayed three times and an average value was determined. RNA quality was assessed on an RNA 6000 NanoLabChip (Agilent Technologies, Palo Alto, CA, USA), using an Agilent 2100 Bioanalyzer to assess the integrity of the 18S and 28S rRNA bands, and an RNA integrity number (RIN) was assigned, with 0 corresponding to fully degraded RNA and 10 corresponding to intact RNA. For all Quantitative real-time PCR (qPCR), only RNA samples with RIN of at least 7.5 were used, with the vast majority of samples having a RIN of at least 8.0. These values meet requirements for reproductible qPCR experiments (Fleige et al., 2006).

QUANTITAVE REAL-TIME PCR

RNA (2 μg), primed with oligo-dT, was reverse-transcribed into cDNA at 37°C for 2 h using the first-strand cDNA synthesis kit (Promega Corporation, Madison, WI, USA) in a 20 μl volume, and stored at −20°C until use, according to manufacturer's instructions. In all cases, a reverse transcriptase negative control was used for testing genomic DNA contamination.

qPCR was performed using the SYBR-Green method with a 2 × Master Mix (Applied Biosystems). Each reaction contained 10 μl of Master Mix, 0.4 μl of each pair of primers (**Table 1**), 3 μl of each cDNA sample in a different serial cDNA quantity for each gene, and MilliQ-grade water up to 20 μl. The amplification reaction took place in an ABI Prism 7000 detection system (Applied Biosystems), with the following conditions: 10 min at 95°C followed by 40 cycles of 15 s at 95°C and 1 min at 60°C depending on each pair of primers. Three PCR reactions were performed for each sample per plate, and each experiment was repeated twice. The ribosomal protein L-19 endogenous gene was used as reference gene.

Table 1 | Primers used in the RT-qPCR study.

Gen	GenBank number	Primer forward	cDNA forward*	Primer reverse	cDNA reverse*	Product size	Slope	E**	R^2
b-act	NM_031144	AGCCATGTACGTAGCCATCC	468–488	ACCCTCATAGATGGGCACAG	563–582	115	−3.15	107.4	0.996
Chrna10	NM_022639	CCTCACCTATGGCTGCTGCT	702–721	GCCAGCAGGGAGATGAACAC	805–824	123	−3.03	113.8	0.993
Prestin	NM_030840	GATTGGAGGTGTGGCCTGTCC	429–448	ACGGACATGGCGACTTTGAC	526–545	117	−3.11	109.6	0.995

**Location of the primers for the rat sequency in the Gene Bank. **Amplification efficiency.*

The comparative threshold cycle (Ct) method was used to collect quantitative data (Schmittgen and Livak, 2008). Following the removal of outliers, raw fluorescence data were used to determine the PCR amplification efficiency (E) according to the formula $E = [10^{(-1/slope)} - 1]*100$. All amplifications had an E value of 100 ± 10%, the E value close to 100% being an indicator of efficient amplification. The relative gene expression value ("fold change") for each transcript was calculated according to the equation $E^{-(\Delta Ct\ \text{"condition 1"} - \Delta Ct\ \text{"condition 2"})}$, where "condition 1" corresponds to experimental samples (PSD1, 7 and 15), "condition 2" to samples of control animals and ΔCt of each "condition" is $Ct_{\text{"experimental gene"}} - Ct_{\text{"endogenous gene"}}$ (Livak and Schmittgen, 2001; Schmittgen and Livak, 2008). A standard error for each relative gene expression value was calculated as a measure of data variation.

WESTERN-BLOT

Western blot analyses were performed according to Yu et al. (2011) with slight modifications. The cochleae were lysed in a lysis buffer (5 mM Tris pH 6.8, 2% SDS, 2 mM EDTA, 2 mM EGTA, 1 mM phenylmethylsulfonyl fluoride, 1 μg/mL aprotinin, 2 μg/mL leueptine, 1 mM vanadate, 10 mM sodium fluoride and 20 mM β-glycerophosphate) for 1 h at 4°C with gentle shaking and then centrifuged at 13000 × g for 15 min to eliminate debris. Protein concentration was quantified using Qubit Fluorometric quantification (Life Technologies). Lysates were added 5x SDS buffer and boiled for 6 min to denature the proteins. Proteins (20 μg/sample) were resolved by 7.5% SDS–PAGE and Western blots were performed with antibodies against the different proteins. Blots were developed in WesternBrigth ECL detection kit (Advansta). Films were digitized using an Epson V750 scanner.

Antibodies used were anti-Prestin (1:500) made in rabbit, a kind gift from Dr. Bechara Kachar (Laboratory of Cell Structure and Dynamics, National Institute on Deafness and Other Communication Disorders, NIH, Bethesda, Maryland), anti-beta tubulin (1:4000) and anti-actin (1:4000) from Sigma.

ABR RECORDINGS

ABRs were recorded immediately before and after removal of the ossicular chain, and 7 days post injury. Recordings were performed using a close-field real-time signal processing system (Tucker-Davis Technologies (TDT), System 3, Alachua, Fl, USA), as previously described in Lamas et al. (2013).

On the side of the ossicle chain removal, the four characteristic waves of the rat ABR disappeared, thresholds were increased up to 90 dB SPL and did not show any recovery 7 days after the surgery (**Figure 1**). Fifteen days after the injury, waves were visible at 80 dB SPL. The side contralateral to the experimental lesion showed ABR thresholds similar to those of pre-lesion condition at all post lesional times (**Figure 1**). The amplitude of the four waves for this side was increased by 50–100% relative to pre-lesion condition at 15 PSD.

Changes in the ABR from animals with unilateral ablations of the AC have been previously described in Lamas et al. (2013). Briefly, on the side of the lesion the amplitude of the waves was decreased by 25–40% relative to pre-lesion condition at 1 PSD, and recovered at 7 PSD. The side contralateral to the ablation showed ABR amplitudes similar to those of pre-lesion condition at all post-lesion times.

STATISTICAL ANALYSIS

Real-time PCR results are shown as mean ± SD and were tested for significance using one-way ANOVA with Scheffe and Bonferroni *post hoc* tests. Ipsi- vs. contralateral statistical comparisons were carried out with Student's *t*-test. Differences were considered significant at the $p < 0.05$ level. Statistical analysis was performed using the SPSS-IBM software, version 20 (SPSS Inc., Chicago, IL, USA).

LOCALIZATION OF THE LESIONS IN AC

The localization of the lesions in AC was performed as described in Lamas et al. (2013). Briefly, after perfusion fixation and brain removal, the lateral surface of the brain was photographed using a Nikon camera located 21 cm above the cortex surface, and the photograph was superimposed to a purposely built coordinates map (Lamas et al., 2013). The extension of the lesion expressed in percent area of AC was calculated using the "area dimensioning tool" of Canvas X software (Lamas et al., 2013).

All ablations specifically encroached the major subdivisions of the AC (primary, dorsal and ventral cortices), and affected all AC layers but not the underlaying white matter. Lesions included a region ranging from 70 to 100% of the total AC area (**Table 2**).

RESULTS

PRESTIN PROTEIN OLIGOMERIZATION AFTER SOUND ATTENUATION BY UNILATERAL MIDDLE EAR OSSICLE REMOVAL

Western blotting was performed to assess oligomerization and relative amount of Prestin protein in the cochlea at two survival times (7 or 15 PSD) after unilateral removal of the middle ear ossicles. Protein levels in the sides ipsi- and contralateral to

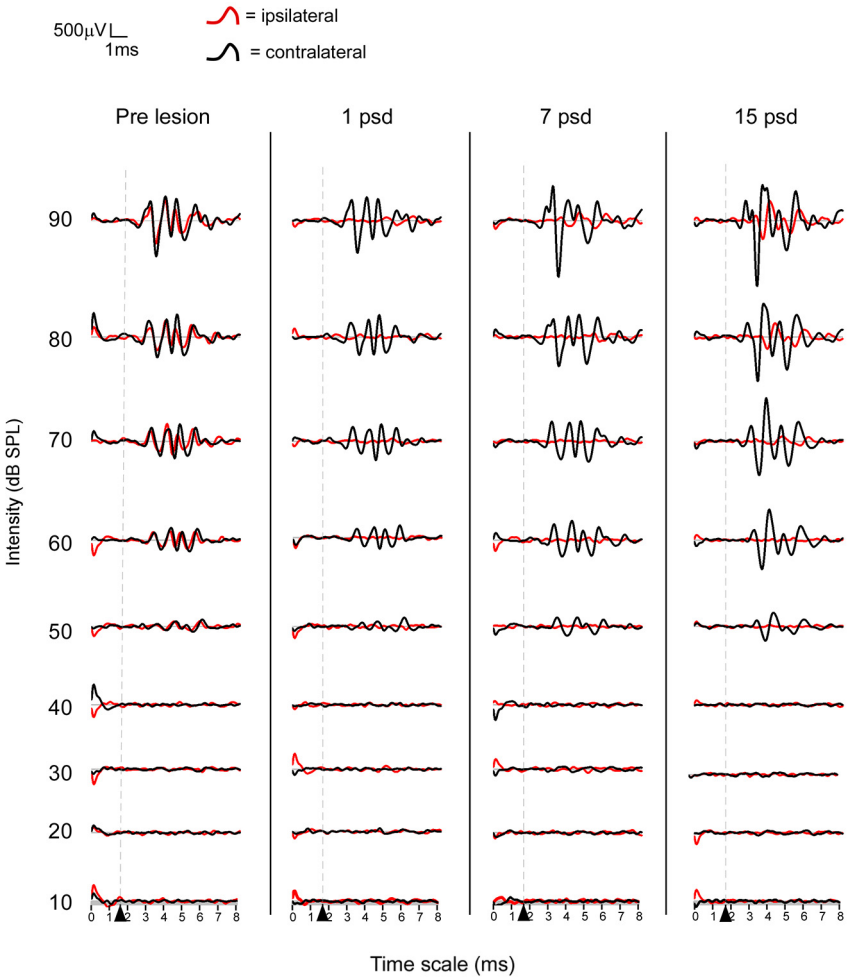

FIGURE 1 | Average ABR waveform obtained before and after the unilateral removal of the ossicular chain at different post surgery days (PSD), 1, 7 and 15. The stimulus onset starts at 1.7 ms and all waves were visible at 50 dB SPL in both ears before the lesion. Note that only waves from the contralateral ear to the surgery remain visible at 50 dB SPL after the lesion.

Table 2 | Extent of lesions in the rat brain AC.

Post surgery days	Percentage of AC ablated (WB study)	Percentage of AC ablated (RT-qPCR study)
1	73.33 ± 20.12	71.79 ± 8.33
7	75.73 ± 6.89	76.81 ± 9.24
15	81.79 ± 11.09	72.99 ± 5.27

This table shows the percentage of AC affected by lesions in the experimental groups. Data are presented by Mean ± standard deviation. WB = Western Blott. RT-qPCR = Reverse Transcription quantitative polymerase chain reaction.

the lesion were compared. After blotting cochlear samples with antiprestin antibodies, Prestin was displayed in Western blots from control animals in bands corresponding mostly to 80, 160 and 240 kDa (**Figure 2**—7 PSD, control animals on the two left tracks), in accordance with the reported molecular weights of the monomers, dimers and trimers of this protein, respectively (Matsuda et al., 2004).

There were no major differences in the pattern of immunoblot staining between both survival groups after middle ear ossicle removal. **Figure 2** shows Western blots from three representative cases at 7 PSD. Western blots from animals at 15 PSD are not shown. Bands corresponding to Prestin monomers in animals after ossicle removal were comparable to those seen in control animals, regardless of survival time (**Figure 2**, lower arrow). However, the bands corresponding to prestin dimers (160 kDa) stood out more strongly labeled in animals with unilateral conductive deafness. This 160 kDa band was more marked in the side contralateral to the lesioned ear (**Figure 2**, second arrow from bottom). In general, bands corresponding to trimers were attenuated or absent at 7 and 15 PSD both in the cochleae ipsi- and contralateral to the lesion. Interestingly, however, in one case at 7 PSD after unilateral ossicle chain removal, the band corresponding to prestin trimers in the cochlea contralateral to the lesion, was comparable in intensity to that of controls (**Figure 2**, third arrow from the bottom).

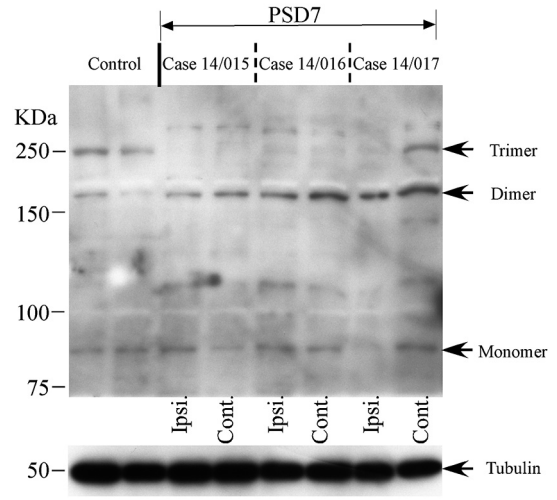

FIGURE 2 | Changes in prestin protein expression after unilateral removal of the ossicular chain. Results from the ipsilateral (Ipsi.) and contralateral (Cont.) cochleae from three animals at 7 days after surgery (PSD7). The two tracks on the left are from two normal control animals.

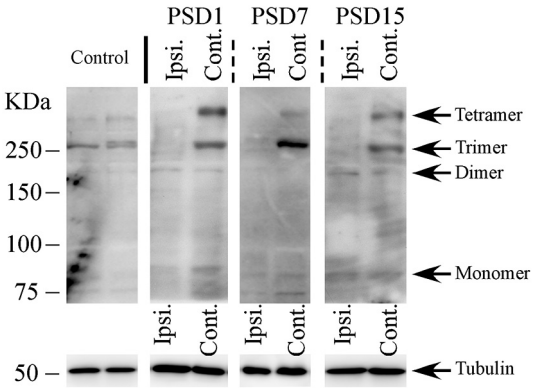

FIGURE 3 | Changes in the protein expression of prestin after unilateral ablation of AC at different post surgery days (PSD). Data represent the western blott results from both ipsilateral and contralateral ears to the surgery obtained at PSD1, 7 and 15. Ipsi = ipsilateral ear to the surgery. Contr. = contralateral ear to the surgery.

Bands corresponding to the potential localization of tetramers (320 kDa) were faint or undetectable either in controls or in the conductive deafness experimental group at any survival time.

PRESTIN PROTEIN OLIGOMERIZATION AFTER ATTENUATION OF DESCENDING INPUT TO THE COCHLEA BY UNILATERAL AC ABLATION

The effects of unilateral AC ablation on the oligomerization and relative amount of prestin protein in the cochlea, were also tested by Western blot. In the cochleae ipsilateral to the AC lesion, there were no immunolabeled bands above 160 KDa, indicating disappearance of trimeric Prestin forms relative to controls, with tetrameric forms being absent, like in control animals. Bands corresponding to monomers and dimers were unchanged relative to controls (**Figure 3**).

Western blot analysis of the cochleae contralateral to the AC lesion showed a banding pattern for monomers and dimers similar to that found in the ipsilateral side and therefore comparable to control cochleae. However, different to the ipsilateral side, dense bands at the 240 kDa location, corresponding to an intense expression of Prestin trimers were detected in most animals (**Figure 3**) at all survival times. A band at 320 kDa corresponding to Prestin tetramers was also visible in the side contralateral to the lesion.

No major differences were seen in the patterns of Prestin expression detected by Western blot at any of the three tested survival times, 1, 7 or 15 PSD (**Figure 3**).

nAchR α10-SUBUNIT, PRESTIN AND BETA-ACTIN mRNA LEVELS AFTER PARTIAL INACTIVATION OF DESCENDING INPUT TO THE COCHLEA BY AC ABLATION

We carried out qRT-PCR to assess changes in the expression of the α10-subunit of the OHC nAChR, Prestin and β-actin mRNA in the cochlea ipsi and contralateral to the lesion at different times after AC ablations. Collectively, these three markers should give an indication of how partial inactivation of MOC affects the molecular machinery of the OHC involved in electromotility.

The α10-subunit transcripts of the nAChR showed a significant decrease in the cochleae ipsilateral to the lesion at 1 PSD after the AC ablation (**Figure 4A**). However, both at 7 and 15 PSD, α10 mRNA levels were significantly increased (**Figure 4A** gray bars). The increase in the α10-subunit transcripts was above two fold relative to control values at 7 PSD and above four fold at 15 PSD (**Figure 4A**).

The cochleae contralateral to the lesion did not show statistically significant changes in the expression of the α10 subunit at 1 PSD. However, both at 7 PSD and 15 PSD α10 mRNA levels were increased. These increases were four fold relative to control values at 7 PSD, and two fold at 15 PSD, respectively (**Figure 4A** white bars).

Prestin transcripts showed a significant threefold increase relative to control values in the cochlea ipsilateral to the lesion, at 1 PSD (**Figure 4B** gray bar). Increased transcript levels were even larger at 7 PSD, reaching six fold relative to controls, and returned to values similar to those of controls at 15 PSD (**Figure 4B** gray bars).

The cochlea contralateral to the lesion did not show any significant change in the expression of prestin at 1 PSD. An eight fold increase relative to control values was found at 7 PSD whereas at 15 PSD there was a significant decrease below control values (**Figure 4B** white bars).

The analysis of β-actin transcripts showed a significant decrease relative to control values in the cochlea ipsilateral to the lesion at 1 PSD following AC ablation. β-actin transcript levels returned to values comparable to those of controls at 7 PSD and decreased again at 15 PSD ($p < 0.001$)

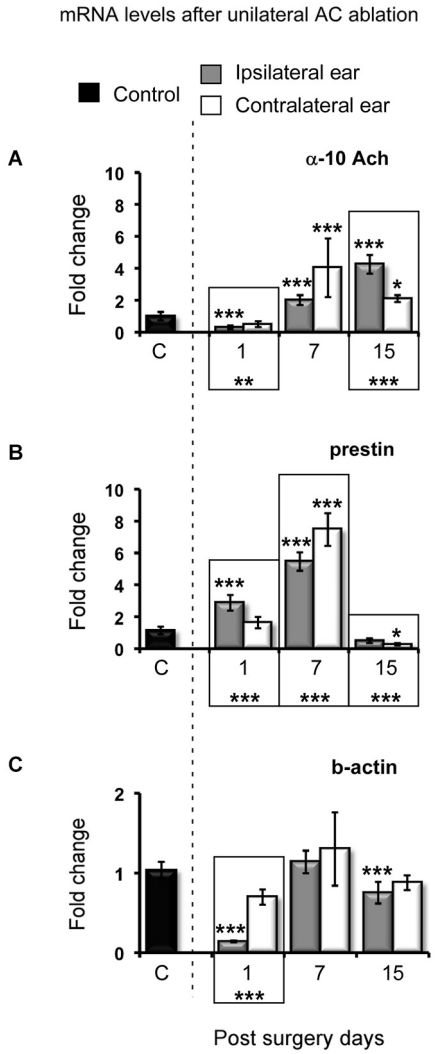

FIGURE 4 | Changes in the mRNA levels of α-10 subunit, prestin and β-actin after unilateral AC ablations at different post surgery days, 1, 7 and 15. **(A)** Data of the *α-10 subunit* from the outer hair cell cholinergic receptor. **(B)** Data of *prestin*. **(C)** Data of β-*actin*. Results are presented by the mean ± stdev of the fold change. The statistical significance of the comparison between the fold changes of the post-surgery days and control condition is shown at the top of the bars. Bars from the same survival time that present differences between the ipsi- and contralateral ears are framed in a box, and their statistical significance is shown at the bottom. $*p < 0.05$; $**p < 0.01$; $***p < 0.001$.

(**Figure 4C** gray bars). No statistically significant changes were found in the expression of the β-actin gene in the contralateral cochlea at any PSD after AC ablation (**Figure 4C** white bars).

DISCUSSION

The first key finding reported in this paper is that oligomerization of the OHC membrane motor protein Prestin is regulated by the interaction of acoustic input and centrifugal efferent cholinergic neurotransmission on OHCs.

In the normally functioning auditory receptor, monomeric and oligomeric forms of Prestin coexist, as shown in Western blots from control animals (see **Figures 2**, **3**). Prestin oligomers include mostly dimers and trimers, whereas tetrameric forms are barely detectable in cochlear homogenates from control animals. The absence of tetrameric forms in our control Western blots is compatible with current views of Prestin oligomerization. Whereas tetramers may actually be present but not detectable in our control cochleae, the view that prestin functions strictly as a tetramer (Hallworth and Nichols, 2012) has been seriously challenged. Correlative electrophysiological and dynamic fluorescence measurements suggest that sub-tetrameric oligomers, or even monomers, are functional (Bian et al., 2013) and not mere precursors for the assembly of tetramers.

Dampened acoustic input subsequent to unilateral middle ear ossicle removal, diminishes prestin trimers, often below detection levels, in Western blots from cochleae in the side of the lesion. Dimeric forms, however, are preserved or even increased. These findings suggest that Prestin oligomerization beyond dimers requires normal acoustic input. Actually, Xia et al. (2013) have reported global increases in Prestin protein levels in the cochlea after noise-induced hearing loss, but these authors did not provide evidence as to whether such an increase was attributable to monomers or one or several oligomeric forms. The mechanism and role of this activity-dependent oligomerization will have to be elucidated. Shutting off oligomerization of larger Prestin forms while simultaneously increasing dimeric forms, might represent a mechanism to adapt cochlear micromechanics and amplification to diminished acoustic stimuli. On the other hand, the finding of relatively more dense dimeric bands in the cochlea contralateral to the lesion along with less frequent loss of trimers, may be related to subtle compensatory changes in the unmanipulated cochlea, driven by acoustic input imbalance between both ears, as discussed further in detail.

A second most relevant finding is that activity of the cochlear efferent system is also required to regulate Prestin oligomeric assembly. Evidence comes from results of ablation of the AC. Descending projections are complex, and include direct corticopontine and indirect colliculopontine pathways. At least corticopontine projections, are bilateral and symmetric, although more dense in the ipsilateral side (Doucet et al., 2002; Doucet and Ryugo, 2003; Schofield and Coomes, 2005), and innervate MOC in the ventral nucleus of the trapezoid body (Mulders and Robertson, 2000). MOC, in turn, send efferent axons bilaterally to OHCs, modulating its micro-mechanical properties (Guinan, 2006). Due to the excitatory nature of the corticofugal projection (Feliciano and Potashner, 1995), its degeneration after unilateral AC ablation induces loss of excitation on MOC, more marked in the ipsilateral side and, therefore an imbalance of efferent input between both ears (León et al., 2012).

After unilateral ablation of the AC, Prestin trimers were barely detectable in the cochlea ipsilateral to the lesion, whereas monomer and dimer bands were generally comparable to controls. In contrast, dense trimer bands were visible in the cochlea contralateral to the AC ablation. Prestin tetramers were also clearly detectable in the cochlea contralateral to the lesion.

These findings suggest that diminished efferent activity on OHCs in the side of the AC ablation, also limits the assembly of higher forms of Prestin oligomers. Thus, monomeric and dimeric forms of Prestin might represent stable pools, relatively unaffected by changes in the acoustic or efferent input to the cochlea, at least after manipulations like those reported here. It is relevant that in the cochlea contralateral to the AC lesion, less affected by loss of efferent activity, Prestin trimers and tetramers are more intensely expressed. This may represent a mechanism to adapt cochlear amplification to efferent imbalance between both ears, whose intrinsic molecular nature is unknown.

Taken together, these findings support that Prestin oligomerization (Zheng et al., 2006; Mio et al., 2008) is regulated both by acoustic input and efferent activity. This may be part of mechanisms to adapt electromotility and cochlear amplification to altered inputs, including input imbalance between both ears. This prediction is worth pursuing through further experimental work.

A third finding is that efferent activity also regulates the expression of key genes involved in electromotility. The expression of the alpha10 subunit of the nAchR, Prestin and beta-actin genes are affected by diminished and unbalanced activity in the MOC, probably also as part of adaptations to altered input.

The main neurotransmitter in MOC is Ach (Warr, 1975; Altschuler et al., 1985; Vetter et al., 1991) which binds to an α9/α10 nAchR on OHCs (Elgoyhen et al., 1994, 2001), modulating motility and axial stiffness (Sziklai and Dallos, 1993; Sziklai et al., 1996, 2001; Dallos et al., 1997; Kalinec et al., 2000). In our unilateral AC ablation model, an expected loss of MOC cholinergic activity correlates with an acute (1 PSD) decrease in the gene expression of the α-10 subunit. This is followed by increased expression at 7 and 15 PSD, which is comparatively greater in the side ipsilateral to the AC lesion, where the activity of the descending corticopontine projection likely is less affected (Doucet et al., 2002; Doucet and Ryugo, 2003; Schofield and Coomes, 2005). This changes in the expression of the nAChR alpha-10 subunit point to OHC adaptation to loss of cholinergic input. The nature and function of such adaptations are unknown and need to be investigated in the future.

Likely as part of adaptive responses to limited MOC activity on OHCs, Prestin gene up regulation is seen in the cochlea ipsilateral to the AC ablation at short times (1 and 7 PSD) after the lesion, with a return to control values at 15 PSD. In the cochlea contralateral to the AC lesion, however, increased Prestin mRNA levels are found just at 7 PSD, with levels at 15 PSD slightly decreased relative to controls. Whereas these oscillations in Prestin gene expression do not bear a linear relation with changes in protein levels seen in Western blots, they probably represent additional levels of regulation by efferent activity or an indirect effect of GABA or CGRP release by the MOC terminals (Maison et al., 2003).

It is also interesting that there is a significant drop in the expression of the β-actin gene at 1 PSD in the cochlea ipsilateral to the cortical lesion. Down-regulation of the β-actin gene could be partly responsible of a greater motor deactivation (Matsumoto et al., 2010) and may reflect the effect on one of the final targets of efferent regulation on OHCs. This may be related to decreased activity in the ipsilateral cochlea, with higher thresholds and a decrease in the amplitude of ABR waves, after unilateral AC lesions (Lamas et al., 2013). In this regard it is interesting to note that at 15 days PSD, prestin gene expression returns to levels similar to controls, while expression levels of the nAChR α10 subunit are still increased. This change, which coincides in time with the recovery of the ABRs previously observed by us (Lamas et al., 2013), may reflect an OHC electromotile "resetting" induced by nAchr receptor adaptations at the MOC-OHC synapse. Therefore, the activity-dependent regulation of the α10 subunit, prestin and β-actin genes reported in this paper may reflect OHC adaptations to changes in MOC activity to compensate for limited and/or unbalanced corticofugal excitation.

In conclusion in this paper we suggest that at least two mechanisms are at work in combination to balance the micromechanical response of the OHC after a decrease in inner ear activity: changes in oligomerization of Prestin and MOC cholinergic neurotransmission along with regulation of the expression of Prestin and β-actin genes.

AUTHORS CONTRIBUTIONS

Miguel A. Merchán and Veronica Lamas designed the experiments. Veronica Lamas and Juan C. Arévalo performed the experiments and analyzed data. Veronica Lamas, Juan C. Arévalo, José M. Juiz and Miguel A. Merchán participated in the discussion of the results. José M. Juiz, Miguel A. Merchán and Veronica Lamas, wrote the paper.

ACKNOWLEDGMENTS

The authors would like to thank Javier Herrero Turrión for his excellent technical assistance, and Dr. Bechara Kachar for providing us with the prestin antibody. This research was supported by the grants from the Ministry of Economy and Competitiveness of the Government of Spain, BFU2012-39982-C02 and BFU2012-39982-C01. This article was written in memory of Dr. Pablo Gil Loyzaga (1954–2013).

REFERENCES

Altschuler, R. A., Kachar, B., Rubio, J. A., Parakkal, M. H., and Fex, J. (1985). Immunocytochemical localization of choline acetyltransferase-like immunoreactivity in the guinea pig cochlea. *Brain Res.* 338, 1–11. doi: 10.1016/0006-8993(85)90242-2

Batta, T. J., Panyi, G., Szucs, A., and Sziklai, I. (2004). Regulation of the lateral wall stiffness by acetylcholine and GABA in the outer hair cells of the guinea pig. *Eur. J. Neurosci.* 20, 3364–3370. doi: 10.1111/j.1460-9568.2004.03797.x

Bian, S., Navaratnam, D., and Santos-Sacchi, J. (2013). Real time measures of prestin charge and fluorescence during plasma membrane trafficking reveal subtetrameric activity. *PLoS One* 8:e66078. doi: 10.1371/journal.pone.0066078

Dallos, P., He, D. Z., Lin, X., Sziklai, I., Mehta, S., and Evans, B. N. (1997). Acetylcholine, outer hair cell electromotility and the cochlear amplifier. *J. Neurosci.* 17, 2212–2226.

Doucet, J. R., Rose, L., and Ryugo, D. K. (2002). The cellular origin of corticofugal projections to the superior olivary complex in the rat. *Brain Res.* 925, 28–41. doi: 10.1016/s0006-8993(01)03248-6

Doucet, J. R., and Ryugo, D. K. (2003). Axonal pathways to the lateral superior olive labeled with biotinylated dextran amine injections in the dorsal cochlear nucleus of rats. *J. Comp. Neurol.* 461, 452–465. doi: 10.1002/cne.10722

Elgoyhen, A. B., and Franchini, L. F. (2011). Prestin and the cholinergic receptor of hair cells: positively-selected proteins in mammals. *Hear. Res.* 273, 100–108. doi: 10.1016/j.heares.2009.12.028

Elgoyhen, A. B., Johnson, D. S., Boulter, J., Vetter, D. E., and Heinemann, S. (1994). α9: an acetylcholine receptor with novel pharmacological properties expressed in rat cochlear hair cells. *Cell* 79, 705–715. doi: 10.1016/0092-8674(94)90555-x

Elgoyhen, A. B., Vetter, D. E., Katz, E., Rothlin, C. V., Heinemann, S. F., and Boulter, J. (2001). α10: a determinant of nicotinic cholinergic receptor function in mammalian vestibular and cochlear mechanosensory hair cells. *Proc. Natl. Acad. Sci. U S A* 98, 3501–3506. doi: 10.1073/pnas.051622798

Feliciano, M., and Potashner, S. J. (1995). Evidence for a Glutamatergic pathway from the Guinea Pig auditory cortex to the inferior Colliculus. *J. Neurochem.* 65, 1348–1357. doi: 10.1046/j.1471-4159.1995.65031348.x

Fleige, S., Walf, V., Huch, S., Prgomet, C., Sehm, J., and Pfaffl, M. W. (2006). Comparison of relative mRNA quantification models and the impact of RNA integrity in quantitative real-time RT-PCR. *Biotechnol. Lett.* 28, 1601–1613. doi: 10.1007/s10529-006-9127-2

Guinan, J. J. (2006). Olivocochlear efferents: anatomy, physiology, function and the measurement of efferent effects in humans. *Ear. Hear.* 27, 589–607. doi: 10.1097/01.aud.0000240507.83072.e7

Hallworth, R., and Nichols, M. G. (2012). Prestin in HEK cells is an obligate tetramer. *J. Neurophysiol.* 107, 5–11. doi: 10.1152/jn.00728.2011

He, D. Z., and Dallos, P. (1999). Somatic stiffness of cochlear outer hair cells is voltage-dependent. *Proc. Natl. Acad. Sci. U S A* 96, 8223–8228. doi: 10.1073/pnas.96.14.8223

He, D. Z., and Dallos, P. (2000). Properties of voltage-dependent somatic stiffness of cochlear outer hair cells. *J. Assoc. Res. Otolaryngol.* 1, 64–81. doi: 10.1007/s101620010006

He, D. Z. Z., Lovas, S., Ai, Y., Li, Y., and Beisel, K. W. (2014). Prestin at year 14: progress and prospect. *Hear. Res.* 311, 25–35. doi: 10.1016/j.heares.2013.12.002

Kalinec, F., Zhang, M., Urrutia, R., and Kalinec, G. (2000). Rho GTPases mediate the regulation of cochlear outer hair cell motility by acetylcholine. *J. Biol. Chem.* 275, 28000–28005. doi: 10.1074/jbc.M004917200

Lamas, V., Alvarado, J. C., Carro, J., and Merchán, M. A. (2013). Long-term evolution of brainstem electrical evoked responses to sound after restricted ablation of the auditory cortex. *PLoS One* 8:e73585. doi: 10.1371/journal.pone.0073585

León, A., Elgueda, D., Silva, M. A., Hamamé, C. M., and Delano, P. H. (2012). Auditory cortex basal activity modulates cochlear responses in chinchillas. *PLoS One* 7:e36203. doi: 10.1371/journal.pone.0036203

Livak, K. J., and Schmittgen, T. D. (2001). Analysis of relative gene expression data using real-time quantitative PCR and the 2(-Delta Delta C(T)) method. *Methods* 25, 402–408. doi: 10.1006/meth.2001.1262

Maison, S. F., Adams, J. C., and Liberman, M. C. (2003). Olivocochlear innervation in the mouse: immunocytochemical maps, crossed versus uncrossed contributions and transmitter colocalization. *J. Comp. Neurol.* 455, 406–416. doi: 10.1002/cne.10490

Maison, S. F., Luebke, A. E., Liberman, M. C., and Zuo, J. (2002). Efferent protection from acoustic injury is mediated via alpha9 nicotinic acetylcholine receptors on outer hair cells. *J. Neurosci.* 22, 10838–10846.

Maison, S. F., Vetter, D. E., and Liberman, M. C. (2007). A novel effect of cochlear efferents: in vivo response enhancement does not require α9 cholinergic receptors. *J. Neurophysiol.* 97, 3269–3278. doi: 10.1152/jn.00067.2007

Matsuda, K., Zheng, J., Du, G.-G., Klöcker, N., Madison, L. D., and Dallos, P. (2004). N-linked glycosylation sites of the motor protein prestin: effects on membrane targeting and electrophysiological function. *J. Neurochem.* 89, 928–938. doi: 10.1111/j.1471-4159.2004.02377.x

Matsumoto, N., Kitani, R., Maricle, A., Mueller, M., and Kalinec, F. (2010). Pivotal role of actin depolymerization in the regulation of cochlear outer hair cell motility. *Biophys. J.* 99, 2067–2076. doi: 10.1016/j.bpj.2010.08.015

Mazurek, B., Haupt, H., Amarjargal, N., Yarin, Y. M., Machulik, A., and Gross, J. (2007). Up-regulation of prestin mRNA expression in the organs of Corti of guinea pigs and rats following unilateral impulse noise exposure. *Hear. Res.* 231, 73–83. doi: 10.1016/j.heares.2007.05.008

Mio, K., Kubo, Y., Ogura, T., Yamamoto, T., Arisaka, F., and Sato, C. (2008). The motor protein prestin is a bullet-shaped molecule with inner cavities. *J. Biol. Chem.* 283, 1137–1145. doi: 10.1074/jbc.m702681200

Mulders, W. H., and Robertson, D. (2000). Evidence for direct cortical innervation of medial olivocochlear neurones in rats. *Hear. Res.* 144, 65–72. doi: 10.1016/s0378-5955(00)00046-0

Schmittgen, T. D., and Livak, K. J. (2008). Analyzing real-time PCR data by the comparative C(T) method. *Nat. Protoc.* 3, 1101–1108. doi: 10.1038/nprot.2008.73

Schofield, B. R., and Coomes, D. L. (2005). Auditory cortical projections to the cochlear nucleus in guinea pigs. *Hear. Res.* 199, 89–102. doi: 10.1016/j.heares.2004.08.003

Sumner, C. J., Tucci, D. L., and Shore, S. E. (2005). Responses of ventral cochlear nucleus neurons to contralateral sound after conductive hearing loss. *J. Neurophysiol.* 94, 4234–4243. doi: 10.1152/jn.00401.2005

Sziklai, I., and Dallos, P. (1993). Acetylcholine controls the gain of the voltage-to-movement converter in isolated outer hair cells. *Acta Otolaryngol.* 113, 326–329. doi: 10.3109/00016489309135818

Sziklai, I., He, D. Z., and Dallos, P. (1996). Effect of acetylcholine and GABA on the transfer function of electromotility in isolated outer hair cells. *Hear. Res.* 95, 87–99. doi: 10.1016/0378-5955(96)00026-3

Sziklai, I., Szõnyi, M., and Dallos, P. (2001). Phosphorylation mediates the influence of acetylcholine upon outer hair cell electromotility. *Acta Otolaryngol.* 121, 153–156. doi: 10.1080/000164801300043280

Vetter, D. E., Adams, J. C., and Mugnaini, E. (1991). Chemically distinct rat olivocochlear neurons. *Synapse* 7, 21–43. doi: 10.1002/syn.890070104

Vetter, D. E., Katz, E., Maison, S. F., Taranda, J., Turcan, S., Ballestero, J., et al. (2007). The α10 nicotinic acetylcholine receptor subunit is required for normal synaptic function and integrity of the olivocochlear system. *Proc. Natl. Acad. Sci. U S A* 104, 20594–20599. doi: 10.1073/pnas.0708545105

Warr, W. B. (1975). Olivocochlear and vestibular efferent neurons of the feline brain stem: their location, morphology and number determined by retrograde axonal transport and acetylcholinesterase histochemistry. *J. Comp. Neurol.* 161, 159–181. doi: 10.1002/cne.901610203

Xia, A., Song, Y., Wang, R., Gao, S. S., Clifton, W., Raphael, P., et al. (2013). Prestin regulation and function in residual outer hair cells after noise-induced hearing loss. *PLoS One* 8:e82602. doi: 10.1371/journal.pone.0082602

Yang, K., Huang, Z.-W., Liu, Z.-Q., Xiao, B.-K., and Peng, J.-H. (2009). Long-term administration of salicylate enhances prestin expression in rat cochlea. *Int. J. Audiol.* 48, 18–23. doi: 10.1080/14992020802327998

Yu, T., Calvo, L., Anta, B., López-Benito, S., Southon, E., Chao, M. V., et al. (2011). Regulation of trafficking of activated TrkA is critical for NGF-mediated functions. *Traffic* 12, 521–534. doi: 10.1111/j.1600-0854.2010.01156.x

Yu, N., Zhu, M.-L., Johnson, B., Liu, Y.-P., Jones, R. O., and Zhao, H.-B. (2008). Prestin up-regulation in chronic salicylate (aspirin) administration: an implication of functional dependence of prestin expression. *Cell. Mol. Life Sci.* 65, 2407–2418. doi: 10.1007/s00018-008-8195-y

Zheng, J., Du, G.-G., Anderson, C. T., Keller, J. P., Orem, A., Dallos, P., et al. (2006). Analysis of the oligomeric structure of the motor protein prestin. *J. Biol. Chem.* 281, 19916–19924. doi: 10.1074/jbc.m513854200

Conflict of Interest Statement: The authors declare that the research was conducted in the absence of any commercial or financial relationships that could be construed as a potential conflict of interest.

Received: 21 October 2014; accepted: 24 December 2014; published online: 20 January 2015.

*Citation: Lamas V, Arévalo JC, Juiz JM and Merchán MA (2015) Acoustic input and efferent activity regulate the expression of molecules involved in cochlear micromechanics. Front. Syst. Neurosci. **8**:253. doi: 10.3389/fnsys.2014.00253*

This article was submitted to the journal Frontiers in Systems Neuroscience.

Advantages of publishing in Frontiers

OPEN ACCESS
Articles are free to read, for greatest visibility

COLLABORATIVE PEER-REVIEW
Designed to be rigorous – yet also collaborative, fair and constructive

FAST PUBLICATION
Average 85 days from submission to publication (across all journals)

COPYRIGHT TO AUTHORS
No limit to article distribution and re-use

TRANSPARENT
Editors and reviewers acknowledged by name on published articles

SUPPORT
By our Swiss-based editorial team

IMPACT METRICS
Advanced metrics track your article's impact

GLOBAL SPREAD
5'100'000+ monthly article views and downloads

LOOP RESEARCH NETWORK
Our network increases readership for your article

Frontiers
EPFL Innovation Park, Building I • 1015 Lausanne • Switzerland
Tel +41 21 510 17 00 • Fax +41 21 510 17 01 • info@frontiersin.org
www.frontiersin.org

Find us on